



UNIVERSIDADE ESTADUAL DE CAMPINAS
FACULDADE DE ENGENHARIA DE ALIMENTOS

RAQUEL COSTA CHEVALIER

**EMULSÕES PICKERING ESTABILIZADAS COM NANOFIBRAS DE CELULOSE PARA
INCORPORAÇÃO EM FILMES E COBERTURAS BIODEGRADÁVEIS**

**PICKERING EMULSIONS STABILIZED WITH CELLULOSE NANOFIBERS FOR INCORPORATION
IN BIODEGRADABLE FILM AND COATINGS**

CAMPINAS

2024

RAQUEL COSTA CHEVALIER

**EMULSÕES PICKERING ESTABILIZADAS COM NANOFIBRAS DE CELULOSE PARA
INCORPORAÇÃO EM FILMES E COBERTURAS BIODEGRADÁVEIS**

**PICKERING EMULSIONS STABILIZED WITH CELLULOSE NANOFIBERS FOR INCORPORATION
IN BIODEGRADABLE FILM AND COATINGS**

Tese apresentada à Faculdade de Engenharia de Alimentos da Universidade Estadual de Campinas como parte dos requisitos exigidos para a obtenção do título de Doutora em Engenharia de Alimentos.

Thesis presented to the School of Food Engineering of the University of Campinas in partial fulfillment of the requirements for the degree of Doctor in Food Engineering.

Orientadora: Profa. Dra. Rosiane Lopes da Cunha

ESTE TRABALHO CORRESPONDE À VERSÃO FINAL DA TESE DEFENDIDA PELA ALUNA RAQUEL COSTA CHEVALIER, E ORIENTADA PELO(A) PROF(A). DR(A). ROSIANE LOPES DA CUNHA.

CAMPINAS

2024

Ficha catalográfica
Universidade Estadual de Campinas (UNICAMP)
Biblioteca da Faculdade de Engenharia de Alimentos
Claudia Aparecida Romano - CRB 8/5816

C427p Chevalier, Raquel Costa, 1993-
Pickering emulsions stabilized with cellulose nanofibers for incorporation in biodegradable film and coatings / Raquel Costa Chevalier. – Campinas, SP : [s.n.], 2024.

Orientador: Rosiane Lopes da Cunha.
Tese (doutorado) – Universidade Estadual de Campinas (UNICAMP), Faculdade de Engenharia de Alimentos.

1. Alimentos - Embalagens. 2. Emulsões de Pickering. 3. Nanofibra de celulose. 4. Revestimentos. I. Cunha, Rosiane Lopes da. II. Universidade Estadual de Campinas (UNICAMP). Faculdade de Engenharia de Alimentos. III. Título.

Informações Complementares

Título em outro idioma: Emulsões pickering estabilizadas com nanofibras de celulose para incorporação em filmes e coberturas biodegradáveis

Palavras-chave em inglês:

Food - Packaging

Pickering emulsions

Cellulose nanofibers

Coatings

Área de concentração: Engenharia de Alimentos

Titulação: Doutora em Engenharia de Alimentos

Banca examinadora:

Rosiane Lopes da Cunha [Orientador]

William Renzo Cortez Vega

Luís Marangoni Júnior

Franciele Maria Pelissari

Ana Letícia Rodrigues Costa Lelis

Data de defesa: 05-07-2024

Programa de Pós-Graduação: Engenharia de Alimentos

Identificação e informações acadêmicas do(a) aluno(a)

- ORCID do autor: 0000-0003-2738-0050

- Currículo Lattes do autor: <http://lattes.cnpq.br/0319086152875324>

COMISSÃO EXAMINADORA

Prof(a). Dr(a). Rosiane Lopes da Cunha
Presidente e Orientadora – FEA/UNICAMP

William Renzo Cortez Vega
Membro Titular
UFAM

Luís Marangoni Júnior
Membro Titular
UNICAMP

Franciele Maria Pelissari Molina
Membro Titular
UFVJM

Ana Letícia Rodrigues Costa Lelis
Membro Titular
UFV

A Ata de Defesa com as respectivas assinaturas dos membros encontra-se no SIGA/Sistema de Fluxo de Dissertações/Teses e na Secretaria do Programa de Pós-Graduação

Ao único Deus sábio, Salvador nosso, seja glória e majestade, domínio e poder, agora, e para todo o sempre.
Judas 1:25

**AO MEU AMADO ESPOSO,
AOS MEUS QUERIDOS PAIS E IRMÃS**

AGRADECIMENTOS

Confesso que por muitas vezes posterguei escrever essa seção, pois sabia que me lembraria de muitas coisas, e seria um mix de muitos sentimentos, pois essa fase final me parece ser a mais desgastante de todo o processo, não pelo fato de escrever em si, mas por todo o significado desse momento de finalização de ciclos e seguir rumo ao ainda desconhecido.

Primeiramente, agradeço ao meu amado e bom Deus. Sim, a ele toda honra e glória, pois eu não sou nada sem ele em minha vida. Nos momentos de maior dificuldade, é ele que segura na minha mão e me diz: Eu te amo Filha, continua, pois eis que estarei convosco todos os dias da sua vida. Ele que me dá toda força, proteção e sempre ilumina os meus caminhos, permitindo que eu superasse todos os desafios desta nada fácil jornada.

Ao meu amado esposo, Gustavo Ferreira, que esteve ao meu lado nessa longa jornada. Ele viu as minhas aflições, preocupações, as noites em claro, os finais de semana trabalhando, seja em casa ou no laboratório, onde ele nunca reclamou e sempre esteve ao meu lado, para que eu não ficasse sozinha. Mas também esteve ao meu lado nos momentos de muitas alegrias, onde pudemos viver juntos o intercâmbio, comemorar as aprovações de artigos e dentre outras conquistas. Deus sabia exatamente que eu precisava de você como companheiro para finalizar esse ciclo. Sou eternamente grata por tudo que fez e faz por mim. Eu te amo muito.

Aos meus pais, Maurício e Marli Chevalier, que sempre estiveram comigo, mesmo que a distância, me ouvindo, me incentivando e torcendo por mim e comigo. Por terem sempre priorizado os meus estudos e hoje colhemos esses frutos, desse tamanho investimento. Por me amar de forma incondicional, sempre querer o melhor pra mim e por nunca interferir nas minhas escolhas profissionais, sempre me apoiando em cada passo que dei. E por sempre orar sem cessar pela minha vida, eu sei que se cheguei até aqui foi porque eu pude contar sempre com vocês. Sou eternamente grata pela vida de vocês e os amo demais.

A minha querida irmã pequena, Dani, que é a minha princesinha, que desde pequena teve que entender as minhas ausências, sofreu por estarmos longes, mas em cada encontro me ajudava a seguir em frente com seu amor e carinho. Você foi um presente de Deus em nossa família, obrigada por nos escolher. Eu amo muito você Tchan Tchan.

A minha irmã mais velha Rapha e seu esposo Igor, meus sobrinhos lindos e amados, Ícaro e Eloá Vitória, obrigada por sempre torcerem por mim, entender as minhas ausências, e mesmo com toda distância, sempre sonharam os sonhos, acreditaram em mim e festejavam as conquistas mesmo sem entender plenamente. Amo demais vocês.

As minhas queridas avós, Darci Carneiro e Alice Chevalier, por orarem por mim, me amarem e mesmo com toda distância sempre se fizeram presentes. Infelizmente a Vó Alice nos deixou no meio dessa jornada, mas eu entendi que foi melhor assim, que a senhora descansou nos braços do Pai. Mas agradeço a oportunidade de ter cuidado da senhora, e estado ao seu lado mesmo nos últimos dias. Tenho certeza que a senhora e o Vô Moacir Chevalier, estão muito orgulhosos que a “formiguinha preta” será agora Doutora em Engenharia de Alimentos. A vó Darci, por todas as orações, principalmente quando fui pro exterior, ela ficou tão aflita, mas sempre com palavras doces, de incentivo e com muita alegria em cada vídeo chamada e sempre ficava abismada com a diferença de horário. Te amo muito Vozinha.

A Família Carneiro, Tia Euzir, meus primos Raphael, Camilia e Kíssila, por todo carinho, desde quando eu era pequena cuidaram de mim, se preocupando comigo e sempre torcendo por mim, e estando presentes em cada fase da minha vida, mesmo que estejamos distantes fisicamente.

A Família Chevalier, Tio Carlos, Tia Vânia, e primo Victor, por torcerem por mim, sempre comemorar as minhas conquistas e sempre presente em cada fase da minha vida, mesmo que estejamos distantes fisicamente.

À minha querida orientadora Prof. Dra. Rosiane Lopes da Cunha pela pessoa humana, dedicada e por toda a ajuda, além da excelente orientação. Por todos os conselhos dentro e fora da área acadêmica, nesse período de 6 anos em que estivemos juntas. Muito obrigada por tudo.

A técnica do laboratório Vanessinha, por toda ajuda, suporte e por toda dedicação em todos os dias para me ajudar, aconselhar e até mesmo desabafar em relação as preocupações. Muito Obrigada.

E jamais poderia deixar de agradecer a um casal que mostrou esse caminho da pesquisa, que são meus orientadores da época da graduação, Prof. Dr. William Renzo e Prof. Dra. Sandriane Pizato. Por todos os ensinamentos, conselhos e por me instruírem nas minhas decisões, para que eu fizesse a melhor escolha.

Aos amigos, parceiros de experimentos e colegas de laboratório LEP- Laboratório de Engenharia de Processos, que conheci na UNICAMP que fizeram parte dessa jornada. Meu muito obrigada a todos.

Aos meus amigos que são do Rio de Janeiro, que mesmo não entendendo porque não paro de estudar, sempre procuram me encontrar e se alegram com as minhas conquistas, mesmo não nos vendo com tanta frequência como gostaríamos.

Aos membros da banca examinadora pelos conselhos e pelas correções que auxiliaram no aprimoramento do trabalho exposto.

À FEA (Faculdade de Engenharia de Alimentos), aos professores e funcionários sempre dispostos a nos ajudar, nos fornecendo um aprendizado diário.

Ao Laboratório de Ciência de Superfícies (LCS) do Laboratório Nacional de Nanotecnologia (LNNano - CNPEM) (Campinas, Brasil) por me receber e sempre serem muitos solícitos no acompanhamento das análises de AFM.

A Universidade do Minho, principalmente na pessoa do Prof. Dr. Antônio Vicente, que me recebeu de braços abertos no LIP, onde pude me sentir em casa, mesmo estando em Portugal. A todos os colegas de laboratório, os “Lipinhos”, que me acompanharam, me ajudaram e me auxiliaram em tudo que precisei. E principalmente a pessoa do Dr. Jorge Miguel, que foi o meu Coorientador e abraçou junto comigo o meu projeto. Muito obrigada por tudo. Ao órgão de fomento Conselho Nacional de Desenvolvimento Científico e Tecnológico (CNPq) pela bolsa de doutorado sanduiche no exterior, nº 200248/2022-7.

Este estudo foi financiado pela Coordenação de Aperfeiçoamento de Pessoal de Nível Superior – Brasil (CAPES) - Código Financeiro 001. Agradeço a Fundação de Amparo à Pesquisa do Estado de São Paulo - FAPESP (2019/27354-3). Agradeço ao órgão de fomento Conselho Nacional de Desenvolvimento Científico e Tecnológico (CNPq) pelo suporte financeiro (404753/2023-0).

RESUMO

A preocupação global com o grave problema ambiental resultante do grande acúmulo de resíduos de embalagens plásticas deve-se ao uso de materiais à base de polímeros de petróleo não biodegradáveis. Portanto, a utilização de biopolímeros naturais em embalagens é uma alternativa, embora não apresentem boas propriedades de barreira à água e resistência mecânica. Além dos biopolímeros formadores de filmes, como pectina, alginato e gelatina, nanofibras produzidas a partir da celulose (CNF) podem ser usadas como sistema de reforço em filmes/revestimentos sustentáveis, apresentando as vantagens de abundância natural e biodegradabilidade deste polissacarídeo. A incorporação de emulsões Pickering (PE) em uma matriz filmogênica também traz melhorias às propriedades de barreira dos filmes, além de poder veicular compostos ativos lipofílicos. Neste contexto, este trabalho visou avaliar o efeito do CNF como material de reforço e/ou também como estabilizante de PE dentro da matriz formadora de filme. Na primeira etapa, CNFs foram produzidas a partir de casca de mandioca por hidrólise ácida ou hidrólise enzimática (usando xilanase) seguida de ultrassom. A capacidade emulsificante e digestibilidade das CNFs de casca de mandioca foi comparada com a da etilcelulose comercial submetida a processo de ultrassom. As dimensões das CNFs exerceram influência na estabilidade das emulsões, sendo o tipo de processo determinante para estas propriedades. A hidrólise química foi capaz de quebrar de forma mais eficiente a estrutura celulósica, favorecendo uma melhor capacidade estabilizante das CNFs em emulsões. Como o método enzimático foi menos eficiente e o objetivo era a produção de CNFs usando um método sustentável, uma associação de enzimas (xilanase + celulase) foi aplicada usando diferentes tempos de hidrólise com celulase. A etapa de hidrólise com xilanase seguiu as mesmas condições de processo da primeira etapa (150 rpm; 35°C por 24 h). Nesta segunda etapa buscou-se produzir CNFs com propriedades similares às obtidas por hidrólise química. As CNFs obtidas após 6 e 12 horas da hidrólise com celulase foram as escolhidas para dar prosseguimento aos estudos de aplicação das CNFs como estabilizantes de emulsão Pickering incorporando óleo essencial de orégano (OEO) que apresenta atividade antimicrobiana. O OEO foi incorporado em uma matriz emulsionada associado ao óleo de girassol para minimizar o odor forte e volatilidade do OEO. A atividade antimicrobiana foi melhorada frente a bactérias (*Staphylococcus aureus*, *Escherichia coli* e *Listeria monocytogenes*) e fungo (*Alternaria Alternata*) analisados. Diante destes resultados, seguiu-se para a terceira etapa, na qual foram produzidos filmes de pectina usando CNFs como agente de reforço e estabilizante da emulsão Pickering incorporada na solução filmogênica. Todos os filmes eram transparentes, e a incorporação da emulsão promoveu uma redução da hidrofobicidade e barreira completa à luz UV, características desejáveis em embalagens para alimentos. Por fim, esta matriz foi usada como revestimento em tomates e o *shelf-life* foi avaliado por 12 dias. De forma geral, houve ganho na incorporação das CNFs e da emulsão Pickering como revestimento nos tomates, principalmente devido à incorporação do OEO que inibiu o crescimento de fungos, podendo estes revestimentos serem usados para ampliação da vida útil de frutos.

Palavras-chave: filmes nanocompósitos; emulsão Pickering; nanofibras de celulose; revestimentos.

ABSTRACT

Global concern about the serious environmental problem resulting from the large accumulation of plastic packaging waste is due to the use of materials based on non-biodegradable petroleum polymers. Therefore, the use of natural biopolymers in packaging is an alternative, although they do not present good water barrier properties and mechanical resistance. In addition to film-forming biopolymers, such as pectin, alginate and gelatin, nanofibers produced from cellulose (CNF) can be used as a reinforcement system in sustainable films/coatings, presenting the advantages of the natural abundance and biodegradability of this polysaccharide. The incorporation of Pickering emulsions (PE) into a film-forming matrix also improves the barrier properties of the films, in addition to being able to transport lipophilic active compounds. In this context, this work aimed to evaluate the effect of CNF as a reinforcing material and/or also as a PE stabilizer within the film-forming matrix. In the first stage, CNFs were produced from cassava peel by acid hydrolysis or enzymatic hydrolysis (using xylanase) followed by ultrasound. The emulsifying capacity and digestibility of CNFs from cassava peel were compared with those of commercial ethylcellulose subjected to the ultrasound process. The dimensions of the CNFs influenced the stability of the emulsions, with the type of process determining these properties. Chemical hydrolysis was able to more efficiently break down the cellulosic structure, favoring a better stabilizing capacity of CNFs in emulsions. As the enzymatic method was less efficient and the objective was to produce CNFs in a sustainable way, a combination of enzymes (xylanase + cellulase) was applied using different hydrolysis times with cellulase. The hydrolysis step with xylanase followed the same process conditions as the first step (150 rpm; 35°C for 24 h). In this second stage, we sought to produce CNFs with properties similar to those obtained by chemical hydrolysis. The CNFs obtained after 6 and 12 hours of hydrolysis with cellulase were chosen to continue studies on the application of CNFs as stabilizers of Pickering emulsions incorporating oregano essential oil (OEO), which has antimicrobial activity. OEO was incorporated into an emulsified matrix associated with sunflower oil to minimize the strong odor and volatility of OEO. The antimicrobial activity was improved against the bacteria (*Staphylococcus aureus*, *Escherichia coli* and *Listeria monocytogenes*) and fungi (*Alternaria Alternata*) analyzed. Given these results, the third stage was carried out, in which pectin films were produced using CNFs as a reinforcing and stabilizing agent for the Pickering emulsion incorporated in the film-forming solution. All films were transparent, and the incorporation of the emulsion promoted reduced hydrophilicity and a complete barrier to UV light, desirable characteristics in food packaging. Finally, this matrix was used as a tomato cover and the shelf life was evaluated for 12 days. In general, there was a gain in the incorporation of CNFs and Pickering emulsion as a coating on tomatoes, mainly due to the incorporation of OEO, which inhibited the growth of fungi, and these coatings can be used to extend the shelf life of fruits.

Keywords: nanocomposite films; Pickering emulsion; cellulose nanofibers; coatings.

SUMÁRIO

CAPÍTULO I	13
1.1 INTRODUÇÃO GERAL	14
1.2 OBJETIVOS	16
1.2.1 OBJETIVO GERAL	16
1.2.2 OBJETIVO ESPECÍFICOS.....	16
1.3 ESTRUTURA DA TESE	17
1.4 REFERÊNCIAS	18
CAPÍTULO II	21
Main production methods of cellulose nanofibers: perspectives on emerging technologies.....	22
CAPÍTULO III	62
Modulating digestibility and stability of Pickering emulsions based on cellulose nanofibers.....	63
CAPÍTULO IV	98
Antimicrobial potential of oregano essential oil vehiculated in Pickering cellulose nanofibers-stabilized emulsions	99
CAPÍTULO V	141
Cellulose nanofibers as stabilizer of Pickering emulsions and reinforcement of pectin films covering tomatoes	142
CAPÍTULO VI	176
6.1 DISCUSSÃO GERAL.....	177
CAPÍTULO VII	182
CONCLUSÃO GERAL.....	182
CAPÍTULO VIII	185
REFERÊNCIAS GERAIS	185
CAPÍTULO IX	188
APÊNDICE	188

CAPÍTULO I

INTRODUÇÃO GERAL

OBJETIVOS GERAL E ESPECÍFICOS

ESTRUTURA DA TESE

1.1 INTRODUÇÃO GERAL

Nas últimas décadas, o interesse pelo desenvolvimento de processos e produtos sustentáveis cresceu em resposta à preocupação com o meio ambiente. Matérias-primas convencionais para embalagens de alimentos são produzidas a partir de recursos não renováveis como o petróleo, que são prejudiciais ao meio ambiente (Travalini et al., 2019). Polissacarídeos, proteínas, lipídeos ou suas misturas são usados para a produção de filmes biodegradáveis, como uma resposta sustentável (Khan et al., 2024). Com o aumento da degradação ambiental, muitos estudos visam a utilização de recursos naturais e renováveis (Riaz et al., 2024), sendo o aproveitamento de resíduos agrícolas uma tendência uma vez que, além do benefício ambiental, seu uso favorece a obtenção de produtos de maior valor agregado. O Brasil é o país que apresenta a maior extensão territorial cultivável mundial, sendo, portanto, uma importante fonte de resíduos de origem vegetal. O cultivo da mandioca (*Manihot esculenta*), classificada como a sexta cultura mais importante do mundo, é amplamente difundido na América Latina, África e Sul da Ásia. No entanto, as cascas de mandioca são frequentemente descartadas, resultando em apodrecimento ou incineração, o que libera metano, produz fumaça e polui a água, o solo e o ar (Zhang et al., 2024). Essas práticas representam sérias ameaças ao meio ambiente. Portanto, é de suma importância aproveitar esses materiais, não apenas para gerar valor e novos produtos, mas também para prevenir a poluição ambiental. Diante disto, muitos materiais podem ser utilizados como alternativas para a produção de filmes a partir de resíduos vegetais, uma vez que estes têm em sua composição biopolímeros tais como: celulose, hemicelulose, lignina e pectina. Embora os filmes baseados em biopolímeros não apresentem as mesmas propriedades físicas dos plásticos sintéticos, estes são uma alternativa que deve ser considerada, pois são de fontes renováveis, não tóxicas, biodegradáveis e biocompatíveis (Pérez-Córdoba et al., 2018).

Soluções filmogênicas a base de biopolímeros de fontes vegetais podem ser usadas como revestimentos biodegradáveis visando a minimização das perdas pós-colheita e, consequentemente, prolongando a vida útil de frutas e hortaliças. Os produtos agrícolas são extremamente susceptíveis à deterioração seja ela na colheita, transporte ou armazenamento (Yang et al., 2024). Segundo uma estimativa feita no Brasil, o maior percentual de perdas de frutas em supermercado e feiras é proveniente do tomate (*Solanum lycopersicum*), o que é principalmente devido ao clima quente e úmido que favorece o rápido amadurecimento e possível contaminação por fungo (*Alternaria Alternata*) e pragas agrícolas (Silva et al., 2024).

Entretanto, é um dos frutos mais consumidos no mundo devido a seu sabor apreciado em diversas culturas, além de ser rico em compostos bioativos como carotenóides, ácido ascórbico, tocoferol e compostos fenólicos. Para proporcionar e disponibilizar esse fruto na mesa do consumidor e evitar as perdas por fatores físicos, químicos e/ou microbiológicos, a utilização de revestimentos ou mesmo de filmes biodegradáveis é uma alternativa interessante.

Considerando a necessidade da melhora das propriedades dos filmes a base de biopolímeros, o uso de nanopartículas de celulose como elemento de reforço pode aprimorar as propriedades mecânicas e diminuir a sensibilidade dos polímeros à presença de água, porém, ainda assim, preservar a biodegradabilidade (Pelissari et al., 2017). As nanofibrilas de celulose possuem características tecnológicas favoráveis para utilização em embalagens, como baixa expansão térmica, elevada razão de aspecto (comprimento em relação ao diâmetro), além de boas propriedades mecânicas devido à sua alta relação superfície / volume (Cengiz-Çallioglu, 2011).

Nos últimos anos, os CNFs têm atraído grande atenção, o que tem levado a um número crescente de estudos sobre métodos para sua obtenção. Tratamentos químicos (por exemplo, álcali, ácido e oxidação), mecânicos (por exemplo, eletrofiação, sopro de solução, homogeneização a alta pressão, microfluidização, moagem de alto cisalhamento e ultrassom de alta intensidade) e enzimáticos (por exemplo, ligninases, xilanases, celulase e hemicelulose) têm sido aplicados para isolar CNFs de microfibrilas de celulose. Além disso, muitas tecnologias emergentes (por exemplo, líquidos iônicos, solvente eutético profundo, micro-ondas, irradiação por feixe de elétrons, plasma frio, campo elétrico pulsado e crioesmagamento) tem surgido como alternativas sustentáveis às metodologias convencionais (Li et al., 2023). Entretanto, entre os diversos processos, a hidrólise enzimática consolida-se como uma vertente interessante por ser ambientalmente amigável e ser feito em condições amenas de processo, evitando a geração de resíduos químicos.

Outra vertente interessante, recentemente explorada, é a aplicação de emulsões em revestimentos, de forma a reduzir a hidrofobicidade da matriz filmogênica e melhorar a resistência ao vapor de água. Diante disso, a utilização de uma fase lipídica incorporada por meio de uma emulsão seria uma estratégia promissora para compensar as deficiências dos filmes a base de biopolímeros (Liu et al., 2020). Além disso, emulsões podem carrear compostos ativos, como óleos essenciais e antioxidantes, agregando novas funcionalidades à

embalagem. Os óleos essenciais são fonte de ingredientes bioativos que apresentam múltiplas funções, como: antioxidantes, antimicrobianas, anti-inflamatórias e anticancerígenas (Ebrahimi et al., 2023). O óleo essencial de orégano - OEO (*Origanum vulgare* L.) é conhecido devido por suas propriedades antifúngicas e ação contra patógenos. No entanto, apresenta um odor forte e irritante, é facilmente oxidado sob condições como luz, calor e oxigênio, se for adicionado diretamente à solução filmogênica. Para contornar essa desvantagens, a veiculação do OEO por meio de emulsão é uma alternativa para proteger o OEO da degradação e volatilização no processo de fabricação dos filmes.

Emulsões Pickering são emulsões estabilizadas por partículas sólidas, no lugar de surfactantes ou materiais anfifílicos (Chevalier & Bolzinger, 2013; Y. et al. Yang et al., 2017), apresentando alta estabilidade contra agregação, coalescência e separação de fases. Emulsões tipo Pickering estabilizadas por partículas sólidas biocompatíveis, como nanofibrilas de celulose (Fujisawa et al., 2017; Nikfarjam et al., 2015), têm atraído o interesse devido à sua baixa toxicidade e respeito ao meio ambiente (Patel, 2020; Tavernier et al., 2016; X. et al. Zhang et al., 2018). Considerando as duas funções que a CNF pode ter em um filme, esta foi usada com duas finalidades, para estabilizar a emulsão incorporada na matriz filmogênica e reforçar filmes compósitos.

1.2 OBJETIVOS

1.2.1 OBJETIVO GERAL

Avaliar as propriedades tecnológicas, físico-químicas e microbiológicas de filmes biodegradáveis incorporados de emulsões Pickering estabilizadas por CNFs e com fase dispersa de OEO.

1.2.2 OBJETIVO ESPECÍFICOS

- Isolar e caracterizar nanofibrilas de celulose (CNFs) obtidas a partir da casca de mandioca e de etil celulose usando pré-tratamento alcalino, hidrólise ácida ou enzimática, além de aplicação de ultrassom
- Avaliar a capacidade estabilizante e digestibilidade *in vitro* de emulsões estabilizadas por CNFs;

- Produzir e caracterizar emulsões Pickering estabilizadas por CNFs produzidas por hidrólise enzimática com xilanase e celulase, tendo óleo essencial de orégano na fase dispersa.
- Avaliar a atividade antimicrobiana de emulsões contendo óleo essencial de orégano e estabilizadas por CNFs produzidas por hidrólise enzimática;
- Produzir e caracterizar filmes de pectina adicionados de emulsões Pickering e reforçados com CNFs;
- Avaliar a vida útil de tomates revestidos com filmes de pectina contendo emulsão Pickering (fase dispersa OEO) estabilizada e reforçada com CNFs.

1.3 ESTRUTURA DA TESE

Esta tese de doutorado foi dividida em 8 capítulos, conforme descrito a seguir.

No primeiro capítulo (**Capítulo 1**) é apresentada a introdução geral do trabalho, seguida pelos objetivos gerais e específicos que contribuíram para a realização dos artigos dessa tese, e por fim a descrição de como a tese foi estruturada.

No **Capítulo 2** é apresentado o artigo de revisão intitulado: “Main production methods of cellulose nanofibers: perspectives on Emerging Technologies”. São abordadas as principais fontes e os métodos mais relevantes de obtenção das nanofibras de celulose. Além disso, são mostradas as principais vantagens e desvantagens atreladas a cada método, e por fim tecnologias emergentes para a produção de nanofibras de celulose. Esse artigo será submetido à revista Cellulose.

No **Capítulo 3** é apresentado o primeiro artigo experimental intitulado “Modulating digestibility and stability of Pickering emulsions based on cellulose nanofibers”. Nesse artigo foram exploradas as hidrólises ácida e enzimática associadas a processo mecânico (ultrassom) para obtenção de nanofibras de celulose a partir de resíduos como a casca da mandioca. Foi traçada uma comparação com a nanofibra de etil celulose produzida apenas por processo mecânico. Foi investigada a capacidade das nanofibras produzidas de estabilizar emulsões óleo/água (O/A), além de ser avaliada a digestibilidade *in vitro* dessas emulsões. Esse artigo foi publicado na revista Food Research International em 2024 (<https://doi.org/10.1016/j.foodres.2024.113963>).

O **Capítulo 4** é continuação do estudo anterior, mas visou aprimorar a hidrólise enzimática para a obtenção das nanofibras de celulose, uma vez que é uma tecnologia verde e mais desejável considerando a sustentabilidade. Além do processo enzimático usado no processo anterior (com xilanase), celulase foi usada em uma segunda etapa de hidrólise enzimática com diferentes tempos de duração, visando a melhora das propriedades tecno-funcionais das nanofibras. OEO foi incorporado na fase oleosa da emulsão devido às suas excelentes atividades antimicrobiana e bioativa. Com isso, um estudo aprofundado da atividade antimicrobiana dessas emulsões contra três bactérias (*Staphylococcus aureus*, *Escherichia coli* e *Listeria monocytogenes*) e um fungo (*Alternaria alternata*) foi realizado. O artigo intitulado “Antimicrobial potential of oregano essential oil vehiculated in Pickering cellulose nanofibers- stabilized emulsions” foi submetido à revista International Journal of Biological Macromolecules.

No **Capítulo 5** é apresentado o último artigo experimental, cujo objetivo era produzir e caracterizar filmes nanocompósitos com a incorporação de emulsão Pickering contendo OEO e estabilizada por CNF. Coberturas obtidas com a mesma solução filmogênica foram usadas em tomates, sendo a vida útil dos tomates revestidos e não revestidos analisada por 12 dias. Este trabalho foi realizado no período do doutorado sanduíche na Universidade do Minho/ Portugal, financiado pelo CNPq, por meio da bolsa 200248/2022-7 durante o período de 6 meses (Março/ Agosto de 2023). O artigo é intitulado “Pectin films incorporating Pickering emulsions and reinforced with cellulose nanofibers as a solution to increase tomato shelf life” e será submetido à revista Food Packaging and Shelf life.

O **Capítulo 6** traz a discussão geral referente a todos os resultados apresentados nesta tese, trazendo a ligação entre os capítulos 3, 4 e 5. Na sequência, o **Capítulo 7** traz a conclusão geral, **Capítulo 8** as referências gerais e o **Capítulo 9** apresenta a produção científica deste trabalho.

1.4 REFERÊNCIAS

- Cengiz-Çallioglu, F. (2011). *Silindirli elektro lif çekim yöntemi ile poliüretan nano lif üretimi. 2011. Tese de Doutorado. Üniversitesi Fen Bilimleri Enstitüsü, Doktora Tezi, Süleyman Demirel , Isparta.*
- Chevalier, Y., & Bolzinger, M. (2013). Emulsions stabilized with solid nanoparticles: Pickering emulsions. *Colloids and Surfaces A: Physicochemical and Engineering Aspects*, 439, 23–34.

- Ebrahimi, R., Fathi, M., & Ghoddusi, H. B. (2023). Nanoencapsulation of oregano essential oil using cellulose nanocrystals extracted from hazelnut shell to enhance shelf life of fruits : Case study : Pears. *International Journal of Biological Macromolecules*, 242(P1), 124704. <https://doi.org/10.1016/j.ijbiomac.2023.124704>
- Fujisawa, S.;Togawa, E.; Kuroda, K. (2017). Nanocellulose-stabilized Pickering emulsions and their applications. *Science and Technology of Advanced MaTeriaLS*, 18(1), 959–971.
- Khan, S., Hashim, S. B. H., Arslan, M., Zhang, K., Bilal, M., Zhiyang, C., Zhihua, L., Elrasheid, H., Zhai, X., Rezaul, M., Shishir, I., & Zou, X. (2024). Berry wax improves the physico-mechanical , thermal , water barrier properties and biodegradable potential of chitosan food packaging film. *International Journal of Biological Macromolecules*, 261(P2), 129821. <https://doi.org/10.1016/j.ijbiomac.2024.129821>
- Li, J., Alamdari, N. E., Aksoy, B., Parit, M., & Jiang, Z. (2023). Chemosphere Integrated enzyme hydrolysis assisted cellulose nanofibril (CNF) fabrication : A sustainable approach to paper mill sludge (PMS) management. *Chemosphere*, 334(April), 138966. <https://doi.org/10.1016/j.chemosphere.2023.138966>
- Liu, Z., Lin, D., Shen, R., & Yang, X. (2020). Characterizations of novel konjac glucomannan emulsion films incorporated with high internal phase Pickering emulsions. *Food Hydrocolloids*, 106088. <https://doi.org/10.1016/j.foodhyd.2020.106088>
- Nikfarjam, N.; Qazvini, N. T.; Deng, Y. (2015). Surfactant free Pickering emulsion polymerization of styrene in w/o/w system using cellulose nanofibrils. *European Polymer Journal*, 64, 179–188.
- Patel, A. R. (2020). Functional and Engineered Colloids from Edible Materials for Emerging Applications in Designing the Food of the Future. *Advanced Functional Materials*, 30(18), 1–34. <https://doi.org/10.1002/adfm.201806809>
- Pelissari, F. M., Andrade-Mahecha, M. M., Sobral, P. J. do A., & Menegalli, F. C. (2017). Nanocomposites based on banana starch reinforced with cellulose nanofibers isolated from banana peels. *Journal of Colloid and Interface Science*, 505, 154–167. <https://doi.org/10.1016/j.jcis.2017.05.106>
- Pérez-Córdoba, L. J., Norton, I. T., Batchelor, H. K., Gkatzionis, K., Spyropoulos, F., & Sobral, P. J. A. (2018). Physico-chemical, antimicrobial and antioxidant properties of gelatin-chitosan based films loaded with nanoemulsions encapsulating active compounds. *Food Hydrocolloids*, 79, 544–559. <https://doi.org/10.1016/j.foodhyd.2017.12.012>
- Riaz, S., Aslam, A. M., Butt, M. S., & Khan, M. K. I. (2024). Valorization of agricultural residues in the development of biodegradable active packaging films. *Industrial Crops & Products*, 215(April), 118587. <https://doi.org/10.1016/j.indcrop.2024.118587>
- Silva, A. C. P. da, Barbosa, J. R., Araújo, C. da S., Batista, J. T. S., Neves, E. M. P. X., Cardoso, D. N. P., Joele, M. R. S. P., & Lourenço, L. de F. H. (2024). A new edible coating of fish gelatin incorporated into açaí oil to increase the post-harvest shelf life of tomatoes. *Food Chemistry*, 438(May 2023). <https://doi.org/10.1016/j.foodchem.2023.138047>
- Tavernier, I. et al., Wijaya, W., Meeren, P. Van der, & Dewettinck, K. (2016). Food-grade particles for emulsion stabilization. *Trends in Food Science & Technology*, 50, 159–174.
- Travalini, A. P., Lamsal, B., Magalhães, W. L. E., & Demiate, I. M. (2019). Cassava starch films reinforced with lignocellulose nanofibers from cassava bagasse. *International Journal of Biological Macromolecules*, 139, 1151–1161. <https://doi.org/10.1016/j.ijbiomac.2019.08.115>
- Yang, W., Zhang, S., Hu, Y., Fu, Q., Cheng, X., Li, Y., Wu, P., Li, H., & Ai, S. (2024). Pectin-based film activated with carboxylated cellulose nanocrystals-stabilized oregano essential oil

- Pickering emulsion. *Food Hydrocolloids*, 151(January), 109781.
<https://doi.org/10.1016/j.foodhyd.2024.109781>
- Yang, Y. et al., Fang, Z., Chen, X., Zhang, W., & Xie, Y. (2017). An overview of Pickering emulsions: solid-particle materials, classification, morphology, and applications. *Frontiers in Pharmacology*, 8, 287.
- Zhang, X. et al., Ren, S., Han, T., Hua, M., & He, S. (2018). New organic–inorganic hybrid polymers as Pickering emulsion stabilizers. *Colloids and Surfaces A: Physicochemical and Engineering Aspects*, 542, 42–51.
- Zhang, Y., Xie, J., Ellis, W. O., Li, J., Appaw, W. O., & Simpson, B. k. (2024). Bioplastic films from cassava peels : Enzymatic transformation and film properties. *Industrial Crops & Products*, 213(August 2023), 118427. <https://doi.org/10.1016/j.indcrop.2024.118427>

CAPÍTULO II

MAIN PRODUCTION METHODS OF CELLULOSE NANOFIBERS: PERSPECTIVES ON EMERGING TECHNOLOGIES

Manuscript prepared to be submitted to Cellulose

Main production methods of cellulose nanofibers: perspectives on emerging technologies

Raquel Costa Chevalier¹, Cristiane Grella Miranda¹, Ana Carla Kawazoe Sato¹, Rosiane Lopes

Cunha^{1*}

¹Department of Food Engineering and Technology (DETA), School of Food Engineering (FEA), University of Campinas (UNICAMP), Rua Monteiro Lobato, 80; Campinas-SP; CEP, 13083- 862, Brazil.

* Corresponding author

Email address: rosiane@unicamp.br (R.L. Cunha).

Abstract - Nanofibers can be produced from several cellulose sources, including waste of different industries. Cellulose nanofibers (CNFs) show features of natural cellulose such as low density, biodegradability, and lightweight. However, several properties such as high surface area-to-volume ratio, excellent mechanical properties, good gas barrier properties, and low thermal expansion are attributed to cellulose only after nanomerization. Different approaches have been introduced to isolate CNFs from a wide range of sources due to the growing interest in cellulose nanomaterials. In this review, we summarize recent progress in production methods, which have been divided into chemical, mechanical, enzymatic and emerging technologies. In addition, the main characteristics of the CNFs obtained from each method are extensively reviewed. In general, studies show the high complexity of establishing a pattern in the CNFs produced, which are dependent on the production method, operating conditions and cellulose source.

Keywords: Nanocellulose; agro-industrial waste; hydrolysis; ultrasound; emerging technologies.

Introduction

The demand for natural polymers extracted from renewable sources has increased considerably due to the environmental impact caused by synthetic polymers. Natural polymers can be obtained from animal (e. g. chitin and chitosan) and plant (e. g. cellulose, lignin and starch) sources, or by microorganisms production (e.g. cellulose produced by *Gluconacetobacter xylinus* and alginate produced by *Azotobacter vinelandii*) (Thomas et al., 2013). Among the various biopolymers, cellulose is the most abundant natural polymer available on Earth, playing an important structural role in plants due to being fibrous, tough

and water-insoluble (Du et al., 2019)(Dufresne, 2018; George & Sabapathi, 2015). Cellulose can be found in pure form (as in cotton) or in combination with other materials such as lignin and hemicellulose (Dufresne, 2018). Cellulose fibers are composed of several microfibrils linked to each other and to hemicellulose by hydrogen bonds. A growing interest in forming cellulose nanomaterials has arisen, since nanomerization is a strategy to improve the solubility and increase the applicability of biopolymers (Yan et al., 2020). Indeed, nanocellulose shows excellent features such as high tensile strength and elasticity modulus, high specific surface area and low density (Du et al., 2019).

The family of cellulose nanomaterials includes cellulose nanofibers (CNFs), cellulose nanocrystals (CNC) and bacterial nanocellulose (BNC). BNC has a similar chemical structure as that found in plant-based cellulose; however, all bacterial cellulose is necessarily in nanoscale, since bacteria produce cellulose from a unit fibrils on a nanoscale – bottom-up approach (Amorim et al, 2020; Sharma & Bhardwaj, 2019). On the other hand, plant-based cellulose is not found naturally in a nanometric scale; however, CNFs and CNC can be isolated from plant cell walls through chemical, mechanical, enzymatic procedures – top-down approach (Oprea & Voicu, 2020). Since, this review is focused on methodologies for cellulose nanomaterial extraction from plant sources, the discussion related to the BNC is restricted in the current review, nevertheless it has been previously well elaborated in the literature (Amorim et al, 2020; Sharma & Bhardwaj, 2019).

Although, CNFs and CNC share similar chemical composition, physical characteristics such as size, morphology and crystallinity may vary according to nanocellulose material, as well the type and conditions of production methods (Pradhan et al., 2022). Cellulose nanofibers also known as nanofibrillated cellulose and cellulose nanofibrils can be obtained from cellulose microfibrils subjected to chemical, mechanical, and enzymatic treatments. CNFs have outstanding characteristics such as lightweight, high surface area and aspect ratio, network structure, high rigidity, good water absorption capacity, high reactivity and barrier properties (Choudhury et al., 2020). Various applications for cellulose nanofibers have been reported such as milk thickener (Gao et al., 2018), coating of strawberry (Kwak et al., 2021), reinforcement for films (Pelissari et al., 2017), Pickering emulsifier (Costa et al., 2018a), 3D bioink for auricular cartilage (Martínez Ávila et al., 2016), aerogel with fast shape recovery for noncompressible hemorrhage (Fan et al., 2020), membrane for air purification (Zhao et al.,

2019), hydrogel for dental treatments (Favatela et al., 2021) and bionic biosensor for detecting silver ions (Lei Wang et al., 2021).

In recent years, CNFs has attracted great attention, which has led to an increasing number of studies on methods for obtaining them. Chemical (e.g. alkali, acid and oxidation), mechanical (e.g. electrospinning, solution blowing, high-pressure homogenization, microfluidization, high shear grinding, and high-intensity ultrasound), and enzymatic (e.g. ligninases, xylanases, cellulase, and hemicellulose) treatments have been successfully applied to isolate CNFs from cellulose microfibrils. In addition, many emerging technologies (e.g. ionic liquids, deep eutectic solvent, microwave, electron beam irradiation, cold plasma, pulsed electric field, and cryocrushing) have arisen as sustainable alternatives to conventional methodologies. However, there is a lack of information about the characteristics of the CNFs obtained in each methodology and the advantages/disadvantages associated with each process. Thus, to address this knowledge gap, this review aims to discuss cellulose structure, its derivatives, and the main plant sources used to produce cellulose nanofibers. The most common methods (chemical, mechanical, and enzymatic) for obtaining CNFs are presented, considering their setup and working principle. The main characteristics of CNFs obtained from each methodology are discussed. Finally, some emerging technologies are discussed according to their operational characteristics and examples of CNFs produced by these techniques are presented.

2. Cellulose

2.1 Cellulose and its derivatives

Cellulose is one of the most widespread substances in nature, known to be insoluble in water and indigestible by humans. It was discovered in 1838 by the French chemist Anselme Payen and since then it has been widely used as a material in the chemical, food, cosmetic, medical and energy fields (Oprea & Voicu, 2020). Even though cellulose could be obtained from plants, animal and microorganisms, plant sources are the most extensively studied, especially due to abundance and inexpensive nature (Zyl and Coburn, 2019). The most studied plant source has been wood, as it is an abundant cellulose source. However, competition with the furniture, pulp and paper industry, as well as building products, which also widely use wood as a raw material, has reduced the interest of this source in obtaining nanocellulose (Trache et al., 2017). Hence, several other plant sources have been studied, mainly agricultural

crops and their by-products. Cotton (Farahbakhsh et al., 2015), corn (Bian et al., 2020), sugar palm (Rushdan Ahmad Ilyas et al., 2018), banana peels (Pelissari et al., 2017), pineapple leaf (Balakrishnan et al., 2017), mulberry pulp (L. F. Wang et al., 2017) and others (Table 1) have been studied as a source of cellulose. It is worth mentioning that the source and isolation method of cellulose derivatives contribute to their specific properties, such as degree of polymerization, morphology, surface charge, geometric dimensions, crystallinity, surface area, porosity, mechanical properties, thermal stability and others (Du et al., 2019; Mu et al., 2019; Trache et al., 2017).

Chemical structure of cellulose is based on repeating D-glucose units joined by β -1,4 glycosidic bonds (Ganguly et al., 2020; He et al., 2021). Although cellulose molecules are synthesized individually, interactions between cellulose chains build higher-order structures such as layers, cell walls and fibers (Wertz et al., 2010). As a consequence of the intense interactions, cellulose molecules organize themselves in a hierarchical structure (Amorim et al., 2020). Intramolecular and intermolecular interactions by hydrogen bonds and van der Waals forces between cellulose chains give rise to structures called cellulose microfibrils (CMF) (Oprea & Voicu, 2020; Wertz et al., 2010). CMF are responsible for forming the cellulose microstructure (Figure 1), which is composed of an outer primary P-wall and an inner secondary S-wall. P-wall contains a loose network of microfibrils while S-wall is composed of three layers (S1, S2 e S3). These three layers differ from each other according to their wall thickness. S1 and S3 layers are nanosized, while S2 is micro-sized in thickness due to the presence of helically wound CMF (Kargarzadeh et al., 2017). Microfibrils are arranged in multiple layers formed by crosslinks between cellulose, pectin and hemicellulose chains. Pectin and hemicellulose molecules fill the gaps between cellulose chains that maintain the strength of the microfibril network and influence crystallinity, creating amorphous regions (Oprea & Voicu, 2020; Wertz et al., 2010).

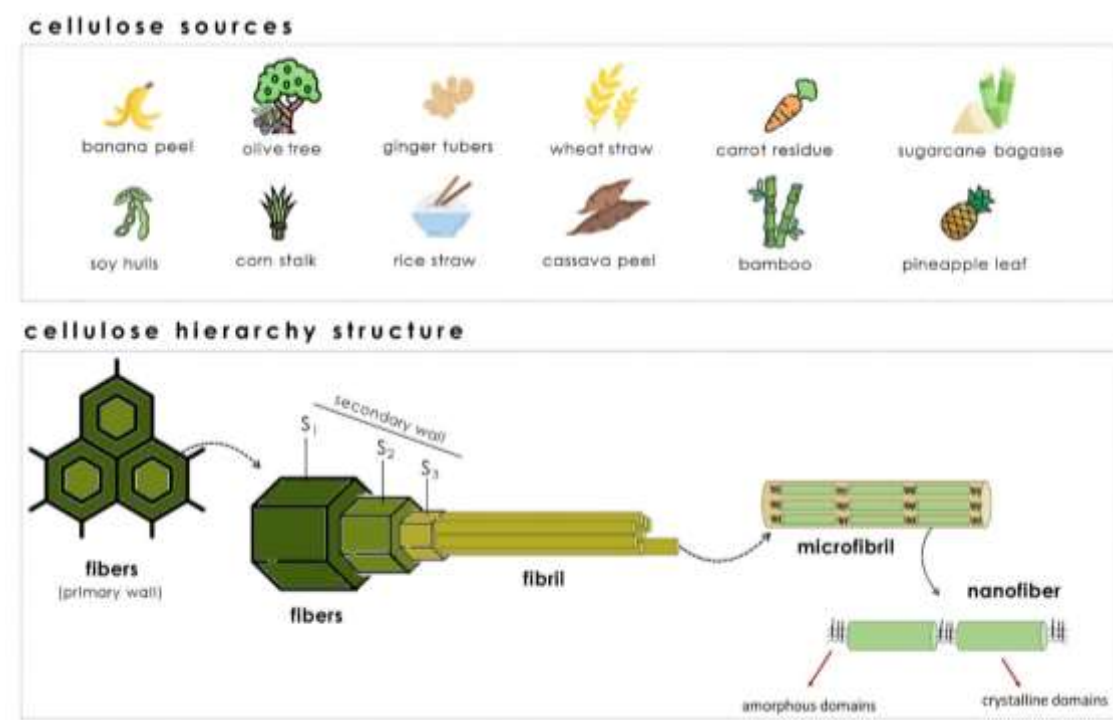


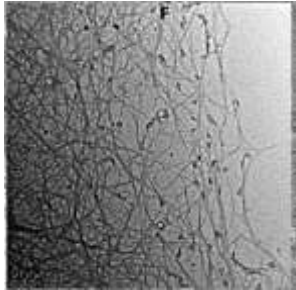
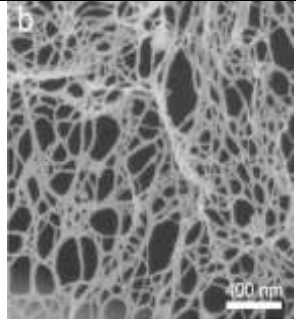
Figure 1. Some cellulose sources from agro-industrial waste and cell wall model of cellulose fibers.

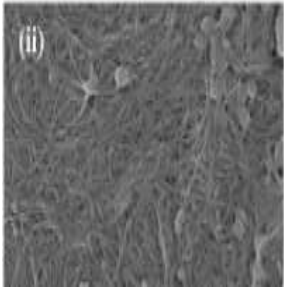
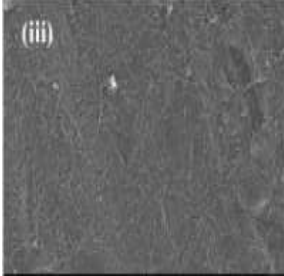
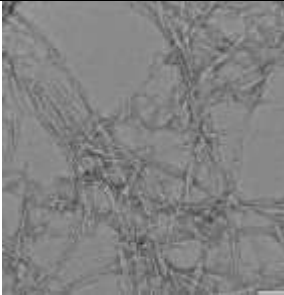
As aforementioned, cellulose has several advantages, such as biodegradability, biocompatibility, renewability, non-toxicity and being environmentally friendly. However, the disadvantage of low solubility in water and other common solvents, due to intra- and inter-chain interactions, limits the use of cellulose (He et al., 2021; Yan et al., 2020). Fiber size reduction by mechanical and chemical processes has been applied as an alternative to improve cellulose solubility, mechanical stiffness and specific surface area (Anusiya & Jaiganesh, 2022; Dufresne, 2018; Thomas et al., 2013). On the other hand, some relevant features such as low density, high specific strength and Young modulus, renewability, biodegradability and non-toxicity are maintained after size reduction.



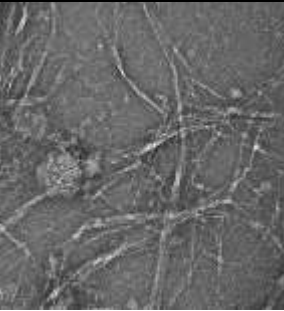
Nanomerization of cellulose from plant sources can be obtained depending on the preparation techniques, generating varying size and morphology (Du et al., 2019; Mu et al., 2019). Microcrystalline cellulose (MCC), cellulose nanofibrils (CNFs), cellulose nanocrystal (CNC), amorphous nanocellulose (ANC) and cellulose nanoyarn (CNY) can be obtained after mechanical and chemical processes (Chizitere et al., 2023; Du et al., 2019; Mu et al., 2019). MCC is a porous, aggregate, white and odorless powder, in which both diameter and length are on microscale (He et al., 2021; Nsor-Atindana et al., 2017). CNFs are composed of aggregates of elementary nanofibrils, which alternate crystalline and amorphous domains.

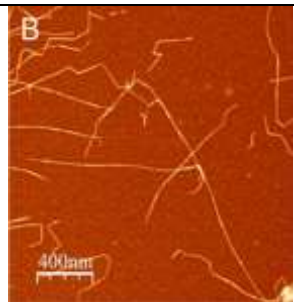
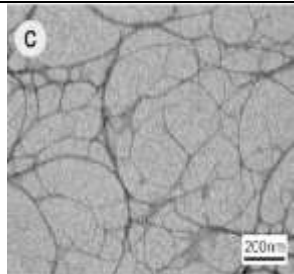
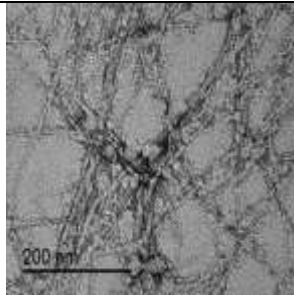
CNC (also known as nanocrystalline cellulose, nanowhiskers, nanorods and rod-like cellulose crystals) is produced from acid hydrolysis of crystalline domain of nanofibrils. Finally, CNY is a cellulose particle obtained by electrospinning a solution containing cellulose (Hubbe et al., 2008; Kargarzadeh et al., 2017; Khattab et al., 2017).

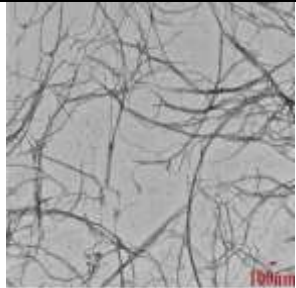
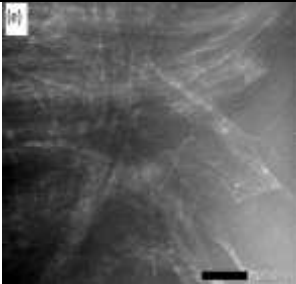
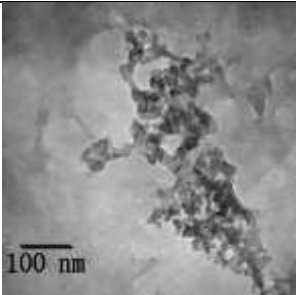
Table 1. Cellulose derivatives: sources, production methods, characteristics, and applications.

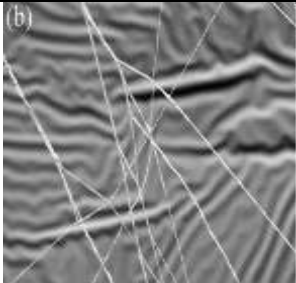
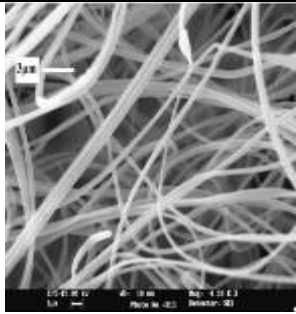
Cellulose Source	Production methods		CNFs features			References
	Pre-treatment	Main treatment	Mean diameter	Crystallinity	Appearance	
Pineapple pomaces	Alkali	Acid Hydrolysis	4.18 – 33.22 nm	68%		(Neenu et al., 2022)
Soybean residue	Alkali	Acid hydrolysis + High Pressure Homogenization	50 nm	75.9%		(Wang et al., 2021)

Wheat straw	Alkali	Acid Hydrolysis	17 nm	70%		(Ceaser & Chimphango, 2021)
Wheat straw	Alkali	Enzymatic	17 nm	48%		(Ceaser & Chimphango, 2021)
Cassava peel	Alkali	Acid Hydrolysis	8.62 nm	53.42%		(Czaikoski et al., 2020)

Cassava peel	Alkali	Acid Hydrolysis + High intensity ultrasound	16 nm	53.47%		(Czaikoski et al., 2020)
Cassava peel	Alkali	TEMPO-Oxidation	5 nm	46.67%		(Czaikoski et al., 2020)
Cassava peel	Alkali	TEMPO-Oxidation + High intensity ultrasound	8 nm	46.82%		(Czaikoski et al., 2020)

Olive tree	-	TEMPO-Oxidation + Microfluidization	1 nm	82%		(Fillat et al., 2018)
Wood	Alkali	High intensity ultrasound	5 – 20 nm	68.69%		(Chen et al., 2011)
Bamboo	Microwave + bleaching	High intensity ultrasound	2 – 30 nm	67.4%		(Xie et al., 2016)

Softwood pulp	Bleaching	Enzymatic treatment + High shear grinding	0.10 – 2.20 nm	68.44%		(Liu et al., 2019)
<i>Agave gigantea</i> leaves	Alkali + bleaching	High shear grinding	15 – 20 nm	65.21%		(Syafri et al., 2022)
Sugarcane bagasse	Alkali	High Pressure Homogenization	10 – 20 nm	36%		(Li et al., 2012)

Cellulose pulp	-	Solution Blowing	800 nm	-		(Zhuang et al., 2012)
Cellulose	-	Electrospinning	1 μm	58.8%		(Kim et al, 2006)

3. Methods of producing cellulose nanofibers (CNFs)

3.1 Chemical Methods

3.1.1 Pretreatments

The use of *alkali* as a pretreatment aims to solubilize lignin, hemicellulose and pectin (Abdul Khalil et al., 2014). This process is normally carried out in association with acid hydrolysis. The cellulosic material is added to a solution of sodium hydroxide (NaOH), ammonium hydroxide (NH₄OH) or anhydrous ammonia (NH₃) to increase the surface area of cellulosic fibers and make them more susceptible to hydrolysis. Investigating the best time and temperature, as well as the concentration of bases, is relevant since these parameters will influence the morphology and dimensions of the fibers obtained in the subsequent treatments, such as in the hydrolysis reaction.

Another relevant pretreatment process is the *bleaching* that aims to remove residual lignin and it is known as delignification. Bleaching is usually carried out with the help of chemicals such as chlorine dioxide (ClO₂), hydrogen peroxide (H₂O₂), sodium hypochlorite (NaClO), ozone (O₃) or peracetic acid (CH₃CO₃H). A disadvantage is that bleaching with chlorine and its derivatives for purification of lignocellulosic materials produces highly toxic and dangerous pollutants (Tripathi et al., 2019). Thus, to eliminate or reduce this effect, studies have been carried out using oxygen, ozone or enzymes prior to bleaching to circumvent this limitation (Dhali et al., 2021; Tripathi et al., 2019).

3.1.2 Acid hydrolysis

Acid hydrolysis is a process capable of removing the amorphous regions of the raw cellulosic material and, consequently, promoting the isolation of micro and nanofibers with a high degree of crystallinity. Typically, mineral acids such as hydrochloric acid (HCl), sulfuric acid (H₂SO₄) or phosphoric acid (H₃PO₄) are used for the solubilization of hemicellulose. Nanofibers features are influenced by acid concentration, time and temperature of the hydrolysis reaction (Abdul Khalil et al., 2014; Frone et al., 2011). Acid hydrolysis treatment can be combined with other processes such as ultrasound, bleaching, alkaline and/or enzymatic hydrolysis. For instance, the combination of acid hydrolysis, bleaching and ultrasound allowed obtaining long and tangled fibers from sugarcane bagasse, with a nanoscale diameter (20-30 nm) and several micrometers in length. On the other hand, in wheat straw or cassava husk,

the use of alkaline pre-treatment and subsequent acid hydrolysis produced more crystalline and monodisperse fibers than the combination of alkaline pretreatment-enzymatic hydrolysis. In fact, crystallinity is always higher when using acid hydrolysis combined or not with other processes (Asem et al., 2021; Ceaser & Chimphango, 2021; Czaikoski et al., 2020) compared to enzymatic hydrolysis. Despite being a very popular method, this treatment has some disadvantages such as high use of water and generation of acidic effluents, long processing time, high operating and maintenance costs, risk of equipment corrosion, formation of inhibitors and not being environmentally friendly (Teo & Wahab, 2020).

3.1.3 Oxidation

TEMPO-mediated oxidation is a method in which 2,2,6,6-tetramethylpiperidine-1-oxyl (TEMPO) and its analogues are applied, aiming at the oxidation of hydroxyl groups of carbohydrates to generate carboxyl and/or aldehyde groups (Isogai et al., 2011). Several advantages can be attributed to TEMPO reagent, such as i) ability to oxidize primary and secondary groups under mild conditions, ii) reduced reaction time, iii) use of mild and catalytic conditions and iv) tolerance to sensitive functional groups (M. De Souza, 2006). Several studies have applied TEMPO-oxidation to oxidize cellulose from different sources. Selectively, the C6 primary alcohols of cellulose are oxidized to aldehydes which are further oxidized to carboxylates. This conversion influences characteristics of nanofibers such as surface charge and mass loss at low temperature, improving thermal stability (Bian et al., 2020; Hua et al., 2014; Tang et al., 2024). For example, nanofibers obtained from corn stalk and husk by TEMPO-oxidation achieved maximum mass loss at a lower temperature than other processes for obtaining nanofibers (Bian et al., 2020; Madivoli et al., 2022). Furthermore, the negative charge of nanofibers can increase after the TEMPO-oxidation process, as observed for green algae (Hua et al., 2014). Nanofibers crystallinity seems to be dependent on the cellulose source, since different degrees of crystallinity were observed for green algae (92%), corn stalk (76.1%), corn husk (63%) *Oryza sativa* residue (42%) and cassava peel (46,7%) (Bian et al., 2020; Czaikoski et al., 2020; Du et al., 2019; Hua et al., 2014; Madivoli et al., 2022). Finally, the diameters and lengths of CNFs produced by TEMPO-oxidation ranged between 16 - 50 nm, and 10 - 100 nm, respectively (Bian et al., 2020; Czaikoski et al., 2020; Soni et al., 2015). One of the advantages of applying this process is the low energy consumption, simple process and

use of mild conditions. Among the disadvantages, there is the use of toxic reagents (Zhang et al., 2020) that prevents human consumption.

3.2 Enzymatic Methods

Enzymes can be applied for pre-treatment or hydrolysis, depending on the raw material to be used for the production of cellulose nanofibers. Enzymes such as ligninases, xylanases and others are able to degrade lignin and hemicellulose while maintaining the cellulose structure. On the other hand, cellulolytic enzymes, that is, cellulases, help to hydrolyze cellulosic fibers. Cellulases can be divided into three groups: (1) endoglucanases or β -1,4-endoglucanases (also called type A and B cellulases), which randomly hydrolyze β -1,4 - accessible glucosidic bonds in non-crystalline cellulose domains, generating damaged fibers with new chain ends; (2) exoglucanases (cellobiohydrolases), also called type C and D cellulases, which act at the ends of the chain to release soluble cellobiose as a major product; and (3) β -glucosidases, which hydrolyze cellobiose to glucose (Kargarzadeh et al., 2017; Squinca et al., 2022). Association of enzymes, such as xylanases and endoglucanases can improve the accessibility of enzymes to the cellulosic component (J. Hu et al., 2018). In this sense, the use of endoglucanase and a mixture of hemicellulases and pectinases was efficient in obtaining cellulosic nanoparticles with preserved cellulose (Campos et al., 2013). Furthermore, with suitable process conditions, sugar beet residue was converted into cellulose nanofibers by enzymatic treatment, showing properties similar to nanofibers obtained by chemical treatment, with diameters around 20-40 nm (Perzon et al., 2020). Cellulose nanofibers obtained from banana peels were also produced by enzymatic treatment, and presented diameters between 3.7 and 8.8 nm (H Tibolla et al., 2019). It is worth mentioning that it is an eco-friendly method, although expensive. However, enzyme concentration to obtain a good performance is very low, in the range of $\mu\text{l/g}$ of pulp (Perzon et al., 2020), which means that under optimized conditions, the cost can be adequate considering the positive aspects of this green process.

3.3 Physical Methods

3.3.1 Electrospinning

The electrospinning method is one of the most promising and effective ways to produce nanofibers. Electrospinning is a straightforward method of producing fibers with

controlled surface morphology and diameters ranging from micro- to nanometers (Long et al., 2019; Refate et al., 2023). Generally, electrospinning is conducted at room temperature and atmospheric pressure. Typically, the basic electrospinning setup (Figure 2) is composed of a syringe, fiber collector, high-voltage power supply and flow control pump. A plastic syringe attached to a metal needle is used as a spinneret (specifically a thin metal needle) and acts as an electrode. The process consists of transporting the polymer (cellulose) solution through the spinneret that has one end connected to the syringe pump and the other end connected to the positive electrode of the power supply. The fiber collector is connected to the negative electrode. The high-voltage power supply provides an electric field between the two electrodes. In the basic electrospinning setup, the collector is usually placed 10-25 cm from the needle tip. There is a variety of equipment configurations and the most traditional one is described here.

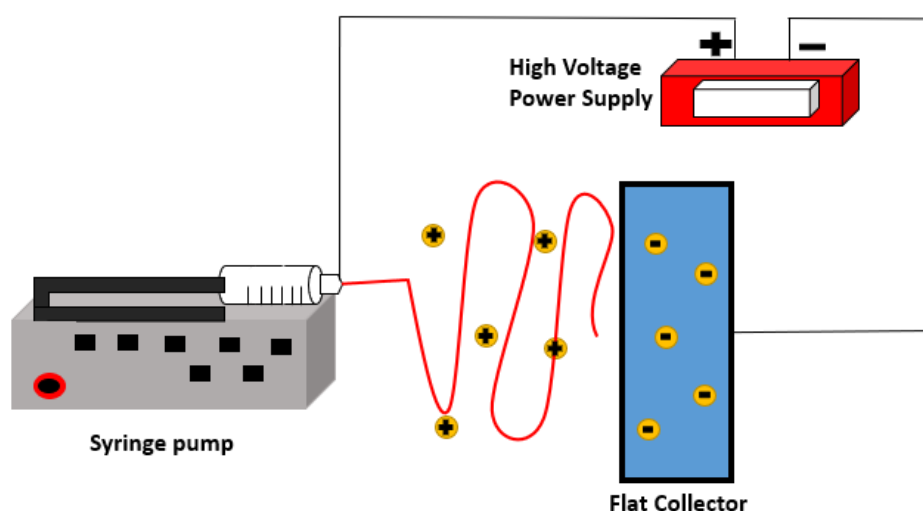


Figure 2. Schematic of a basic electrospinning setup.

Two methodologies have been used to form fibers by electrospinning. The first methodology called solvent electrospinning requires a solvent capable of dissolving the polymer to form a homogenous solution. This solution containing a charged polymer is subjected to a high voltage and is ejected to be transformed into fibers by solvent evaporation (Jiang et al., 2015; Muerza-cascante et al., 2015). The second methodology, named melt electrospinning, is a solvent-free method. The fiber is formed by cooling the ejected ultrafine jet containing molten (heated) charged polymer (Detta et al., 2010; Xiuyan Li et al., 2012). The

use of solvent is the most used configuration of this technique, which may or may not be combined with other treatments to produce nanofibers.

The characteristics of the nanofibers will depend on the parameters used during electrospinning, such as: temperature, flow, applied voltage, distance between the nozzle and the collector, as well as the use or not of co-solvent. A decrease in nanofiber diameters was observed using co-solvent during the process, due to the higher polarity and lower viscosity of the co-solvent (Ahn et al., 2012; Robles-García et al., 2018). In a study using commercial cellulose, a decrease in the degree of crystallinity (around 40%) was observed at low nozzle temperature (25°C). Furthermore, a similar behavior is observed if the sample is subjected to a shorter residence or crystallization time during electrospinning (i.e., shorter nozzle-collector distance and/or higher flow rate) (Kim et al., 2006). The main advantage is that it is a simple and a versatile method that can be used with a wide variety of materials. Variations in the basic electrospinning configuration can be used to produce nanofibers with a number of morphological and functional properties for specific applications. One of the disadvantages is the cost of equipment and maintenance (Angel et al., 2022).

3.3.2 Solution blowing

Solution blowing is an innovative process for spinning micro-/nano-fibers from polymer solutions using high-velocity gas flow as the driving force for fiber formation (Zhuang et al., 2012). Figure 3 shows a schematic view of solution blowing. The setup consists of a source of compressed hot gas equipped with a pressure regulator, an injection pump containing the polymer solution, a nozzle and a collector. Nanofibers are formed when the polymer solution is stretched through a straight part (nozzle) under high pressure with a significant reduction in diameter. The high air temperature decreases the solution viscosity facilitating jet formation, while air-blowing accelerates evaporation during fibers collection (X. Wang et al., 2005). This technique was developed because some high viscosity polymer solutions cannot be successfully electrospun. Thus, several biopolymers have been used to produce nanofibers by solution blowing such as soy protein, chitosan, lignin and zein, in addition to cellulose (Zhuang et al., 2012). As solution blowing is a relatively recent technology, some operational parameters such as nozzle dimensions, air pressure, collecting distance and polymer solution rheology still need to be optimized (A. Kumar & Sinha-Ray, 2018) for different materials.

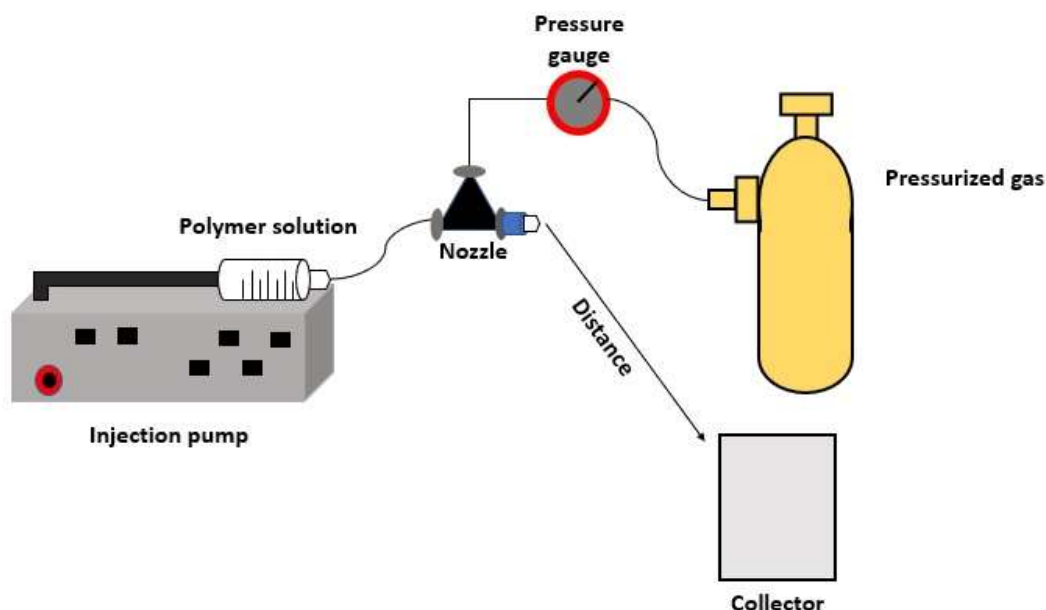


Figure 3: Schematic view of solution blowing.

The solution blowing technique has two main advantages: i) scalability and ii) the ability to mix biopolymers, since in this technique the polymer is extruded and not melted, avoiding denaturalization when using high temperature (A. Kumar & Sinha-Ray, 2018). Cellulose nanofibers were produced from wood pulp with different degrees of polymerization (DP) showing that the higher the degree of polymerization, the finer the nanofibers were formed. Furthermore, as the air velocity increased, an increase in the crystal orientation and fiber crystallinity index were observed (Zhang et al., 2020).

3.3.3 High-pressure homogenization

High-pressure homogenization has been reported as an effective mechanical treatment to create nanocellulose (R. A. Ilyas et al., 2019; Wu et al., 2021). The principle of operation is based on the application of pressures between 50 and 200 MPa by passing the polymer solution through a very narrow channel or orifice (Rahman et al., 2021) (Figure 4). The increase in dynamic pressure and reduction in static pressure (below the vapor pressure of the aqueous phase) of the polymer solution stream results in the formation of gas bubbles. After the suspension leaves the homogenization gap, the phenomenon of implosion occurs as the solution is again subjected to normal atmospheric pressure (around 100 kPa). The

formation and implosion of gas bubbles induce the formation of shock waves and cavitation, which cause the rupture of the fibrillar structure of the cellulose (Müller et al., 2001). The width of the homogenization gap varies between 5 and 20 μm depending on the viscosity of the suspension and applied pressure (Kargarzadeh et al., 2017). Factors responsible for fiber size reduction are large pressure drop, high shear forces, turbulent flow and interparticle collisions. The number of cycles and the applied pressure will define the fiber length (Kalia et al., 2014). An increase in pressure and a longer time of repetitions (cycles) reduces the fiber size, but to optimize the energy expenditure it is necessary to investigate the pressure and the number of cycles to be adopted for each material.

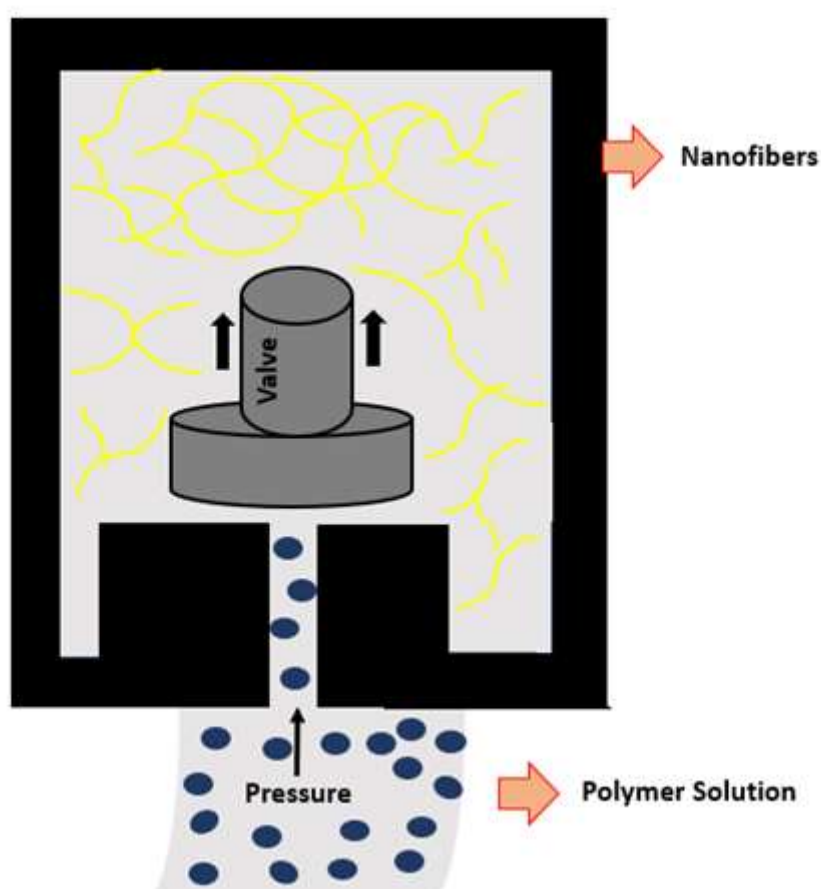


Figure 4. Schematic of a high-pressure homogenizer.

Despite being a very effective method, the high pressure homogenizer presents some problems such as: insufficient disintegration of the fibers and equipment clogging, high energy consumption and damage to the crystalline structure of CNFs (Rebouillat & Pla, 2013). The association of this mechanical process with chemical pre-treatments can improve energy

consumption and assist in the disintegration of fibers to non-pure materials, such as waste. Application of this process in combination with bleaching for 30 minutes with sodium hypochlorite (NaClO) provided an improvement in the fiber formation process (Tarrés et al., 2020). The association of alkaline and acid hydrolysis, followed by high pressure homogenization, produced cellulose nanofibers from soybean residue, with high crystallinity (75.9%) and diameters around 50nm, negative surface charge (-22.5 mV) and high thermal stability (Li Wang et al., 2021). Advantages of using high pressure homogenizer are i) free from generation of effluents, ii) no need to use chemical solvents and iii) fast process, with a simple configuration and adaptable to an industrial scale (Teo & Wahab, 2020).

3.3.4 Microfluidization

A microfluidizer is composed of microchannels, a chamber, a pump and check valves, and may also have a heat exchanger (Figure 5). Unlike the homogenizer that operates at constant pressure, the microfluidizer operates at a constant shear rate (Kargarzadeh et al., 2017). The fluid is pumped through the intensifier pump and passes through a Z- or Y-shaped interaction and impact chamber containing microchannels through which the fluid passes at high speeds. The Y-type chamber is mainly used for liquid-liquid dispersions, while the Z-type chamber is normally applied to disperse solid materials in suspensions and destroy cell structures, such as cellulose suspensions aiming to obtain nanofibers (Mert, 2020). The degree of fibrillation is improved by repeating the cycles and associating different chamber sizes. Typically, as the number of cycles increases, the fiber size decreases. In general, pressure applied and type of raw material also influence the properties of nanofibers. Number of cycles and pressure to be used are defined from preliminary tests and observation of the desired degree of fibrillation (Abdul Khalil et al., 2014; Kalia et al., 2014). A specific characteristic of this process is that the smaller the size of the chamber, the greater the degree of defibrillation, that is, the capacity of opening and exposure of the nanofibers (Missoum et al., 2013).

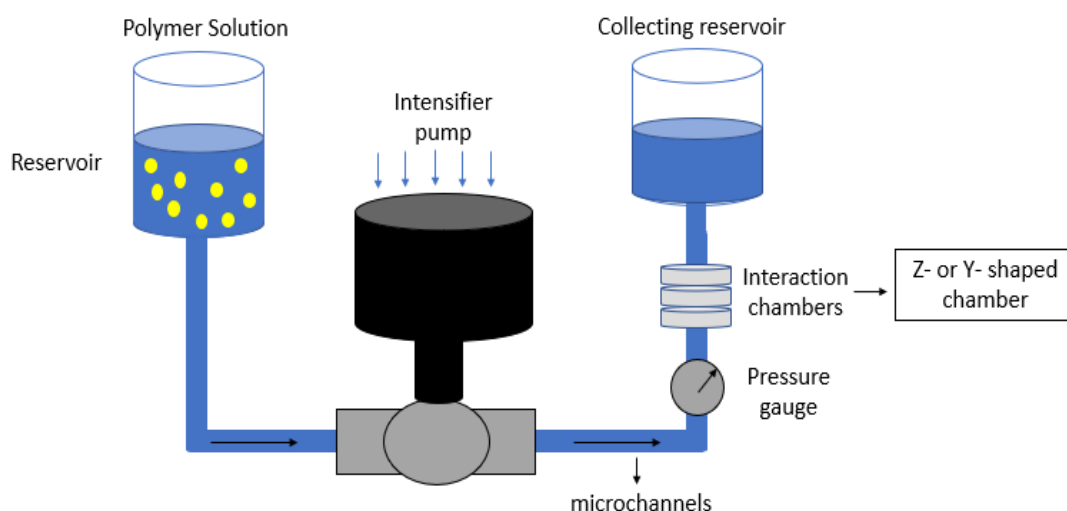


Figure 5. Schematic of microfluidizer.

Microfluidization is usually preceded by chemical processes to remove hemicellulose and other undesirable components (Kargarzadeh et al., 2018), since the mechanical process aims only to reduce the cellulose fiber size. Furthermore, the number of chambers in the microfluidizer can define the characteristics of nanofibers. Nanofibrils were obtained from bleached commercial cellulose, hydrolyzed with HCl and subjected to microfluidization in two Z-shaped chambers (diameter <10 nm) (Naderi et al., 2015). A microfluidizer equipped with two chambers was also used to produce cellulose nanofibers from birch pulp (BP) with diameters ranging from 5.9 to 6.9 nm (Sirviö & Lakovaara, 2021). Wheat cellulose nanofibers were obtained using a microfluidizer with three chambers that had a small diameter (4-6 nm) (Sehaqui et al., 2017). From this, we can observe that the association of chambers favored the reduction of nanofibers.

3.3.5 High shear grinding

High shear grinding is another mechanical method used to produce CNFs. In this technique, shear forces are applied to the polymer solution that passes between two grinding stones, one stone being fixed while the other is rotating. The distance between these stones can be adjusted, allowing to avoid clogging problems. The fibrillation mechanism occurs from the disruption of hydrogen bonds and cell wall structure by shear forces, consequently, leading to individualization of the pulp to nanoscale fibers (Missoum et al., 2013; Ngasotter et

al., 2022). As previously described for other mechanical methods, the combination with a pretreatment can be favorable in the production of CNFs. For instance, cellulose nanofibrils extracted from sugarcane bagasse were produced from a pretreatment with endoglucanase (enzyme) followed by a mechanical grinding process (Nie et al., 2018). The combination of methods provides a wide range of CNFs size and other desirable structural characteristics. Cellulose nanofibers from eucalyptus sawdust with a diameter of around 30 nm were prepared by combining alkaline pretreatment, bleaching and high shear grinding. In fact, pretreatment is essential for the production of CNFs to be economically viable, due to the reduction in milling energy expenditure (Liu et al., 2019). The use of *Agave gigantea* for the production of cellulose nanofibers was carried out through the association of chemical treatment and grinding, obtaining a diameter of 15-20 nm and a crystallinity of 65.21% (Syafri et al., 2022). Smaller diameters could be obtained with enzymatic treatments prior to grinding. Commercial cellulose subjected to enzymatic hydrolysis and grinding resulted in nanofibers with diameters ranging from 8 to 30 nm and crystallinity index of up 77%, depending on the intensity of the enzymatic treatment (X. Liu et al., 2019). However, despite being an efficient method, high shear grinding has disadvantages such as high cost, high energy consumption, overheating of raw materials and low uniformity of nanocellulose (Teo & Wahab, 2020). In fact, pretreatment is essential for the production of CNFs to be economically viable, due to the reduction in grinding energy consumption (X. Liu et al., 2019).

3.3.6 High - Intensity Ultrasound

The ultrasound method is a mechanical method capable of extracting cellulose nanofibers through the hydrodynamic forces of ultrasound. Cavitation is generated, causing the formation, explosion and implosion of microscopic water bubbles. As a consequence, intermolecular hydrogen bonds are broken within the fiber structure (Kargarzadeh et al., 2017; Phanthong et al., 2018), resulting in high heat generation that requires the use of auxiliary equipment for cooling temperature (5 at 10°C) and heat transfer to control. The three main independent parameters in the ultrasound process are power, time and cellulose concentration in the polymer solution (Pradhan et al., 2022; Salimi et al., 2019). As reported for other mechanical treatments, combined treatments must be performed to obtain nanofibers efficiently.

For instance, bamboo cellulose nanofibers were obtained by combining microwave liquefaction, chemical treatment (bleaching and alkali treatment) and ultrasound. The combination of microwave liquefaction and chemical treatment was an efficient approach to remove non-cellulosic materials from bamboo, while the ultrasound process resulted in reduced crystallinity of the cellulose nanofibers (Xie et al., 2016). Another study used sugarcane bagasse treated by the alkaline and acid hydrolysis, in addition to being assisted by ultrasound, obtaining a network of long tangled nanofibers with a nanoscale diameter (20-30 nm) and a crystallinity of 42% (Asem et al., 2021). It was also possible to isolate cellulose nanofibers from banana peels with the aid of high-intensity ultrasound combined with chemical treatment. A reduction in diameter was observed with gradual increase in ultrasound power, ranging from 32 nm (400 W) to 20 nm (1000 W) (Xie et al., 2016). The combination of chemical pre-treatments with ultrasound also produced wood cellulose nanofibers with varying dimensions, depending on the ultrasound power. There was a decrease in diameter with increasing power, although it had no effect on the crystallinity of the nanofibers (69%) (Chen et al., 2011). With this, we can observe, in general, a decrease in size with increasing power, although there should be a plateau, where the values reach a limit and no further changes are observed. Among the advantages of using this method to obtain cellulose nanofibers is the fact that this process is ecologically friendly and efficient. However, one of the disadvantages is the high energy consumption as observed in other mechanical treatments.

4. Emerging technologies

In recent times, considering aspects of sustainability and environmental preservation, new technologies have been developed with the aim of being less aggressive, using less solvents and reducing costs. Thus, in this topic we will present some of the emerging methodologies most commonly found in the literature, such as ionic liquids, deep eutectic solvent, microwaves, electron beam irradiation, cold plasma, pulsed electric field and cryocrushing (Figure 6).

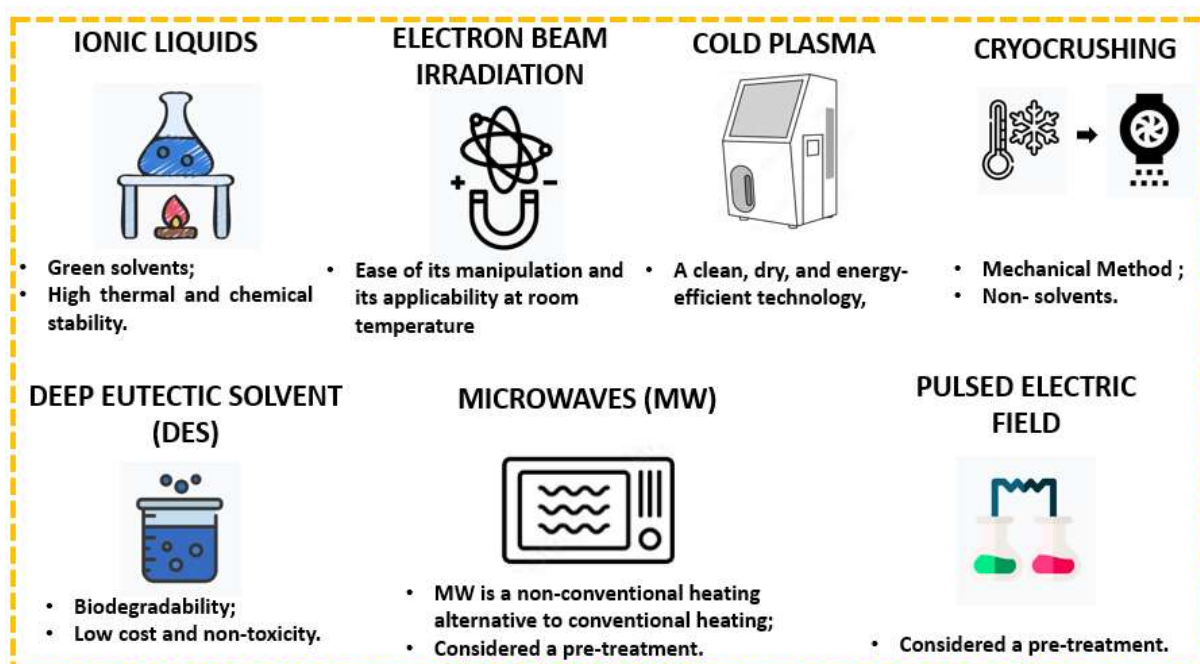


Figure 6. Emerging methodologies most commonly found in the literature.

Ionic liquids (IL) are salts composed of cations and anions with a relatively low melting point, which form stable liquids at temperature below 100 °C (Haron et al., 2021). ILs show low vapor pressure, high thermal and chemical stability, non-flammability and recyclability, the two later characterizing them as green solvents (Menezes et al., 2021). Recently, CNFs have been obtained from orange bagasse cellulose, rubber wood, and bagasse residue by ILs treatment (Menezes et al., 2021; Ninomiya et al., 2018; Onkarappa et al., 2020). The CNFs obtained from orange bagasse cellulose were around 100 nm in diameter (Menezes et al., 2021), while rubber wood nanofibers showed an average size between 200 – 300 nm (Onkarappa et al., 2020). Several studies have applied ILs as a fibrillation method for CNFs obtained from mechanical processes, since ILs can permeate through the lignocellulose structure, breaking inter- and intramolecular bonds during mechanical processes (Haron et al., 2021). In this sense, ILs have been used in combination with ball milling, high pressure homogenizer (HPH) and electrospinning to produce CNFs from cellulose powder, sugarcane bagasse and wood pulp. These studies reported that CNFs with 10 – 25 nm in diameter can be obtained in processes combining ILs and ball milling or HPH; however, CNFs obtained by ILs and electrospinning were larger in diameter (100 -1000 nm) (J. Li et al., 2012; Phanthong et al., 2017; Vinogradova & Chen, 2016). Crystallinity is greatly affected by ILs treatment and ILs-

assisted mechanical processes. For instance, Li et al., (2012) reported that the crystallinity of nanofibers obtained from sugarcane bagasse decreased from 60% to 52%, after ILs treatment, and to 36% after high pressure homogenization. Similarly, Phanthong et al. (2017) reported that crystallinity of cellulose nanofibers decreased from 73.7% to 71.4% after ILs, and to 65.8% after ball milling. Moreover, Vinogradova and Chen (2016) reported that the decrease in crystallinity is also dependent on the type of ILs. The crystallinity of wood pulp decreased from 81.76% to 63.07% using 1-butyl- 3-methylimidazolium chloride ([BMIM]Cl) and to 58.60% using 1-ethyl-3-methylimidazolium acetate ([EMIM]Ac).

Deep eutectic solvents (DES) are defined as binary and ternary mixture of compounds, which can self-associate via hydrogen bonds (El Achkar et al., 2021). Usually, DESs are recognized as a class of ILs as both share similar characteristics such as high thermal stability, low volatility, low vapor pressure, and tunable polarity. However, due to characteristics such as biodegradability, low cost and non-toxicity, much attention has been paid to the DESs methodology (Hansen et al., 2021). Similar to ILs, DESs have been applied in combination with mechanical processes to produce CNFs in order to increase mechanical process efficiency. CNFs with average size between 2 – 65 nm were produced by DESs associated with ultrasound, high pressure homogenization, microfluidization, microwave, and ball milling with a number of raw materials such as kraft pulp, okara, cane bagasse, softwood pulp, ramie and silk fibers (Y. Hu et al., 2020; Panpan Li et al., 2018; Peiyi Li et al., 2020; C. Liu et al., 2020; Ma et al., 2019; Sirviö et al., 2020; Yu et al., 2019). An example of the efficiency of the process combination is that ramie fiber CNFs showed a size distribution between 100 – 1000 nm after 11h of milling, while DES-treated ramie fibers only needed 5 h to achieve a similar size distribution (Yu et al., 2019). In addition, pretreatment with DES was more efficient than conventional solvents (HCl) to produce CNFs at small diameters after homogenization using okara as raw material. Indeed, pretreatment with HCl produced CNFs with a diameter distribution between 51 – 79 nm, while those pretreated with DES had a diameter distribution between 11 – 65 nm (Peiyi Li et al., 2020). Finally, kraft pulp can hardly be fibrillated into nanocellulose after the ultrasound process. On the other hand, kraft pulp treated with DES at 10% and 20% resulted in CNFs and CNCs, respectively, after the ultrasound process (Ma et al., 2019).

Microwaves (MW) are electromagnetic radiation with a frequency ranging from 300 MHz to 300 GHz and a wavelength from 1 mm to 1 m (Pradhan et al., 2022). MW is a non-conventional heating alternative to conventional heating. In MW, heat is transferred by direct

conversion of electromagnetic energy into heat, unlike conventional heating in which heat transfer occurs by convection, conduction and radiation (Pradhan et al., 2022; Romero-Zúñiga et al., 2021). In the production of nanocellulose, MW has been applied as a pretreatment for the gradual removal of cementing material (e.g. lignin, hemicellulose and pectin). Several plant matrices such as bamboo, corn cob, rape straw, lime residue, cane bagasse and wheat straw were pretreated by MW to reduce lignin and hemicellulose. After treatment with MW, an increase in crystallinity was observed, from 52.3% to 70.6% for bamboo nanofibers and from 45.85% to 61.5% for wheat straw nanofibers (Q. Liu et al., 2017; Xie et al., 2016). Despite the high efficiency of MW in reducing cementing materials, a chemical treatment could be necessary to remove the brownish color in the liquefied residue after MW treatment (Xie et al., 2016)Huang et al., 2017). In addition, fibers are converted into microfibrils after MW treatment and, therefore, a mechanical process is still required to convert microfibrils into nanofibers. CNFs with average size between 2 - 43 nm were produced by MW associated with ultrasound, high pressure homogenization, high shear homogenization, microfluidization and milling (Impoolsup et al., 2020; Peiyi Li et al., 2020; Q. Liu et al., 2017; Louis & Venkatachalam, 2020).

The electron beam irradiation (EBI) technique can be used both to reduce the size of cellulose fibers to the nanometer scale and as a pretreatment to isolate cellulose fibers from lignocellulosic raw material. It is an emerging technology in the field of production of cellulose nanofibers and still few studies are found. In this technique, accelerated electron beams are used to irradiate lignocellulosic biomass in order to break the structure of cell wall polymers (lignin, cellulose, hemicellulose) producing free radical, inducing cross-link formation or promoting chain scission and/or decreased degree of polymerization (Hassan et al., 2018). Cellulose nanofibers were obtained from cotton linters using electron beam irradiation, in the range of 10-100 KGy, observing that the radiation interferes with the size and crystallinity of the nanofibers. The increase in radiation decreases the crystallinity and slightly affects the size range of nanofibers obtained from cotton linter, with the crystallinity varying from 75.3% to 65.5% and the width of nanofibers ranging from 30 to 70 nm to 50 to 70 nm (Van Hai & Seo, 2016).

Cold plasma treatment is considered an emerging green technology. Plasma is an ionized gas, considered the fourth state of matter. It can be defined as a medium consisting

of gaseous or fluid mixtures of a wide range of charged particles, such as free electrons, ions, radicals and metastable molecules (Pradhan et al., 2022). The gas is electrically charged and under atmospheric or reduced pressure, the generation of plasma occurs (Morent et al., 2011). The parameters that affect plasma generation are: electrode material and geometry, electrical energy and the nature of the gases, since different gases can be used such as CH₄, NH₃, N₂, O₂, Ar and He (Rauscher et al., 2010). Despite the few reports found in the literature regarding the use of plasma in the production of cellulose nanofibers, some advantages of using this technique can be cited as a clean, dry and energy efficient technology, as well as the use of a low concentration of acids. Cellulose nanofibers from wheat straw were obtained by pretreatment with cold plasma. The process was able to reduce the total energy consumption by 90.4% compared to conventional nanofiber processing (Shaghaleh et al., 2021). Regarding the disadvantages, the need for a continuous large-scale process and the huge surface area of the materials that need to be treated are highlighted (Pradhan et al., 2022; Shaghaleh et al., 2021).

The pulsed-electric field is a technique that uses a simple device, composed of two electrodes, which subjects the raw material to non-thermal voltage pulses. The process duration is short, from approximately nano to milliseconds, and uses a high pulse amplitude, approximately 0.1–100 kV/cm (B. Kumar et al., 2020). This allows the breakdown of the structure, resulting in the loss of semi permeability. If pulsed-electric field is associated with other processes such as enzymatic hydrolysis, it is possible to obtain nanofibers (Barba et al., 2015). The specific intensity of the treatment process depends on the conductivity of the material to be treated, the voltage supplied and the distance and geometry of the electrodes (Gómez et al., 2019). One of the disadvantages is the few studies in the literature on the technique and its influence on the formation of nanofibers. A comparison of alkaline pretreatment (NaOH) with pulsed electric field process was performed to obtain cellulose nanofibers from Mendong fiber (*Fimbristylis globulosa*), observing a slight improvement in crystallinity (from 83% to 86%) using the pulsed electric field (Suryanto et al., 2018).

The cryocrushing process uses a mechanical process for the formation of nanofibers. In this process, the fibers are immersed in water and, after absorbing the water, liquid nitrogen is applied to freeze them and then crushed them by applying high shear forces (Abdul Khalil et al., 2014). Due to the pressure exerted by the ice crystals and the application of high

impact forces, the frozen fibers break the cell wall and release the cellulose nanofibers (Siró & Plackett, 2010). The disadvantages of this process are low recovery and low uniformity of the nanofiber, high cost and high energy consumption (Teo & Wahab, 2020). Cellulose nanofibers from soybean residue were produced using cryocrushing associated with high pressure homogenization. The obtained nanofibers had a diameter around 50 -100 nm and 48% of crystallinity (B. Wang & Sain, 2007). Water hyacinth weeds were used as a source of obtaining cellulose nanofibers from several processes, including cryocrushing, showing diameter ranging from 20 to 100 nm (Thiripura Sundari & Ramesh, 2012).

Finding remarks

Cellulose is the most abundant natural polymer found in many sources, and the substitution of conventional polymers by cellulose-based polymers is a way of building a more sustainable industry. Cellulose nanofibers are a kind of cellulose nanomaterial that can be obtained by numerous chemical and physical treatments. In this review, we summarize the main chemical and physical treatments for CNFs production. We focus on elucidating the main characteristics of the CNF production methods. It is difficult to establish a clear relationship between method of obtaining and CNFs characteristics, since a combination of techniques is necessary to transform cellulose in nanofibers. The numerous methods associated with the CNF production and the complexity of the cellulose source promote a huge influence on the CNFs characteristics. Finally, we highlight the most promising emerging technologies for CNFs production, as these technologies aim to match the new pattern of sustainability, which is an innovative trend in nanocellulose production.

ACKNOWLEDGMENTS

This study was financed by Coordenação de Aperfeiçoamento de Pessoal de Nível Superior – Brazil (CAPES) - Finance Code 001 and Fundação de Amparo à Pesquisa do Estado de São Paulo - FAPESP (2019/27354-3). Chevalier and Miranda thanks CAPES-Brazil for the scholarship (88887.479720/2020-00; 88887479710/2020-00). Cunha and Chevalier thanks CNPq (404753/2023-0). Cunha and Sato thanks CNPq (307094/2021-9/ 309326/2022-2) for the productivity grant.

References

- Abdul Khalil, H. P. S., Davoudpour, Y., Islam, M. N., Mustapha, A., Sudesh, K., Dungani, R., & Jawaidd, M. (2014). Production and modification of nanofibrillated cellulose using various mechanical processes: A review. *Carbohydrate Polymers*, 99, 649–665. <https://doi.org/10.1016/j.carbpol.2013.08.069>
- Ahn, Y., Hu, D. H., Hong, J. H., Lee, S. H., Kim, H. J., & Kim, H. (2012). Effect of co-solvent on the spinnability and properties of electrospun cellulose nanofiber. *Carbohydrate Polymers*, 89(2), 340–345. <https://doi.org/10.1016/j.carbpol.2012.03.006>
- Angel, N., Li, S., Yan, F., & Kong, L. (2022). Recent advances in electrospinning of nanofibers from bio-based carbohydrate polymers and their applications. *Trends in Food Science and Technology*, 120(January), 308–324. <https://doi.org/10.1016/j.tifs.2022.01.003>
- Asem, M., Jimat, D. N., Jafri, N. H. S., Wan Nawawi, W. M. F., Azmin, N. F. M., & Abd Wahab, M. F. (2021). Entangled cellulose nanofibers produced from sugarcane bagasse via alkaline treatment, mild acid hydrolysis assisted with ultrasonication. *Journal of King Saud University - Engineering Sciences*, xxxx. <https://doi.org/10.1016/j.jksues.2021.03.003>
- Balakrishnan, P., Sreekala, M. S., Kunaver, M., Huskić, M., & Thomas, S. (2017). Morphology, transport characteristics and viscoelastic polymer chain confinement in nanocomposites based on thermoplastic potato starch and cellulose nanofibers from pineapple leaf. *Carbohydrate Polymers*, 169, 176–188. <https://doi.org/10.1016/j.carbpol.2017.04.017>
- Barba, F. J., Parniakov, O., Pereira, S. A., Wiktor, A., Grimi, N., Boussetta, N., Saraiva, J. A., Raso, J., Martin-Belloso, O., Witrowa-Rajchert, D., Lebovka, N., & Vorobiev, E. (2015). Current applications and new opportunities for the use of pulsed electric fields in food science and industry. *Food Research International*, 77, 773–798. <https://doi.org/10.1016/j.foodres.2015.09.015>
- Bian, H., Tu, P., & Chen, J. Y. (2020). Fabrication of all-cellulose nanocomposites from corn stalk. *Journal of the Science of Food and Agriculture*, 100(12), 4390–4399. <https://doi.org/10.1002/jsfa.10476>
- Campos, A., Correa, A. C., Cannella, D., de M Teixeira, E., Marconcini, J. M., Dufresne, A., Mattoso, L. H. C., Cassland, P., & Sanadi, A. R. (2013). Obtaining nanofibers from curauá and sugarcane bagasse fibers using enzymatic hydrolysis followed by sonication. *Cellulose*, 20(3), 1491–1500. <https://doi.org/10.1007/s10570-013-9909-3>
- Ceaser, R., & Chimphango, A. F. A. (2021). Comparative analysis of physical and functional properties of cellulose nanofibers isolated from alkaline pre-treated wheat straw in optimized hydrochloric acid and enzymatic processes. *International Journal of Biological Macromolecules*, 171, 331–342. <https://doi.org/10.1016/j.ijbiomac.2021.01.018>
- Chen, W., Yu, H., Liu, Y., Chen, P., Zhang, M., & Hai, Y. (2011). Individualization of cellulose nanofibers from wood using high-intensity ultrasonication combined with chemical

- pretreatments. *Carbohydrate Polymers*, 83(4), 1804–1811.
<https://doi.org/10.1016/j.carbpol.2010.10.040>
- Choudhury, R. R., Sahoo, S. K., & Gohil, J. M. (2020). Potential of bioinspired cellulose nanomaterials and nanocomposite membranes thereof for water treatment and fuel cell applications. *Cellulose*, 27(12), 6719–6746. <https://doi.org/10.1007/s10570-020-03253-z>
- Costa, A. L. R., Gomes, A., Tibolla, H., Menegalli, F. C., & Cunha, R. L. (2018). Cellulose nanofibers from banana peels as a Pickering emulsifier: High-energy emulsification processes. *Carbohydrate Polymers*, 194(April), 122–131.
<https://doi.org/10.1016/j.carbpol.2018.04.001>
- Czaikoski, A., da Cunha, R. L., & Menegalli, F. C. (2020). Rheological behavior of cellulose nanofibers from cassava peel obtained by combination of chemical and physical processes. *Carbohydrate Polymers*, 248(July), 116744.
<https://doi.org/10.1016/j.carbpol.2020.116744>
- De Souza, M. (2006). TEMPO (2,2,6,6-tetramethylpiperidine-N-oxyl) an Important Reagent in Alcohol Oxidation and its Application in Synthesis of Natural Products. *Mini-Reviews in Organic Chemistry*, 3(2), 155–165. <https://doi.org/10.2174/157019306776819244>
- Detta, N., Brown, T. D., Edin, F. K., Albrecht, K., Chiellini, F., Chiellini, E., Dalton, D., & Dietmar, W. (2010). *Melt electrospinning of polycaprolactone and its blends with poly (ethylene glycol)*. August, 1558–1562. <https://doi.org/10.1002/pi.2954>
- Dhali, K., Ghasemlou, M., Daver, F., Cass, P., & Adhikari, B. (2021). A review of nanocellulose as a new material towards environmental sustainability. *Science of the Total Environment*, 775, 145871. <https://doi.org/10.1016/j.scitotenv.2021.145871>
- Du, H., Liu, W., Zhang, M., Si, C., Zhang, X., & Li, B. (2019). Cellulose nanocrystals and cellulose nanofibrils based hydrogels for biomedical applications. *Carbohydrate Polymers*, 209(November 2018), 130–144.
<https://doi.org/10.1016/j.carbpol.2019.01.020>
- Dufresne, A. (2018). Cellulose nanomaterials as green nanoreinforcements for polymer nanocomposites. *Philosophical Transactions of the Royal Society A: Mathematical, Physical and Engineering Sciences*, 376(2112). <https://doi.org/10.1098/rsta.2017.0040>
- El Achkar, T., Greige-Gerges, H., & Fourmentin, S. (2021). Basics and properties of deep eutectic solvents: a review. *Environmental Chemistry Letters*, 19(4), 3397–3408.
<https://doi.org/10.1007/s10311-021-01225-8>
- Fan, X., Li, Y., Li, X., Wu, Y., Tang, K., Liu, J., Zheng, X., & Wan, G. (2020). Injectable antibacterial cellulose nanofiber/chitosan aerogel with rapid shape recovery for noncompressible hemorrhage. *International Journal of Biological Macromolecules*, 154, 1185–1193. <https://doi.org/10.1016/j.ijbiomac.2019.10.273>
- Farahbakhsh, N., Roodposhti, P. S., Ayoub, A., Venditti, R. A., & Jur, J. S. (2015). Melt

- extrusion of polyethylene nanocomposites reinforced with nanofibrillated cellulose from cotton and wood sources. *Journal of Applied Polymer Science*, 132(17), 1–10. <https://doi.org/10.1002/app.41857>
- Favatela, F., Horst, M. F., Bracone, M., Gonzalez, J., Alvarez, V., & Lassalle, V. (2021). Gelatin/Cellulose nanowhiskers hydrogels intended for the administration of drugs in dental treatments: Study of lidocaine as model case. *Journal of Drug Delivery Science and Technology*, 61(July 2019), 101886. <https://doi.org/10.1016/j.jddst.2020.101886>
- Fillat, Ú., Wicklein, B., Martín-Sampedro, R., Ibarra, D., Ruiz-Hitzky, E., Valencia, C., Sarrión, A., Castro, E., & Eugenio, M. E. (2018). Assessing cellulose nanofiber production from olive tree pruning residue. *Carbohydrate Polymers*, 179(June 2017), 252–261. <https://doi.org/10.1016/j.carbpol.2017.09.072>
- Frone, A. N., Panaitescu, D. M., & Donescu, D. (2011). *SOME ASPECTS CONCERNING THE ISOLATION OF CELLULOSE MICRO- AND NANO- FIBERS*. 73.
- Ganguly, P., Sengupta, S., Das, P., & Bhowal, A. (2020). Valorization of food waste: Extraction of cellulose, lignin and their application in energy use and water treatment. *Fuel*, 280(July), 118581. <https://doi.org/10.1016/j.fuel.2020.118581>
- Gao, H., Duan, B., Lu, A., Deng, H., Du, Y., Shi, X., & Zhang, L. (2018). Fabrication of cellulose nanofibers from waste brown algae and their potential application as milk thickeners. *Food Hydrocolloids*, 79, 473–481. <https://doi.org/10.1016/j.foodhyd.2018.01.023>
- George, J., & Sabapathi, S. N. (2015). Cellulose nanocrystals: Synthesis, functional properties, and applications. *Nanotechnology, Science and Applications*, 8, 45–54. <https://doi.org/10.2147/NSA.S64386>
- Gómez, B., Munekata, P. E. S., Gavahian, M., Barba, F. J., Martí-Quijal, F. J., Bolumar, T., Campagnol, P. C. B., Tomasevic, I., & Lorenzo, J. M. (2019). Application of pulsed electric fields in meat and fish processing industries: An overview. *Food Research International*, 123(April), 95–105. <https://doi.org/10.1016/j.foodres.2019.04.047>
- Hansen, B. B., Spittle, S., Chen, B., Poe, D., Zhang, Y., Klein, J. M., Horton, A., Adhikari, L., Zelovich, T., Doherty, B. W., Gurkan, B., Maginn, E. J., Ragauskas, A., Dadmun, M., Zawodzinski, T. A., Baker, G. A., Tuckerman, M. E., Savinell, R. F., & Sangoro, J. R. (2021). Deep Eutectic Solvents: A Review of Fundamentals and Applications. *Chemical Reviews*, 121(3), 1232–1285. <https://doi.org/10.1021/acs.chemrev.0c00385>
- Haron, G. A. S., Mahmood, H., Noh, M. H., Alam, M. Z., & Moniruzzaman, M. (2021). Ionic Liquids as a Sustainable Platform for Nanocellulose Processing from Bioresources: Overview and Current Status. *ACS Sustainable Chemistry and Engineering*, 9(3), 1008–1034. <https://doi.org/10.1021/acssuschemeng.0c06409>
- Hassan, S. S., Williams, G. A., & Jaiswal, A. K. (2018). Emerging technologies for the pretreatment of lignocellulosic biomass. *Bioresource Technology*, 262(March), 310–318. <https://doi.org/10.1016/j.biortech.2018.04.099>

- He, X., Lu, W., Sun, C., Khalesi, H., Mata, A., Andaleeb, R., & Fang, Y. (2021). Cellulose and cellulose derivatives: Different colloidal states and food-related applications. *Carbohydrate Polymers*, 255(August), 117334. <https://doi.org/10.1016/j.carbpol.2020.117334>
- Hu, J., Tian, D., Renneckar, S., & Saddler, J. N. (2018). Enzyme mediated nanofibrillation of cellulose by the synergistic actions of an endoglucanase, lytic polysaccharide monooxygenase (LPMO) and xylanase. *Scientific Reports*, 8(1), 4–11. <https://doi.org/10.1038/s41598-018-21016-6>
- Hu, Y., Liu, L., Yu, J., Wang, Z., & Fan, Y. (2020). Preparation of Natural Multicompatible Silk Nanofibers by Green Deep Eutectic Solvent Treatment. *ACS Sustainable Chemistry and Engineering*, 8(11), 4499–4510. <https://doi.org/10.1021/acssuschemeng.9b07668>
- Hua, K., Carlsson, D. O., Ålander, E., Lindström, T., Strømme, M., Mihranyan, A., & Ferraz, N. (2014). Translational study between structure and biological response of nanocellulose from wood and green algae. *RSC Advances*, 4(6), 2892–2903. <https://doi.org/10.1039/c3ra45553j>
- Huang, X., De Hoop, C. F., Li, F., Xie, J., Hse, C. Y., Qi, J., Jiang, Y., & Chen, Y. (2017). Dilute Alkali and Hydrogen Peroxide Treatment of Microwave Liquefied Rape Straw Residue for the Extraction of Cellulose Nanocrystals. *Journal of Nanomaterials*, 2017. <https://doi.org/10.1155/2017/4049061>
- Hubbe, M. A., Rojas, O. J., Lucia, L. A., & Sain, M. (2008). Cellulosic nanocomposites: A review. *International Journal of Interactive Mobile Technologies*, 12(3), 929–980. <https://doi.org/10.15376/biores.3.3.929-980>
- Ilyas, R. A., Sapuan, S. M., Ishak, M. R., & Zainudin, E. S. (2019). Sugar palm nanofibrillated cellulose (*Arenga pinnata* (Wurmb.) Merr): Effect of cycles on their yield, physico-chemical, morphological and thermal behavior. *International Journal of Biological Macromolecules*, 123, 379–388. <https://doi.org/10.1016/j.ijbiomac.2018.11.124>
- Ilyas, Rushdan Ahmad, Sapuan, S. M., Ishak, M. R., & Zainudin, E. S. (2018). Water transport properties of bio-nanocomposites reinforced by sugar palm (*arenga pinnata*) nanofibrillated cellulose. *Journal of Advanced Research in Fluid Mechanics and Thermal Sciences*, 51(2), 234–246.
- Impoolsup, T., Chiewchan, N., & Devahastin, S. (2020). On the use of microwave pretreatment to assist zero-waste chemical-free production process of nanofibrillated cellulose from lime residue. *Carbohydrate Polymers*, 230(October 2019), 115630. <https://doi.org/10.1016/j.carbpol.2019.115630>
- Isogai, A., Saito, T., & Fukuzumi, H. (2011). TEMPO-oxidized cellulose nanofibers. *Nanoscale*, 3(1), 71–85. <https://doi.org/10.1039/c0nr00583e>
- Jiang, T., Carbone, E. J., & Lo, K. W. (2015). Progress in Polymer Science Electrospinning of polymer nanofibers for tissue regeneration. *Progress in Polymer Science*, 46, 1–24. <https://doi.org/10.1016/j.progpolymsci.2014.12.001>

- Kalia, S., Boufi, S., Celli, A., & Kango, S. (2014). Nanofibrillated cellulose: Surface modification and potential applications. *Colloid and Polymer Science*, 292(1), 5–31. <https://doi.org/10.1007/s00396-013-3112-9>
- Kargarzadeh, H., Ioelovich, M., Ahmad, I., Thomas, S., & Dufresne, A. (2017). Methods for Extraction of Nanocellulose from Various Sources. *Handbook of Nanocellulose and Cellulose Nanocomposites*, 1–49. <https://doi.org/10.1002/9783527689972.ch1>
- Kargarzadeh, H., Mariano, M., Gopakumar, D., Ahmad, I., Thomas, S., Dufresne, A., Huang, J., & Lin, N. (2018). Advances in cellulose nanomaterials. In *Cellulose* (Vol. 25, Issue 4). Springer Netherlands. <https://doi.org/10.1007/s10570-018-1723-5>
- Khattab, M. M., Abdel-Hady, N. A., & Dahman, Y. (2017). Cellulose nanocomposites: Opportunities, challenges, and applications. In *Cellulose-Reinforced Nanofibre Composites: Production, Properties and Applications*. Elsevier Ltd. <https://doi.org/10.1016/B978-0-08-100957-4.00021-8>
- Kim, C. W., Kim, D. S., Kang, S. Y., Marquez, M., & Joo, Y. L. (2006). Structural studies of electrospun cellulose nanofibers. *Polymer*, 47(14), 5097–5107. <https://doi.org/10.1016/j.polymer.2006.05.033>
- Kumar, A., & Sinha-Ray, S. (2018). A review on biopolymer-based fibers via electrospinning and solution blowing and their applications. *Fibers*, 6(3), 1–53. <https://doi.org/10.3390/fib6030045>
- Kumar, B., Bhardwaj, N., Agrawal, K., Chaturvedi, V., & Verma, P. (2020). Current perspective on pretreatment technologies using lignocellulosic biomass: An emerging biorefinery concept. *Fuel Processing Technology*, 199(November 2019). <https://doi.org/10.1016/j.fuproc.2019.106244>
- Kwak, H., Shin, S., Kim, J., Kim, J., Lee, D., Lee, H., Lee, E. J., & Hyun, J. (2021). Protective coating of strawberries with cellulose nanofibers. *Carbohydrate Polymers*, 258(January), 117688. <https://doi.org/10.1016/j.carbpol.2021.117688>
- Li, J., Wei, X., Wang, Q., Chen, J., Chang, G., Kong, L., Su, J., & Liu, Y. (2012). Homogeneous isolation of nanocellulose from sugarcane bagasse by high pressure homogenization. *Carbohydrate Polymers*, 90(4), 1609–1613. <https://doi.org/10.1016/j.carbpol.2012.07.038>
- Li, Panpan, Sirviö, J. A., Asante, B., & Liimatainen, H. (2018). Recyclable deep eutectic solvent for the production of cationic nanocelluloses. *Carbohydrate Polymers*, 199(June), 219–227. <https://doi.org/10.1016/j.carbpol.2018.07.024>
- Li, Peiyi, Wang, Y., Hou, Q., Liu, H., Lei, H., Jian, B., & Li, X. (2020). Preparation of cellulose nanofibrils from okara by high pressure homogenization method using deep eutectic solvents. *Cellulose*, 27(5), 2511–2520. <https://doi.org/10.1007/s10570-019-02929-5>
- Li, X., Liu, H., Wang, J., & Li, C. (2012). Preparation and characterization of poly (3 - caprolactone) nonwoven mats via melt electrospinning. *Polymer*, 53(1), 248–253.

<https://doi.org/10.1016/j.polymer.2011.11.008>

- Liu, C., Li, M. C., Chen, W., Huang, R., Hong, S., Wu, Q., & Mei, C. (2020). Production of lignin-containing cellulose nanofibers using deep eutectic solvents for UV-absorbing polymer reinforcement. *Carbohydrate Polymers*, 246(May), 116548. <https://doi.org/10.1016/j.carbpol.2020.116548>
- Liu, Q., Lu, Y., Aguedo, M., Jacquet, N., Ouyang, C., He, W., Yan, C., Bai, W., Guo, R., Goffin, D., Song, J., & Richel, A. (2017). Isolation of High-Purity Cellulose Nanofibers from Wheat Straw through the Combined Environmentally Friendly Methods of Steam Explosion, Microwave-Assisted Hydrolysis, and Microfluidization. *ACS Sustainable Chemistry and Engineering*, 5(7), 6183–6191. <https://doi.org/10.1021/acssuschemeng.7b01108>
- Liu, X., Jiang, Y., Song, X., Qin, C., Wang, S., & Li, K. (2019). A bio-mechanical process for cellulose nanofiber production – Towards a greener and energy conservation solution. *Carbohydrate Polymers*, 208(November 2018), 191–199. <https://doi.org/10.1016/j.carbpol.2018.12.071>
- Long, Y., Yan, X., Wang, X., Zhang, J., & Yu, M. (2019). Chapter 2 - Electrospinning: The Setup and Procedure. In *Electrospinning: Nanofabrication and Applications*. Elsevier Inc. <https://doi.org/10.1016/B978-0-323-51270-1.00002-9>
- Louis, A. C. F., & Venkatachalam, S. (2020). Energy efficient process for valorization of corn cob as a source for nanocrystalline cellulose and hemicellulose production. *International Journal of Biological Macromolecules*, 163, 260–269. <https://doi.org/10.1016/j.ijbiomac.2020.06.276>
- Ma, Y., Xia, Q., Liu, Y., Chen, W., Liu, S., Wang, Q., Liu, Y., Li, J., & Yu, H. (2019). Production of Nanocellulose Using Hydrated Deep Eutectic Solvent Combined with Ultrasonic Treatment. *ACS Omega*, 4(5), 8539–8547. <https://doi.org/10.1021/acsomega.9b00519>
- Madivoli, E. S., Kareru, P. G., Gachanja, A. N., Mugo, S. M., Sujee, D. M., & Fromm, K. M. (2022). Isolation of Cellulose Nanofibers from Oryza sativa Residues via TEMPO Mediated Oxidation. *Journal of Natural Fibers*, 19(4), 1310–1322. <https://doi.org/10.1080/15440478.2020.1764454>
- Martínez Ávila, H., Schwarz, S., Rotter, N., & Gatenholm, P. (2016). 3D bioprinting of human chondrocyte-laden nanocellulose hydrogels for patient-specific auricular cartilage regeneration. *Bioprinting*, 1–2, 22–35. <https://doi.org/10.1016/j.bprint.2016.08.003>
- Menezes, D. B., Diz, F. M., Romanholo Ferreira, L. F., Corrales, Y., Baudrit, J. R. V., Costa, L. P., & Hernández-Macedo, M. L. (2021). Starch-based biocomposite membrane reinforced by orange bagasse cellulose nanofibers extracted from ionic liquid treatment. *Cellulose*, 28(7), 4137–4149. <https://doi.org/10.1007/s10570-021-03814-w>
- Mert, I. D. (2020). The applications of microfluidization in cereals and cereal-based products: An overview. *Critical Reviews in Food Science and Nutrition*, 60(6), 1007–1024. <https://doi.org/10.1080/10408398.2018.1555134>

- Missoum, K., Belgacem, M. N., & Bras, J. (2013). Nanofibrillated cellulose surface modification: A review. *Materials*, 6(5), 1745–1766. <https://doi.org/10.3390/ma6051745>
- Morent, R., De Geyter, N., Desmet, T., Dubruel, P., & Leys, C. (2011). Plasma surface modification of biodegradable polymers: A review. *Plasma Processes and Polymers*, 8(3), 171–190. <https://doi.org/10.1002/ppap.201000153>
- Mu, R., Hong, X., Ni, Y., Li, Y., Pang, J., Wang, Q., Xiao, J., & Zheng, Y. (2019). Recent trends and applications of cellulose nanocrystals in food industry. *Trends in Food Science and Technology*, 93(December 2018), 136–144. <https://doi.org/10.1016/j.tifs.2019.09.013>
- Muerza-cascante, M. L., Haylock, D., Hutmacher, D. W., & Dalton, P. D. (2015). *Melt Electrospinning and Its Technologization*. 21(2), 187–202. <https://doi.org/10.1089/ten.teb.2014.0347>
- Müller, R. H., Jacobs, C., & Kayser, O. (2001). Nanosuspensions as particulate drug formulations in therapy: Rationale for development and what we can expect for the future. *Advanced Drug Delivery Reviews*, 47(1), 3–19. [https://doi.org/10.1016/S0169-409X\(00\)00118-6](https://doi.org/10.1016/S0169-409X(00)00118-6)
- Naderi, A., Lindström, T., Sundström, J., Pettersson, T., Flodberg, G., & Erlandsson, J. (2015). Microfluidized carboxymethyl cellulose modified pulp: a nanofibrillated cellulose system with some attractive properties. *Cellulose*, 22(2), 1159–1173. <https://doi.org/10.1007/s10570-015-0577-3>
- Neenu, K. V., Midhun Dominic, C. D., Begum, P. M. S., Parameswaranpillai, J., Kanoth, B. P., David, D. A., Sajadi, S. M., Dhanyasree, P., Ajithkumar, T. G., & Badawi, M. (2022). Effect of oxalic acid and sulphuric acid hydrolysis on the preparation and properties of pineapple pomace derived cellulose nanofibers and nanopapers. *International Journal of Biological Macromolecules*, 209(PB), 1745–1759. <https://doi.org/10.1016/j.ijbiomac.2022.04.138>
- Ngasotter, S., Sampath, L., & Xavier, K. A. M. (2022). Nanochitin: An update review on advances in preparation methods and food applications. *Carbohydrate Polymers*, 291(March), 119627. <https://doi.org/10.1016/j.carbpol.2022.119627>
- Nie, S., Zhang, C., Zhang, Q., Zhang, K., Zhang, Y., Tao, P., & Wang, S. (2018). Enzymatic and cold alkaline pretreatments of sugarcane bagasse pulp to produce cellulose nanofibrils using a mechanical method. *Industrial Crops and Products*, 124(July), 435–441. <https://doi.org/10.1016/j.indcrop.2018.08.033>
- Ninomiya, K., Abe, M., Tsukegi, T., Kuroda, K., Tsuge, Y., Ogino, C., Taki, K., Taima, T., Saito, J., Kimizu, M., Uzawa, K., & Takahashi, K. (2018). Lignocellulose nanofibers prepared by ionic liquid pretreatment and subsequent mechanical nanofibrillation of bagasse powder: Application to esterified bagasse/polypropylene composites. *Carbohydrate Polymers*, 182, 8–14. <https://doi.org/10.1016/j.carbpol.2017.11.003>
- Nsor-Atindana, J., Chen, M., Goff, H. D., Zhong, F., Sharif, H. R., & Li, Y. (2017). Functionality

- and nutritional aspects of microcrystalline cellulose in food. *Carbohydrate Polymers*, 172, 159–174. <https://doi.org/10.1016/j.carbpol.2017.04.021>
- Onkarappa, H. S., Prakash, G. K., Pujar, G. H., Rajith Kumar, C. R., Latha, M. S., & Betageri, V. S. (2020). Hevea brasiliensis mediated synthesis of nanocellulose: Effect of preparation methods on morphology and properties. *International Journal of Biological Macromolecules*, 160, 1021–1028. <https://doi.org/10.1016/j.ijbiomac.2020.05.188>
- Oprea, M., & Voicu, S. I. (2020). Recent advances in composites based on cellulose derivatives for biomedical applications. *Carbohydrate Polymers*, 247(April), 116683. <https://doi.org/10.1016/j.carbpol.2020.116683>
- Pelissari, F. M., Andrade-Mahecha, M. M., Sobral, P. J. do A., & Menegalli, F. C. (2017). Nanocomposites based on banana starch reinforced with cellulose nanofibers isolated from banana peels. *Journal of Colloid and Interface Science*, 505, 154–167. <https://doi.org/10.1016/j.jcis.2017.05.106>
- Perzon, A., Jørgensen, B., & Ulvskov, P. (2020). Sustainable production of cellulose nanofiber gels and paper from sugar beet waste using enzymatic pre-treatment. *Carbohydrate Polymers*, 230(November 2019), 115581. <https://doi.org/10.1016/j.carbpol.2019.115581>
- Phanthong, P., Karnjanakom, S., Reubroycharoen, P., Hao, X., Abudula, A., & Guan, G. (2017). A facile one-step way for extraction of nanocellulose with high yield by ball milling with ionic liquid. *Cellulose*, 24(5), 2083–2093. <https://doi.org/10.1007/s10570-017-1238-5>
- Phanthong, P., Reubroycharoen, P., Hao, X., Xu, G., Abudula, A., & Guan, G. (2018). Nanocellulose: Extraction and application. *Carbon Resources Conversion*, 1(1), 32–43. <https://doi.org/10.1016/j.crcon.2018.05.004>
- Pradhan, D., Jaiswal, A. K., & Jaiswal, S. (2022). Emerging technologies for the production of nanocellulose from lignocellulosic biomass. *Carbohydrate Polymers*, 285(January), 119258. <https://doi.org/10.1016/j.carbpol.2022.119258>
- Rahman, S., Petroudy, D., Chabot, B., Loranger, E., Naebe, M., Shojaeiarani, J., Gharehkhani, S., Ahvazi, B., Hu, J., & Thomas, S. (2021). *Recent Advances in Cellulose Nanofibers Preparation through Energy-Efficient Approaches : A Review*. 1–31.
- Rauscher, H., Perucca, M., & Buyle, G. (2010). Plasma Technology for Hyperfunctional Surfaces: Food, Biomedical, and Textile Applications. In *Plasma Technology for Hyperfunctional Surfaces: Food, Biomedical, and Textile Applications*. <https://doi.org/10.1002/9783527630455>
- Rebouillat, S., & Pla, F. (2013). State of the Art Manufacturing and Engineering of Nanocellulose: A Review of Available Data and Industrial Applications. *Journal of Biomaterials and Nanobiotechnology*, 04(02), 165–188. <https://doi.org/10.4236/jbnnb.2013.42022>
- Robles-García, M. Á., Del-Toro-Sánchez, C. L., Márquez-Ríos, E., Barrera-Rodríguez, A.,

- Aguilar, J., Aguilar, J. A., Reynoso-Marín, F. J., Ceja, I., Dórame-Miranda, R., & Rodríguez-Félix, F. (2018). Nanofibers of cellulose bagasse from Agave tequilana Weber var. azul by electrospinning: preparation and characterization. *Carbohydrate Polymers*, 192(January), 69–74. <https://doi.org/10.1016/j.carbpol.2018.03.058>
- Romero-Zúñiga, G. Y., González-Morones, P., Sánchez-Valdés, S., Yáñez-Macías, R., Sifuentes-Nieves, I., García-Hernández, Z., & Hernández-Hernández, E. (2021). Microwave Radiation as Alternative to Modify Natural Fibers: Recent Trends and Opportunities—A Review. *Journal of Natural Fibers*, 00(00), 1–17. <https://doi.org/10.1080/15440478.2021.1952140>
- Salimi, S., Sotudeh-Gharebagh, R., Zarghami, R., Chan, S. Y., & Yuen, K. H. (2019). Production of Nanocellulose and Its Applications in Drug Delivery: A Critical Review. *ACS Sustainable Chemistry and Engineering*, 7(19), 15800–15827. <https://doi.org/10.1021/acssuschemeng.9b02744>
- Sehaqui, H., Kulasinski, K., Pfenninger, N., Zimmermann, T., & Tingaut, P. (2017). Highly Carboxylated Cellulose Nanofibers via Succinic Anhydride Esterification of Wheat Fibers and Facile Mechanical Disintegration. *Biomacromolecules*, 18(1), 242–248. <https://doi.org/10.1021/acs.biomac.6b01548>
- Shaghaleh, H., Wang, S., Xu, X., Guo, L., Dong, F., Hamoud, Y. A., Liu, H., Li, P., & Zhang, S. (2021). Innovative two-phase air plasma activation approach for green and efficient functionalization of nanofibrillated cellulose surfaces from wheat straw. *Journal of Cleaner Production*, 297. <https://doi.org/10.1016/j.jclepro.2021.126664>
- Siró, I., & Plackett, D. (2010). Microfibrillated cellulose and new nanocomposite materials: A review. *Cellulose*, 17(3), 459–494. <https://doi.org/10.1007/s10570-010-9405-y>
- Sirviö, J. A., Hyypiö, K., Asaadi, S., Junka, K., & Liimatainen, H. (2020). High-strength cellulose nanofibers produced: Via swelling pretreatment based on a choline chloride-imidazole deep eutectic solvent. *Green Chemistry*, 22(5), 1763–1775. <https://doi.org/10.1039/c9gc04119b>
- Sirviö, J. A., & Lakovaara, M. (2021). A Fast Dissolution Pretreatment to Produce Strong Regenerated Cellulose Nanofibers via Mechanical Disintegration. *Biomacromolecules*, 22(8), 3366–3376. <https://doi.org/10.1021/acs.biomac.1c00466>
- Soni, B., Hassan, E. B., & Mahmoud, B. (2015). Chemical isolation and characterization of different cellulose nanofibers from cotton stalks. *Carbohydrate Polymers*, 134, 581–589. <https://doi.org/10.1016/j.carbpol.2015.08.031>
- Suryanto, H., Fikri, A. A., Permanasari, A. A., Yanuhar, U., & Sukardi, S. (2018). Pulsed electric field assisted extraction of cellulose from mendong fiber (*Fimbristylis globulosa*) and its characterization. *Journal of Natural Fibers*, 15(3), 406–415. <https://doi.org/10.1080/15440478.2017.1330722>
- Syafri, E., Jamaluddin, Sari, N. H., Mahardika, M., Amanda, P., & Ilyas, R. A. (2022). Isolation and characterization of cellulose nanofibers from Agave gigantea by chemical-

- mechanical treatment. *International Journal of Biological Macromolecules*, 200(December 2021), 25–33. <https://doi.org/10.1016/j.ijbiomac.2021.12.111>
- Tarrés, Q., Oliver-Ortega, H., Boufi, S., Àngels Pèlach, M., Delgado-Aguilar, M., & Mutjé, P. (2020). Evaluation of the fibrillation method on lignocellulosic nanofibers production from eucalyptus sawdust: A comparative study between high-pressure homogenization and grinding. *International Journal of Biological Macromolecules*, 145, 1199–1207. <https://doi.org/10.1016/j.ijbiomac.2019.10.046>
- Teo, H. L., & Wahab, R. A. (2020). Towards an eco-friendly deconstruction of agro-industrial biomass and preparation of renewable cellulose nanomaterials: A review. *International Journal of Biological Macromolecules*, 161, 1414–1430. <https://doi.org/10.1016/j.ijbiomac.2020.08.076>
- Thiripura Sundari, M., & Ramesh, A. (2012). Isolation and characterization of cellulose nanofibers from the aquatic weed water hyacinth - Eichhornia crassipes. *Carbohydrate Polymers*, 87(2), 1701–1705. <https://doi.org/10.1016/j.carbpol.2011.09.076>
- Thomas, S., VISAKH, P. M., & Mathew, A. P. (2013). Advanced in Natural Polymers-Composites and Nanocomposites. In *Springer* (Vol. 18). <http://www.springer.com/series/8611>
- Tibolla, H., Pelissari, F. M., Martins, J. T., Lanzoni, E. M., Vicente, A. A., Menegalli, F. C., & Cunha, R. L. (2019). Banana starch nanocomposite with cellulose nano fi bers isolated from banana peel by enzymatic treatment : In vitro cytotoxicity assessment. *Carbohydrate Polymers*, 207(November 2018), 169–179. <https://doi.org/10.1016/j.carbpol.2018.11.079>
- Trache, D., Hussin, M. H., Haafiz, M. K. M., & Thakur, V. K. (2017). Recent progress in cellulose nanocrystals: Sources and production. *Nanoscale*, 9(5), 1763–1786. <https://doi.org/10.1039/c6nr09494e>
- Tripathi, S., Sharma, N., Alam, I., & Bhardwaj, N. K. (2019). Effectiveness of different green chemistry approaches during mixed hardwood bamboo pulp bleaching and their impact on environment. *International Journal of Environmental Science and Technology*, 16(8), 4327–4338. <https://doi.org/10.1007/s13762-018-1887-4>
- Van Hai, L., & Seo, Y. B. (2016). Effects of electron beam treatment on cotton linter for the preparation of nanofibrillated cellulose. *Palpu Chongi Gisul/Journal of Korea Technical Association of the Pulp and Paper Industry*, 48(2), 68–74. <https://doi.org/10.7584/ktappi.2016.48.2.068>
- Vinogradova, Y. S., & Chen, J. Y. (2016). Micron- and nano-cellulose fiber regenerated from ionic liquids. *Journal of the Textile Institute*, 107(4), 472–476. <https://doi.org/10.1080/00405000.2015.1040693>
- Wang, B., & Sain, M. (2007). Dispersion of soybean stock-based nanofiber in a plastic matrix. *Polym Int*, 56, 961–969. <https://doi.org/10.1002/pi>

- Wang, L. F., Shankar, S., & Rhim, J. W. (2017). Properties of alginate-based films reinforced with cellulose fibers and cellulose nanowhiskers isolated from mulberry pulp. *Food Hydrocolloids*, 63, 201–208. <https://doi.org/10.1016/j.foodhyd.2016.08.041>
- Wang, Lei, Guo, W., Zhu, H., He, H., & Wang, S. (2021). Preparation and properties of a dual-function cellulose nanofiber-based bionic biosensor for detecting silver ions and acetylcholinesterase. *Journal of Hazardous Materials*, 403(June 2020), 123921. <https://doi.org/10.1016/j.jhazmat.2020.123921>
- Wang, Li, Cui, Q., Pan, S., Li, Y., Jin, Y., Yang, H., Li, T., & Zhang, Q. (2021). Facile isolation of cellulose nanofibers from soybean residue. *Carbohydrate Polymer Technologies and Applications*, 2, 100172. <https://doi.org/10.1016/j.carpta.2021.100172>
- Wang, X., Um, I. C., Fang, D., Okamoto, A., Hsiao, B. S., & Chu, B. (2005). Formation of water-resistant hyaluronic acid nanofibers by blowing-assisted electro-spinning and non-toxic post treatments. *Polymer*, 46(13), 4853–4867. <https://doi.org/10.1016/j.polymer.2005.03.058>
- Wertz, J.-L., Bédoué, O., & Mercier, J. P. (2010). *Introduction. In Cellulose Science and Technology, EPFL Press, Taylor and Francis group, Boca Raton, 1st Edition.*
- Wu, C., McClements, D. J., He, M., Zheng, L., Tian, T., Teng, F., & Li, Y. (2021). Preparation and characterization of okara nanocellulose fabricated using sonication or high-pressure homogenization treatments. *Carbohydrate Polymers*, 255(June 2020), 117364. <https://doi.org/10.1016/j.carbpol.2020.117364>
- Xie, J., Hse, C. Y., De Hoop, C. F., Hu, T., Qi, J., & Shupe, T. F. (2016). Isolation and characterization of cellulose nanofibers from bamboo using microwave liquefaction combined with chemical treatment and ultrasonication. *Carbohydrate Polymers*, 151, 725–734. <https://doi.org/10.1016/j.carbpol.2016.06.011>
- Yan, G., Chen, B., Zeng, X., Sun, Y., Tang, X., & Lin, L. (2020). Recent advances on sustainable cellulosic materials for pharmaceutical carrier applications. *Carbohydrate Polymers*, 244(April), 116492. <https://doi.org/10.1016/j.carbpol.2020.116492>
- Yu, W., Wang, C., Yi, Y., Zhou, W., Wang, H., Yang, Y., & Tan, Z. (2019). Choline chloride-based deep eutectic solvent systems as a pretreatment for nanofibrillation of ramie fibers. *Cellulose*, 26(5), 3069–3082. <https://doi.org/10.1007/s10570-019-02290-7>
- Zhang, J., Kitayama, H., & Gotoh, Y. (2020). High strength ultrafine cellulose fibers generated by solution blow spinning. *European Polymer Journal*, 125(October 2019). <https://doi.org/10.1016/j.eurpolymj.2020.109513>
- Zhao, X., Chen, L., Guo, Y., Ma, X., Li, Z., Ying, W., & Peng, X. (2019). Porous cellulose nanofiber stringed HKUST-1 polyhedron membrane for air purification. *Applied Materials Today*, 14, 96–101. <https://doi.org/10.1016/j.apmt.2018.11.012>
- Zhuang, X., Yang, X., Shi, L., Cheng, B., Guan, K., & Kang, W. (2012). Solution blowing of submicron-scale cellulose fibers. *Carbohydrate Polymers*, 90(2), 982–987.

<https://doi.org/10.1016/j.carbpol.2012.06.031>

CAPÍTULO III

MODULATING DIGESTIBILITY AND STABILITY OF PICKERING EMULSIONS BASED ON CELLULOSE NANOFIBERS

Article published in Food Research International

Vol.178 (2024), p. 113963

<https://doi.org/10.1016/j.foodres.2024.113963>

Modulating digestibility and stability of Pickering emulsions based on cellulose nanofibers

Chevalier, Raquel Costa^a, Oliveira Júnior, Fernando Divino^a, Cunha, Rosiane Lopes^{a*}

^a Department of Food Engineering and Technology (DETA), School of Food Engineering (FEA), University of Campinas (UNICAMP); Rua Monteiro Lobato, 80; Campinas-SP; CEP: 13083-862; Brazil

* Corresponding author: rosiane@unicamp.br

Abstract

Cellulose nanofibers (CNF) have been widely studied for their biodegradability and for their unique advantages as a stabilizer in Pickering-type emulsions. However, it is challenging to produce cellulose nanofibers from agroindustry waste with good techno-functional properties, without the use of harsh process conditions. Green alternatives (eco-friendly) have been studied to obtain nanofibers, such as enzymatic hydrolysis and/or application of mechanical processes. In this work, we used acid hydrolysis (as a control and example of an efficient method), enzymatic hydrolysis and a mechanical process (ultrasound) to obtain cellulose nanofibers. We also evaluated the effect of the presence of ethyl groups in the cellulosic matrix (ethylcellulose) on the stabilizing mechanism of emulsions. All cellulose nanofibers were able to produce Pickering emulsions at concentrations of 0.01-0.05% (w/w), although showing differences in emulsion stability and digestibility. Morphology of the different cellulose nanofibers affected the viscosity of the aqueous suspensions used as continuous phase. Emulsions with nanofibers obtained from cassava peel (without the presence of ethyl groups) were stabilized only by the Pickering-type mechanism, while ethylcellulose nanofibers also showed surface activity that contributed to the stability of the emulsion. Furthermore, these latter emulsions showed greater release of free fatty acids in *in vitro* digestion compared to emulsions stabilized by cellulose nanofibers. Despite these differences, *in vitro* digestion showed the potential of applying cellulose-stabilized emulsions to control the rate of lipid digestion, due to the low amount of free fatty acids released (less than 20%).

Keywords: chemical hydrolysis; enzymatic hydrolysis; ultrasound; rheology; ethylcellulose; *in vitro* digestion.

1. Introduction

Emulsion-based products are common in food, cosmetics and pharmaceuticals, as they have a number of technological features such as creamy texture, spreadability and acting as a carrier of active compounds. Emulsions can show different phases composition and configurations depending on the application, such as one or more dispersed phases, varied average droplet sizes and more than one interfacial layer (Ho et al., 2022). Oil droplets distributed in a continuous aqueous phase (O/W emulsions) can be stabilized by different types of emulsifiers such as solid particles (Pickering mechanism), natural polymers (proteins and polysaccharides) or low molecular weight surfactants (McClements et al., 2017). Pickering-type emulsions show high resistance to destabilization by coalescence, although they may show flocculation and cream formation during storage. Cream formation indicates loss of stability only when the particles adsorbed at the interface do not prevent the coalescence, hampering redispersion of the droplets after gentle agitation (Y. Chevalier & Bolzinger, 2013). Despite these advantages, the Pickering stabilization of food emulsions is extremely challenging, due to the requirements of regulatory agencies and current consumers that have prioritized biocompatible and eco-friendly ingredients. In response to this demand, emulsion stabilizers based on natural compounds have been developed, including from agroindustry waste.

Cellulose is composed of repeating units of two anhydroglucose rings connected by a β -1,4-glycosidic bond, and is considered the most abundant biopolymer in the world (Tanpichai et al., 2022). Due to its unique properties, such as mechanical strength, renewability, biocompatibility, biodegradability and chemical stability, cellulose has been widely used for various purposes, including the stabilization of Pickering emulsions. Ethylcellulose is a cellulose derivative, obtained by the controlled replacement of surface hydroxyl groups by ethyl groups, increasing the hydrophobicity of the material (Parajuli & Ureña-Benavides, 2022). The reaction is often stopped after the ethoxy content ranges from 47.5% to 49%, which is equivalent to a degree of substitution of 2.5 (Liu et al., 2021). Cellulose-based nanoparticles, such as nanocrystals or nanofibers, can be obtained from mechanical, physical and/or chemical processes. However, some processes conditions are not environmental friendly. For instance, in acid hydrolysis with sulfuric acid (H_2SO_4) there is the generation of toxic acid effluents that must be subsequently neutralized (Liu et al., 2016).

Therefore, the use of ecofriendly methods, such as enzymatic hydrolysis and physical methods, such as ultrasound, are interesting alternatives. In addition, the association of methods improves and enhances the properties of the produced nanofibers (Czaikoski et al., 2020). Regarding the morphology of the nanofibers, they appear as filamentous networks that have diameters of less than 1 μm . These ultrafine fibers have unique characteristics such as high porosity, high surface area/volume ratio and good mechanical properties, in addition to extreme flexibility (Mohiti-Asli & Lobo, 2016). Pickering-type emulsions stabilized by cellulose nanofibrils (CNF) have aroused interest due to their low toxicity (Patel, 2020) and unique physical properties. Besides, they can be obtained from different sources and among them, agro-industrial waste. In addition to their peculiar properties as a Pickering-stabilizer, nanocellulose particles can control fat intake due to be non-responsive to small intestine physiological conditions. Therefore, this study aimed to produce and evaluate emulsions stabilized by cellulose nanofibers from cassava peel or commercial ethyl cellulose in order to seek alternatives for the production of Pickering-type stabilizers for food emulsions, which present different hydrophilicity/hydrophobicity properties. Therefore, the main objectives of the study were evaluating how the nature and method of production of these stabilizers affect the interface and emulsion properties, thus obtaining a better understanding of the role of different nanofibers on the stability and digestion of cellulose nanofibers-based emulsions.

2. Material and methods

2.1 Material

Crushed cassava husk was kindly donated by Plaza Ind. Com. Ltda (Brazil). Ethyl cellulose was kindly provided by Ashland Brazil (Brazil) and sunflower oil by Cargill (Brazil). Enzymes and reagents for the digestibility assays were obtained from Merck KGaA (Germany). All chemicals used were of analytical grade.

2.2 Obtaining cellulose nanofibers from cassava husk

Preparation steps of cellulose nanofibers from cassava peel are shown in Fig. 1 and described in detail in the following sections.

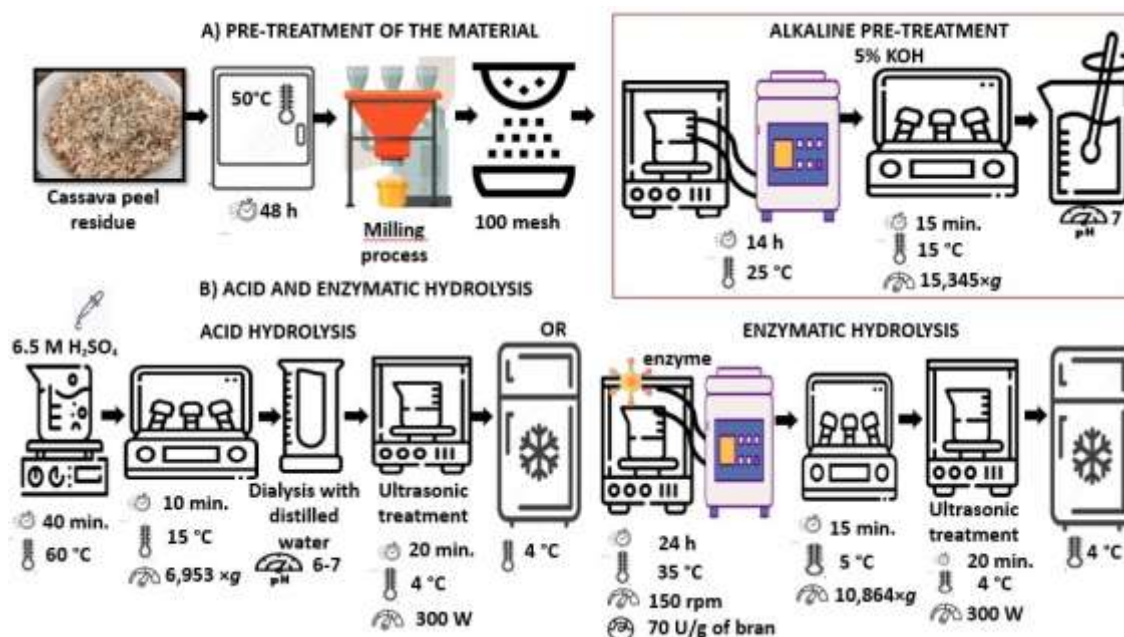


Fig. 1. Obtaining cellulose nanofibers from cassava husk. A) Physical and chemical pre-treatment and B) acid or enzymatic treatment combined with ultrasound.

2.2.1 Raw material preparation

First, the crushed cassava peel was washed, then sanitized with the aid of a sodium hypochlorite solution (250 ppm) for 10 min and dried in a forced convection oven at 50 °C for 48 h. Then, this material was ground in a knife mill and minced in a high-performance professional blender (Metalúrgica Siemens Ltda, Brazil). The material sieved through an opening of 0.15 mm (100-mesh) was subjected to the chemical (alkaline) pre-treatment described in section 2.2.2.

2.2.2 Alkaline pre-treatment

Minced cassava peels were subjected to alkaline pre-treatment with KOH solution (5% w/v), at a ratio of 1:18 (peel samples: KOH solution) at 25 °C under mechanical agitation for 14 h (Czaikoski et al., 2020). Then, these suspensions were successively washed and centrifuged (15,345×g/15 °C/15 min). Insoluble material was added in distilled water and centrifuged until the color of supernatant no longer changed. The remaining insoluble residue was added in distilled water and the pH adjusted to 7.0 using sulfuric acid (6.5 M) before being subjected to acid (section 2.2.3) or enzymatic (section 2.2.4) hydrolysis.

2.2.3 Acid hydrolysis treatment

Acid hydrolysis process was performed according to the method described below (E. de M. Teixeira et al., 2009). First, 10 g of pre-treated material were dispersed in 200 ml of 6.5 M sulfuric acid in a flask under vigorous mechanical stirring at 60 °C/40 min. Excess sulfuric acid was removed from the suspension by successive washes and centrifugation at 6,953 ×g for 10 min. Then, the suspension was subjected to dialysis with distilled water through a cellulose membrane until the pH reached 6–7. Finally, the resulting suspension was subjected to ultrasonic treatment (QR 750 W, Ultronique, Brazil) for approximately 20 minutes with a power of 300 W, coupled to a thermostatic bath at 4 °C. This material was named cellulose nanofibers obtained by acid hydrolysis (CNF-C) and stored at 4 °C in a sealed container.

2.2.4 Enzymatic hydrolysis treatment

Enzymatic hydrolysis was performed according to the method described below (Heloisa Tibolla et al., 2014). Erlenmeyer flasks containing 15% substrate (material obtained after alkaline treatment) in 0.1 M acetate buffer (pH 7) were placed on a thermostatic shaker (temperature of 35 °C) for 10 min, so that the medium reached thermal equilibrium. Then, the xylanase enzyme (concentration of 70 U/g of bran) was added to the mixture, which was kept at the same temperature for 24 h under agitation (150 rpm). After this period, the suspensions were placed on a thermostatic bath at 80 °C for 30 min to denature the enzyme. Then, the residual pulp was washed with deionized water and the solid was separated by centrifugation (10,864×g, 5 °C, 15 min) and resuspended in deionized water. Finally, the resulting suspension was subjected to ultrasonic treatment (QR 750 W, Ultronique, Brazil) for approximately 20 minutes with a power of 300 W, coupled to a thermostatic bath at 4 °C. This material was named cellulose nanofibers obtained by enzymatic hydrolysis (CNF-ENZ) and stored at 4 °C in a sealed container.

2.3 Obtaining ethyl cellulose nanofibers (CNF-EC)

First, the same procedure for obtaining CNF-C was applied using ethylcellulose as substrate, but nanofibers were not obtained as could not be observed from microscopy (section 2.4.1). Thus, a second procedure was carried out applying only ultrasound (QR 750 W, Ultronique, Brazil) on a suspension of 10% (w/v) of ethylcellulose in water for approximately 10 minutes with a power of 300 W, coupled to a thermostatic bath at 4 °C. This material named as CNF-EC was stored at 4 °C in a sealed container.

2.4 Characterization of nanofibers (CNF-C, CNF-ENZ and CNF-EC)

2.4.1 Morphology

Morphology of nanofibers was evaluated by atomic force microscopy (AFM). AFM images were acquired on a Microscope Park Systems, model NX-10 (Suwon, Korea) equipped with Si Nano sensor probe manufactured with a spring constant of 42 N.m⁻¹. The resonance frequency was about 320 kHz and the acquired images were treated with the GWYDDION software version 2.4. In order to determine the average diameter of CNFs, 20 measurements were taken from the AFM images.

2.4.2 Zeta potential

Zeta potential of CNFs suspended in Milli-Q water (0.01% w/w) was determined in triplicate using a Zetasizer model Nano ZS from Malvern Instruments Ltd. (United Kingdom, U.K) at a detection angle of 173°. Measurements of zeta potential were performed at room temperature (25 °C) for each sample.

2.4.3 Contact angle

The contact angle between oil or water and the cellulose nanofibrils was measured at 25°C, using the Tracker S tensiometer (Teclis, Longessaigne, France). The tests were performed with the formation and detachment of a droplet of oil or water (2 µL) kept in contact with compressed samples of lyophilized cellulose nanofibrils. The contact angle values were automatically measured for 60 s and determined in triplicate.

2.4.4 Fourier-transform infrared spectroscopy (FTIR)

The analysis of the functional groups in cassava husk flour, commercial ethyl cellulose and CFNs was performed by infrared absorption spectroscopy (4000 to 650 cm⁻¹) and determined in triplicate. A Fourier-transform infrared spectrometer (FTIR), Perkin Elmer Spectrum One, equipped with a UATR (universal attenuated total reflectance) accessory was used (Vicentini et al., 2005).

2.4.5 Rheological measurements

Rheological behavior of aqueous CNF suspensions (1.0%, 1.5%, 2.0%, 2.5% and 3.0% w/w) was studied using a controlled-stress rheometer (AR1500ex, TA Instruments, England) at 25°C. Flow curves were obtained using a rough plate (6 cm diameter, 1750 µm gap) by an up-down-up step program with shear rate ranging from 0 to 50 s⁻¹. Viscosity of emulsions was

evaluated at 50 s⁻¹. Emulsions were evaluated immediately after their preparation and after 7 days of storage in triplicate at 25 °C.

2.4.6 Specific surface area

CNF-ENZ and CNF-EC nanofibers were freeze-dried and stored under refrigeration prior to the analysis. Next, 1.0 g of freeze-dried nanofiber was incubated at 40 °C for 12 h, in order to remove residual water from the surface of the fibers. Then, N₂ physisorption measurements were carried out on a surface area and porosity analyzer (Micromeritics, model ASAP 2000, USA). N₂ isotherms of adsorption (Volume adsorbed/g x Relative Pressure (N₂ Pressure/N₂ Equilibrium Pressure)) were obtained at room temperature and the data were fitted to the isotherm models of Brunauer, Emmett, and Teller (BET) and Langmuir (Brunauer, Emmett & Teller, 1938; Langmuir, 1918).

CNF-C could not be evaluated since the sample presented liquid aspect, even after freeze-drying and conventional drying (105 °C, 30 min) pre-treatments.

2.5 Preparation of emulsions

The oil phase was composed of sunflower oil. Cellulose nanofibers at 0.01%; 0.02% and 0.05% w/w (CNF-C, CNF-ENZ or CNF-EC) dispersed in water were the aqueous continuous phase. The minimum concentration of CNF was determined based on preliminary tests in order to obtain emulsions without oil separation immediately after their preparation. Oil-in-water emulsions were first prepared by homogenizing sunflower oil (2.5% w/w) and aqueous phase (97.5% w/w) in a rotor-stator (Ultra Turrax T18, IKA, Germany) at 13,000 rpm for 2 min. After pre-emulsification, the emulsions were subjected to homogenization in a microfluidizer (Microfluidic, LM20, USA) for 3 cycles at 15,000 psi.

2.6 Characterization of Pickering emulsions

2.6.1 Dynamic interfacial tension

The interfacial tension between the aqueous and oil phases was evaluated at 25 °C using a Tracker-S tensiometer (Teclis, France) by the pendant drop method for 120 min. Such analyzes aimed to evaluate the effect of different types of CNF (CNF-C, CNF-ENZ and CNF-EC) and concentrations (0.01; 0.02 and 0.05% w/w) on interfacial tension of water-oil interface over time. A syringe was used and the tests were carried out with the formation of an oil drop (25 µL) in the CNF dispersion (aqueous phase). Measurements were performed in triplicate.

2.6.2 Droplet size distribution

Droplet size distribution was determined by laser diffraction using a Mastersizer 2000 (Malvern Instruments Ltd, Malvern, UK) with rotational velocity at 1,750 rpm. Water was used as a dispersant and ultrasound was applied for 2 min (before sample introduction) to avoid the presence of bubbles. Measurements were performed on freshly prepared emulsions and after 7 days of storage in triplicate. Some emulsions showed visual phase separation after 7 days of storage, forming a top (cream) and a bottom (serum) phase. For these emulsions, size distribution of each phase was obtained after 7 days. The mean volume-surface diameter ($D_{3,2}$) was calculated according to Eq. (1).

$$D_{3,2} = \frac{\sum n_i d_i^3}{\sum n_i d_i^2} \quad (1)$$

2.6.3 Microscopy

The emulsion microstructure was observed by optical and confocal microscopy. For confocal scanning laser microscopy (CSLM), first, the sunflower oil used to form the emulsions was stained with a Red Nile fluorescent dye before the analysis. Images were collected using 530 nm laser line for Red Nile excitation. Images of the microstructure of emulsions were captured with the software ZEN 3.4 (Carl Zeiss AG, Germany) on an Axio Scope A-1 microscope (Carl Zeiss AG, Germany) with magnifications of 400x and 1000x.

2.6.4 Kinetic stability – laser scanning turbidimetry

Emulsion stability was monitored using the optical scanning instrument Turbiscan ASG (Formulation, France). Emulsions were placed in flat-bottomed cylindrical glass tubes (140 mm, height; 16 mm, diameter) and stored at 25 ± 2 °C. Backscattered light at 880 nm was measured right after emulsions preparation and after 7 days. A backscattered light plot, BS (%), was performed on the y-axis and the sample height (mm) on the x-axis. A sample height of 0 mm corresponds to the bottom of the measuring cell. Measurements were performed in triplicate.

2.7 *In vitro* digestion assays and free fatty acids release

Digestibility assays were performed according to the international COST INFOGEST protocol (Brodkorb et al., 2019). First, enzymatic activities of pepsin and pancreatin were determined. To perform the assays, 10 mL of the Pickering emulsion (CNF-C, CNF-ENZ, or CNF-

EC) were diluted 1:1 (v:v) with simulated salivary fluid (KCl 15.1 mM, KH_2PO_4 3.7 mM, NaHCO_3 13.6 mM, $\text{MgCl}_2(\text{H}_2\text{O})_6$ 0.15 mM, $(\text{NH}_4)_2\text{CO}_3$ 0.06 mM, HCl 1.1 mM, $\text{CaCl}_2(\text{H}_2\text{O})_2$ 1.5 mM), and the pH of the medium was adjusted to 7.0. After two minutes of incubation at 37 °C, the oral mixture was diluted 1:1 (v:v) with simulated gastric fluid (KCl 6.9 mM, KH_2PO_4 0.9 mM, NaHCO_3 25 mM, NaCl 47.2 mM, $\text{MgCl}_2(\text{H}_2\text{O})_6$ 0.12 mM, $(\text{NH}_4)_2\text{CO}_3$ 0.5 mM, HCl 15.6 mM, $\text{CaCl}_2(\text{H}_2\text{O})_2$ 0.15 mM), and pH was adjusted to 3.0. Then, pepsin (2,000 U/mL) was added to the mixture and incubation for 2 h at 37 °C was carried out. Next, gastric chime was diluted 1:1 (v:v) with simulated intestinal fluid (KCl 6.8 mM, KH_2PO_4 0.8 mM, NaHCO_3 85 mM, NaCl 38.4 mM, $\text{MgCl}_2(\text{H}_2\text{O})_6$ 0.33 mM, HCl 8.4 mM, $\text{CaCl}_2(\text{H}_2\text{O})_2$ 0.6 mM), and the pH of the medium was adjusted to 7.0. Bile extract and pancreatin were added (10 mM and 100 U/mL in the final mixture, respectively) and the sample was incubated for 2 h at 37 °C. The pH at each step was controlled using an automatic titrator (Metrohm, Switzerland). HCl 1 M and NaOH 1 M were employed as titration solutions throughout the assays and HCl 6 M was applied to decrease the pH to 3.0 in the gastric step. Aliquots were taken at the end of the gastric and intestinal phases to characterize the digesta by particle size distribution (section 2.6.2) and microscopy (section 2.6.3), using the same procedure for emulsions before digestion.

Also, the free fatty acid release (% FFA) at the intestinal step was determined by using a pH-stat methodology. NaOH 1 M was used to maintain the pH of the system (pH = 7.0) and the volume added to the reactor was monitored through the intestinal phase. Next, it was assumed that the complete digestion of one molecule of triacylglycerol releases two molecules of free fatty acids, and then, % FFA was calculated by Equation 2.

$$\% \text{ FFA} = \frac{V_{\text{NaOH}} * M_{\text{NaOH}} * MW_{\text{lipid}}}{2 * W_{\text{lipid}}} \quad (2)$$

Where V_{NaOH} is the cumulative volume of NaOH 1 M added to the reactor, M_{NaOH} is the molarity of the NaOH solution, MW_{lipid} is the molecular weight of the sunflower oil, and W_{lipid} is the total mass of oil at the beginning of the intestinal step. A so-called blank sample was performed, without adding the emulsion, to account for the fatty acid released and its value was discounted directly from the analyzed samples. The digestion of emulsions, as well as the characterization of each digestive phase, were performed in triplicate.

2.8 Statistical analysis

To compare the differences between the mean values obtained for the properties of the different CNFs, an analysis of variance (ANOVA) and a Tukey test of multiple comparisons with a significance level of 5% were performed using the Statistica 7.0 software (StatSoft Inc., Tulsa, Oklahoma, USA).

3. Results and discussion

3.1 Characterization of cellulose nanofibers

3.1.1 Morphology, zeta potential and contact angle

AFM images confirmed the presence of nanofibers regardless of the treatments or raw materials used (Fig. 2). The images suggest that amorphous components such as hemicelluloses, lignin and pectin were practically removed as little cementing material is seen around the fiber bundles, which are the largest particles in the image (Pelissari et al., 2014). In general, the nanofibers appeared as a network of long, tangled cellulosic filaments. However, differences in the structure of the nanofibrils can be observed depending on the treatment. Nanofibrils obtained from acidic treatment and subsequent sonication showed the thinnest fibers dispersed in a network with many branches. Such characteristics are attributed to the breakage of the nanofibrils previously formed with the chemical process and posterior sonication process (Sanchez-Salvador et al., 2022). However, after the enzymatic treatment, the fibers showed a more elongated structure and some traces of amorphous components, which hampered the enzyme penetration in the cellulose chains (Heloisa Tibolla et al., 2014). Ultrasound application could promote an additional breakage of the nanofibrils. In fact, only the sonication process was sufficient to produce nanofibrils with ethyl cellulose, although the CNF-EC showed larger diameters and agglomerated structure (fibers bundle). These characteristics were associated to its low solubility in water. Diameter values of CNCs ranged between 7 - 14 nm, with the CNF-ENZ and CNF-EC showing the largest diameters (Table 1).

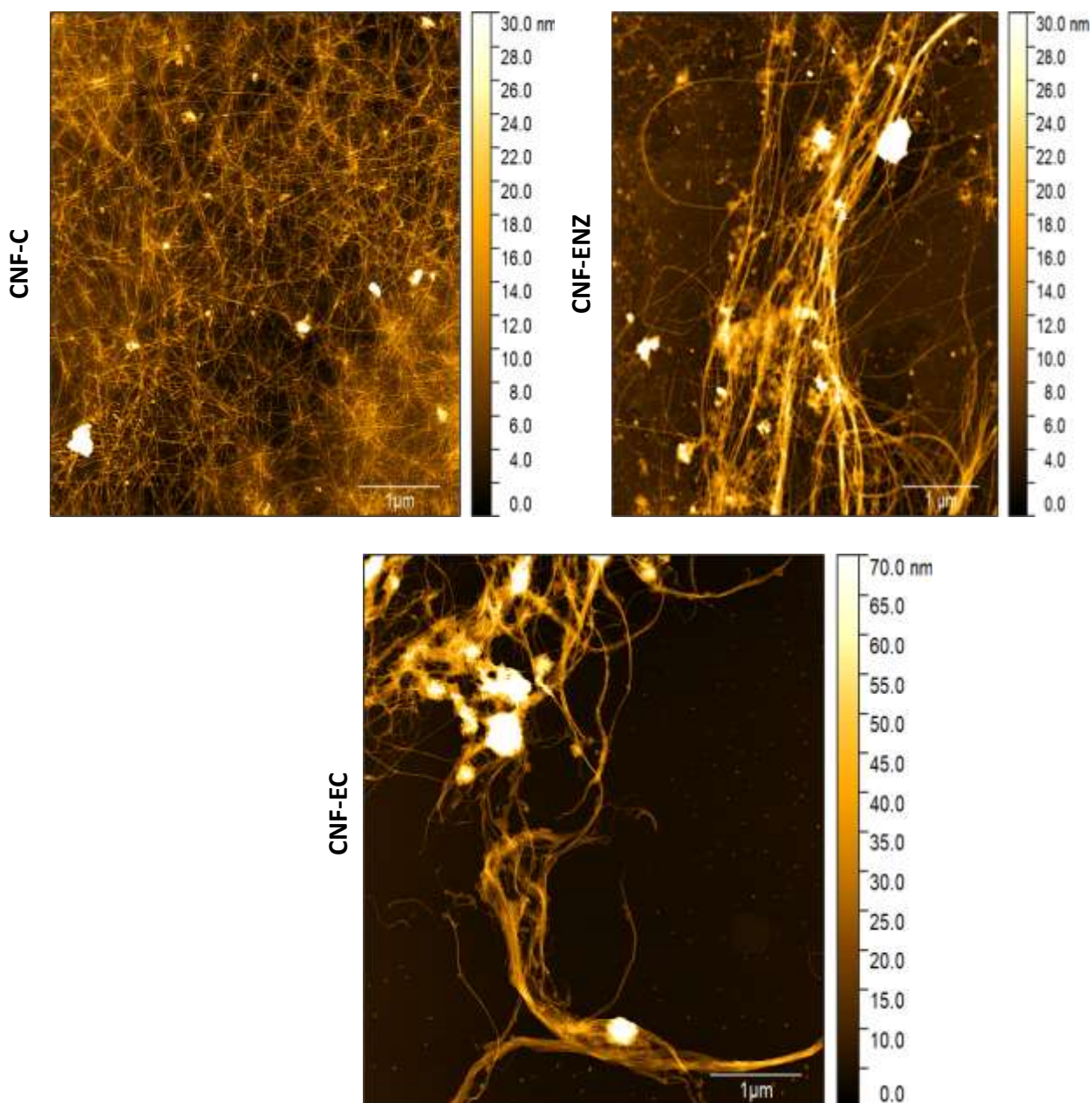


Fig. 2. AFM images of cellulose nanofibers obtained after acid/ultrasound process (CNF-C), enzymatic/ultrasound process (CNF-ENZ) and only ultrasound process (CNF-EC) (scale bar = 1 μm).

The zeta potential of the nanofibrils is shown in Table 1. Since zeta potential is related to the surface charge, the evaluation of this property can help to verify the performance of nanofibers as, for example, reinforcing agent in films and stabilizing emulsions. All cellulose nanofiber suspensions had a pH close to 7. Aqueous CNF suspensions showed negative zeta potential values, ranging from -23.94 to -27.63 mV with no significant differences between them. The ultrasound process used in all treatments probably promoted good mixing of the

suspension and great contact between the nanofibrils and oxygen, favoring the generation of negative charge on the surface of the CNFs due to the partial oxidation of the particles (Kitamura et al., 2016). Such an increase in zeta potential may favor the use of these particles as emulsion stabilizers, due to the electrostatic repulsion effect between the CNFs adsorbed on the interface, although it can limit the confinement of the particles at the interface (Costa et al., 2018b).

Table 1. Physical characteristics of cellulose nanofibers obtained from acid/ultrasound process (CNF-C) and enzymatic/ultrasound process (CNF-ENZ) using cassava husk as raw material; and from ultrasound (CNF-EC) using commercial ethyl cellulose as raw material.

Sample	Mean diameter (nm)	Zeta potential (mV)	Water contact angle (°)	Oil contact angle (°)
CNF- C	7.40±2.0 ^b	-26.76±4.08 ^a	-	24.94±1.23 ^b
CNF- ENZ	14.74±5.07 ^a	-23.94±3.13 ^a	-	39.85±2.95 ^a
CNF-EC	14.79±2.36 ^a	-27.63±2.10 ^a	52.45±2.72	41.19±2.96 ^a

Different letters in the same column indicate a statistically significant difference ($p < 0.05$).

The measurement of the contact angle was performed as a way of evaluating the wettability of the surface of the nanofibrils. Typically, a highly wetting or hydrophilic surface has a contact angle $\sim 0^\circ$ ($\cos \theta \sim 1$, for complete wetting) with water, while a non-wetting or hydrophobic surface has a contact angle $\geq 90^\circ$ ($\cos \theta \sim -1$, for non-wetting) (S. Kumar et al., 2022). The effect of the processes on the wettability of CNFs was measured by the contact angle between the CNFs films and water (Table 1). The droplet of water was quickly absorbed by the CNFs films obtained from the cassava peel (high hydrophilicity), and it was not possible to detect the angle. The CNF-EC presented an angle of 52.45° and less than 90° , thus demonstrating that, due to the wettability of CNF in water, it can be used to produce oil-in-water emulsions (Pang et al., 2018). A contact angle of $15^\circ < \theta < 90^\circ$ is necessary for O/W emulsions, while the W/O emulsions require a contact angle of $90^\circ < \theta < 165^\circ$ (Kaptay, 2006). However, the values of the contact angle with the oil were also lower than 90° , showing a good affinity of the particles with the oil. Although CNFs show smaller angles with water (except CNF-EC which has a slight smaller angle with oil), these results show that the nanoparticles act on the interface, forming networks capable of stabilizing the interface of O/W Pickering emulsions.

3.1.2 Fourier-transform infrared spectroscopy (FTIR)

FTIR spectroscopy analysis was performed to evaluate the chemical structure of different CNFs, cassava peel flour and commercial ethyl cellulose (Fig. 3). The peaks of the ethyl cellulose derivatives were very similar, while the cellulose derivatives varied greatly depending on the treatment. However, all samples showed characteristic absorption peaks around $3650\text{--}3000\text{ cm}^{-1}$ corresponding to the hydroxyl (OH) stretching vibration (Tsakani et al., 2022). The band observed at 3337 cm^{-1} corresponds to intramolecular hydrogen bonding of cellulose II, showing that CNF-C band was quite small in comparison to CNF-ENZ and flour. The region at 2920 cm^{-1} refers to the stretching vibrations of the CH bonds of cellulose and hemicellulose. Cassava flour showed a prominent peak, suggesting that chemical and enzymatic processes were effective in removing hemicellulose from cassava husk (Pelissari et al., 2014). The peak presented at about 1640 cm^{-1} was attributed to the hydroxyl bending vibration of the adsorbed water (Mahardika et al., 2018). The 1430 cm^{-1} band corresponds to the vibration of CH_2 bonds and is attributed to the "band of crystallinity" of cellulose, showing a less expressive peak for CNF-C. Cellulose II can be produced from cellulose I (naturally occurring cellulose) via alkaline treatment or solubilization and recrystallization (regeneration). Type II cellulose has advantages over type I cellulose, such as greater wettability, pore volume and surface area, in addition to being an easily digestible product (Nagarajan et al., 2017). Indeed, the transition from cellulose I to II of CNF-C was confirmed by the very expressive region in the absorption region around 1102 cm^{-1} (Costa et al., 2018b), which was less clear for CNF-ENZ. The well-pronounced peak observed in CNF-C between $554\text{--}666\text{ cm}^{-1}$ can correspond to S-S bonds, related to process using sulfuric acid during acid hydrolysis (El Fawal et al., 2022).

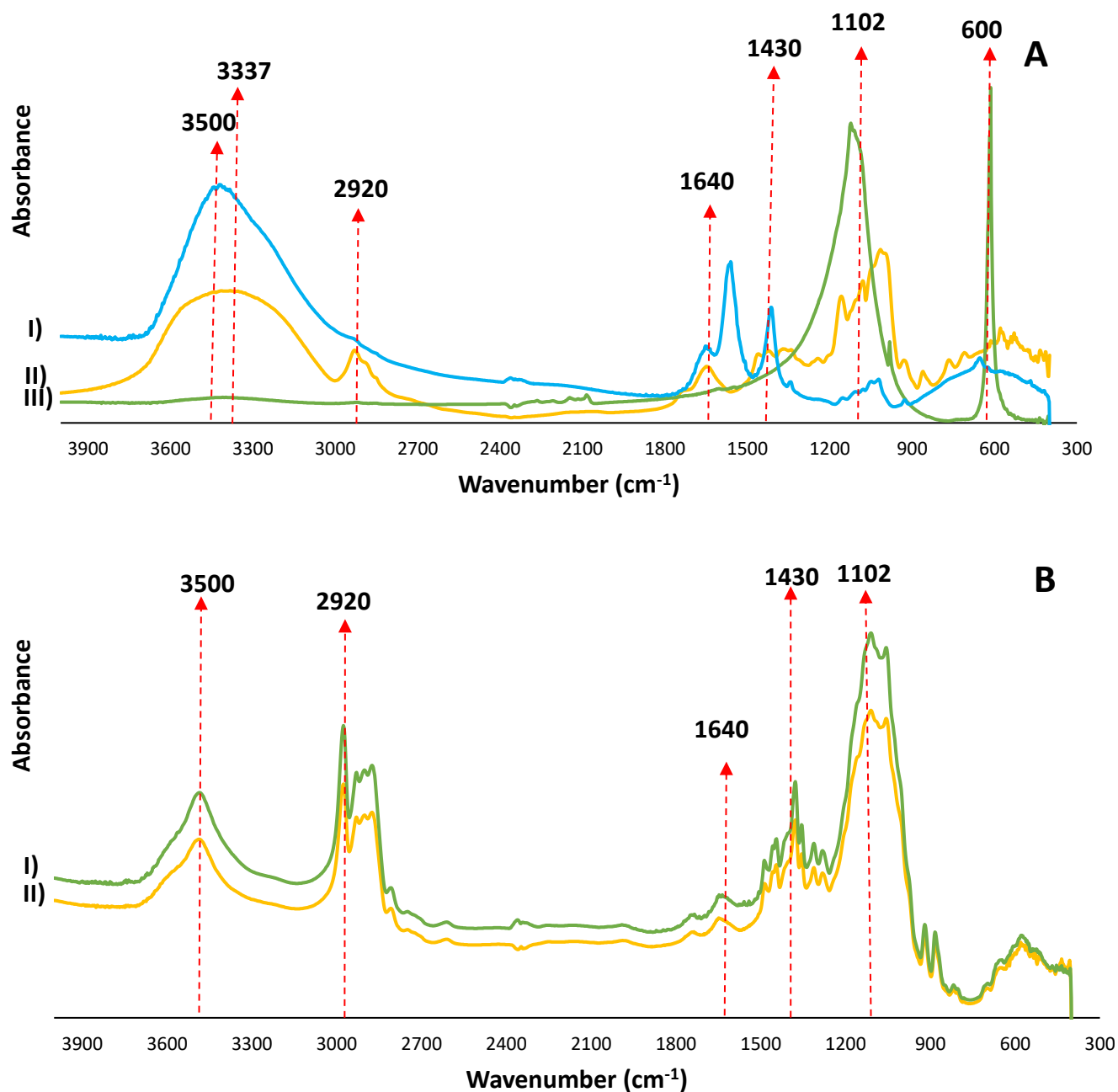


Fig. 3. FTIR spectra of A) derivatives of cassava peel and B) ethyl cellulose. In A: I) CNF-ENZ; II) cassava husk flour and III) CNF-C. In B: I) CNF-EC and II) ethyl cellulose.

3.1.3 Rheological assessment

The suspensions showed different behaviors, depending on the nanofibril production process and the raw material used. Rheological behavior of CNC-C and CNC-ENZ suspensions was Newtonian, while CNC-EC showed a shear thinning behavior. Greater pseudoplasticity was observed by increasing the concentration of CNF-EC, indicating a more complex interaction between these nanofibers. At low shear stresses, the elongated structure tends to

form networks and be more rigid, due to the hydrogen bonds between the nanofibrils. As the shear rate increases, the hydrogen bonds are broken and the network is disrupted, thus decreasing the viscosity until it reaches a plateau (Kayes et al., 2022; Nechyporchuk & Belgacem, 2016).

Table 2 shows the viscosity of the nanofibers suspensions at 50 s^{-1} , since this shear rate is typical in different processes such as swallowing and mixing. The viscosity tended to increase with increasing concentrations of nanofibrils, indicating a more interconnected and compact structure. The highest values of viscosity were observed in ethyl cellulose nanofibril suspensions, followed by the enzymatic process and, lastly, by the acid process. The increase in viscosity is related to the degree of fibrillation obtained by the processes, whether mechanical, chemical or enzymatic (Naderi, 2017). Thus, although the CNF-EC presented a fiber with a diameter as large as the CNF-ENZ, the former showed greater interaction between the fibers in relation to the others. The rheological behavior of CNFs is complex and influenced by several parameters, such as entanglement, branching, concentration, composition or specific surface area of CNFs (Koponen, 2020). Fig. 2 shows a lower dispersability and specific surface area of CNF-EC compared to other CNFs, mainly CNF-C (Sanchez-Salvador et al., 2022). This same behavior was also observed by specific surface area measurements (Fig S.3 and Table S1), which can be attributed to a lower affinity for the solvent (water) (Table 1).

Table 2. Viscosity values (η) at 50 s^{-1} of nanofiber suspensions.

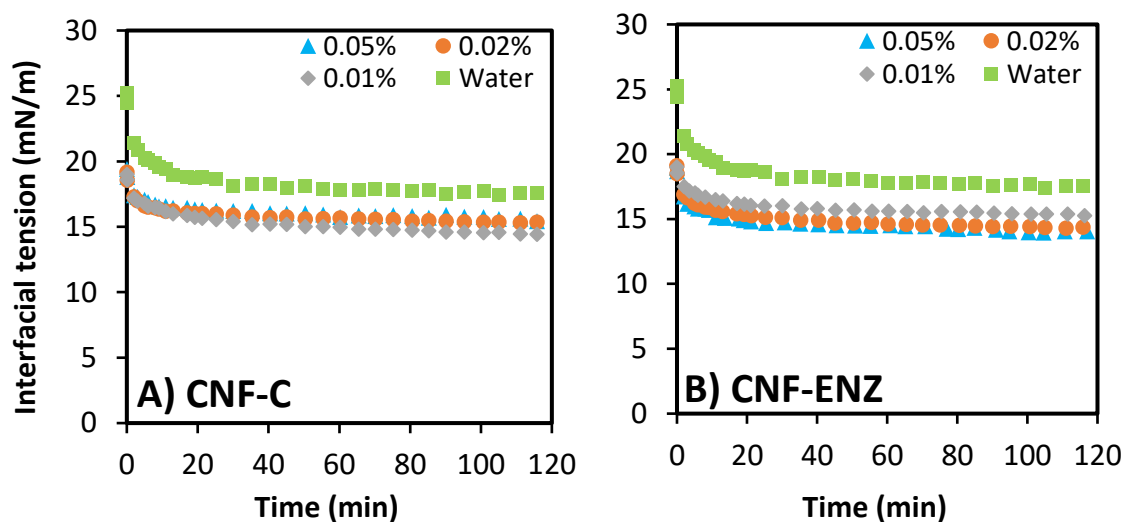
Concentration (% w/w)	η (mPa.s)		
	CNF-C	CNF-ENZ	CNF-EC
1.0	$3.00 \pm 0.08^{\text{Bb}}$	$6.52 \pm 0.20^{\text{Aa}}$	$7.31 \pm 1.07^{\text{Aa}}$
1.5	$3.10 \pm 0.05^{\text{Cb}}$	$6.33 \pm 0.05^{\text{Ba}}$	$10.40 \pm 1.52^{\text{Aa}}$
2.0	$3.63 \pm 0.18^{\text{Ca}}$	$6.30 \pm 0.04^{\text{Ba}}$	$9.56 \pm 1.57^{\text{Aa}}$
2.5	$3.51 \pm 0.10^{\text{Ca}}$	$6.38 \pm 0.14^{\text{Ba}}$	$12.30 \pm 0.87^{\text{Aa}}$
3.0	$3.83 \pm 0.24^{\text{Ca}}$	$6.46 \pm 0.05^{\text{Ba}}$	$11.40 \pm 4.52^{\text{Aa}}$

Different letters in the same line or column indicate significant differences ($p < 0.05$). Capital letters: differences among samples with different nanofiber manufacturing process and the same nanofibers concentration. Lowercase letters: differences between nanofiber concentrations, but the same manufacturing process.

3.2 Emulsions stabilized by cellulose nanofibers

3.2.1 Dynamic interfacial tension

Interfacial tension measurements were performed to assess whether CNFs were able to reduce the interfacial tension between water and oil, elucidating the stabilization mechanism of cellulose nanofibrils. The interfacial tension curves over time of all systems are shown in Fig. 4. The interfacial tension of sunflower oil droplet in pure water was measured as the control experiment. At equilibrium, the interfacial tension between the oil droplet and water was around 18 mN/m, while for the different CNF suspensions the values were lower, regardless of the CNF concentration. The initial interfacial tension values of water and CNF-EC systems were similar and higher than CNF-ENZ and CNF-C systems, around 25 mN/m. However, a progressive decrease of interfacial tension over time was observed, with a more pronounced decrease being evidenced at the highest concentration of the CNF-EC suspension (up to 12 mN/m). On the other hand, variation of interfacial tension over time and with increasing concentration was small in the presence of CNF-C and CNF-ENZ, showing the low surface activity of these nanofibers. On the other hand, the more pronounced reduction in interfacial tension over time and with increasing concentration of CNF-EC indicates that not only the Pickering-type mechanism could be responsible for the stabilization of emulsions in the presence of these nanoparticles.



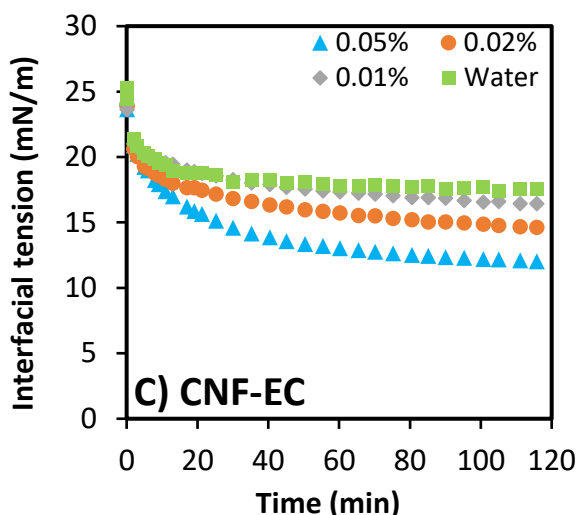


Fig. 4. Dynamic interfacial tension between sunflower oil and water or aqueous dispersions of cellulose nanofibers obtained from different treatments and sources (CNF-C, CNF-ENZ or CNF-EC).

Conventional emulsifiers can decrease the interfacial tension between the oil-water phases, favoring droplet breakage during the emulsification process and increasing the kinetic stability of emulsions (Wachira et al., 2016). Our results showed that the interfacial tension values between the aqueous suspensions of CNFs and the oil were lower when compared to the control system (water), although CNF-EC can further decrease the interfacial tension over time, as typical of conventional emulsifiers. However, nanofibrils can mainly irreversibly adsorb (high desorption energy) and organize themselves at the interface, forming a rigid structure that has the ability to prevent coalescence in a Pickering mechanism (Parajuli & Ureña-Benavides, 2022).

3.2.2 Droplet size distribution and confocal microscopy

The droplet size distribution and the mean diameter (D_{32}) of fresh emulsions and after 7 days of storage, stabilized by the different concentrations and types of cellulose nanofibers (CNF-C, CNF-ENZ and CNF-EC), are shown in Fig. S.1 and Table 3, respectively. All fresh emulsions, produced by pre-homogenization in the rotor-stator followed by homogenization in the microfluidizer, showed monomodal size distribution and small average droplet diameter (0.7- 1.1 μm). However, CNF-ENZ shows a distinct behavior (Fig. 5) since the fresh emulsions stabilized by this cellulose nanofibril showed flocculation and coalescence of the droplets. Absence of flocculation and coalescence was observed in CNF-EC stabilized emulsions, while

some flocculation was noticed in CNF-C (mainly at high concentration). In this sense, the type of process to obtain CNF affected droplets size of the emulsions, which became more evident after 7 days of storage.

Table. 3. Mean droplet diameter (D_{32}) of fresh O/W emulsions (day 0) and after 7 days of storage.

Nanofibrils concentration (%)	$D_{32}(\mu\text{m})$ CNF-C		$D_{32}(\mu\text{m})$ CNF-ENZ			$D_{32}(\mu\text{m})$ CNF-EC	
	0 day	7 days	0 day	7 days aged	7 days aged	0 day	7 days
		aged		Cream phase	Serum phase		aged
0.01%	0.71±0.22 ^{Aa}	0.69±0.28 ^{Aa}	1.09±0.11 ^{Aab}	1.38±0.22 ^{Aa}	0.88±0.23 ^{Ab}	0.81±0.16 ^{Aa}	0.72±0.04 ^{Aa}
0.02%	0.74±0.14 ^{Aa}	0.57±0.02 ^{Aa}	0.83±0.10 ^{Ba}	0.90±0.05 ^{Ba}	0.79±0.08 ^{Aa}	0.70±0.02 ^{Aa}	0.69±0.13 ^{Aa}
0.05%	0.67±0.04 ^{Aa}	0.56±0.07 ^{Aa}	1.12±0.04 ^{Aa}	1.31±0.05 ^{Aa}	0.99±0.22 ^{Aa}	0.72±0.03 ^{Aa}	0.69±0.02 ^{Aa}

Different letters indicate significant differences ($p < 0.05$) between D_{43} values. Capital letters: differences between different CNF concentration using the same type of CNF. Lower case letters: differences between different days of storage, but with the same concentration and type of CNF.

Mean diameter of the droplets stabilized by CNF-C and CNF-EC did not show significant differences over the 7 days of storage, maintaining the monomodal size distribution and without visual phase separation. However, a clear phase separation was observed in the CNF-ENZ stabilized emulsions. The increase in mean droplet size and a multimodal distribution of the droplets was observed at different concentrations of CNF-ENZ, in the two phases (cream and serum) formed during storage. This phase separation was favored by the larger initial droplet size of the emulsions stabilized by CNF-ENZ (Table 3) that can induce creaming (McClements, 2015).

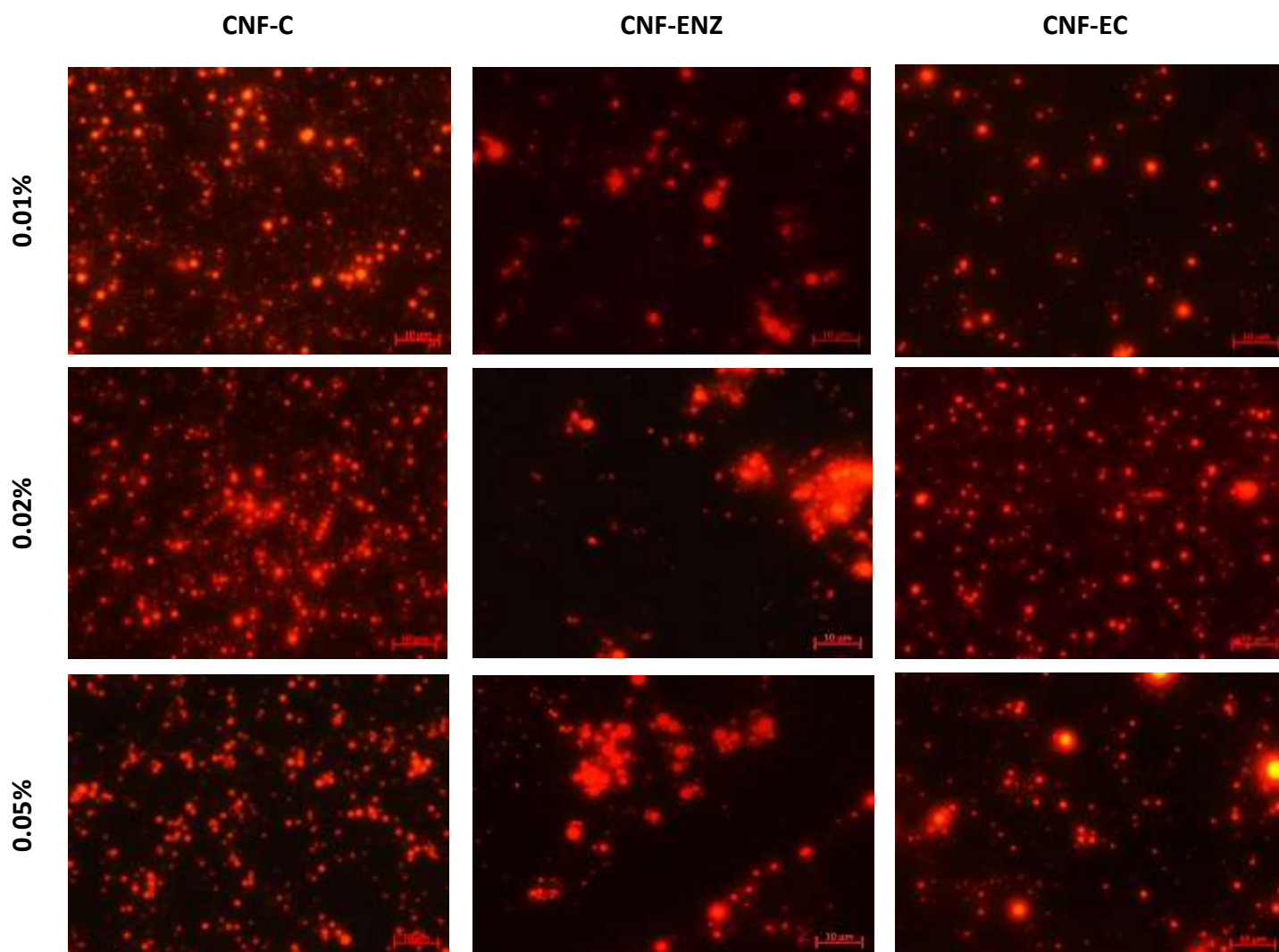


Fig. 5. Confocal micrographs of O/W fresh Pickering emulsions (red areas show oil phase stained with Red Nile fluorescent dye, black areas show aqueous phase). Scale: 10 μm .

3.2.3 Kinetic stability – laser scanning turbidimetry

The physical stability of the emulsions was determined from turbidimetric measurements, analyzing the backscattering profiles. The multiple light scattering technique (backscattering profiles) allows to detect emulsion destabilization phenomena before any effective visual observation (Dima & Dima, 2020). The backscattering (BS) profiles of the emulsions fresh and stored for 7 days at $25 \pm 2^\circ\text{C}$ are shown in Fig. 6. The fresh emulsions showed the following approximate mean values of BS: 50% for CNF-C, 40-25% for CNF-EC and the lowest values (30 -10%) for CNF-ENZ. The lower values of the emulsions stabilized by CNF-ENZ is due to the larger droplet size, as can be seen in the microscopy images (Fig. 5) and particle size distribution (Fig. S.1 and Table 3). It should be noted that the higher

concentrations of CNFs generally favored the reduction of backscattering values, mainly for CNF-ENZ.

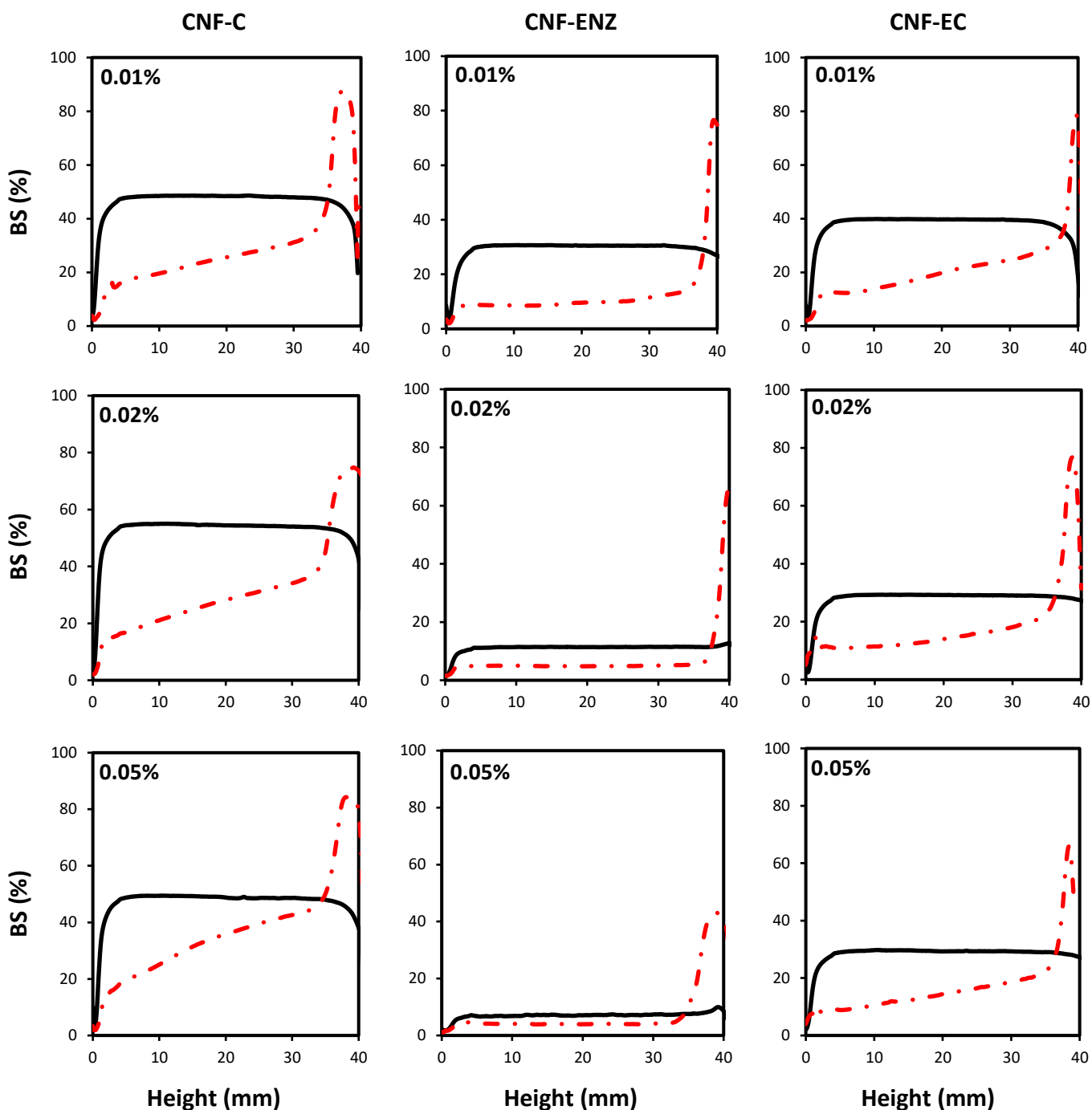


Fig. 6. Backscattering profiles of O/W emulsions stabilized by different types and concentration of CNF (CNF-C, CNF-ENZ or CNF-EC). Fresh emulsions (solid line) and after 7 days of storage (dashed red line).

BS values were evaluated as a function of the height of the measurement cell. Back scattering results showed that all emulsions presented a decrease in BS values at the bottom of the measuring cell and a pronounced increase at the top of the cell after 7 days of storage,

which is associated to phase separation. However, a clear phase separation was observed only for emulsions prepared with CNF-ENZ, while for CNF-C and CNF-EC systems only a slight creaming was visually observed (Fig. S.2). Images show that after 7 days of storage and after agitation, only emulsions stabilized by CNF-ENZ (Fig. S.2) were unstable, showing flocculation even soon after preparation. On the other hand, the emulsions that showed the greatest stability were those stabilized by CNF-C and CNF-EC. CNF-C were shorter and, consequently, more uniformly distributed in dispersion, facilitating the deposition onto the droplets of the emulsion. Although CNF-EC had a longer size and diameter as CNF-ENZ, the former showed the advantage of having surface activity (associated with the ethylation of cellulose), thus minimizing the difficulty of deposition on the droplets.

3.2.4 *In vitro* digestion

Emulsions stabilized by different types of CNF were subjected to *in vitro* digestion assays, with aliquots of gastric and intestinal digesta analyzed for droplet size distribution (Fig. 7) and microscopy (Fig. 8).

All emulsions showed an increase in droplet size in the gastric and intestinal steps (Fig. 7). The high ionic strength and the acidic conditions of the stomach environment decrease the net charge of the CNF particles, decreasing the electrostatic repulsion between the emulsion droplets and allowing their flocculation (Le et al., 2020; Liu et al., 2019). Furthermore, the presence of large oil droplets at the gastric phase suggests the simultaneous occurrence of an Ostwald ripening destabilization mechanism (Fig. 7) (Liu et al., 2019), as the Pickering particles at the interface should prevent the coalescence of the droplets. Despite the increase in droplet size of CNF-EC emulsions, microscopy images show less evident destabilization considering the small oil droplets at the end of the stomach step. As aforementioned, CNF-EC particles have interfacial properties that promote greater stability of CNF-EC emulsions in the harsh conditions of the gastric phase.

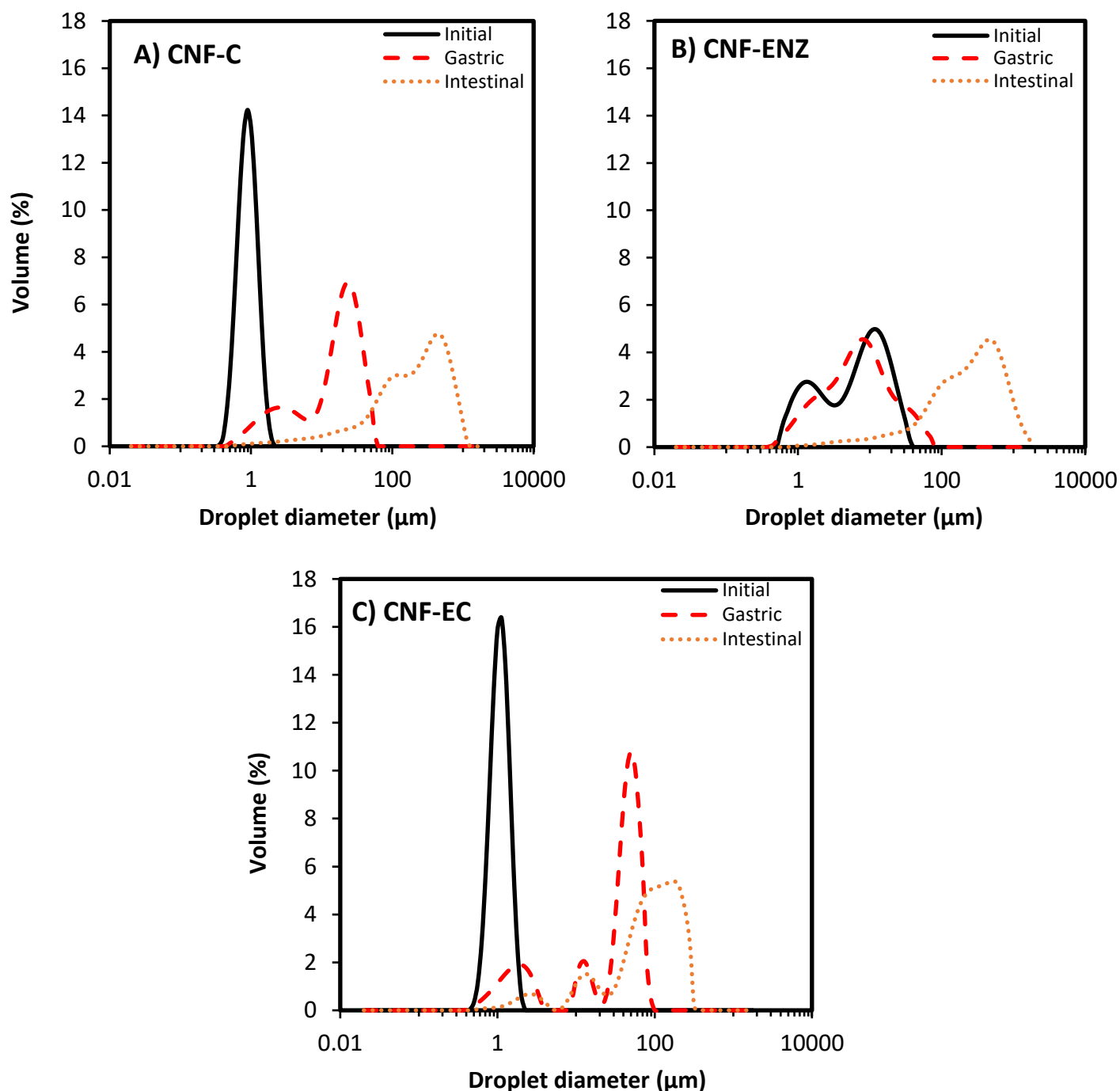
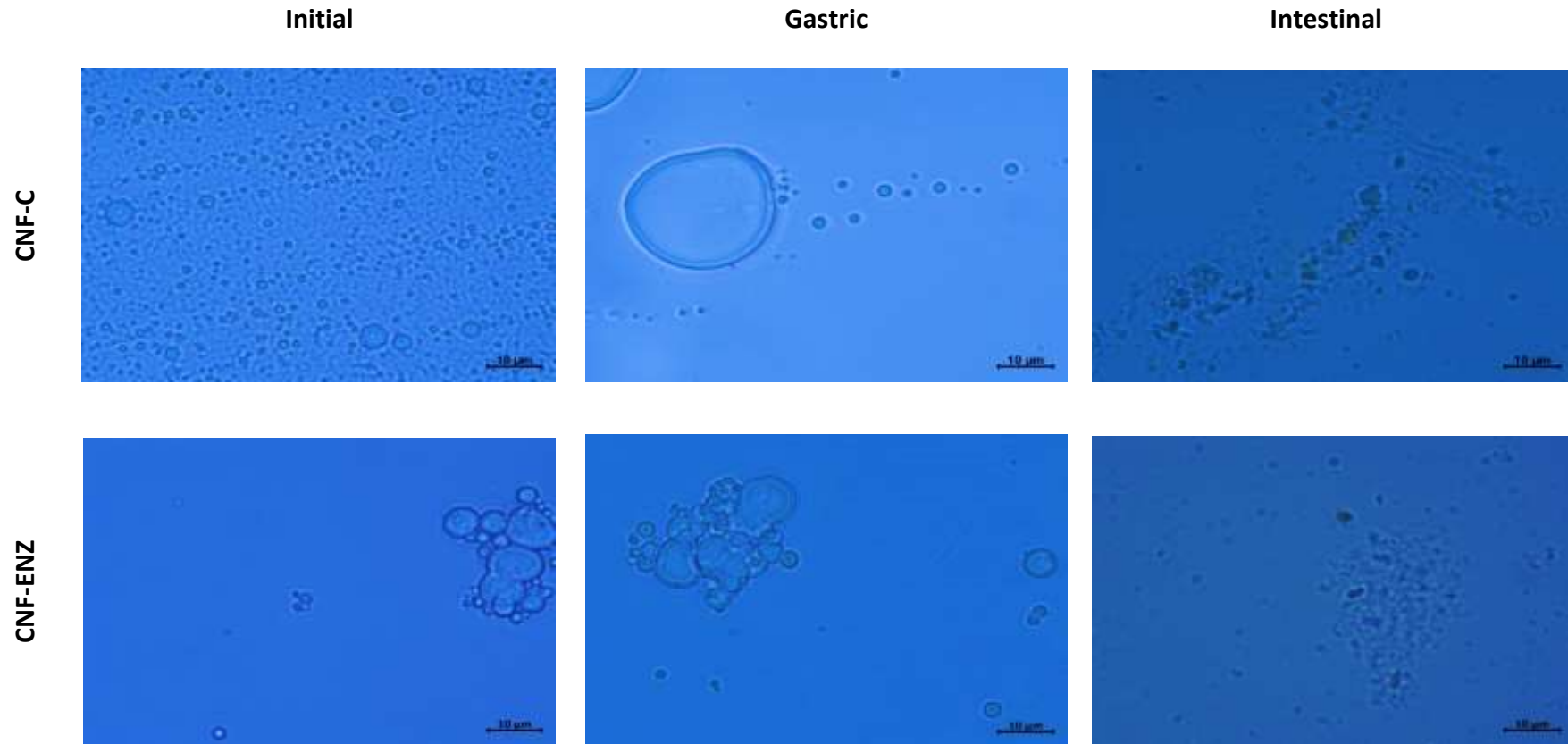


Fig. 7. Volume size distribution of the Pickering emulsions before digestion, after gastric and intestinal steps.

At the end of the gastric step, emulsions are diluted by adding SIF to the medium. At the beginning of the intestinal phase (5-10 minutes), as Pickering particles are not able to fully cover the surface of the droplets (Xia Li et al., 2022), pancreatic lipase adsorbs at the oil/water interface and promotes lipolysis and breakdown of the droplets into smaller structures, as observed by microscopy (Fig. 8). As lipid digestion proceeds, low molecular weight surfactants

(monoacylglycerol and diacylglycerol) are released. These molecules are able to remove and replace lipase adsorbed on the surface of oil droplets, which stabilizes the oil/water interface and stops the lipolytic process (Xia Li et al., 2022; Lu & Huang, 2020). Size distribution of the intestinal digesta was multimodal and presented larger size fractions ($>100\ \mu\text{m}$), although it was not possible to observe oil droplets in the microscopy images (Fig. 8) due to dilution effects.



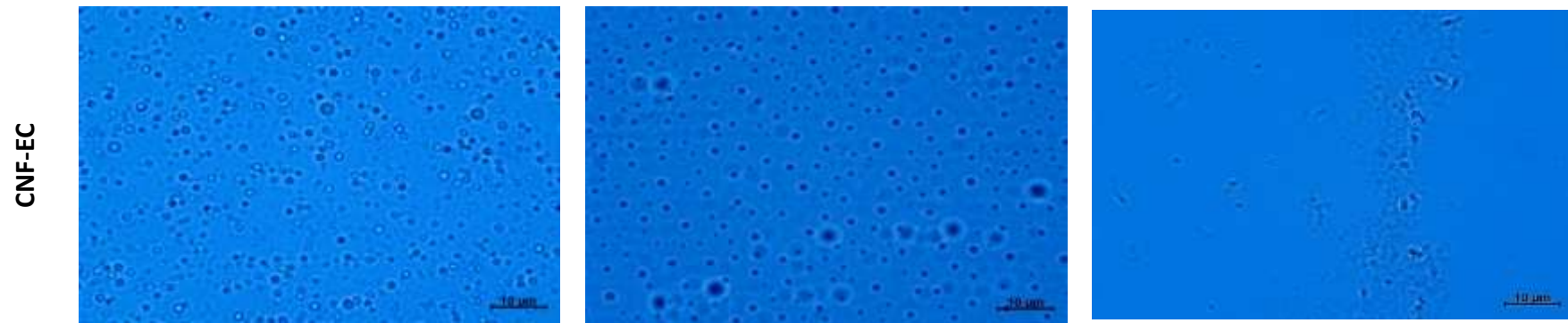


Fig. 8. Microscopy of the CNF-stabilized emulsions before digestion (initial) and after gastric and intestinal steps. Scale bar: 10 μm .

The extension of lipolysis was evaluated by quantifying the percentage of free fatty acids released (FFA) from intestinal digestion (Fig. 9). All CNF-stabilized emulsions showed a low amount of released FFA. CNF-EC emulsions showed the highest % FFA (around 20 % at the end of digestion), while CNF-C and CNF-ENZ systems presented similar and the lowest values (13-15 %). As observed by microscopy, CNF-EC emulsions had the smallest droplet size at the end of the gastric phase. Since lipolysis occurs at the surface of the droplets, the lipolysis rate increases with increasing surface area (or decreasing droplet size) (Oliveira Júnior & Cunha, 2022), explaining the highest %FFA of CNF-EC. In the small intestine environment, bile salts can also contribute to lipid digestion as they promote the orogenic displacement of emulsifiers at the surface of the droplets, which facilitates the adsorption of lipase (Corstens et al., 2017). Thereby, as CNF-EC emulsions are stabilized by a combination of Pickering and emulsifying mechanisms, their lipolysis was enhanced due to the presence of the bile salts in the medium. Otherwise, bile salts had no effect on the digestion of CNF-C and CNF-ENZ emulsions, as Pickering-type particles possess high desorption energies (Le et al., 2020).

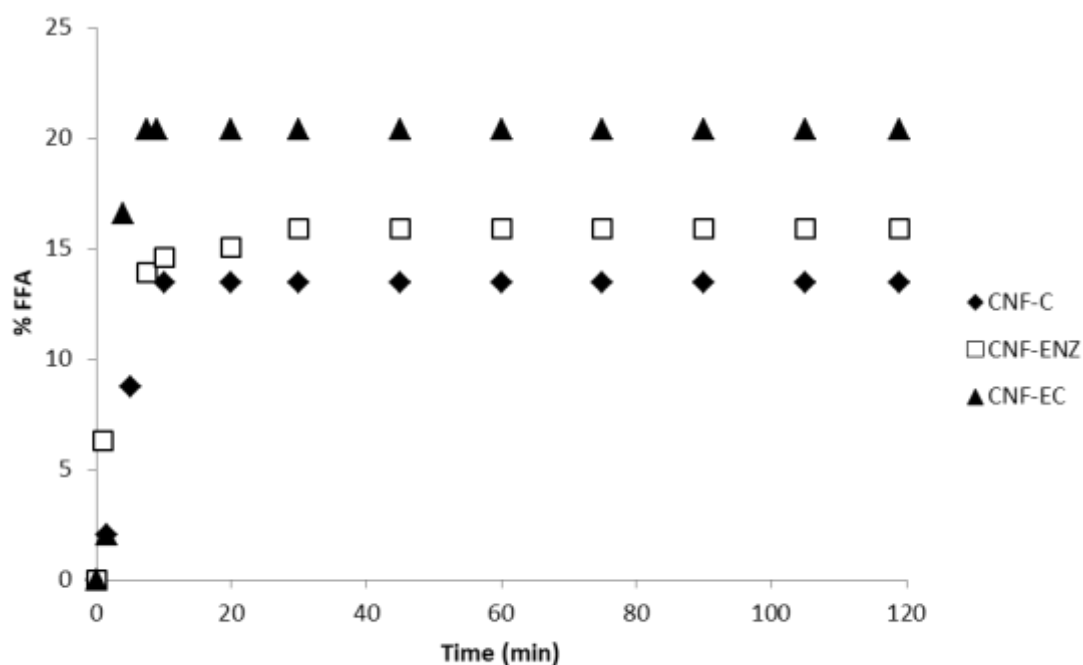


Fig. 9. Kinetics of free fatty acids (FFA) release under simulated intestinal conditions.

Cellulose nanofibers showed different characteristics and among them the most relevant are shown in Fig. 10. In order to draw a comparison between the effect of the

different nanofibers on the relevant properties associated with the stability and digestibility of the emulsions, the ratio between the value of a property for a given CNF and the calculated average value of the same property for the three CNFs was calculated. Thus, a value equal to 1 (called as reference) means that the value obtained for a given property is equal to the average value obtained for the three CNFs. The reference line allows observing how the variations of values in the characteristics of the cellulose nanofibers affect the stability of the emulsions, since the lowest TSI values (Turbiscan Stability Index) of CNF-C and CNF-EC mean more stable emulsions. CNF-C and CNF-ENZ showed no reduction in interfacial tension, being attributed a predominantly Pickering mechanism in the stabilization of the emulsions. On the other hand, CNF-EC showed surface activity, favoring the stability of the emulsion. In terms of zeta potential, no difference was observed between the nanofibers, while viscosity of nanofiber aqueous dispersions was related to their size. CNF-C had a smaller diameter and length, therefore, a lower viscosity than CNF-ENZ and CNF-EC. Considering these results, we believe that the good stability of CNF-EC is mainly associated with its surface activity. On the other hand, the good stability of CNF-C may be associated with the shorter length of the nanofibers, which can promote the formation of a network between the small droplets and favor greater stability of the emulsions. Regarding digestibility, emulsions stabilized by CNF-EC showed higher FFA release or lipolysis rate due to the smaller droplet size. On the other hand, although emulsions stabilized by CNF-ENZ showed a slightly lower digestion than CNF-C, CNF-ENZ is produced in a totally eco-friendly and sustainable way.

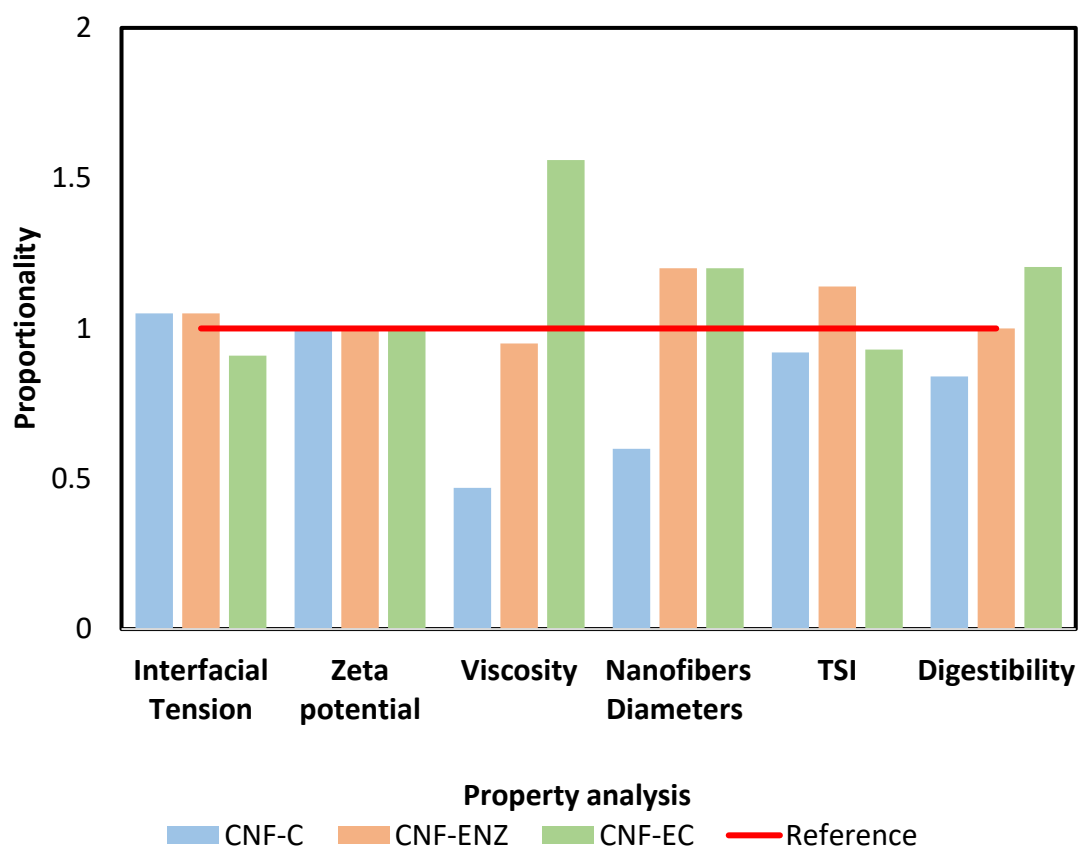


Fig. 10. Summary of the main characteristics of the nanofibers and their influence on emulsion stability and digestibility.

4. Conclusion

Chemical, enzymatic and mechanical processes were effective for the production of cellulose nanofibers from different materials. All nanofibers showed greater affinity with water (except CNF-EC). However, the intermediate contact angle values with both water and oil (wettability in both phases) showed that these particles are proper to stabilize oil-water emulsions. CNF-stabilized emulsions showed high stability in terms of coalescence, demonstrating that a Pickering-type was the main emulsion stabilizing mechanism, regardless of the concentration and type of CNF. However, emulsions stabilized by CNF-EC showed, in addition to the Pickering mechanism, reduction of the interfacial tension that improved the stability of the emulsion. The replacement of hydroxyl groups by ethyl groups proved to be an interesting modification of cellulose to produce an efficient emulsion stabilizer, which combined with mechanical treatment (for the formation of nanofibrils) produced an efficient emulsion stabilizer. On the other hand, the reduction in diameter and length of the fibers provided by the drastic

conditions of the acid process favor the formation of a network of droplets, stabilizing the emulsions. Regarding the digestion, these emulsions can be used for incorporation in low calorie foods, since they presented a low release of free fatty acids. Although emulsion stabilized by CNF-ENZ did not present a good stability, we believe that the improvement of the enzymatic hydrolysis conditions (different enzyme or more than one enzyme) should promote a more pronounced breakage of the nanofibers and the formation of a similar network of CNF-C. Thus, emulsions could be stabilized by nanofibers produced from an eco-friendly process, in addition to using an agroindustry waste in line with the concept of sustainability.

Author contributions

Raquel Costa Chevalier: Conceptualization, Methodology, Formal analysis, Investigation, Data curation, Writing - original draft, Visualization. **Fernando Divino Oliveira Júnior:** Conceptualization, Methodology, Formal analysis, Investigation, Data curation, Writing - original draft, Visualization. **Rosiane Lopes Cunha:** Conceptualization, Writing - review & editing, Supervision, Project administration, Funding acquisition.

Conflict of interest

The authors declare that they have no known competing financial interests or personal relationships that could have appeared to influence the work reported in this paper.

Acknowledgments

This study was financed by Coordenação de Aperfeiçoamento de Pessoal de Nível Superior – Brazil (CAPES) - Finance Code 001 and Fundação de Amparo à Pesquisa do Estado de São Paulo - FAPESP (2019/27354-3). Chevalier and Oliveira Júnior thanks CAPES-Brazil for the scholarship (88887.479720/2020-00; 88887.682855/2022-00). Cunha thanks CNPq (307094/2021-9) for the productivity grant. The authors thank the Laboratory for Surface Science (LCS) of the National Nanotechnology Laboratory (LNNano - CNPEM) (Campinas, Brazil) for AFM analyses.

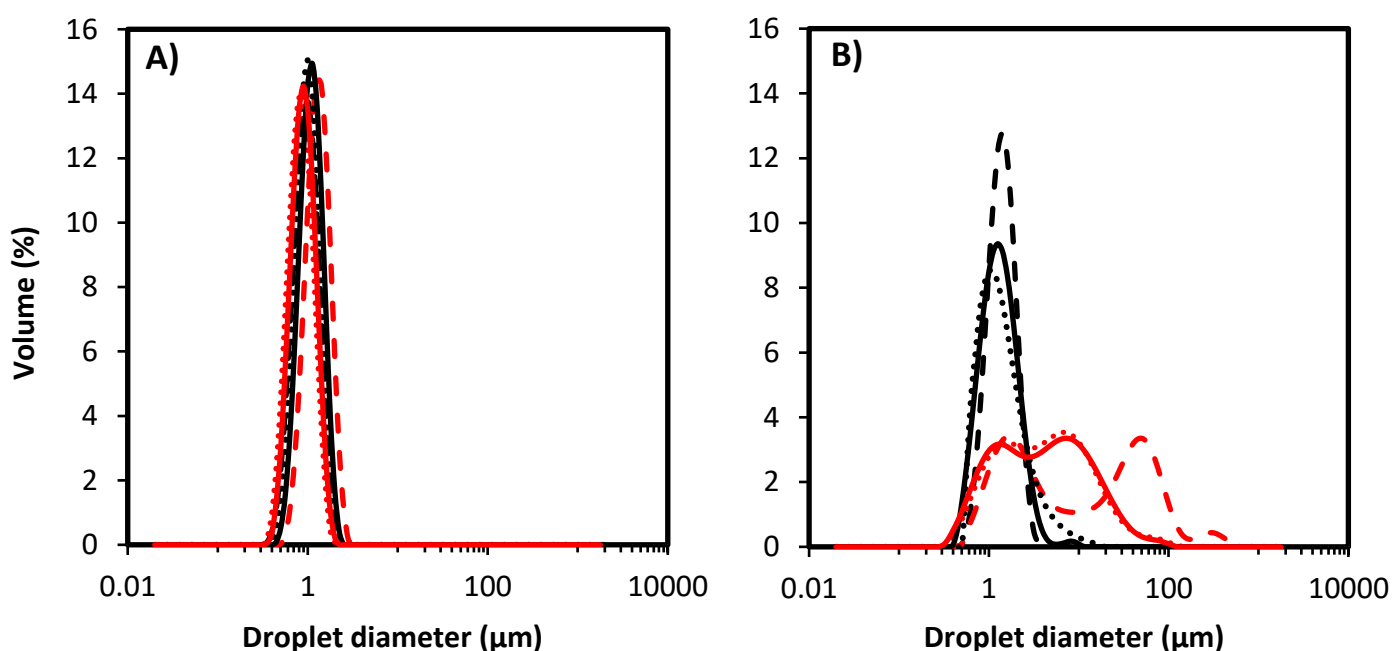
Supplementary Information

Table S.1 Specific surface areas of freeze-dried nanofibers.

	CNF-ENZ	CNF-EC
BET Surface Area (m²/g)	0.6005±0.0592 ^A	0.3723±0.0236 ^B
Langmuir Surface Area (m²/g)	0.8853±0.0904 ^A	0.5274±0.0290 ^B

Different letters in the same line indicate significant differences ($p < 0.05$) among samples with different nanofiber manufacturing process.

Figure S.1. Droplet size distribution of emulsions stabilized by different CNF. A) CNF-C; B) CNF-ENZ and C) CNF-EC. The concentrations of cellulose nanofibers were 0.01% (---), 0.02% (....) and 0.05% (___). Black line are fresh emulsions and red line are emulsions after seven days of storage. The droplet size distribution of CNF-ENZ after storage refers to the cream phase, since this emulsion separated into two phases.



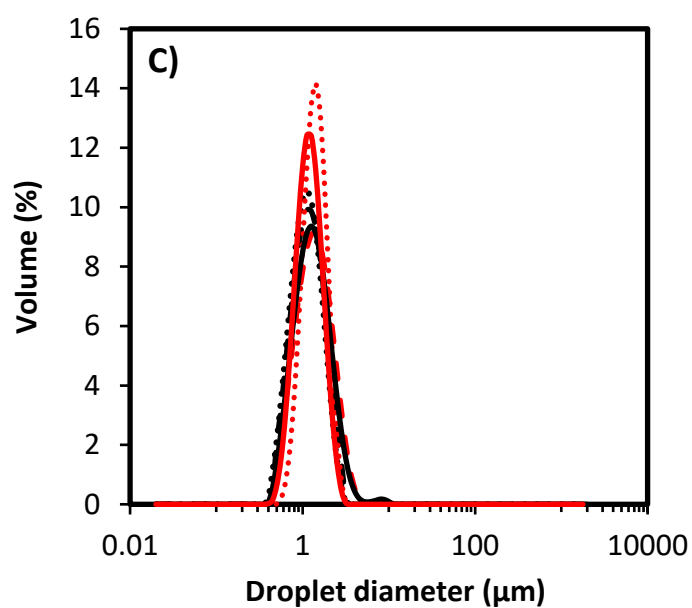
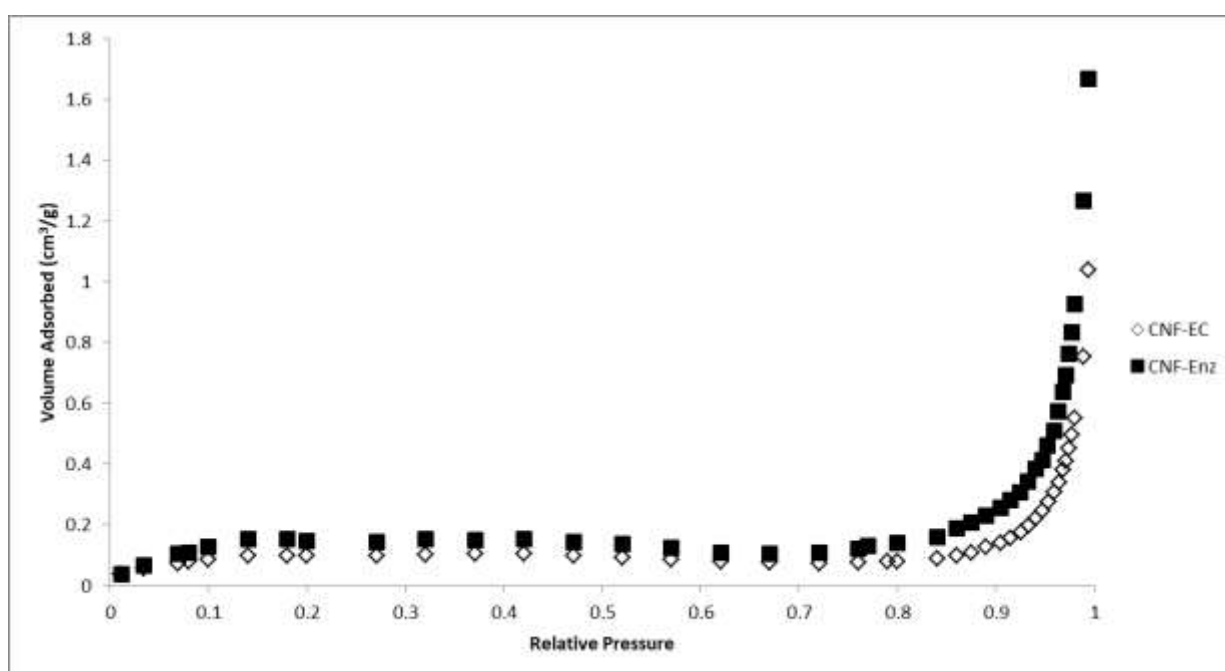


Figure S.2. Images of the measurement cells containing emulsions stabilized by different CNF at 0 and after 7 days of storage. After 7 days, the emulsions were manually homogenized.





Figure S.3 N₂ adsorption isotherms of cellulose nanofibers (CNF-ENZ and CNF-EC).



References

- Brodkorb, A., Egger, L., Alminger, M., Alvito, P., Assunção, R., Ballance, S., Bohn, T., Bourlieu-lacanal, C., Boutrou, R., & Carrière, F. (2019). INFOGEST static in vitro simulation of gastrointestinal food digestion. *Nature Protocols*, 14(April), 991–1014.
- Chevalier, Y., & Bolzinger, M. A. (2013). Emulsions stabilized with solid nanoparticles: Pickering emulsions. *Colloids and Surfaces A: Physicochemical and Engineering Aspects*, 439, 23–34. <https://doi.org/10.1016/j.colsurfa.2013.02.054>
- Corstens, M. N., Caltenco Osorio, L. A., Vries, R. De, Schroën, K., & Berton-carabin, C. C. (2017). Interfacial behaviour of biopolymer multilayers : Influence of in vitro digestive conditions. *Colloids and Surfaces B: Biointerfaces*, 153, 199–207. <https://doi.org/10.1016/j.colsurfb.2017.02.019>
- Costa, A. L. R., Gomes, A., Tibolla, H., Menegalli, F. C., & Cunha, R. L. (2018). Cellulose nanofibers from banana peels as a Pickering emulsifier: High-energy emulsification processes. *Carbohydrate Polymers*, 194(January), 122–131. <https://doi.org/10.1016/j.carbpol.2018.04.001>
- Czaikoski, A., da Cunha, R. L., & Menegalli, F. C. (2020). Rheological behavior of cellulose nanofibers from cassava peel obtained by combination of chemical and physical processes. *Carbohydrate Polymers*, 248(July), 116744. <https://doi.org/10.1016/j.carbpol.2020.116744>
- Dima, C., & Dima, S. (2020). Bioaccessibility study of calcium and vitamin D 3 co-microencapsulated in water-in-oil-in-water double emulsions. *Food Chemistry*, 303(January 2019), 125416. <https://doi.org/10.1016/j.foodchem.2019.125416>
- El Fawal, G., Abu-Serie, M. M., El-Gendi, H., & El-Fakharany, E. M. (2022). Fabrication, characterization and in vitro evaluation of disulfiram-loaded cellulose acetate/poly(ethylene oxide) nanofiber scaffold for breast and colon cancer cell lines treatment. *International Journal of Biological Macromolecules*, 204(February), 555–564. <https://doi.org/10.1016/j.ijbiomac.2022.01.145>
- Ho, T. M., Razzaghi, A., Ramachandran, A., & Mikkonen, K. S. (2022). Emulsion characterization via microfluidic devices: A review on interfacial tension and stability to coalescence. *Advances in Colloid and Interface Science*, 299(September 2021), 102541. <https://doi.org/10.1016/j.cis.2021.102541>
- Kaptay, G. (2006). On the equation of the maximum capillary pressure induced by solid particles to stabilize emulsions and foams and on the emulsion stability diagrams. *Colloids and Surfaces A*, 283, 387–401. <https://doi.org/10.1016/j.colsurfa.2005.12.021>
- Kayes, M., Farooq, A., Yinan, F., Chaudary, A., Rashedul, S., Zhao, Y., Ge, A., Wang, F., & Liu, L. (2022). Structure and rheological studies of phosphorylated cellulose nanofibrils suspensions. *Industrial Crops & Products*, 178(January), 114581. <https://doi.org/10.1016/j.indcrop.2022.114581>
- Kitamura, Y., Okawa, H., Kato, T., & Sugawara, K. (2016). Effect of ultrasound intensity on the size and morphology of synthesized scorodite particles. *Advanced Powder Technology*, 27(3), 891–897. <https://doi.org/10.1016/j.appt.2016.02.005>
- Koponen, A. I. (2020). The effect of consistency on the shear rheology of aqueous suspensions of cellulose micro- and nanofibrils: a review. *Cellulose*, 27(4), 1879–1897. <https://doi.org/10.1007/s10570-019-02908-w>

- Kumar, S., Tewatia, P., Samota, S., Rattan, G., & Kaushik, A. (2022). Ameliorating properties of castor oil based polyurethane hybrid nanocomposites via synergistic addition of graphene and cellulose nanofibers. *Journal of Industrial and Engineering Chemistry*, xxxx. <https://doi.org/10.1016/j.jiec.2022.02.035>
- Le, H. D., Loveday, S. M., Singh, H., & Sarkar, A. (2020). Gastrointestinal digestion of Pickering emulsions stabilised by hydrophobically modified cellulose nanocrystals : Release of short-chain fatty acids. *Food Chemistry*, 320(November 2019), 126650. <https://doi.org/10.1016/j.foodchem.2020.126650>
- Li, X., Kuang, Y., Jiang, Y., Dong, H., Han, W., & Ding, Q. (2022). In vitro gastrointestinal digestibility of corn oil-in-water Pickering emulsions stabilized by three types of nanocellulose. *Carbohydrate Polymers*, 277(August 2021), 118835. <https://doi.org/10.1016/j.carbpol.2021.118835>
- Liu, Ahmed, S., Sameen, D. E., Wang, Y., Lu, R., Dai, J., Li, S., & Qin, W. (2021). A review of cellulose and its derivatives in biopolymer-based for food packaging application. *Trends in Food Science & Technology*, 112(April), 532–546. <https://doi.org/10.1016/j.tifs.2021.04.016>
- Liu, B., Zhu, Y., Tian, J., Guan, T., Li, D., Bao, C., Norde, W., Wen, P., & Li, Y. (2019). Inhibition of oil digestion in Pickering emulsions stabilized by oxidized cellulose nanofibrils for low- calorie food design. *RSC Adv*, 9, 14966–14973. <https://doi.org/10.1039/c9ra02417d>
- Liu, Li, B., Du, H., Lv, D., Zhang, Y., & Yu, G. (2016). Properties of nanocellulose isolated from corncob residue using sulfuric acid , formic acid , oxidative and mechanical methods. *Carbohydrate Polymers*, 151, 716–724. <https://doi.org/10.1016/j.carbpol.2016.06.025>
- Lu, X., & Huang, Q. (2020). Stability and in vitro digestion study of curcumin- encapsulated in different milled cellulose particle stabilized Pickering emulsions. *Food & Function*, 11, 606–616. <https://doi.org/10.1039/c9fo02029b>
- Mahardika, M., Abral, H., Kasim, A., Arief, S., & Asrofi, M. (2018). Production of Nanocellulose from Pineapple Leaf Fibers via High-Shear Homogenization and Ultrasonication Melbi. *Fibers*, 6(28), 1–12. <https://doi.org/10.3390/fib6020028>
- McClements. (2015). *Food Emulsions*.
- McClements, D. J., Bai, L., & Chung, C. (2017). Recent Advances in the Utilization of Natural Emulsifiers to Form and Stabilize Emulsions. In *Annual Review of Food Science and Technology* (Vol. 8, pp. 205–236). Annual Reviews Inc. <https://doi.org/10.1146/annurev-food-030216-030154>
- Mohiti-Asli, M., & Lobo, E. G. (2016). Nanofibrous smart bandages for wound care. In *Wound Healing Biomaterials* (Vol. 2, pp. 483–499). Elsevier Inc. <https://doi.org/10.1016/B978-1-78242-456-7.00023-4>
- Naderi, A. (2017). Nanofibrillated cellulose : properties reinvestigated. *Cellulose*, 24(5), 1933–1945. <https://doi.org/10.1007/s10570-017-1258-1>
- Nagarajan, S., Skillen, N. C., Irvine, J. T. S., Lawton, L. A., & Robertson, P. K. J. (2017). Cellulose II as bioethanol feedstock and its advantages over native cellulose. *Renewable and Sustainable Energy Reviews*, 77(March), 182–192. <https://doi.org/10.1016/j.rser.2017.03.118>
- Nechyporchuk, O., & Belgacem, M. N. (2016). *Current Progress in Rheology of Cellulose Nano fi bril Suspensions*. <https://doi.org/10.1021/acs.biomac.6b00668>
- Oliveira Júnior, F. D., & Cunha, R. L. (2022). Soy protein-based delivery systems as

- carriers of trans-resveratrol : Bioaccessibility using different in vitro digestion models. *Food Research International*, 161(February), 111837.
<https://doi.org/10.1016/j.foodres.2022.111837>
- Pang, B., Liu, H., Liu, P., Peng, X., & Zhang, K. (2018). Water-in-oil Pickering emulsions stabilized by stearylated microcrystalline cellulose. *Journal of Colloid And Interface Science*, 513, 629–637. <https://doi.org/10.1016/j.jcis.2017.11.079>
- Parajuli, S., & Ureña-Benavides, E. E. (2022). Fundamental aspects of nanocellulose stabilized Pickering emulsions and foams. In *Advances in Colloid and Interface Science* (Vol. 299). Elsevier B.V. <https://doi.org/10.1016/j.cis.2021.102530>
- Patel, A. R. (2020). Functional and Engineered Colloids from Edible Materials for Emerging Applications in Designing the Food of the Future. *Advanced Functional Materials*, 30(18), 1–34. <https://doi.org/10.1002/adfm.201806809>
- Pelissari, F. M., Jose, P., & Menegalli, F. C. (2014). *Isolation and characterization of cellulose nanofibers from banana peels*. 417–432.
<https://doi.org/10.1007/s10570-013-0138-6>
- Sanchez-salvador, J. L., Campano, C., Balea, A., Tarr, Q., Blanco, A., & Negro, C. (2022). Critical comparison of the properties of cellulose nanofibers produced from softwood and hardwood through enzymatic , chemical and mechanical processes. *International Journal of Biological Macromolecules*, 205, 220–230.
<https://doi.org/10.1016/j.ijbiomac.2022.02.074>
- Tanpichai, S., Boonmahitthisud, A., Soykeabkaew, N., & Ongthip, L. (2022). Review of the recent developments in all-cellulose nanocomposites: Properties and applications. In *Carbohydrate Polymers* (Vol. 286). Elsevier Ltd.
<https://doi.org/10.1016/j.carbpol.2022.119192>
- Teixeira, E. de M., Pasquini, D., Curvelo, A. A. S., Corradini, E., Belgacem, M. N., & Dufresne, A. (2009). Cassava bagasse cellulose nanofibrils reinforced thermoplastic cassava starch. *Carbohydrate Polymers*, 78(3), 422–431.
<https://doi.org/10.1016/j.carbpol.2009.04.034>
- Tibolla, H., Pelissari, F. M., & Menegalli, F. C. (2014). Cellulose nanofibers produced from banana peel by chemical and enzymatic treatment. *LWT - Food Science and Technology*, 59(2P2), 1311–1318. <https://doi.org/10.1016/j.lwt.2014.04.011>
- Tsakani, J., Nuapia, Y., Mxolisi, M., Oranso, T., & Etale, A. (2022). Green chemistry approaches for extraction of cellulose nanofibers (CNFs): A comparison of mineral and organic acids. *Materials Today: Proceedings*.
<https://doi.org/10.1016/j.matpr.2022.02.088>
- Vicentini, N. M., Dupuy, N., Leitzelman, M., Cereda, M. P., & Sobral, P. J. A. (2005). Prediction of cassava starch edible film properties by chemometric analysis of infrared spectra. *Spectroscopy Letters*, 38(6).
- Wachira, W., Ho, K., Tey, B., & Chan, E. (2016). Effects of environmental factors on the physical stability of pickering- emulsions stabilized by chitosan particles. *Food Hydrocolloids*, 60, 543–550. <https://doi.org/10.1016/j.foodhyd.2016.04.023>

CAPÍTULO IV

**ANTIMICROBIAL POTENTIAL OF OREGANO ESSENTIAL OIL VEHICULATED IN
PICKERING CELLULOSE NANOFIBERS- STABILIZED EMULSIONS**

Manuscript prepared to be submitted to International Journal of Biological
Macromolecules

Antimicrobial potential of oregano essential oil vehiculated in Pickering cellulose nanofibers- stabilized emulsions

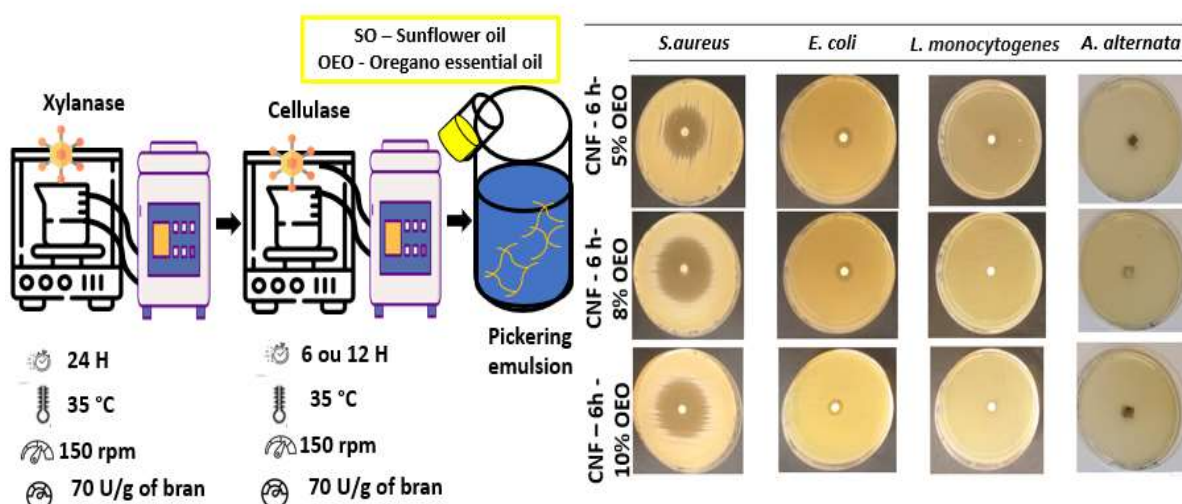
Raquel Costa Chevalier¹, Naara Aparecida Almeida², Liliana de Oliveira Rocha², Rosiane Lopes Cunha^{1*}

¹Laboratory of Process Engineering (LEP), Department of Food Engineering and Technology (DETA), School of Food Engineering (FEA), University of Campinas (UNICAMP), 13083-862, Campinas, São Paulo Brazil.

²Food Microbiology Laboratory I, Department of Food Science and Nutrition, School of Food Engineering (FEA), University of Campinas (UNICAMP), 13083-862, Campinas, São Paulo, Brazil.

* Corresponding author: rosiane@unicamp.br

Graphical abstract



Highlights

- Cellulose nanofibers were obtained by hydrolysis using different enzymes and process time;
- Droplet sizes and emulsion stability depended on the composition of the oil phase and cellulose nanofibers properties.
- The mixture of oregano essential oil and sunflower oil was used as the oily phase, showing good antimicrobial activity mainly against the bacteria *S. aureus* and *E. coli* and the fungus *A. alternata*.

Abstract

Essential oils show several biological properties, such as antimicrobial activity, but have limitations regarding their availability and stability. To maximize their antimicrobial

effect and protection against environmental conditions, Pickering-type emulsions were used to vehiculate oregano essential oil using cellulose nanofibers as emulsion stabilizers. Enzymatic hydrolysis was used to produce CNF from a food industry waste (cassava peel), obtaining an environmentally sustainable emulsifier. The differences in the properties of the nanofibers obtained and how these properties affect the stabilization of the emulsions were evaluated. Excellent antimicrobial activity was observed, mainly in emulsions, highlighting the ability of these systems to inhibit the growth of microorganisms. An improvement in the stability of emulsions was observed when using a mixture of oils, which is extremely advantageous considering costs and greater stability to heat treatments, since the desired antimicrobial activity was maintained. Furthermore, these systems could be incorporated into biodegradable materials used in packaging.

Keywords: antimicrobial activity; enzymatic hydrolysis; Pickering emulsions.

1. Introduction

Pickering emulsions are emulsified systems stabilized by colloidal particles, such as starch, chitosan and cellulose. The stabilization of these systems occurs from different steps. First, irreversible adsorption of particles occurs at the oil-water interface hindering phase separation. Then, the aggregation of these particles occurs in the continuous phase forming a network, and finally, bridges are built between the colloidal particles generating a three-dimensional network (Y. Liu et al., 2023; Peddireddy et al., 2016). Unlike conventional emulsified systems, Pickering emulsions have, in theory, high stability against coalescence, although they may be susceptible to other destabilizing mechanisms (Dizaj et al., 2016). Therefore, improving the stability of these emulsions is still a challenge. Some factors such as the concentration of the colloidal particles, oil and aqueous phase, as well as the conditions of the emulsification process, directly affect the Gibbs energy of the system and can lead to phase separation from different destabilization mechanisms (Feng et al., 2023). Other factors that can influence the properties of Pickering emulsions include particle size and shape (Sun et al., 2022).

Cellulose is the most abundant and widely distributed biopolymer in nature. It can be found in plant fibers, marine plants, algae, fungi, invertebrates and bacteria

(Czaikoski et al., 2020; Purves, 1954). Cellulose nanofiber (CNF) is one of the ideal sustainable sources of colloidal particles, especially when based on the reuse of agro-industrial waste (Y. Liu et al., 2023). Cassava (*Manihot esculenta*) is a root crop widely cultivated in several countries, generating a large amount of waste such as husks and residual bagasse during the production of cassava starch or other food products. Consequently, the use of cassava waste in the production of CNF is promising within the concept of sustainability.

Regarding morphology, CNFs have in their structure at least one of their dimensions on the nanometer scale, therefore being suitable for stabilizing micrometer-sized oil droplets typical of food products. Different processes can be used to produce CNF, such as chemical, enzymatic and physical processes. Among these, the enzymatic process stands out as an ecofriendly and sustainable approach that reduces the generation of toxic waste. Several studies suggest that the combination of enzymes can enhance accessibility to the cellulosic matrix, thus facilitating the production of cellulose nanofibers (Campos et al., 2013; Ceaser & Chimphango, 2021; J. Hu et al., 2018; Rossi et al., 2021). Although it is considered an expensive process, the enzyme concentration to obtain good performance is very low, in the range of $\mu\text{l/g}$ of pulp (Perzon et al., 2020). Therefore, under optimized processing conditions, it becomes an advantageous technique.

Faced with the immense demand for more sustainable processes, in addition to the search for healthier foods, the use of natural compounds to control microorganisms has gained prominence. Essential oils (EOs) are aromatic and volatile oily liquids extracted from specific parts of plants. Several essential oils have antibacterial, antifungal, antiviral and antioxidant properties (Zhou et al., 2018). Among these, oregano essential oil (OEO), from *Origanum vulgare* (*Lamiaceae*), has antioxidant and antimicrobial activity, probably due to the presence of carvacrol and thymol. Furthermore, it shows other associated benefits such as antiproliferative, anti-inflammatory and antidiabetic effects, in addition to having cancer suppressive activity (Leyva-I et al., 2017; Viana et al., 2019). Due to its high volatility, the use of OEO combined with an oil showing higher vapor pressure as part of the composition of the oily phase of emulsified systems is an interesting alternative to overcome drawbacks arising from certain process conditions. OEO easily evaporates or decomposes during

food processing (e.g., heat treatment), drug formulation, and incorporation into biodegradable films, due to direct exposure to heat, pressure, light or oxygen (Fakhreddin et al., 2013). Therefore, in order to maximize the antimicrobial action of OEO and reduce costs, the mixture of oils vehiculated in emulsions is the proposed strategy to be used for conservation of food products. However, before applying these emulsions, it is necessary to know the CNF stabilization mechanisms and the antimicrobial action of OEO to understand their advantages and limitations. In this sense, the objective of this study is to produce stable Pickering emulsions, with OEO as part of the oily phase, for subsequent application in the development of biodegradable coatings and packaging for potential use in food products.

2. Materials and methods

2.1 Materials

Crushed cassava husk was kindly donated by Plaza Ind. Com. Ltda (Brazil). Soybean oil was kindly donated by Cargill (Brazil) and OEO was purchased from Ferquima (Brazil). All other chemicals used were of analytical grade.

2.2 Cellulose nanofibers production

2.2.1 Raw material preparation

First, the crushed cassava husk was washed in running water, subsequently sanitized with sodium hypochlorite solution (250 ppm) for 10 min and dried in a forced convection oven at 50 °C for 48 h. This material was then ground in a knife mill and minced in a high-performance professional blender (Metalúrgica Siemens Ltda, Brazil). The material sieved through an opening of 0.15 mm (100-mesh) was subjected to the chemical pre-treatment described in section 2.2.2.

2.2.2 Alkaline pre-treatment

Minced cassava peels were subjected to alkaline treatment with a KOH solution (5 % w/v) in a ratio of 1:18 (peel samples: KOH solution) at 25 °C under mechanical agitation for 14 h (Czaikoski et al., 2020). These suspensions were then subjected to centrifugation (15,345×g /15 °C/15 min). Insoluble material was separated, added with distilled water and centrifuged again. This procedure was carried out until the color of supernatant no longer changed. The remaining insoluble residue was added to distilled

water and the pH adjusted to 7.0 using sulfuric acid (6.5 M) before being subjected to enzymatic hydrolysis (section 2.2.3).

2.2.3 Enzymatic hydrolysis

Enzymatic hydrolysis was carried out in two steps, using two different enzymes. First, Erlenmeyer flasks containing 15% substrate (material obtained after alkaline treatment) in 0.1 M acetate buffer (pH 7) were placed on a thermostatic shaker (temperature of 35 °C) for 10 min, so that the medium reached thermal equilibrium. Then, the xylanase enzyme (concentration of 70 U/g of bran) was added to the mixture, which was maintained at the same temperature for 24 h under agitation (150 rpm). After this period, the suspensions were placed in a thermostatic bath at 80 °C for 30 min to denature the enzyme. After cooling, the cellulase enzyme (concentration of 70 U/g of bran) was added. The same pH and temperature conditions as the first hydrolysis were maintained for 3, 6, 12 and 24 hours. Then, the residual pulp was washed with deionized water and the solid was separated by centrifugation (10,864×g, 5 °C, 15 min) and resuspended in deionized water (Heloisa Tibolla et al., 2014). Finally, this suspension was subjected to ultrasonic treatment (QR 750 W, Ultronique, Brazil) for approximately 20 minutes with a power of 300 W, before being stored at 4 °C in a sealed container.

2.3 Characterization of nanofibers

2.3.1 Morphology

The morphology of nanofibers was evaluated by atomic force microscopy (AFM). AFM images were acquired on a Microscope Park Systems, model NX-10 (Suwon, Korea) equipped with a Si nano sensor probe manufactured with a spring constant of 42 N.m⁻¹. The resonance frequency was about 320 kHz and the acquired images were treated with the GWYDDION software version 2.4. In order to determine the average size of CNFs, 20 measurements of diameter and length were taken from the AFM images.

2.3.2 Zeta potential

Zeta potential was determined using the Zetasizer model Nano ZS from Malvern Instruments Ltd. (United Kingdom, U.K) at a detection angle of 173°. Zeta potential measurements were performed at room temperature (25 °C) for each sample. The zeta potential of CNFs suspended in Milli-Q water (0.01% w/w) was determined in triplicate.

2.3.3 Fourier-transform infrared spectroscopy (FTIR)

The analysis of the functional groups in cassava husk flour and CNFs was performed by infrared absorption spectroscopy (4000 to 650 cm^{-1}). A Fourier-transform infrared spectrometer (FTIR), Perkin Elmer Spectrum One, equipped with a UATR (universal attenuated total reflectance) accessory was used (Vicentini et al., 2005).

2.4 Preparation of emulsions

The oily phase was composed of sunflower oil (SO) and OEO, while the aqueous dispersion of CNF (0.01% w/w) was the continuous phase. The minimum concentration of CNF was determined based on preliminary tests in order to obtain emulsions without phase separation immediately after their preparation. The oil mixture was made prior to emulsification in ratios of 5:5, 8:2 and 10:0 OEO: SO. The oil-in-water emulsions were first prepared by homogenizing the oil mixture (10% w/w of OEO + SO) and aqueous phase (90% w/w) in a rotor-stator (Ultra Turrax T18, IKA, Germany) at 13,000 rpm for 5 min. After pre-emulsification, the emulsions were subjected to homogenization in a microfluidizer (Microfluidic, LM20, USA) for 3 cycles at 15,000 psi.

2.5 Characterization of Pickering emulsions

2.5.1 Dynamic interfacial tension

The interfacial tension between the aqueous and oil phases was evaluated at 25 °C using a Tracker-S tensiometer (Teclis, France) by the pendant drop method for 60 min. Such analyzes aimed to evaluate the effect of 0.01% (w/w) CNF as the aqueous phase and different oil compositions (5:5, 8:2 and 10:0 OEO:SO) on the interfacial tension of the water-oil interface over time. A syringe was used and the tests were carried out by forming a drop of oil (25 μL) in the CNF suspension (aqueous phase). Measurements were performed in triplicate.

2.5.2 Screening for antimicrobial activity

The disk diffusion method was used to screen the antimicrobial activity of OEO, SO and different emulsions. The experiment was performed in accordance with the National Committee for Clinical Laboratory Standards (Wayne, 2002, 2015). In brief, bacterial colonies were reactivated overnight at 37 °C and the bacterial suspensions were prepared at 10^8 cells/mL in saline solution using the 0.5 McFarland scale. Bacteria *Staphylococcus aureus* ATCC 6538, *Escherichia coli* ATCC 11229 and *Listeria monocytogenes* ATCC 7644 were tested. Afterwards, 100 μL of the suspensions were

spread evenly on the surface of Mueller Hinton agar (MHA) and allowed to dry for five minutes. Sterile filter paper discs (Whatman No. 1, Brazil) were placed individually on the surface of the MHA, and 20 µl of OEO:SO mixtures (0:10; 5:5, 8:2 and 10:0) or emulsions with different oil compositions, were added. Subsequently, the cultures were incubated for 24 h at 37 °C. The diameters (mm) of the inhibition zones were measured and calculated with three replicates for each treatment. The control value was deducted from the sample means. As a negative control, bacteria were grown on MHA without any treatment and as a positive control, chloramphenicol was added to the culture medium. Diameters of the inhibition zones of the extracts were interpreted as sensitive (>18 mm), intermediate (14–17 mm), and resistant (<14 mm) (Mohamed et al., 2020).

To evaluate the activity of OEO, SO and different emulsions against fungi, *A. alternata* ATCC 8739 was selected, due to its importance in the spoilage of several fruits and vegetables. The fungus suspension was adjusted to 1×10^5 spores/mL, using a hemocytometer, and 100 µl of the suspension was spread on Potato Dextrose Agar (PDA). A sterile disk of 6mm containing 20 µL of the tested sample concentrations was transferred to the cultures. Tested concentrations showing inhibition halos equal to or greater than 10 mm were considered effective against *A. alternata* (Ahmet et al., 2002). As a negative control, *A. alternata* was grown in PDA without any inhibitor. As a positive control, thiabendazole (0.3g/L) was used.

2.5.3 Particle size distribution

Droplet size distribution was determined by using a Mastersizer 2000 (Malvern Instruments Ltd, Malvern, UK) with a rotational speed at 1750 rpm. Water was used as a dispersant and ultrasound was applied for 2 min (before introducing the sample) to avoid the presence of bubbles. The droplet size was expressed as the mean volume diameter (D_{43}), calculated according to Eq. (1). The polydispersity (*Span*) was also evaluated according to Eq. (2). Measurements were performed on freshly prepared emulsions and after 7 days of storage in triplicate.

$$D_{43} = \frac{\sum n_i d_i^4}{\sum n_i d_i^3} \quad (1)$$

$$Span = \frac{(D_{90} - D_{10})}{D_{50}} \quad (2)$$

where n_i is the number of droplets with diameter D_i , and D_{10} , D_{50} and D_{90} are diameters at 10, 50 and 90% of cumulative volume, respectively.

2.5.4 Optical microscopy

The microstructure of the emulsion was observed under an optical microscope (Axio Scope.A1, Carl Zeiss, Germany) with a 100x oil immersion objective lens. Images were captured using AxioVision Rel software 4.8 (Carl Zeiss, Germany).

2.5.5 Kinetic stability – laser scanning turbidimetry

Emulsion stability was monitored using the Turbiscan ASG optical scanning instrument (Formulaction, France). Emulsions were placed in flat-bottomed cylindrical glass tubes (140 mm height; 16 mm diameter) and stored at 25 ± 2 °C. Backscattered light at 880 nm was measured in fresh emulsions and after 7 days of storage. A plot of backscattered light, BS (%), was performed on the y-axis and the sample height (mm) on the x-axis. A sample height of 0 mm corresponds to the bottom of the measuring cell. Measurements were performed in triplicate. A sample height of 0 mm corresponds to the bottom of the measuring cell. The Turbiscan Stability Index (TSI), calculated as the sum of all destabilization processes in the sample along the measurement cell, was quantified according to Eq. (3).

$$TSI = \sum_j |scan_{ref}(h_j) - scan_i(h_i)| \quad (3)$$

2.5.6 Rheological assessment

Rheological behavior of the emulsions was studied using a stress-controlled rheometer (AR1500ex, TA Instruments, England) at 25 °C. Flow curves were obtained using a rough plate (6 cm diameter, 0.208 mm gap, 2° cone truncation) by an up-down-up step program with shear rate ranging from 0 to 50 s^{-1} . Emulsions were evaluated immediately after their preparation, in triplicate at 25 °C.

2.6 Statistical analysis

To compare the differences between the mean values obtained for the properties of the different CNFs, an analysis of variance (ANOVA) and a Tukey test of

multiple comparisons were performed with a significance level of 5% using the Statistica 7.0 software (StatSoft Inc., Tulsa, Oklahoma, USA).

3. Results and discussion

3.1 Production and characterization of CNFs

Cellulose hydrolysis using xylanase to produce nanofibers has been previously optimized in terms of pH, temperature, enzyme and substrate concentration (Tibolla et al., 2017). The best conditions to produce nanofibers from banana bran in terms of yield and physical properties have been used to produce nanofibers from cassava peel (R. C. Chevalier et al., 2024). However, cellulose nanofibers obtained from enzymatic hydrolysis (using only xylanase) presented thicker and longer nanofibers compared to CNFs produced from acidic chemical process. Longer nanofibers produced from the later process were better emulsion stabilizer than shorter and thicker CNFs. The role of xylanase is to remove residual hemicellulose (Dias et al., 2022) and facilitate the action of cellulolytic enzymes, but it does not act directly on the breakdown of cellulose. Therefore, in order to improve CNFs properties, a two-step hydrolysis process was used in the present study. In the first step, xylanase was used, while cellulase was evaluated in the second hydrolysis carried out at different process times to obtain CNFs characteristics more favorable for stabilizing emulsions and reinforcing nanocomposite films (Rossi et al., 2021). Addition of cellulases after xylanase in a second hydrolysis step improves the overall hydrolysis yield, potentially reducing the total enzyme dose. Cellulase also acts by increasing the hydrolysis of carbohydrates (cellulose and hemicellulose), which can efficiently loosen the structure of materials due to the breakdown of cellulose into smaller molecules (Hefferon et al., 2020; Lao et al., 2020). The nanofibers obtained were deeply characterized before being applied as emulsion stabilizers.

3.1.1 Morphology and zeta potential

AFM micrographs of CNFs (Fig. 1) provided insight into the morphological changes of CNFs produced at different times of enzymatic treatment (3, 6, 12 and 24 h) with cellulase. In general, the nanofibers appeared as a network of long and tangled cellulosic filaments. However, differences in the structure of nanofibrils can be observed depending on the enzymatic hydrolysis time. At the lower and upper limits of the

hydrolysis time (Fig. 1 A), distinct behaviors were observed. The nanofibers were agglomerated and closed in the shortest time, while the fibers were quite isolated in the longest hydrolysis time. CNFs produced at intermediate times (Fig. 1 B) showed fibers more similar to those produced by acid chemical hydrolysis (R. C. Chevalier et al., 2024). Considering these results, the CNFs produced at intermediate times of 6 (CNF- 6h) and 12 (CNF- 12h) h were further evaluated for application in emulsions. From AFM images, the diameter and length of nanofibrils were measured based on image processing. Although the length shows a high standard deviation (given the difficulty of measurement), the values presented serve as a guide to evaluate the differences between the aspect ratio of CNFs. Table 1 shows the mean values of diameter, length and aspect ratio, in addition to the zeta potential of the CNFs. The smallest diameters and largest lengths of the nanofibers, with a consequent higher aspect ratio, were observed after 6 h of hydrolysis. With increasing hydrolysis time, more pronounced breakage (shorter length) and an increase in diameter (2.61 nm) were observed, which can be associated with the aggregation of nanofibers. Aspect ratio was considerably high for CNF- 6 h, with a value higher than 1,000. It is noteworthy that the performance of CNFs to be used as reinforcing material in polymeric matrices is measured by their aspect ratio (Leite et al., 2017). The zeta potential is related to the surface charge of the particles in a given medium and the evaluation of this property can help verify the performance of nanofibers as, for example, reinforcing agent in films and emulsion stabilizer. The zeta potential values of the nanofibers, although statistically different, presented close values between -36 and -43 mV at pH 7, indicating electrostatic repulsion between droplets covered by CNF and favored kinetic stability of the emulsion.

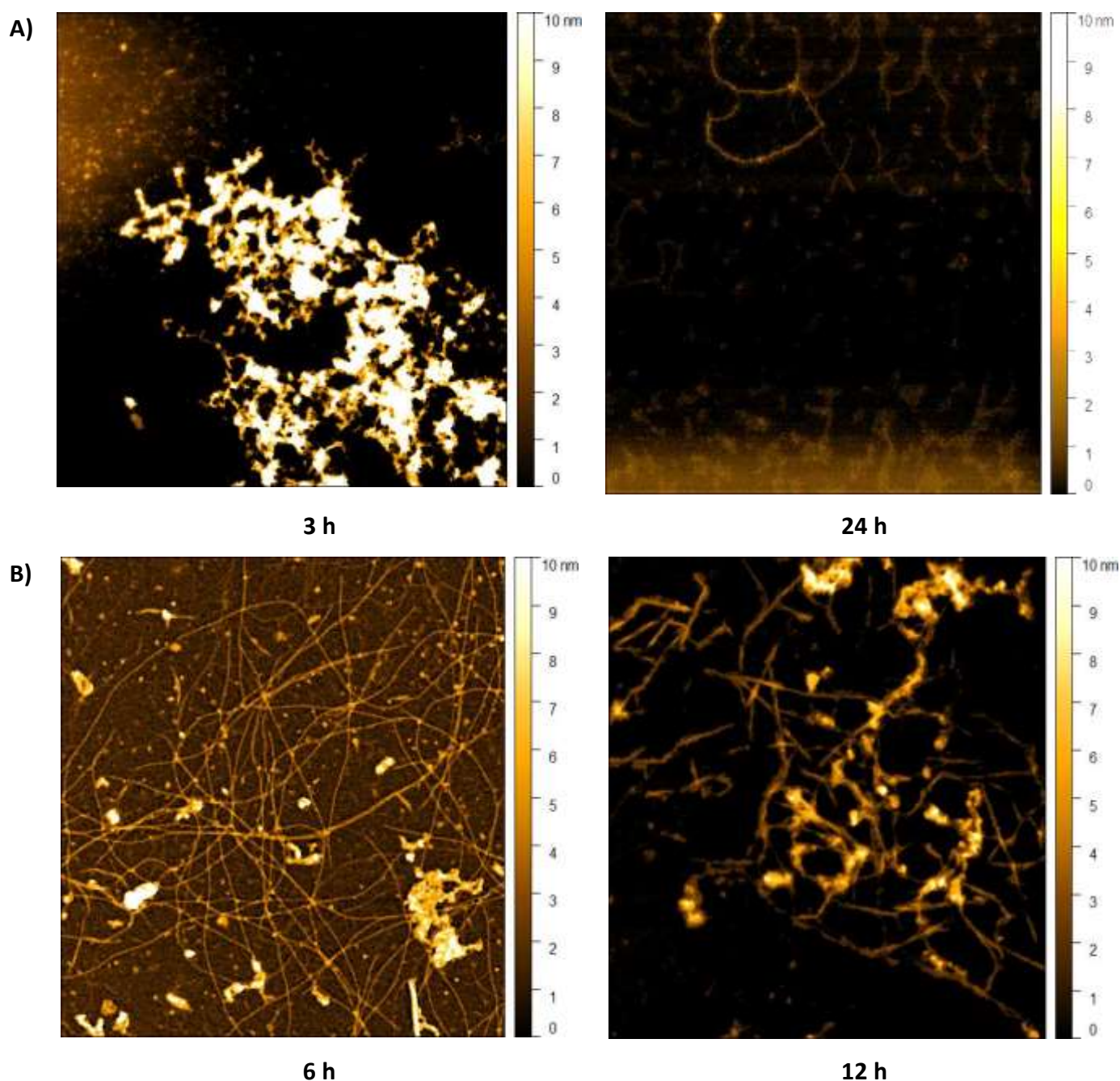


Fig. 1. AFM images of cellulose nanofibers obtained from different times of enzymatic hydrolysis/ultrasound process. A) Shortest and longest (3 and 24 h) and B) intermediate (6 h and 12 h) hydrolysis times.

Table 1. Physical properties of CNFs obtained from enzymatic/ultrasound process using different hydrolysis times (6h and 12h).

Sample	Mean diameter D (nm)	Length L (nm)	Aspect ratio (L/D)	Zeta potential (mV)
6h	0.53 ± 0.12^b	580.52 ± 22.62^a	1096.24 ± 33.52^a	-42.90 ± 1.15^a
12h	2.61 ± 0.56^a	130.87 ± 15.87^b	46.92 ± 14.21^b	-36.00 ± 1.41^b

Different letters in the same column indicate a statistically significant difference ($p < 0.05$).

3.1.2 Fourier-transform infrared spectroscopy (FTIR)

The spectra of cassava peel and CNFs obtained by enzymatic hydrolysis performed at different times are presented in Fig. 2. The region of 3421 cm^{-1} corresponds to the -OH stretching vibrations and hydrogen bonding molecules (Sánchez-Gutiérrez et al., 2020). High peaks were observed in all analyzed samples, but the highest were for CNFs due to the higher relative cellulose content with the elimination of lignin fractions (Ventura-Cruz and Tecante, 2019). The peak at 2912 cm^{-1} is related to the presence of alkane groups in the cellulose. A smaller peak was observed at 1735 cm^{-1} , which is characteristic of the vibrations of the acetyl and uronic ester groups of hemicelluloses or the ester bond of the carboxylic group of ferulic and p-coumaric acids of lignin. This demonstrates that even using alkaline pre-treatment, enzymatic hydrolysis and ultrasound, it is still observed that the total removal of hemicellulose and lignin from CNFs did not occur (Lima et al., 2023). In the absorption bands around 1566 cm^{-1} , peaks for CNFs are observed, characteristic of the stretching of the aromatic groups of lignin. The peak region 1419 cm^{-1} is attributed to the stretching of the C-H groups and the bending mode of the CH_2 bonds (Sánchez-Gutiérrez et al., 2020). These two peaks showed a great difference in relation to the cassava peel, corroborating the relevance of characterizing the composition of the nanoparticles. The small absorbance bands observed between 1500 and 1100 cm^{-1} are attributed to proteins.

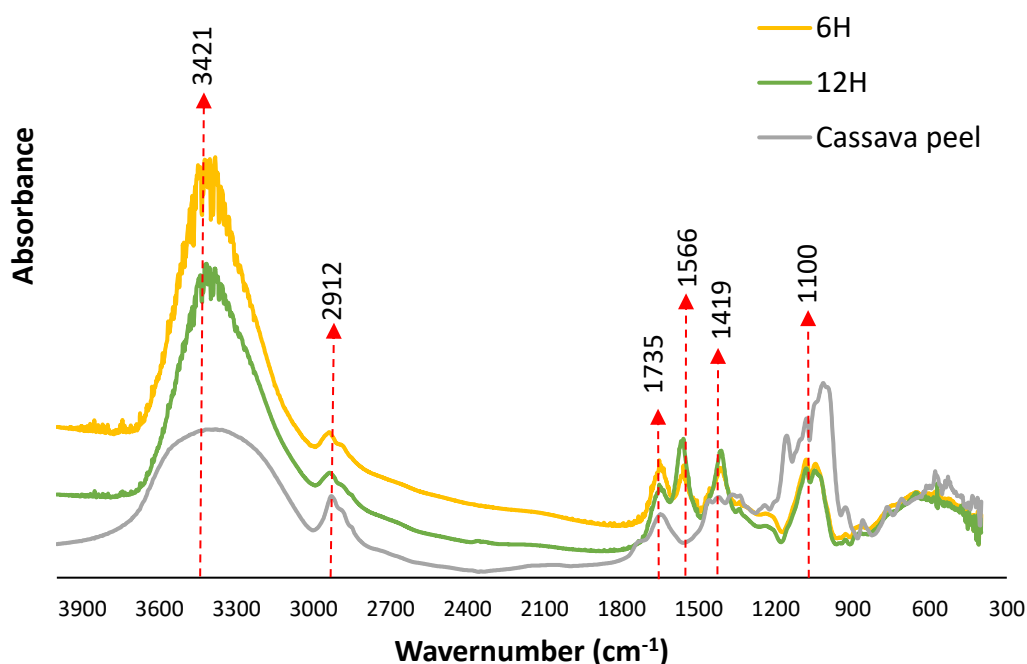


Fig. 2. FTIR spectra of cassava peel and CNFs produced from xylanase hydrolysis followed by cellulase hydrolysis at different times (6h or 12h).

3.2 Screening for antimicrobial activity of essential oil of OEO and SO

Some essential oils, such as oregano oil, have gained prominence due to their antimicrobial properties, which can inhibit several species of bacteria and filamentous fungi. The antimicrobial activities (antibacterial and antifungal) of OEO and oil blends (OEO and SO) are shown in Table 2 and some images of the cultures subjected to treatments are shown in Fig. S1 (Supplementary Material). The results obtained by disk diffusion analysis of OEO:SO against microorganisms demonstrate the efficiency of the essential oil against the bacteria and fungi tested. Overall, the antimicrobial activity of mixtures (5:5, 8:2 and 10:0 OEO:SO) increased with the concentration of oregano oil, regardless of the bacterial species, except for *E. coli*, which showed lower growth in the 8:2 mixture. It is interesting to note that all mixtures were able to inhibit *A. alternata* growth in PDA showing the potential use of this essential oil against *A. alternata* postharvest diseases.

All samples presented a diameter of the inhibition zone (DIZ) greater than 18 mm, therefore the tested strains were considered susceptible to the treatments, when compared to the negative control ($p < 0.05$). Nevertheless, the tested concentrations were more effective against *A. alternata* than against bacteria. The OEO:SO mixtures showed a DIZ from 46.60 - 61.67 mm against *A. alternata*, equivalent to 51.77%; 56.66%; 68.52% and 0% for the different OEO:SO mixtures (5:5, 8:2; 10:0 and 0:10). These results are slightly lower than those found by Soyulu and Kose (2015), who evaluated the use of some essential oils against *A. alternata*. Among the oils studied, oregano presented the greatest reduction, varying from 86.67 to 100% according to the dose of essential oil applied, followed by thyme, bay leaf, lavender and fennel. In another study (Perveen et al. 2020), an 88 % reduction in the growth of *A. alternata* was observed with the action of *Ocimum basilicum* essential oil.

The antimicrobial activity of essential oils is associated with the main active compound, such as carvacrol in OEO, which accumulates and destabilizes the fungal cell membrane. This fact abruptly interrupts proton transfer (Zabka & Pavela, 2013), in addition to affecting the ergosterol biosynthetic pathway and interrupting the

functioning of membrane-bound enzymes (P. S. Kumar et al., 2022). With regard to bacteria, the inhibition halos found were similar for *S. aureus* and lower for *E. coli*, when compared to the results found in the literature (Mollea et al., 2022), since inhibition of up to 40 mm was observed for *Staphylococcus epidermidis* and 46 mm for *E. coli* for oregano oil. Differences in values may occur due to the quality of the oil extraction process, the origin of the plant, how it was stored, the time it was exposed until packaging after processing, in addition to storage in appropriate packaging. If not carried out, losses due to volatilization and even oxidation by light may occur (Y. Li et al., 2022). The efficiency of OEO concentrations on gram-positive bacteria such as *S. aureus* and *L. monocytogenes* in relation to *E. coli* is due to the fact that gram-negative bacteria show greater resistance to essential oils, as they do have hydrophilic lipopolysaccharides in their membrane acting as a barrier (Fathollahi et al., 2019; B. Teixeira et al., 2013).

Table 2. Antibacterial and antifungal activities of OEO:SO mixtures (5:5, 8:2; 10:0 and 0:10). C+ and C- are the positive (strains grown in culture medium containing chloramphenicol for bacteria and thiabendazole for *A. alternata*) and negative controls (strains grown in culture medium only), respectively.

Diameter of the Inhibition Zone - DIZ (mm)				
Sample	<i>S.aureus</i>	<i>E.coli</i>	<i>L. monocytogenes</i>	<i>A.alternata</i>
C-	-	-	-	-
C+	25.00±0.00 ^C	22.30±0.21 ^D	24.30±0.06 ^C	90.00±0.00 ^A
5:5 OEO:SO	33.75±0.25 ^B	23.25±0.28 ^C	37.50±0.60 ^B	46.60±0.23 ^D
8:2 OEO:SO	32.00±2.82 ^B	37.00±2.82 ^A	36.50±1.91 ^B	51.00±0.22 ^C
10:0 OEO:SO	40.66±1.15 ^A	29.50±0.46 ^B	46.00±1.41 ^A	61.67±0.76 ^B
0:10 OEO:SO	9.50±0.58 ^D	10.00±0.81 ^E	0±0 ^D	0±0 ^E

Equal letters indicate that the results showed no statistical difference by Tukey's test ($p < 0.05$).

3.3 Emulsions stabilized by CNFs

3.3.1 Dynamic interfacial tension

Interfacial tension measurements between oil phases (SO; OEO and SO:OEO blends) and aqueous phases (water and 0.01% w/w CNFs) were performed to understand the stabilizing mechanism of CNFs (CNF- 6 h and CNF- 12 h) in emulsions (Fig. 3). The interfacial tension between water and different oil phases was measured as a control experiment (Water_OEO and Water_SO). At equilibrium, the interfacial

tension between droplets of different oil phases and water was similar and around 18 mN/m. The interfacial tension was similarly affected by the addition of 0.01% w/w CNFs, regardless of the different oil phase composition. A more pronounced reduction in interfacial tension was observed for CNF-6 h compared to CNF-12 h. At equilibrium, the interfacial tension between the 0.01% w/w aqueous phase and the different oil phases was approximately 5.8 mN/m and 7.8 mN/m for CNFs-6 h and CNFs-12 h, respectively. These results indicate that the stabilization of emulsions is not purely due to the Pickering mechanism, as in the presence of 0.01% w/w of CNF a significant reduction in interfacial tension is observed, resembling in values the behavior of proteins such as whey protein isolate and sodium caseinate (R. C. Chevalier et al., 2022). The difference between the two CNFs was attributed to the different morphology and organization at the interface of the nanofibers, affecting their adsorption and Pickering-type stabilization mechanism (Parajuli & Ureña-Benavides, 2022).

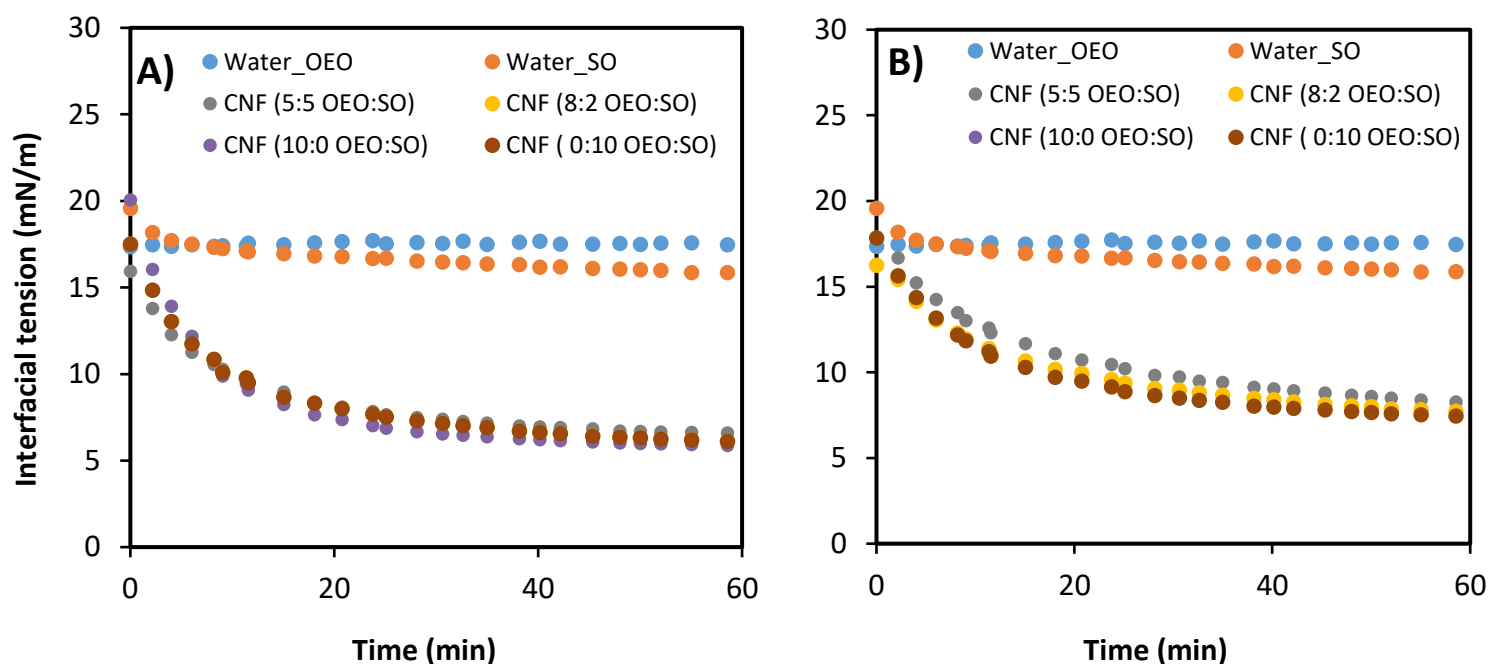


Fig. 3. Dynamic interfacial tension between aqueous phases composed of water or 0.01% w/w CNFs with different oil phases (SO; OEO and blends SO:OEO). A) CNF obtained after 6 h of cellulase hydrolysis time and B) CNF obtained after 12 h of cellulase hydrolysis time.

3.3.2 Droplet size distribution and optical microscopy

The composition of the oil phase, as well as the hydrolysis time of the nanofibers affected the droplet size distribution curves (Fig. 4). A monomodal distribution was observed in fresh emulsions with mixed oil phases (5:5 and 8:2 OEO:SO) and containing only SO (0:10 OEO:SO), stabilized with CNF- 6 h and CNF- 12 h. Bimodal behavior was

observed with fresh emulsions containing only OEO (10:0 OEO:SO). The introduction of SO together with OEO reduced the hydrophilicity of the oil mixture and changed the interaction with CNFs, reducing the droplet size of the emulsions (Y. Chevalier & Bolzinger, 2013; Dai et al., 2023).

After 7 days of storage, monomodal distribution was observed only for emulsions containing OEO:SO blends stabilized with CNF- 12 h. On the other hand, emulsions stabilized by CNF- 6 h showed a bimodal distribution and an increase in the average droplet size over time. Table 3 shows the D_{43} and Span of the emulsions with 0 and 7 days of storage. There was an increase in Span values over the days of storage and showed statistical differences, except for emulsions 5:5 OEO: SO stabilized with CNF- 12 h and 10:0 OEO: SO stabilized with CNF- 6 h. An increase in the D_{43} of the emulsions was observed over the days of storage. However, this increase was subtle with the mixed oily phase 8:2 OEO:SO stabilized by both CNF- 6 h and CNF- 12 h. Furthermore, emulsions with mixed oil phase 5:5 OEO:SO stabilized by CNF-12 h showed no statistical difference in D_{43} over the 7 days of storage.

The results indicate that the incorporation of SO in the mixture with OEO increased the stability of the emulsions, considering the smaller growth in droplet size throughout storage. Given this, one can conclude that the mixture of oils is in fact an interesting and efficient way for applications in the production of films for packaging or coating food products, with the aim of delivering antimicrobial agents, such as OEO. In addition, volatilization losses are reduced and the compatibility between essential oil and the film matrix is improved by mixing with a triacylglycerol, also allowing the reduction of process costs (Etxabide et al., 2017) and increase of emulsions stability.

Micrographs of fresh emulsions and those after 7 days of storage are shown in Fig. 5 and 6. The increase in droplet size associated with the flocculation process and, mainly, droplet coalescence was, in general, observed in emulsions stabilized with CNF- 6h. However, the emulsions containing only oregano oil in the oil phase were those that most clearly showed coalescence, indicating that their greater hydrophilicity impaired the stability of the emulsions stabilized by CNF.

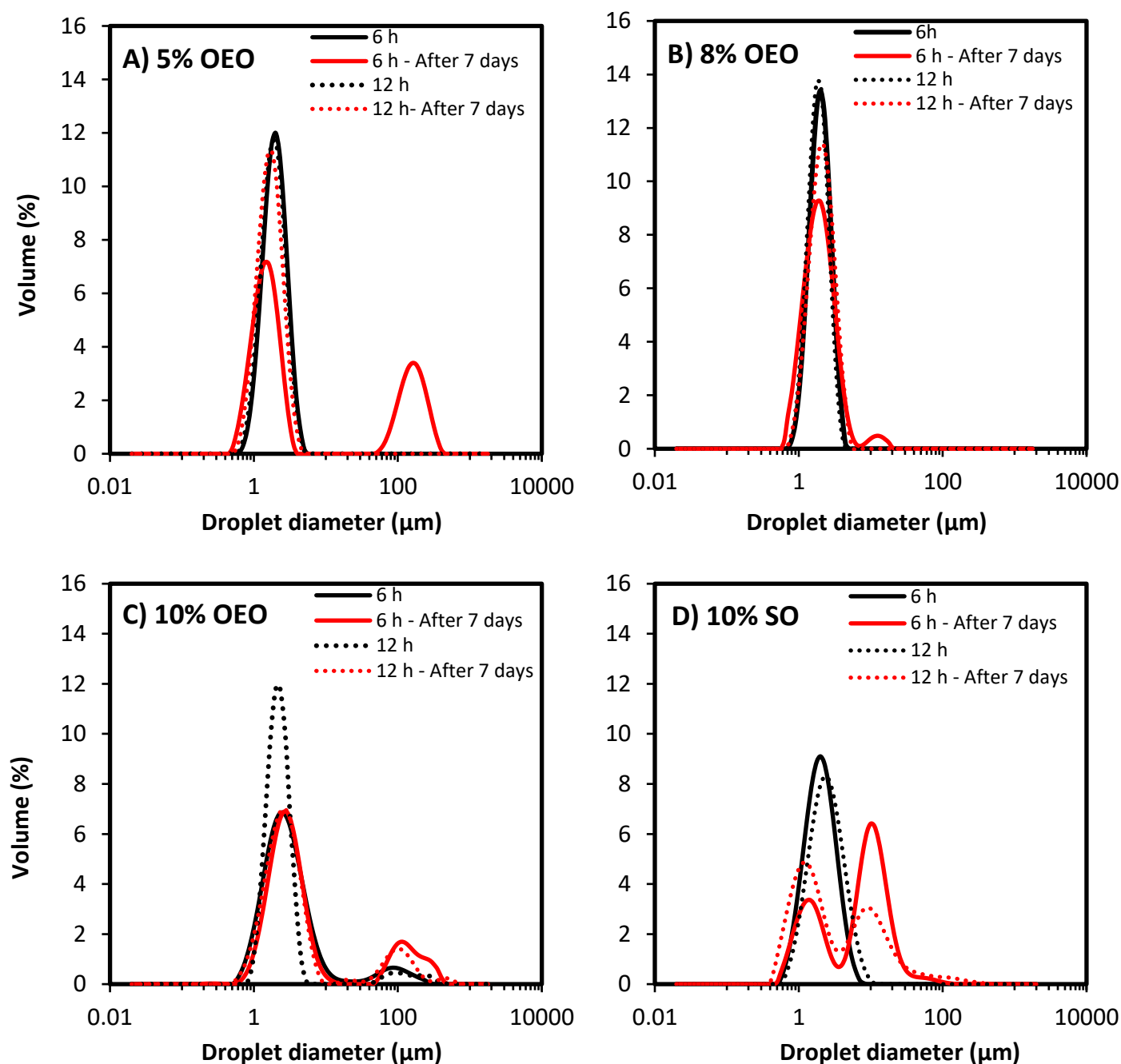


Fig. 4. Droplet size distribution of emulsions with a total oil content of 10% (w/w). Emulsions had different concentrations of essential oil of oregano (OEO): A) 5% (w/w) (5:5 OEO:SO); B) 8% (w/w) (8:2 OEO:SO); C) 10% (w/w) (10:0 OEO:SO); D) 10% (w/w) SO (0:10 OEO:SO). Cellulose nanofiber concentration was set at 0.01% (w/w). Continuous line (—) CNF- 6 h and dotted line (.....) CNF- 12 h. Black line are fresh emulsions and red line are emulsions after seven days of storage.

Table. 3. Mean droplet diameter (D_{43}) and Span of fresh O/W emulsions (day 0) and after 7 days of storage with 10% w/w oil phase stabilized by CNF- 6h or CNF- 12h.

OEO:SO	CNF- 6 h				CNF- 12 h			
	$D_{43}(\mu\text{m})$ 0 day	Span (0 day)	$D_{43}(\mu\text{m})$ 7 days aged	Span (7 days)	$D_{43}(\mu\text{m})$ 0 day	Span (0 day)	$D_{43}(\mu\text{m})$ 7 days aged	Span (7 days)
5:5	2.18±0.01 ^{Bb}	1.07±0.08 ^{Bb}	48.99±15.15 ^{Aa}	33.52±0.70 ^{Ab}	2.05±0.07 ^{Ab}	1.14±0.21 ^{Aab}	2.07±0.19 ^{Ab}	1.14±0.09 ^{Ac}
8:2	2.04±0.21 ^{Bb}	0.81±0.09 ^{Bb}	2.50±0.01 ^{Ac}	1.71±0.50 ^{Ac}	2.05±0.01 ^{Bb}	0.86±0.02 ^{Bb}	2.30±0.07 ^{Ab}	1.25±0.31 ^{Ac}
10:0	35.96±0.92 ^{Aa}	32.67±15.29 ^{Aa}	43.01±9.54 ^{Aab}	48.93±10.20 ^{Aa}	6.50±7.95 ^{Ab}	1.39±0.26 ^{Ba}	19.44±7.44 ^{Aa}	30.79±0.82 ^{Aa}
0:10	2.28±0.07 ^{Bb}	1.26±0.11 ^{Bb}	22.60±8.92 ^{Ab}	2.62±0.59 ^{Ac}	2.53±0.18 ^{Ba}	1.41±0.19 ^{Ba}	15.88±6.72 ^{Aa}	7.14±1.20 ^{Ab}

Different letters indicate significant differences ($p < 0.05$) between D_{43} and span values. Capital letters: differences between 0 and 7 days of storage. Lowercase letters: differences between different concentrations of OEO:SO, always maintaining a proportion of 10% w/w of oil in the emulsion.

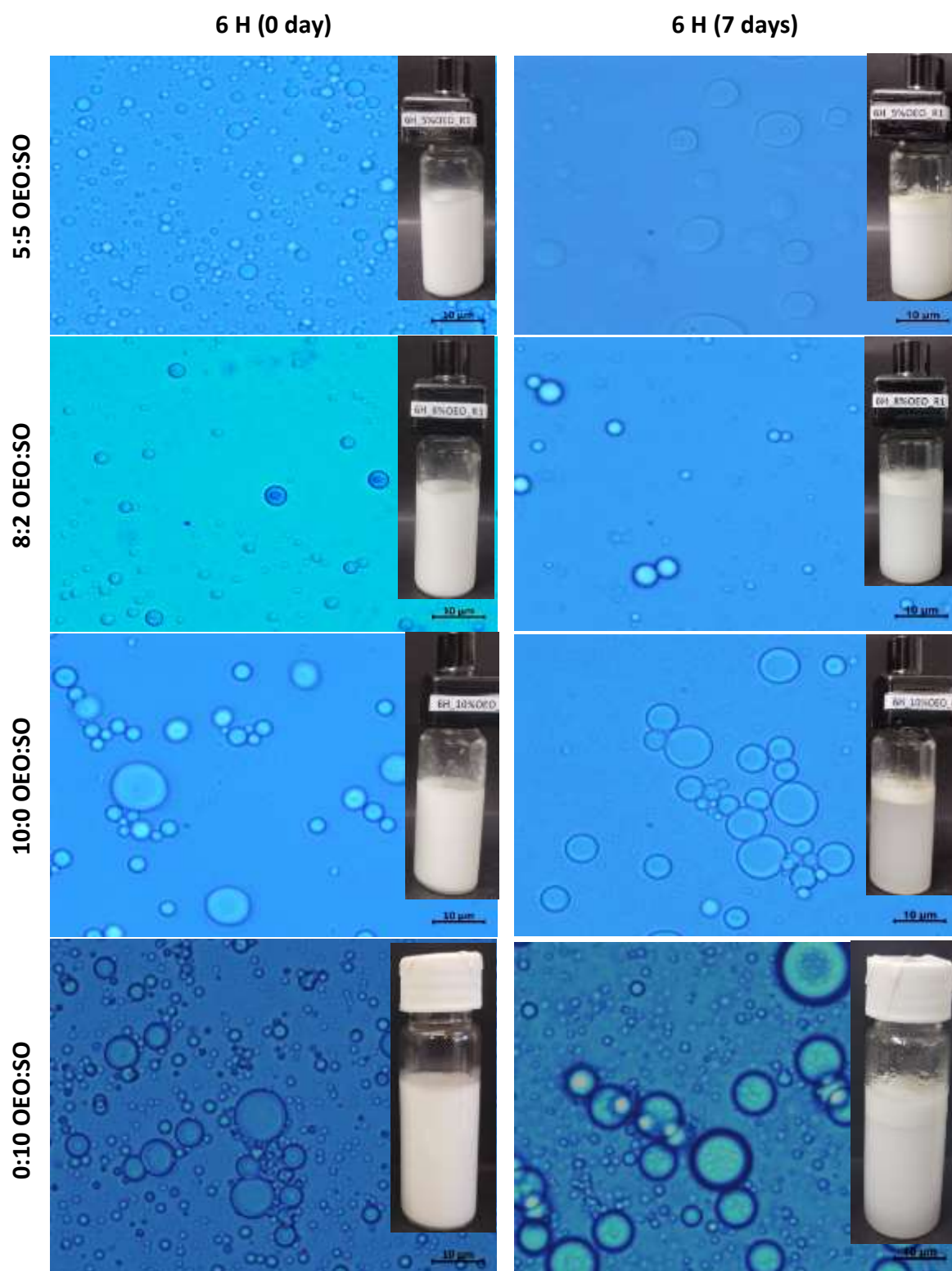


Fig. 5. Optical micrographs of O/W Pickering emulsions. Emulsions stabilized with CNF-6 h. Oil phase was composed of 10% w/w with different ratios OEO:SO (5:5, 8:2, 10:0 and 0:10). Scale bar: 10 μm .

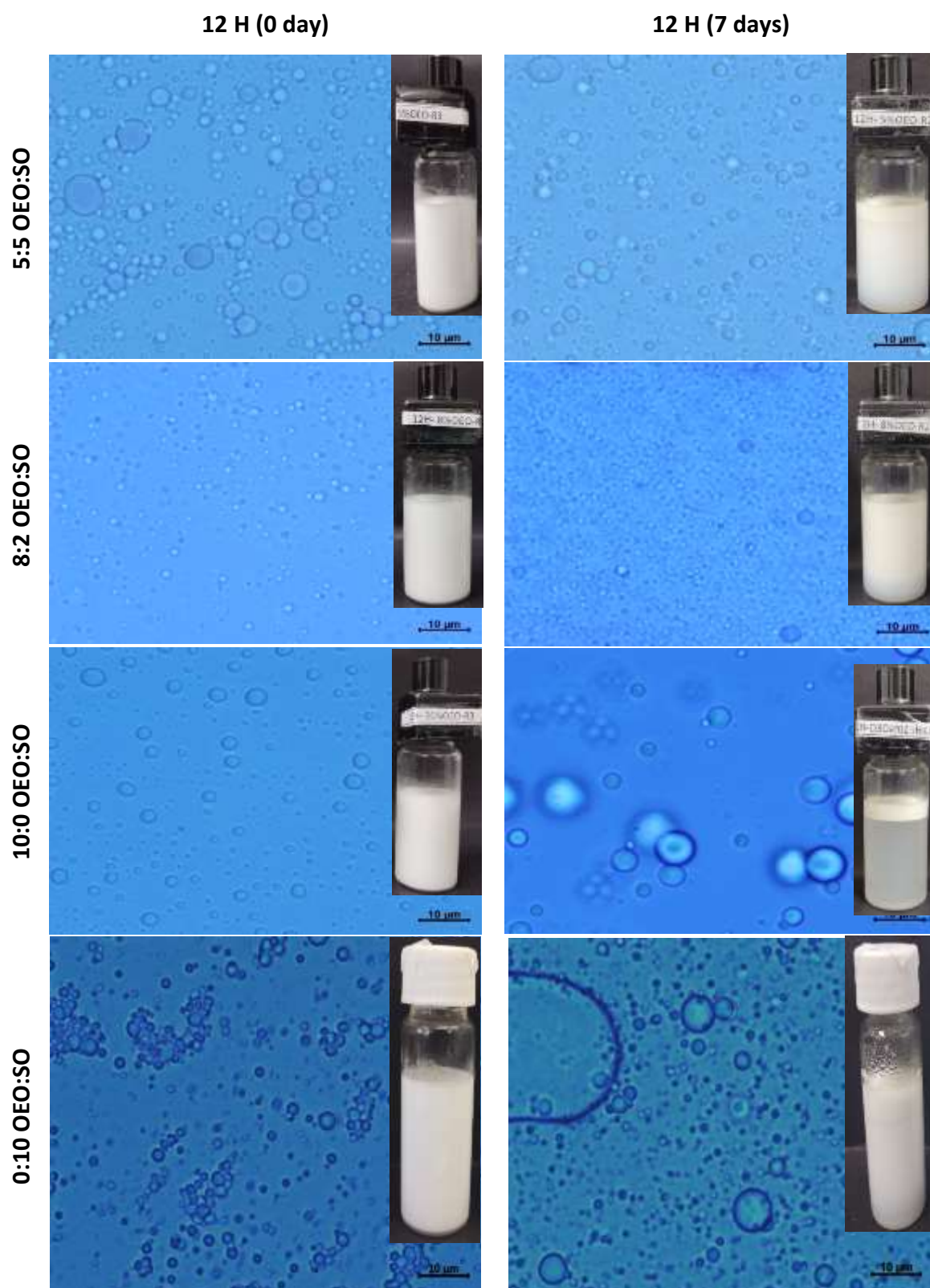
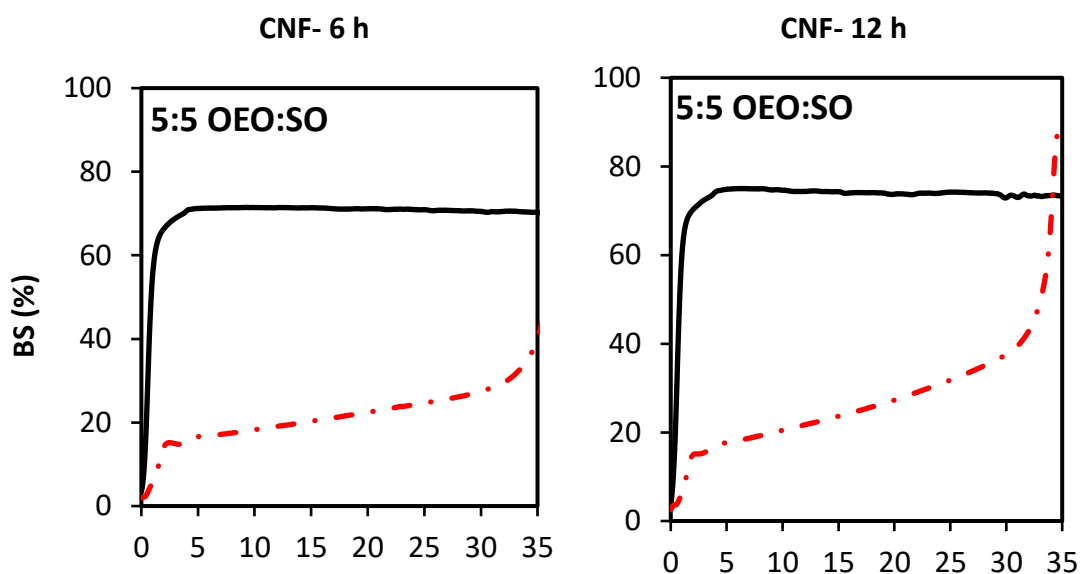


Fig. 6. Optical micrographs of O/W Pickering emulsions. Emulsions stabilized with CNF-12 h. Oil phase was composed of 10% w/w with different ratios OEO:SO (5:5, 8:2, 10:0 and 0:10). Scale bar: 10 μm .

3.3.3 Kinetic stability – laser scanning turbidimetry

The stability of the emulsions was evaluated by light backscattering over 7 days of storage at 25 °C. Storage time was only 7 days, considering that the main objective was to apply the emulsions in film-forming solutions that are subsequently dried. Thus, a longer evaluation time is not necessary. The backscattering profiles (BS) are shown in Fig. 7. This technique allowed the detection of destabilization phenomena even before they became visible. Immediately after preparing the emulsions, there was no variation in the backscattering profiles as a function of the height of the measuring cell. Fresh emulsions stabilized by CNFs presented BS values around 70%, with the exception of emulsions stabilized with CNF- 6 h and the oily phase composed of only OEO (BS of approximately 56%). This can be explained by the droplet size distribution, since BS tends to increase with decreasing droplet diameter if the particle size is larger than the incident wavelength (880 nm). On day 0, the largest droplet size was presented by the emulsion containing only oregano oil (10:0 OEO:SO).



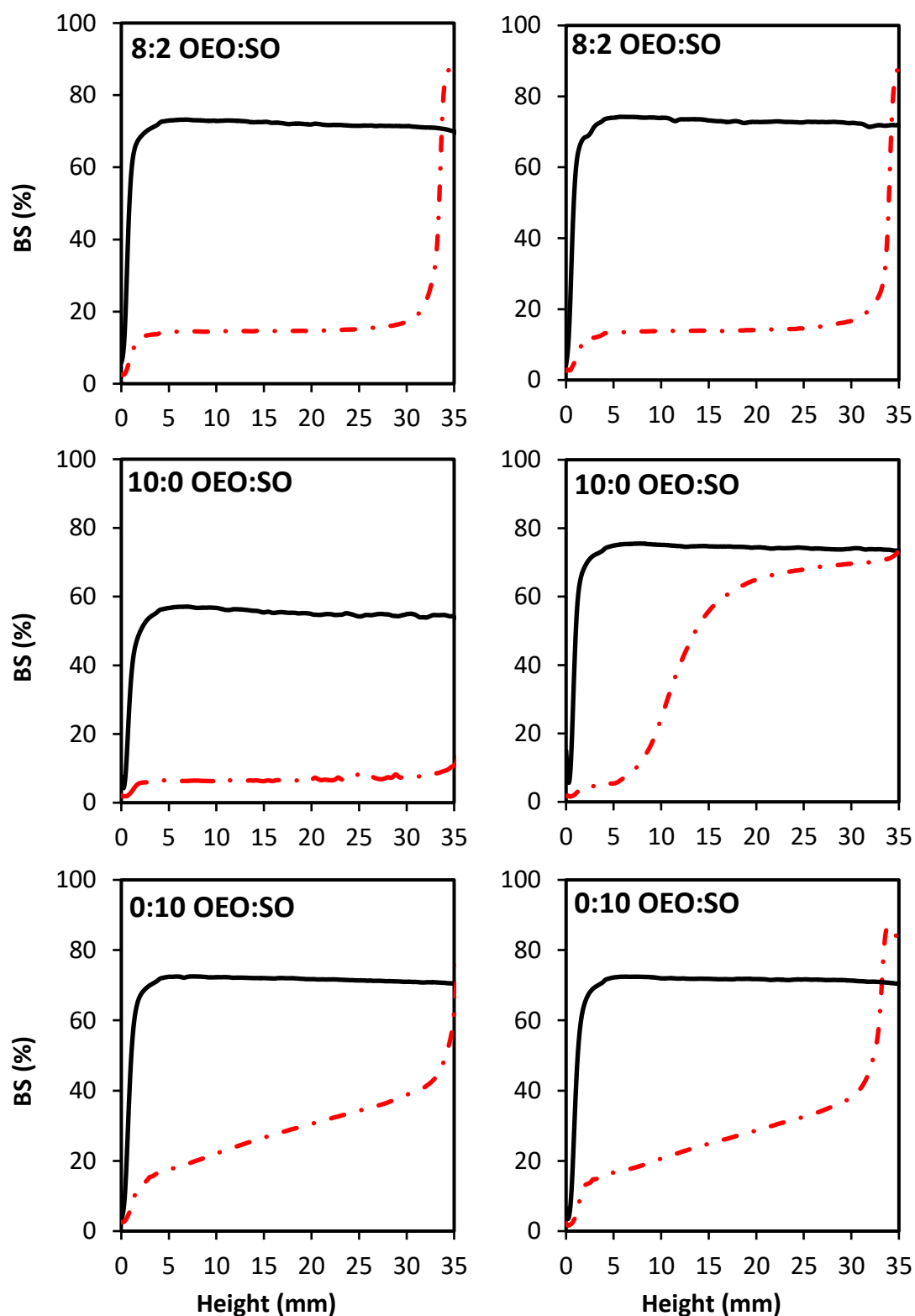


Fig. 7. Backscattering profiles of emulsions with oil phase composed of OEO:SO blends (5:5; 8:2; 10:0 and 0:10) and stabilized by 0.01% w/w CNF- 6 h or CNF- 12 h. Fresh emulsions (solid line) and after 7 days of storage (dashed red line). (For interpretation regarding the colors mentioned in the figure caption, the reader is referred to the web version of this article).

After storage, the emulsions showed signs of destabilization. In general, the results showed a decrease in BS values at the bottom of the measuring cell and a pronounced increase at the top of the cell after 7 days of storage. Table 4 shows the TSI values of the Pickering emulsions over 7 days of storage, showing the kinetic instability due to the high TSI values. Visually, all emulsions showed two distinct phases (serum and cream) after storage. However, it is worth highlighting some differences between the different emulsions. Emulsions containing 5:5 OEO:SO mixture stabilized with CNF-6H and the emulsions with only OEO (regardless of the type of CNF) showed coalescence and the highest TSI values. On the other hand, the most of the emulsions with an oily phase containing SO and stabilized with CNF-6 and 12h presented flocculation and less creaming of the droplets, typical behavior of Pickering-type emulsions. Interestingly, emulsions 8:2 OEO:SO stabilized either for CNF-6h or CNF-12h showed the lowest TSI values, presenting only flocculation and high resistance to coalescence. Regarding emulsions with only OEO, the droplet flocculation mechanism was observed (Fig. 7 and Table 4), although the droplets were larger than the other emulsions and, consequently, with less stability. The results showed that the stabilization of the emulsions is correlated with the composition of the oil phase, as well as the composition/morphology of CNFs.

Table 4. Turbiscan stability index (TSI) values for Pickering O/W emulsions stabilized by CNFs aged for 7 days.

CNF Type	Oil phase composition (OEO:SO)	TSI
CNF- 6 h	5:5	38.17±1.64 ^{Aa}
	8:2	30.63±1.22 ^{Ca}
	10:0	37.30±3.63 ^{ABb}
	0:10	34.90±1.45 ^{ABa}
CNF- 12 h	5:5	36.80±1.00 ^{Ba}
	8:2	29.50±1.74 ^{Ca}
	10:0	53.57±3.21 ^{Aa}
	0:10	34.23±1.70 ^{Ba}

Different letters in the same column indicate significant differences ($p < 0.05$). Capital letters: differences between oil composition and the same type of nanofiber. Lowercase letters: differences between the nanofiber types, but the same oil composition.

The rheological behavior of the emulsions was Newtonian, with no effects of shear time (Fig. S2). Table 5 presents the viscosity of the emulsions, which were very similar and low, showing the influence of the small volumetric fraction of the oil phase associated with the quite low CNF concentration. A small trend towards higher viscosity was observed with increasing SO concentration, due to the higher viscosity of the triacylglycerol. As viscosity values were very low, droplet diameter (D_{43}) was the most important property that influenced the creaming rate of oil droplets in Pickering emulsions (Costa et al., 2018b).

Table. 5. Viscosity values (η) of emulsions as a function of oily phase composition and CNF type.

CNF type	Oil phase composition (OEO:SO)	η (mPa.s)
CNF- 6 h	5:5	2.62±0.00 ^{Cb}
	8:2	2.70±0.07 ^{Ba}
	10:0	2.60±0.03 ^{Ca}
	0:10	3.92±0.00 ^{Aa}
CNF- 12 h	5:5	3.22±0.09 ^{Ba}
	8:2	2.73±0.02 ^{Ca}
	10:0	2.58±0.02 ^{Da}
	0:10	3.60±0.00 ^{Ab}

Different letters in the same column indicate significant differences ($p < 0.05$). Capital letters: differences between oil composition and the same type of nanofiber. Lowercase letters: differences between the nanofiber types, but the same oil composition.

3.3.5 Antimicrobial activity of Pickering emulsions

The antibacterial and antifungal activities of the CNF - 6 h and CNF - 12 h stabilized emulsions are shown in Table 6. Some images of Petri dishes are presented in Fig. S3 and Fig. S4 (Supplementary material). A decrease in antibacterial activity was observed in relation to oils (Table 2), since there was a dilution in emulsified systems. *S. aureus* was sensitive ($\text{DIZ} \geq 18$ mm) to all of the tested emulsions, regardless of the concentration of essential oil and CNFs. The antibacterial activity for *S. aureus* increased with increasing OEO (from 5:5 to 10:0 OEO:SO) in the emulsions ($p \leq 0.05$). The

antibacterial activity of *S. aureus* for emulsions stabilized by CNF-6 h was higher than those stabilized with CNF-12 h.

Regarding the growth of *E. coli*, the inhibition halos were very close in the emulsions stabilized by CNF-6 h and CNF-12 h, with both of them controlling the growth of *E. coli*. The emulsions stabilized with CNF-6 h/5:5 OEO:SO and CNF-12 h/10:0 OEO:SO demonstrated intermediate activity against *E. coli*, with inhibition halos varying from 14 - 17 mm. *L. monocytogenes* also showed intermediate sensitivity (13.5 – 17 mm) to the emulsions stabilized with CNF-6 h, similar findings were observed with emulsions stabilized with CNF-12 h, in which the inhibition halos varied between approximately 13 mm – 18 mm. For antifungal activity, there was no evidence of growth of microorganisms, regardless of OEO concentration. This demonstrates that even with the lowest oil concentration, the growth of *A. alternata* was inhibited.

Table 6. Antibacterial and antifungal activities of emulsions with varied oil composition and stabilized by CNF- 6 h and CNF- 12 h.

		Diameter of the Inhibition Zone - DIZ (mm)							
		CNF- 6 h				CNF- 12 h			
		<i>S. aureus</i>	<i>E. coli</i>	<i>L. monocytogenes</i>	<i>A. alternata</i>	<i>S. aureus</i>	<i>E. coli</i>	<i>L. monocytogenes</i>	<i>A. alternata</i>
Emulsions									
Controls	C-	N.d	N.d	N.d	N.d	N.d	N.d	N.d	N.d
	C+	25.00±0.00 ^C	22.30±0.21 ^A	24.30±0.06 ^A		25.00±0.00 ^C	22.30±0.21 ^A	24.30±0.06 ^{Aa}	*
	5:5	24.50±1.00 ^C	17.33±2.08 ^B	17.00±1.00 ^B	*	22.70±0.42 ^D	22.00±0.67 ^A	12.70±0.09 ^{Bd}	*
Oils composition (OEO: SO)	8:2	29.67±0.57 ^B	20.00±3.60 ^A	13.50±2.12 ^C	*	28.50±0.98 ^B	20.00±0.35 ^B	14.00±0.42 ^{Ac}	*
	10:0	32.33±1.15 ^A	22.50±0.70 ^A	17.00±1.41 ^B	*	30.70±0.09 ^A	17.70±0.31 ^B	18.20±0.09 ^{Ab}	*
							c		
	0:10	N.d	N.d	N.d	N.d	N.d	N.d	N.d	N.d

Equal letters indicate that the results showed no statistical difference by Tukey test ($p < 0.05$). C-: negative control, refers to the culture medium with microbial growth; C+: positive control, refers to the use of established antimicrobial agents against bacteria (chloramphenicol) and fungi (thiabendazole); N.d: Not detected.

* No growth of microorganisms.

Vehiculation of the oil in the emulsion stabilized with CNFs did not increase the antibacterial activity, presenting lower inhibition values than the free oil. These results corroborated the findings of Ferreira et al. (2023), who evaluated the antimicrobial activity of emulsions stabilized by CNFs and loaded with *Melaleuca alternifolia* essential oil. Growth inhibition with free essential oil against *E. coli* and *S. aureus* was 29.5 mm and 41.5 mm respectively, while the results obtained from the emulsion showed a reduction of almost 50% for *S. aureus* (26.5 mm) and *E. coli* (22 to 25 mm). Pickering emulsions loaded with cinnamon essential oil and stabilized by cellulose nanocrystals (CNC) or cellulose nanofibers (CNF) were evaluated. CNC emulsions were more efficient for *Bacillus subtilis* with an inhibition halo of 65 mm than CNF with 30.1 mm, while for *Pseudomonas aeruginosa* there was no difference between the two treatments (Souza et al., 2021). This demonstrates that gram-positive bacteria may be more sensitive to treatments with essential oil than gram-negative bacteria, as aforementioned (Oun et al., 2022). Regarding antifungal activity, the emulsions were effective in inhibiting the growth of the fungus *A. alternata*. One of the possible hypotheses for the increased antimicrobial activity against this fungus is that the generation time is relatively longer than that of bacteria, allowing the complete release of the essential from the emulsion.

4. Conclusion

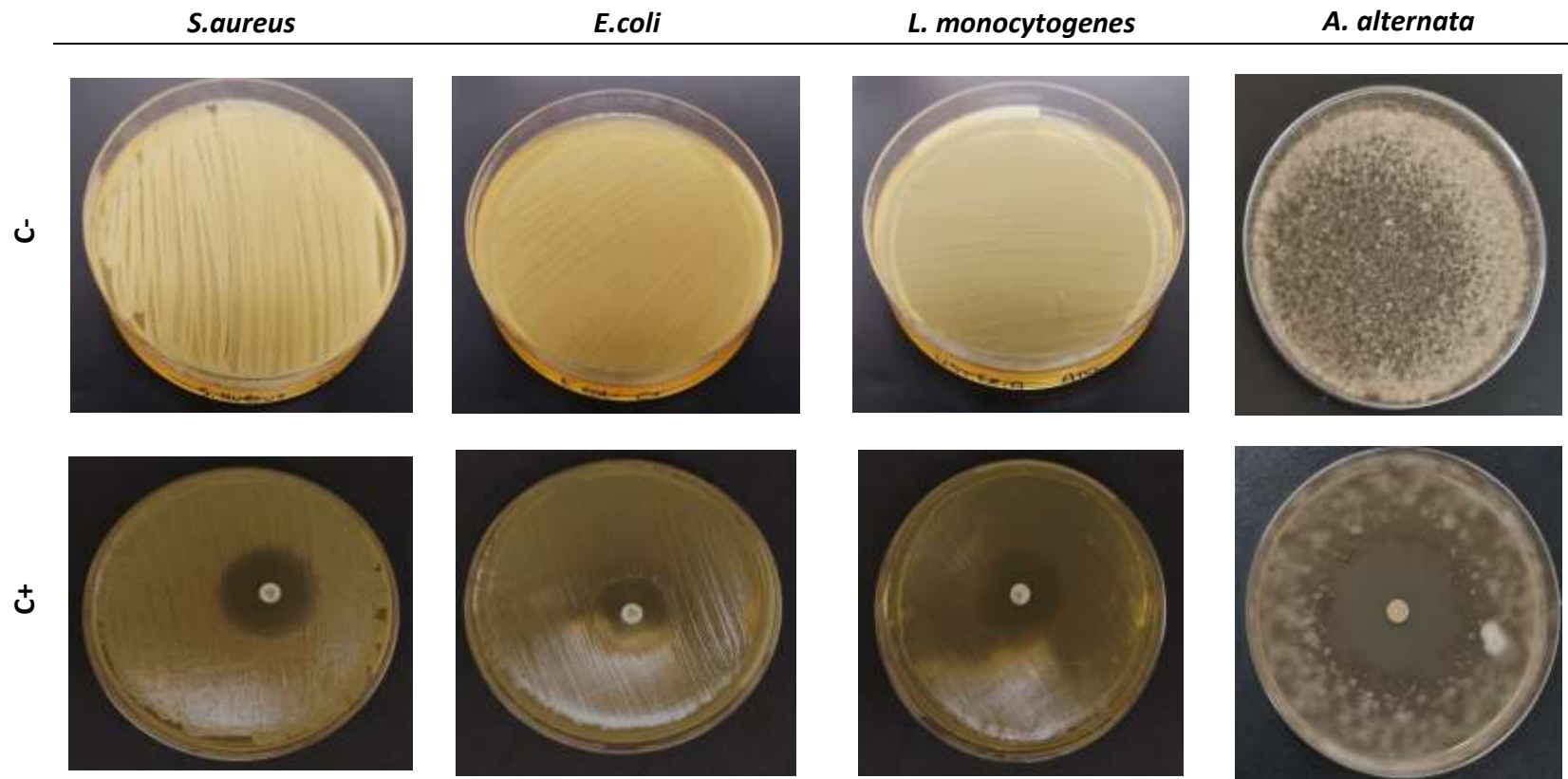
The effects of different types of cellulose nanofibers, manufactured from enzymatic hydrolysis with xylanase followed by a second hydrolysis with cellulase performed at different times was evaluated as Pickering emulsion stabilizers. In addition, mixtures of OEO and SO were evaluated as oil phase of these Pickering emulsions. In general, hydrolysis time influenced the properties of CNF, mainly aspect ratio. Emulsion stabilization by CNFs did not show a pure Pickering mechanism, as a reduction in interfacial tension was observed. The composition of oils blends affected the droplet size and, consequently, the stability of the emulsions. The smallest droplet sizes were observed in emulsions with mixed oil phase (5:5 and 8:2 OEO:SO), regardless of the CNF type. Over the days of storage, the emulsions showed flocculation and high resistance to coalescence, with the exception of the emulsion containing only oregano oil that also showed coalescence. Although SO does not present antimicrobial activity, its presence favored the antimicrobial activity of OEO, proving to be an efficient

alternative for the delivery of OEO, in addition to avoid volatilization and loss of activity during heat processes. Therefore, the emulsions studied have the potential for incorporation into biodegradable films, in order to mainly prevent microbial growth in food matrices.

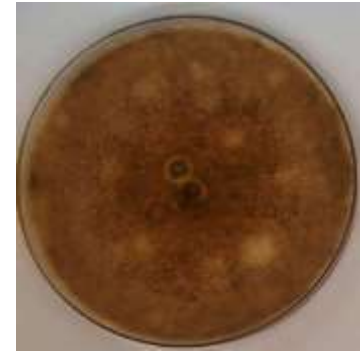
ACKNOWLEDGMENTS

This study was financed by Coordenação de Aperfeiçoamento de Pessoal de Nível Superior – Brazil (CAPES) - Finance Code 001 and Fundação de Amparo à Pesquisa do Estado de São Paulo - FAPESP (2019/27354-3). Chevalier and Almeida thanks CAPES-Brazil for the scholarship (88887.479720/2020-00; 88887485471/2020-00). Cunha and Chevalier thanks CNPq (404753/2023-0). Cunha thanks CNPq (307094/2021-9) for the productivity grant. The authors thank the Laboratory for Surface Science (LCS) of the National Nanotechnology Laboratory (LNNano - CNPEM) (Campinas, Brazil) for AFM analyses.

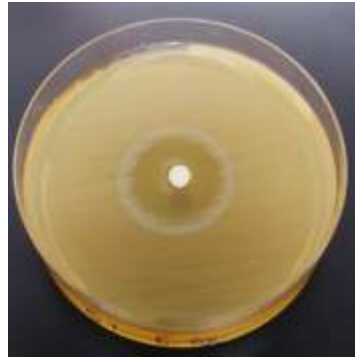
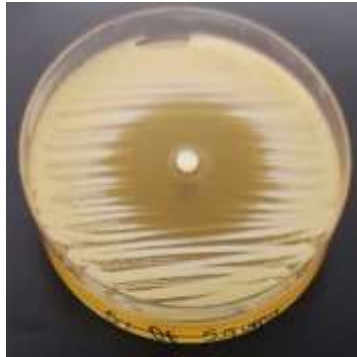
Supplementary Material



0:10 OEO:SO



5:5 OEO:SO



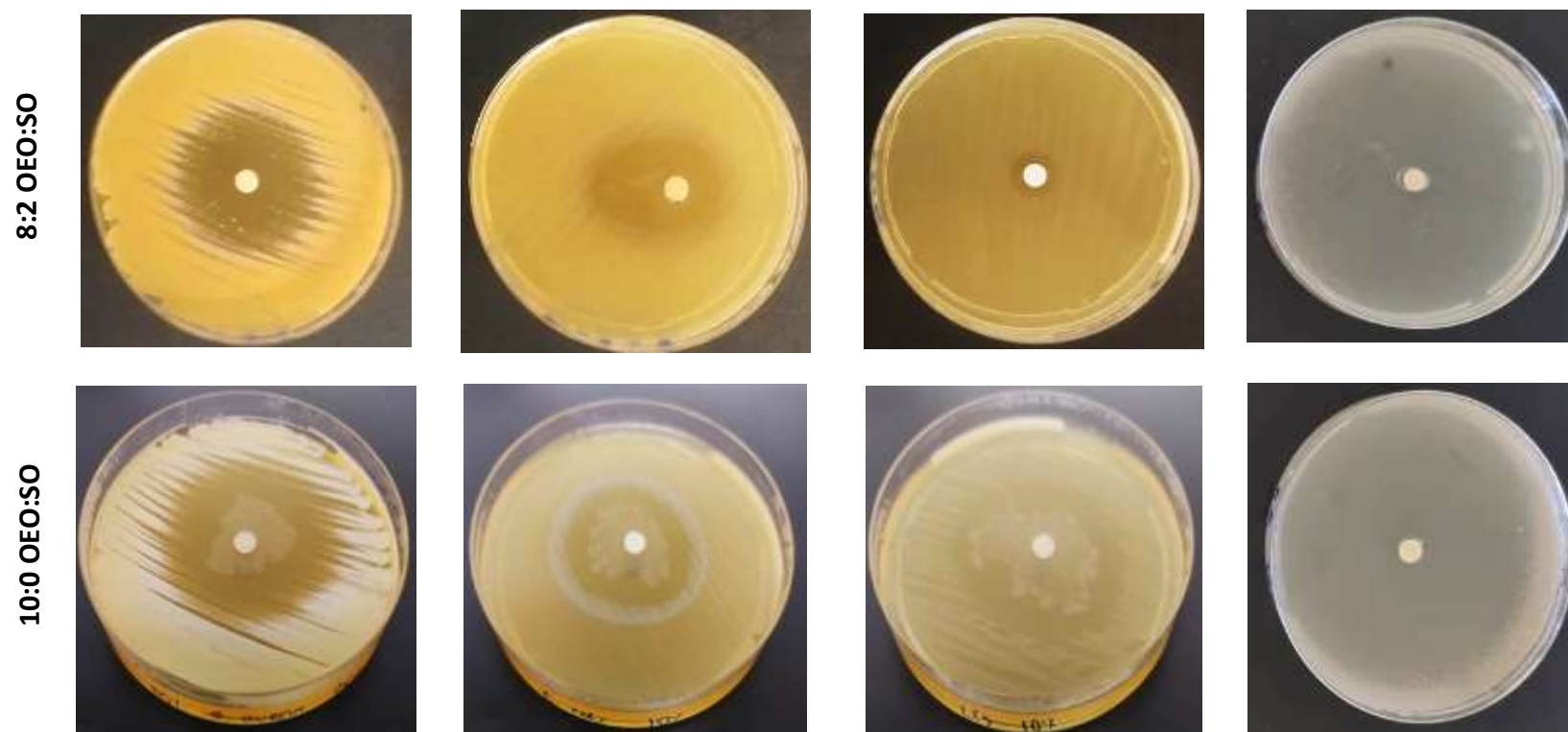


Fig. S1. Images of the plates demonstrating the size of the inhibition zones of the positive controls (strains grown only in culture medium containing chloramphenicol for bacteria and thiabendazole for *A. alternata*) and negative controls (strains grown only in culture medium), and of the OEO mixtures: SO (0:10; 5:5, 8:2 and 10:0).

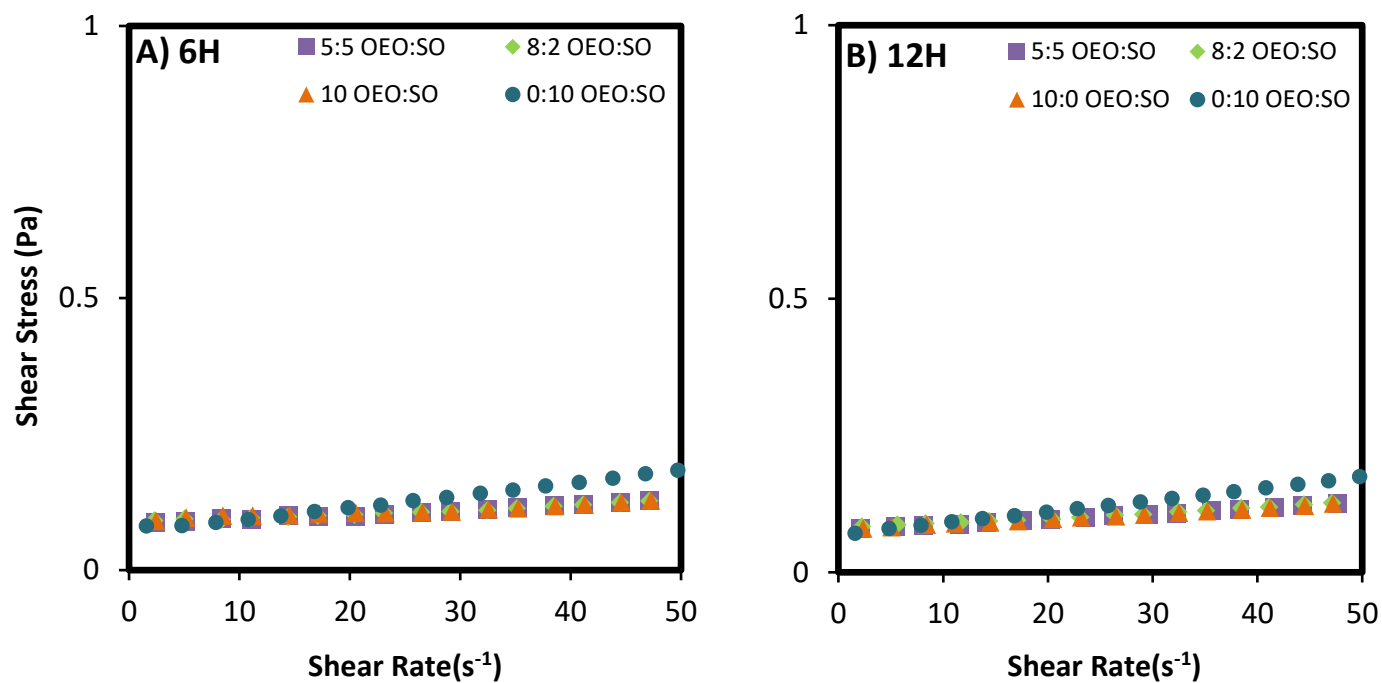
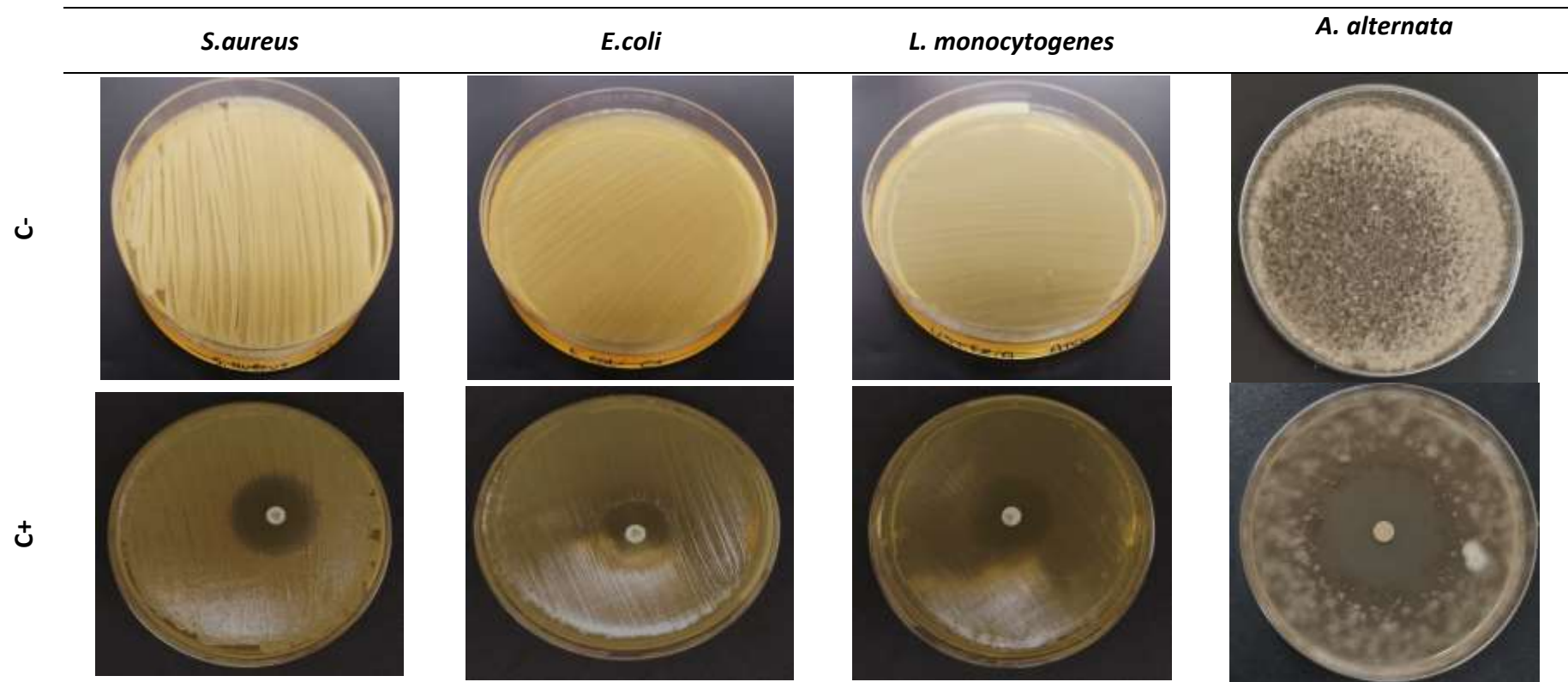


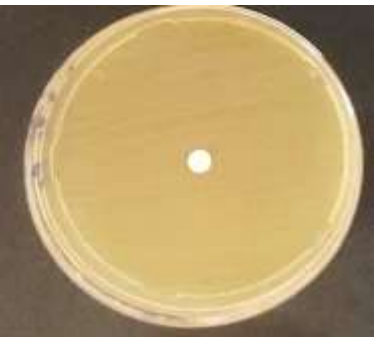
Fig. S2. Flow curves of emulsions with different OEO:SO mixtures (5:5, 8:2; 10:0 and 0:10) and stabilized by cellulose nanofibrils obtained by different enzymatic hydrolysis times: A) 6H and B) 12H.



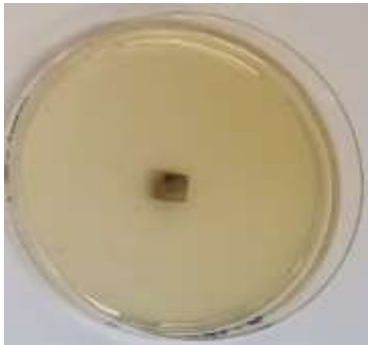
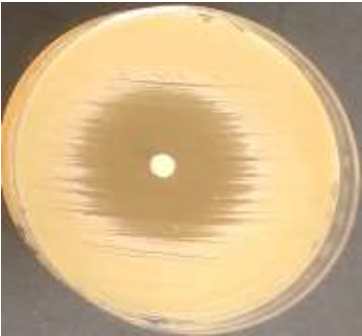
6 h - 5:5 OEO:SO



6 h - 8:2 OEO:SO



6 h - 10:0 OEO:SO



6 h – 0:10 OEO:SO

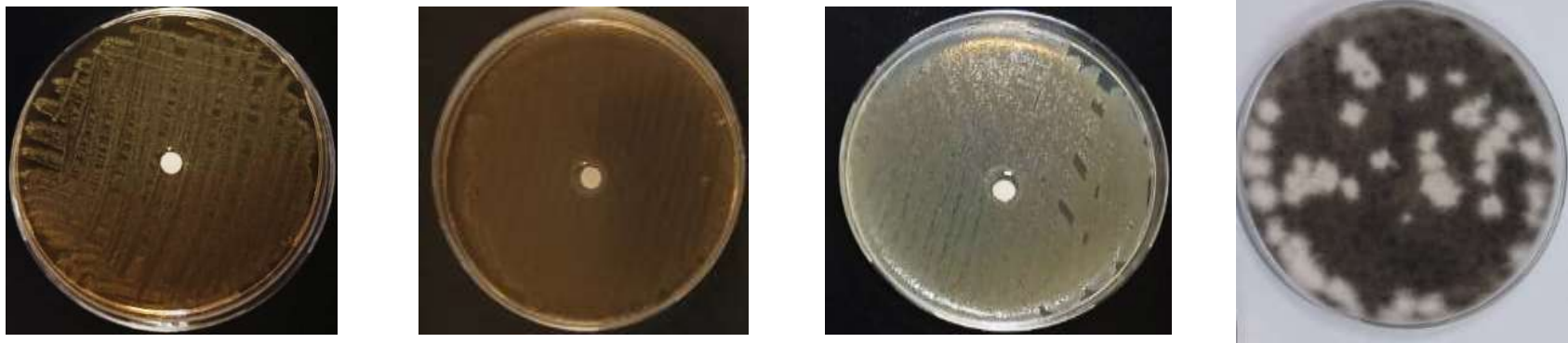
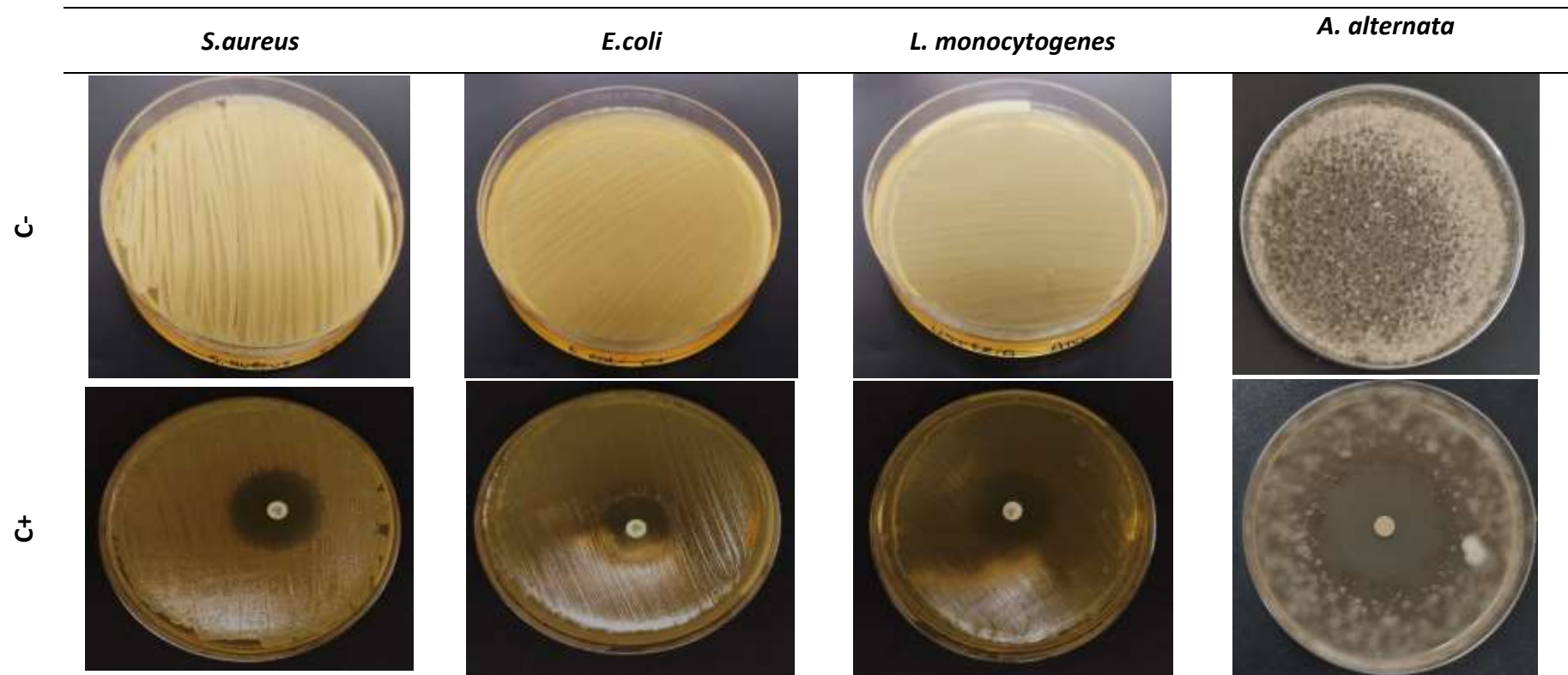
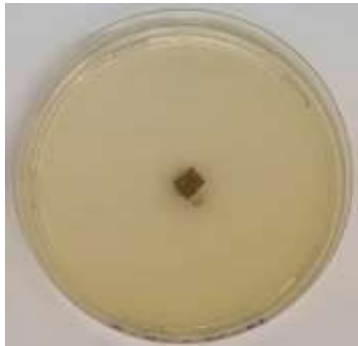
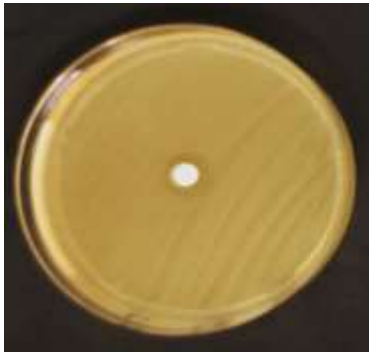


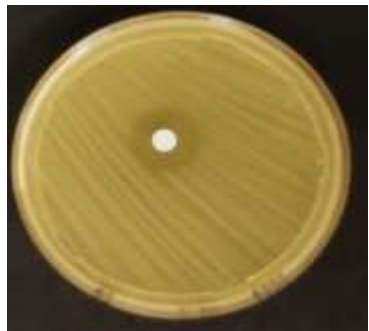
Fig. S3. Images of the plates demonstrating the size of the inhibition zones of positive controls (strains grown in culture medium containing chloramphenicol for bacteria and thiabendazole for *A. alternata*) and negative controls (strains grown only in culture medium), and of emulsions with different mixtures OEO:SO (5:5, 8:2; 10:0 and 0:10) and stabilized by CNF-6 h.



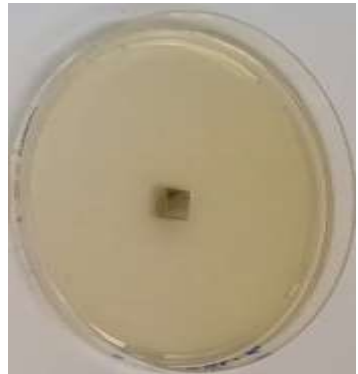
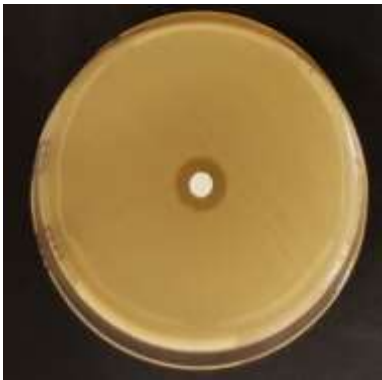
12 h - 5:5 OEO:SO



12 h - 8:2 OEO:SO



12 h - 10:0 OEO:SO



12 h - 0:10 OEO:SO

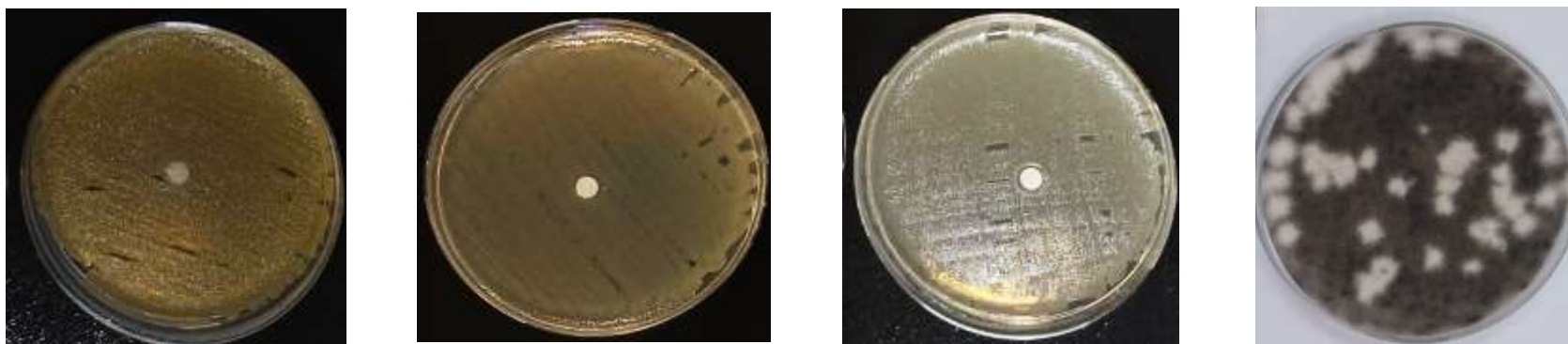


Fig. S4. Images of the plates demonstrating the size of the inhibition zones of positive controls (strains grown in culture medium containing chloramphenicol for bacteria and thiabendazole for *A. alternata*) and negative controls (strains grown only in culture medium), and of emulsions with different mixtures OEO:SO (5:5, 8:2; 10:0 and 0:10) and stabilized by CNF-12 h.

References

- Ahmet, A., Hakan, O., Hamdullah, K., & Bulent, C. (2002). Screening of Antimicrobial Activity of Essential Oil and Methanol Extract of *Satureja hortensis* on Foodborne Bacteria and Fungi. *Czech Journal of Food Sciences*, 25(2), 81–89. <https://doi.org/10.17221/753-CJFS>
- Campos, A., Correa, A. C., Cannella, D., de M Teixeira, E., Marconcini, J. M., Dufresne, A., Mattoso, L. H. C., Cassland, P., & Sanadi, A. R. (2013). Obtaining nanofibers from curauá and sugarcane bagasse fibers using enzymatic hydrolysis followed by sonication. *Cellulose*, 20(3), 1491–1500. <https://doi.org/10.1007/s10570-013-9909-3>
- Ceaser, R., & Chimpango, A. F. A. (2021). Comparative analysis of physical and functional properties of cellulose nanofibers isolated from alkaline pre-treated wheat straw in optimized hydrochloric acid and enzymatic processes. *International Journal of Biological Macromolecules*, 171, 331–342. <https://doi.org/10.1016/j.ijbiomac.2021.01.018>
- Chevalier, R. C., Gomes, A., & Cunha, R. L. da. (2022). Role of aqueous phase composition and hydrophilic emulsifier type on the stability of W / O / W emulsions. *Food Research International*, 156(December 2021), 111123. <https://doi.org/10.1016/j.foodres.2022.111123>
- Chevalier, R. C., JÚNIR, F. D. O., & Cunha, R. L. (2024). Modulating digestibility and stability of Pickering emulsions based on cellulose nanofibers. *Food Research International*, 178(August 2023), 113963. <https://doi.org/10.1016/j.foodres.2024.113963>
- Chevalier, Y., & Bolzinger, M. A. (2013). Emulsions stabilized with solid nanoparticles: Pickering emulsions. *Colloids and Surfaces A: Physicochemical and Engineering Aspects*, 439, 23–34. <https://doi.org/10.1016/j.colsurfa.2013.02.054>
- Costa, A. L. R., Gomes, A., Tibolla, H., Menegalli, F. C., & Cunha, R. L. (2018). Cellulose nanofibers from banana peels as a Pickering emulsifier: High-energy emulsification processes. *Carbohydrate Polymers*, 194(January), 122–131. <https://doi.org/10.1016/j.carbpol.2018.04.001>
- Czaikoski, A., da Cunha, R. L., & Menegalli, F. C. (2020). Rheological behavior of cellulose nanofibers from cassava peel obtained by combination of chemical and physical processes. *Carbohydrate Polymers*, 248(July), 116744. <https://doi.org/10.1016/j.carbpol.2020.116744>
- Dai, H., Chen, Y., Chen, H., Fu, Y., Ma, L., Wang, H., Yu, Y., Zhu, H., & Zhang, Y. (2023). Gelatin films functionalized by lignocellulose nanocrystals-tannic acid stabilized Pickering emulsions : Influence of cinnamon essential oil. *Food Chemistry*, 401(2), 134154. <https://doi.org/10.1016/j.foodchem.2022.134154>
- Dias, I. K. R., Siqueira, G. A., & Arantes, V. (2022). Xylanase increases the selectivity of the enzymatic hydrolysis with endoglucanase to produce cellulose nanocrystals with improved properties. *International Journal of Biological Macromolecules*, 220(April), 589–600. <https://doi.org/10.1016/j.ijbiomac.2022.08.047>
- Dizaj, S. M., Yaqoubi, S., Adibkia, K., & Lotfipour, F. (2016). Nanoemulsion-based

- delivery systems: preparation and application in the food industry. In *Emulsions*. Elsevier Inc. <https://doi.org/10.1016/B978-0-12-804306-6/00009-X>
- Ettxabide, A., Uranga, J., Guerrero, P., & Caba, K. De. (2017). Development of active gelatin films by means of valorisation of food processing waste : A review. *Food Hydrocolloids*, 68, 192–198. <https://doi.org/10.1016/j.foodhyd.2016.08.021>
- Fakhreddin, S., Zandi, M., Rezaei, M., & Farahmandghavi, F. (2013). Two-step method for encapsulation of oregano essential oil in chitosan nanoparticles : Preparation , characterization and in vitro release study. *Carbohydrate Polymers*, 95(1), 50–56. <https://doi.org/10.1016/j.carbpol.2013.02.031>
- Fathollahi, M., Aminzare, M., Mohseni, M., & Hassanzadazar, H. (2019). Antioxidant capacity , antimicrobial activities and chemical composition of Pistacia atlantica subsp . kurdica essential oil. *Veterinary Research Forum*, 10(4), 299–305. <https://doi.org/10.30466/vrf.2018.83910.2103>
- Feng, X., Sun, Y., Tan, H., Ma, L., Dai, H., & Zhang, Y. (2023). Effect of oil phases on the stability of myofibrillar protein microgel particles stabilized Pickering emulsions : The leading role of viscosity. *Food Chemistry*, 413(2), 135653. <https://doi.org/10.1016/j.foodchem.2023.135653>
- Ferreira, S., Daniel, J., Souza, A. G., Yudice, E. D. C., Campos, I. B. De, Dal, R., Mour, A., Martinho, H. S., & Rosa, D. S. (2023). Eco-friendly and effective antimicrobial Melaleuca alternifolia essential oil Pickering emulsions stabilized with cellulose nanofibrils against bacteria and SARS-CoV-2. *International Journal of Biological Macromolecules*, 243. <https://doi.org/10.1016/j.ijbiomac.2023.125228>
- Hefferon, K., Cantero-tubilla, B., Badar, U., & Wilson, D. W. (2020). Plant-Based Cellulase Assay Systems as Alternatives for Synthetic Substrates. *Applied Biochemistry and Biotechnology*, 192, 1318–1330.
- Hu, J., Tian, D., Renneckar, S., & Saddler, J. N. (2018). Enzyme mediated nanofibrillation of cellulose by the synergistic actions of an endoglucanase, lytic polysaccharide monooxygenase (LPMO) and xylanase. *Scientific Reports*, 8(1), 4–11. <https://doi.org/10.1038/s41598-018-21016-6>
- Kumar, P. S., Nattudurai, G., Islam, V. I. H., & Ignacimuthu, S. (2022). The effects of some essential oils on Alternaria alternata , a post - harvest phyto - pathogenic fungus in wheat by disrupting ergosterol biosynthesis. *Phytoparasitica*, 50, 513–525. <https://doi.org/10.1007/s12600-021-00970-4>
- Lao, Y., Zhang, M., Li, Z., & Bhandari, B. (2020). A novel combination of enzymatic hydrolysis and fermentation : Effects on the flavor and nutritional quality of fermented Cordyceps militaris beverage. *LWT - Food Science and Technology*, 120(October 2019), 108934. <https://doi.org/10.1016/j.lwt.2019.108934>
- Leite, A. M. P., Zanon, C. D., & Menegalli, F. C. (2017). Isolation and characterization of cellulose nanofibers from cassava root bagasse and peelings. *Carbohydrate Polymers*, 157, 962–970. <https://doi.org/10.1016/j.carbpol.2016.10.048>
- Leyva-I, N., Guti, E. P., Vazquez-olivo, G., & Heredia, J. B. (2017). *Essential Oils of Oregano : Biological Activity beyond Their Antimicrobial Properties*. <https://doi.org/10.3390/molecules22060989>

- Li, Y., Xie, H., Tang, X., Qi, Y., Li, Y., Wan, N., & Yang, M. (2022). Application of edible coating pretreatment before drying to prevent loss of plant essential oil : A case study of *Zanthoxylum schinifolium* fruits. *Food Chemistry*, 389(September 2021). <https://doi.org/10.1016/j.foodchem.2022.132828>
- Lima, A. R., Cristofoli, N. L., Ana M. Rosa da Costa, A. M., Saraiva, J. A., & Vieira, M. C. (2023). Comparative study of the production of cellulose nanofibers from agro-industrial waste streams of *Salicornia ramosissima* by acid and enzymatic treatment. *Food and Bioproducts Processing*, 137, 214–225. <https://doi.org/10.1016/j.fbp.2022.11.012>
- Liu, Y., Shi, Z., Zou, Y., Yu, J., Liu, L., & Fan, Y. (2023). Comparison of cellulose and chitin nanofibers on Pickering emulsion stability — Investigation of size and surface wettability contribution. *International Journal of Biological Macromolecules*, 235(February), 123754. <https://doi.org/10.1016/j.ijbiomac.2023.123754>
- Mohamed, E. A. A., Muddathir, A. M., & Osman, M. A. (2020). Antimicrobial activity , phytochemical screening of crude extracts , and essential oils constituents of two *Pulicaria* spp . growing in Sudan. *Scientific Reports*, 1–8. <https://doi.org/10.1038/s41598-020-74262-y>
- Mollea, C., Bosco, F., & Fissore, D. (2022). Agar Plate Methods for Assessing the Antibacterial Activity of Thyme and Oregano Essential Oils against *S. epidermidis*. *Antibiotics*, 11.
- Oun, A. A., Hwa, G., & Tae, J. (2022). Multifunctional poly (vinyl alcohol) films using cellulose nanocrystals / oregano and cellulose nanocrystals / cinnamon Pickering emulsions : Effect of oil type and concentration. *International Journal of Biological Macromolecules*, 194(August 2021), 736–745. <https://doi.org/10.1016/j.ijbiomac.2021.11.119>
- Parajuli, S., & Ureña-Benavides, E. E. (2022). Fundamental aspects of nanocellulose stabilized Pickering emulsions and foams. In *Advances in Colloid and Interface Science* (Vol. 299). Elsevier B.V. <https://doi.org/10.1016/j.cis.2021.102530>
- Peddireddy, K. R., Nicolai, T., Benyahia, L., & Capron, I. (2016). Stabilization of Water-in-Water Emulsions by Nanorods. *ACS Macro Lett*, 5, 283–286. <https://doi.org/10.1021/acsmacrolett.5b00953>
- Perveen, K., Bokhari, N. A., Al-rashid, S. A. I., & Al-, L. A. (2020). Chemical Composition of Essential Oil of *Ocimum basilicum* L. and Its Potential in Managing the Alternaria Rot of Tomato. *Journal of Essential Oil Bearing Plants*, 23(6), 1428–1437. <https://doi.org/10.1080/0972060X.2020.1868351>
- Perzon, A., Jørgensen, B., & Ulvskov, P. (2020). Sustainable production of cellulose nanofiber gels and paper from sugar beet waste using enzymatic pre-treatment. *Carbohydrate Polymers*, 230(November 2019), 115581. <https://doi.org/10.1016/j.carbpol.2019.115581>
- Purves, C. (1954). *Chain structure in cellulose and cellulose derivatives: part 1* - Wiley, New York.
- Rossi, B. R., Pellegrini, V. O. A., Cortez, A. A., Chiromito, E. M. S., Carvalho, A. J. F., Pinto, L. O., Rezende, C. A., Mastelaro, V. R., & Polikarpov, I. (2021). Cellulose

- nanofibers production using a set of recombinant enzymes. *Carbohydrate Polymers*, 256(December 2020), 117510.
<https://doi.org/10.1016/j.carbpol.2020.117510>
- Sánchez-Gutiérrez, M., Espinosa, E., Bascón-Villegas, I., Pérez-Rodríguez, F., Carrasco, E., & Rodríguez, A. (2020). Production of Cellulose Nanofibers from Olive Tree Harvest — A Residue with Wide Applications. *Agronomy*, 10(696).
- Souza, A. G. De, Ferreira, R. R., Silva, E., Aguilar, F., Zanata, L., & Rosa, S. (2021). Cinnamon Essential Oil Nanocellulose-Based Pickering Emulsions : Processing Parameters Effect on Their Formation , Stabilization , and Antimicrobial Activity. *Polysaccharides*, 2, 608–625.
- Soylu, E. M., & Kose, F. (2015). Antifungal Activities of Essential Oils Against Citrus Black Rot Disease Agent *Alternaria alternata*. *Journal of Essential Oil Bearing Plants*, 5026(18:4), 894–903. <https://doi.org/10.1080/0972060X.2014.895158>
- Sun, Z., Yan, X., Xiao, Y., Hu, L., Eggersdorfer, M., Chen, D., Yang, Z., & Weitz, D. A. (2022). Particuology Pickering emulsions stabilized by colloidal surfactants : Role of solid particles. *Particuology*, 64, 153–163.
<https://doi.org/10.1016/j.partic.2021.06.004>
- Teixeira, B., Marques, A., Ramos, C., Neng, N. R., Nogueira, J. M. F., Alexandre, J., & Leonor, M. (2013). Chemical composition and antibacterial and antioxidant properties of commercial essential oils. *Industrial Crops & Products*, 43, 587–595.
<https://doi.org/10.1016/j.indcrop.2012.07.069>
- Tibolla, H., Pelissari, F. M., & Menegalli, F. C. (2014). Cellulose nanofibers produced from banana peel by chemical and enzymatic treatment. *LWT - Food Science and Technology*, 59(2P2), 1311–1318. <https://doi.org/10.1016/j.lwt.2014.04.011>
- Ventura-cruz, S., & Tecante, A. (2019). Extraction and characterization of cellulose nano fi bers from Rose stems (*Rosa* spp .). *Carbohydrate Polymers*, 220(May), 53–59. <https://doi.org/10.1016/j.carbpol.2019.05.053>
- Viana, T., Cristina, J., Lima, J., Rogelio, T., Nunes, I., Machinski, M., Martha, J., & Mikcha, G. (2019). Bioactivity of oregano (*Origanum vulgare*) essential oil against *Alicyclobacillus* spp. *Industrial Crops & Products*, 129(September 2018), 345–349.
<https://doi.org/10.1016/j.indcrop.2018.12.025>
- Vicentini, N. M., Dupuy, N., Leitzelman, M., Cereda, M. P., & Sobral, P. J. A. (2005). Prediction of cassava starch edible film properties by chemometric analysis of infrared spectra. *Spectroscopy Letters*, 38(6).
- Wayne. (2002). *Reference method for broth dilution antifungal susceptibility testing of yeasts, approved standard. CLSI document M27-A2.*
- Wayne, P. A. (2015). *Methods for dilution antimicrobial susceptibility test for bacteria that grow aerobically, approved standard. CLSI document M07-A10.*
- Zabka, M., & Pavela, R. (2013). Chemosphere Antifungal efficacy of some natural phenolic compounds against significant pathogenic and toxinogenic filamentous fungi. *Chemosphere*, 93(6), 1051–1056.
<https://doi.org/10.1016/j.chemosphere.2013.05.076>

Zhou, Y., Sun, S., Bei, W., Zahi, M. R., Yuan, Q., & Liang, H. (2018). Preparation and antimicrobial activity of oregano essential oil Pickering emulsion stabilized by cellulose nanocrystals. *International Journal of Biological Macromolecules*, 112, 7–13. <https://doi.org/10.1016/j.ijbiomac.2018.01.102>

CAPÍTULO V

CELLULOSE NANOFIBERS AS STABILIZER OF PICKERING EMULSIONS AND REINFORCEMENT OF PECTIN FILMS COVERING TOMATOES

Manuscript prepared to be submitted to Food Packaging and Shelf Life

Cellulose nanofibers as stabilizer of Pickering emulsions and reinforcement of pectin films covering tomatoes

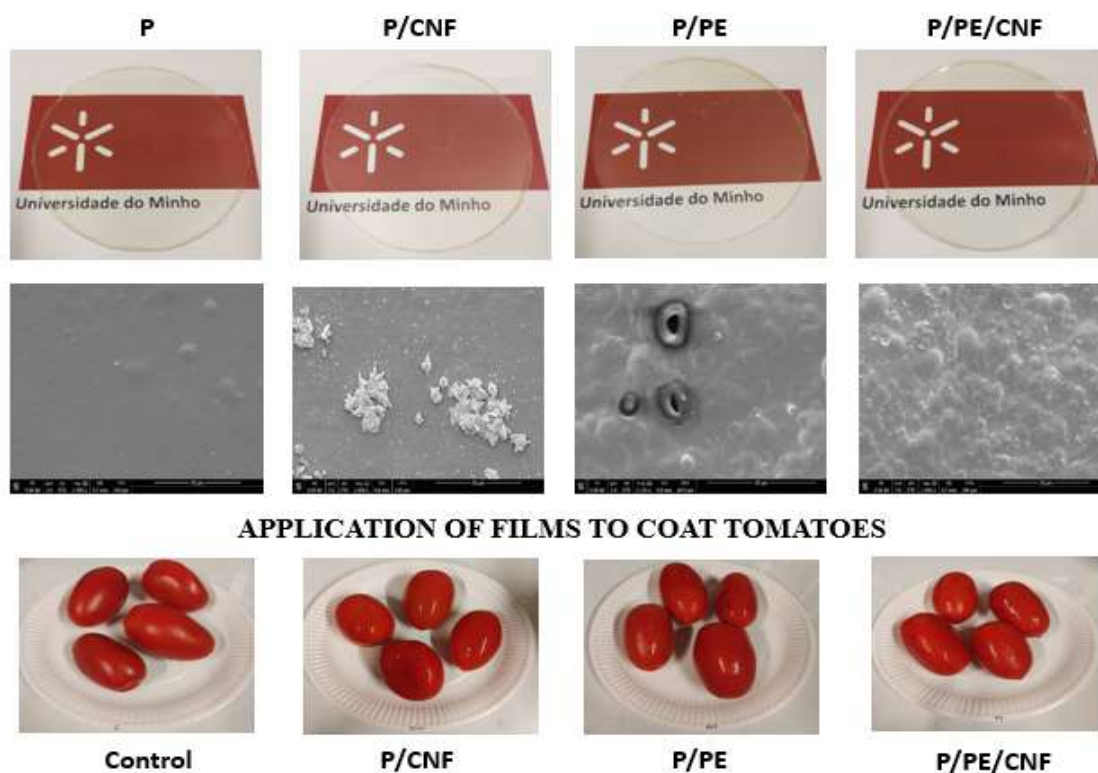
Raquel Costa Chevalier¹, Jorge M. Vieira^{2,3}, Joana T. Martins^{2,3}, Rosiane Lopes Cunha^{1*}, António A. Vicente^{2,3}

¹Laboratory of Process Engineering (LEP), Department of Food Engineering and Technology (DETA), School of Food Engineering (FEA), University of Campinas (UNICAMP), 13083-862, Campinas, São Paulo Brazil.

²CEB - Centre of Biological Engineering, University of Minho, 4710-057 Braga, Portugal

³LBBELS –Associate Laboratory, Braga/Guimarães, Portugal

Graphical abstract



Abstract

Cellulose nanofibers can be used as biocompatible reinforcing agents in biodegradable films to be used to protect food products such as fruits. Tomato is an extremely perishable fruit that can easily spoil due to inadequate handling or storage conditions in the post-harvest period, or even due to contamination by microorganisms. In this context, the aim of this work was to develop biopolymeric films/coatings with improved barrier properties from incorporation of cellulose nanofibers (CNF), in addition to

Pickering emulsions (PE) containing oregano oil as an antimicrobial agent to increase the shelf life of tomatoes. *In vitro* cytotoxicity of CNFs showed that the quantity used to prepare the films did not present toxicity. Pectin (P) films with CNF and/or PE were produced and characterized to understand the role of CNF and PE as reinforcing material and improving water vapor permeability properties, respectively. Moreover, addition of PE and CNF to the films increased their elasticity and hydrophobicity. Interestingly, the incorporation of CNF and PE did not affect the transparency of the films, although films containing only PE or containing PE and CNF had the ability to completely block UV light. Film-forming solutions were used as coatings on the tomato surface. Coated and uncoated tomatoes were stored at 4 °C for 12 days and their physicochemical and microbiological characteristics were assessed during storage. Coating was effective in controlling microbial growth, showing that pectin films incorporating CNF and PE are an attractive solution for extending the shelf-life of perishable fruits such as tomato.

Keywords: Cellulose nanofibers; Pickering emulsions; films; coatings; tomatoes.

1.Introduction

Tomatoes are highly perishable climacteric fruits that ripen quickly and are quite susceptible to post-harvest decay caused by fungal pathogens, in addition to producing some mycotoxins that are harmful to health (Sun et al., 2017). There are several ways to increase the shelf life of climacteric fruits, and the use of coatings/films is an interesting method due to their ability to control oxygen consumption from the environment, reducing the rate of respiration and delaying the premature aging process. Various materials are used in fruit packaging, but the use of biopolymers, such as polysaccharides and proteins, is a more sustainable strategy due to the biocompatibility and eco-friendliness of such materials. Pectin is a plant-derived heteropolysaccharide with excellent properties such as biodegradability, non-toxicity and film-forming capacity. Furthermore, pectin-based films present very interesting characteristics from the consumer perspectives, as they are transparent and have good mechanical properties (Kumar et al., 2020). However, pectin-based films/coatings have limited application on fruits due to their moisture absorption capacity. The incorporation of organic compounds such as oils is a strategy that, in addition to increasing hydrophobicity, can carry functional compounds by developing active films. In fact, antimicrobial agents in coatings, such as essential oils, can improve physiological quality and inhibit the growth of microorganisms (Arnon-rips and Poverenov, 2018).

Oregano essential oil (OEO) contains bioactive components, such as carvacrol and thymol, that can inhibit microbial growth. Nevertheless, the use of OEO as an

antimicrobial agent in fruits has some limitations, as it is easily oxidized when exposed to direct light, heat and oxygen, in addition to having an intense and characteristic odor (Wang et al., 2024). Therefore, encapsulating and protecting OEO from degradation and volatilization in a stable emulsified system can expand applications. Some studies have demonstrated that Pickering emulsions (PE) stabilized by particles such as cellulose nanofibers (CNF) are quite stable to coalescence, due to the high adsorption energy at the droplet interface (Arkoumanis et al., 2019; Jafari et al., 2016; Sahraee et al., 2017). Therefore, vehiculating essential oil in PE in the film-forming solution can be beneficial considering the combination of antibacterial activity (Xu et al., 2023) with barrier properties of the films/coatings. CNF, in addition to being a bionanomaterial produced from the most abundant biopolymer on the planet, cellulose, has interesting features including recyclability, low cost, biodegradability and excellent mechanical properties (Chen et al., 2023), in addition to being included in the concept of circular economy if prepared from industrial waste, such as peels, leaves and fruit hulls. In food films/coatings, the main role of CNF has been its use as structural reinforcement, aiming to improve the quality of the mechanical properties of packaging. Considering the above, pectin films, incorporated with PE and stabilized by CNF obtained from cassava peel, were used to coat tomatoes. Oregano oil was used in the dispersed phase of the emulsions to improve both film barrier properties and antimicrobial activity of the films/coatings that were used to extend the conservation of tomatoes.

2. Material and Methods

2.1 Materials

Crushed cassava peel and enzymes were kindly donated by Plaza Ind. Com. Ltda (Brazil) and Novozymes Latin America Ltda (Brazil), respectively. Oregano essential oil was obtained from Ferquima (Vargem Grande Paulista, Brazil). Low methoxyl pectin (GENU Pectin Type LM-102 AS) was kindly supplied by CP Kelco Brasil S/A (São Paulo, Brazil). All chemicals used in this work were analytical grade.

2.2 Production of cellulose nanofiber (CNF)

Cassava peel was processed using enzymatic hydrolysis. The first step used xylanase (Chevalier et al., 2024), while in the second hydrolysis step cellulase was employed for 12 h (Capítulo IV). The cassava peel was processed using enzymatic

hydrolysis. The first step used xylanase (Chevalier et al., 2024), while in the second hydrolysis step cellulase was used for 12 h (Chapter IV).

2.2.1 CNF cytotoxicity

CNF effect on cell viability was evaluated using the methylthiazolyldiphenyl-tetrazolium bromide (MTT) conversion assay. CNFs were prepared at various concentrations (0.4; 0.9; 1.8; 3.75 and 7.5 % w/w) in supplemented DMEM medium and homogenized. Caco-2 cell suspension was seeded in a 96-well microplate at a density of 2.5×10^5 cells/mL in 200 μ L of supplemented DMEM, and then incubated for 24 hours at 37 °C under a 5% CO₂ environment. Subsequently, the medium was replaced, and CNF solutions were added to the cell culture and further incubated (37 °C; 5% CO₂) for another 24 hours. A blank sample (DMEM without cells) and a positive control (DMEM with cells) were also included in the experiment. Each treatment was performed in quadruplicate. Afterwards, the supernatant was discarded, and 200 μ L of MTT solution (0.5 mg/mL in supplemented DMEM) was added to each well, protected from light, and incubated at 37 °C for 4 hours to allow the formation of purple formazan crystals. Following this, the medium was removed, and the purple formazan crystals were dissolved from the cells using 200 μ L of DMSO. The culture plates were then shaken on an orbital shaker for 30 minutes to completely dissolve the purple formazan crystals. The enzymatic reduction of yellow tetrazolium MTT to purple formazan was quantified using a Synergy™ HT Multi-mode Microplate Reader (Biotek Instruments, Winooski, VT, USA) at 570 nm, with background subtraction performed using readings at 690 nm.

2.3 Production of films

Firstly, an emulsion (PE) was produced with an oily phase fixed at 10% (w/w) and composed of sunflower oil (SO) and OEO in a ratio of 8:2 OEO:SO. An aqueous dispersion of CNF (0.01% w/w) was the continuous aqueous phase. Oil-in-water emulsions were prepared by homogenizing the mixture of oil (10% w/w OEO + SO) and the aqueous phase (90% w/w) in a rotor-stator (Ultra Turrax T18, IKA, Germany) at 13,000 rpm for 10 min.

Films (4 g pectin/100 g of film-forming solution) were produced by the casting method. The film-forming solution (FFS) and, consequently, films varied depending on

the composition. In addition to pectin (P), the films could contain PE (stabilized with 0.01% w/w CNF) and/or CNF as reinforcing material (1% w/w CNF). The films composition and name were: nanocomposite (P + CNF- named P/CNF), emulsified (P + PE - called P/PE) and emulsified nanocomposite (P + PE + CNF - named P/PE/CNF). Films without PE and CNF were produced as control (P).

To prepare the film-forming solutions, first, pectin was hydrated and solubilized for 1 h in water. PE and CNF dispersion (10% w/w and 1% w/w of the film-forming solution, respectively) were added to the FFS dropwise under magnetic stirring (1,000 rpm, AA-2050, Gehaka, Brazil) in nanocomposite and emulsified formulations. Then, glycerol (25 g/100 g of pectin) was added to the FFS under stirring at 10,000 rpm for 5 min (Ultraturrax® IKA T25, Labotechnik, Germany) at room temperature. The FFSs were poured into acrylic plates (140 mm) and then dried at 35 °C for 24 h (MA035/5, Marconi, Brazil). The films were conditioned for 7 days in desiccators with saturated NaBr solution (relative humidity = 58%) at 25 °C before being characterized. The films were also previously conditioned in silica gel for 15 days before microscopy analyses.

2.4 Characterization of the films

2.4.1 Rheology

The viscosity and oscillatory rheological properties of the FFS were determined by a Physica MCR301 rheometer (Anton Paar, Graz, Austria) attached to a parallel plate geometry (diameter 40 mm, gap 0.5 mm). For the evaluation of flow curves (viscosity), FFS were tested at a fixed temperature (25 °C) in three shear rate sweeps (up-down-up) using a shear rate range between 0 and 300 s⁻¹. Oscillatory rheological properties were measured under a fixed strain condition of 1% (within the linear viscoelastic range) and varying angular frequency from 0.1 to 100 rad/s and at 25 °C. Data were analyzed using TRIOS v4.3.1 software.

2.4.2 Thickness and morphology

Film thickness was determined with a digital micrometer (No. 293-5, Mitutoyo, Japan). Ten thickness measurements were randomly taken on each sample. Average values were used to calculate water vapor permeability (WVP) and tensile strength (TS). Ten thickness measurements were made.

The effect of adding PE and CNF on the morphology of the P films was evaluated using a scanning electron microscope (SEM) (Nova NanoSEM 200, Eindhoven, The Netherlands) with an accelerating voltage of 10 to 15 kV under vacuum conditions. The films were mounted on aluminum stubs with carbon tape and then coated with gold to a thickness of about 10 nm. The measurements were performed in triplicate.

2.4.3 Fourier-transform infrared (FTIR) spectroscopy

The films were characterized by Fourier transform infrared spectroscopy (FTIR) on a Bruker FT-IR VERTEX 80/80 v (Boston, USA) in Attenuated Total Reflectance (ATR) mode with a platinum crystal accessory. Sixteen scans were performed with a resolution of 4 cm⁻¹ between 400 and 4000 cm⁻¹. The measurements were performed in triplicate.

2.4.4 Moisture content (MC) and solubility in water (SW)

MC of the films was determined using the gravimetric method by drying the films at 105 °C in an oven with forced air circulation for 24 h. The SW was determined by shaking (60 rpm) film samples (2 cm in diameter and known dry weight) immersed in 50 mL of distilled water at 25 °C for 24 h (Shaker MA- 41, Marconi, Brazil) (Cuq et al., 1996). The non-solubilized part of the films was dried at 105 °C in a forced circulation oven for 24 h. MC and SW were calculated according to Eq. (1).

$$\text{MC or SW (\%)} = \frac{M_i - M_f}{M_i} \times 100 \quad \text{Eq. (1)}$$

Where M_i and M_f are the mass of the initial samples and after drying the films, respectively. The experiments were performed in triplicate.

2.3.5 Water vapor permeability (WVP)

WVP of the films was determined gravimetrically at 20 °C based on the ASTM E96-92 method (Guillard et al., 2003). The films were sealed on the top of a permeation cell containing distilled water (100% RH; vapor pressure of water at 20 °C= 2,337 Pa) and placed in a desiccator with silica gel and 0% RH (vapor pressure of water= 0 Pa). Cells were weighed at 2 h intervals for 10 h. The water transferred through the film and adsorbed by the desiccant was determined from the weight loss of the permeation cell. Steady-state conditions and uniform water pressure were assumed by maintaining constant air circulation outside the cell by means of a mini fan placed inside the desiccator. The slope of the curve representing weight loss versus time (WVTR) was obtained from linear regression. The WVP was determined using Eq. (2).

$$WVP = \frac{WVTR \times L}{\Delta P} \quad \text{Eq. (2)}$$

Where WVTR is the water vapor transmission rate ($\text{g m}^{-2} \text{s}^{-1}$) through the film, L is the average film thickness (m) and ΔP is the water vapor partial pressure difference (Pa) between the two sides of the films. For each film type, WVP measurements were performed in triplicate.

2.4.6 Water contact angle (WCA)

WCA measurements were performed on a face contact angle meter (OCA 20, Dataphysics, Germany). The contact angle was measured using a 500 μL syringe (Hamilton, Switzerland) with a 0.75 mm diameter needle. The contact angle on the film surfaces was measured by the sessile drop method (Coelho et al., 2017). Each measurement was taken within 30 s. At least eight contact angle measurements were obtained for each sample.

2.4.7 Color and opacity

The color of the films was determined with a Minolta digital colorimeter (Konica Minolta, model Chroma Meter CR-400, Osaka, Japan). The CIELab scale was used to determine the color parameters L^* , a^* and b^* . Opacity (Y) was determined as the ratio between the opacity of each sample in the black standard (Y_b) and the opacity of each sample in the white standard (Y_w), using Eq. (3).

$$Y (\%) = \frac{Y_b}{Y_w} \times 100$$

Eq. (3)

Where Y_b is the black pattern and Y_w is the white pattern. Samples were analyzed in triplicate, recording four measurements per triplicate.

2.4.8 UV/Vis light barrier

The barrier properties to ultraviolet and visible light (UV/Vis) were evaluated using a UV-Vis spectrophotometer (Lambda 25 UV/Vis, Perkin-Elmer, USA) in transmittance mode, using a wavelength range from 200 to 800 nm (Bonilla and Sobral, 2016). The films were cut (10×100 mm) and fixed in the cuvette so that light passed through the film sample. Samples were analyzed in triplicate.

2.4.9 Mechanical properties

Mechanical properties such as elongation at break (EB) and Young elastic modulus (YM) were measured with a TA.HD plus Texture Analyzer (Serial RS232, Stable Micro Systems, Surrey, UK Kingdom), with a 5 kg load cell, following ASTM D 882-02 (2010) guidelines. The films were cut (length 10 mm and width 20 mm) to perform the measurements. The initial gripping separation and the crosshead speed were set to 90 mm and 5 mm min⁻¹, respectively. The tests were repeated six times for each sample.

2.5 Shelf- life of tomatoes

2.5.1 Preparation of coatings

Ripe (very red) tomatoes (*Lycopersicon esculentum* Mill.), purchased at the local market, were cleaned in a 2% (w/w) sodium hypochlorite solution to remove dirt from the surface, before being coated. Coating formulations followed the same conditions as the film-forming solutions (section 2.3), that is, P/CNF, P/PE and P/PE/CNF. The tomatoes were immersed in the FFS and subsequently dried at 35 °C on a stove for 20 min. Uncoated tomatoes and tomatoes coated with the different formulations were stored at 5 ± 0.6 °C and relative humidity of 90 ± 3%. Physicochemical and microbiological analyses of tomatoes were carried out at 0, 3, 6, 9 and 12 days of storage.

2.5.2 Physicochemical analyzes

Tomatoes from each treatment (30 g) were crushed in a mixer before proceeding with pH, titratable acidity and total soluble solids analyses. The pH was determined using a pH meter (Hanna Instruments Inc., Romania) in order to check tomato deterioration due to the action of microorganisms. The titratable acidity was determined by the 942.15 AOAC method (AOAC, 1997). The results were expressed in % (grams of citric acid equivalent per 100 g of tomato). Total soluble solids (TSS) were measured using the RHB-32ATC refractometer, previously standardized with water (Hanna Instruments Inc., Romania), according to method 932.12 AOAC (AOAC, 1997). The results were expressed in %. The weight loss of tomatoes was calculated by weighing whole tomatoes on a precision scale (Mettler AE200) on day 0 and on the other days of storage, using the same samples (Vieira et al., 2016). Weight loss was determined by equation 4:

$$\text{Weight loss (\%)} = \frac{w_i - w_f}{w_i} \times 100 \quad \text{Eq. (4)}$$

where W_i is the initial sample weight (day 0) and W_f is the sample weight on day 3, 6, 9 or 12.

Tomato color was measured with a ColorFlex colorimeter (HunterLab, Reston, VA, USA) using the D65 illuminant (Oliveira-Bouzas et al., 2021). The luminosity parameters (L^*), chroma a^* (red/green) and chroma b^* (yellow/blue) were recorded. Color measurements were carried out at 25 ± 1 °C in four different locations on each fruit. Data are presented as average of 4 fruits on each day of shelf life analysis. Texture profile analysis (TPA) was performed on whole tomatoes according to previous studies (Mendes et al., 2023; Zheng et al., 2023) in order to obtain the firmness parameter. A texture analyzer (Stable Micro Systems Ltd., Godalming, UK) equipped with a 250 kg load cell was used to obtain the force-time curves. Coated and uncoated tomatoes were tested in quadruplicate at 21 °C. For data analysis, the Texture Exponent version, software 6.1.1.0 from Stable Microsystems (Surrey, United Kingdom) was used.

2.5.3 Microbiological analyzes

Total viable count (TVC) of tomato samples were assessed on tryptone glucose extract agar after incubation at 30 °C for 2 days according to EN ISO 4833-1:2013. Molds and yeasts count were evaluated on potato dextrose agar (PDA) after incubation at 25 °C for 2 days in accordance to ISO 21527-1/2:2008. The effect of coating on microbial counts of tomato samples stored under refrigerated conditions was evaluated during storage on day 0, 3, 6, 9 and 12. All counts were expressed as log colony forming units ($\log \text{UFC.g}^{-1}$).

2.6 Statistical analysis

To compare the differences between the average values obtained for the properties of the different films and the physicochemical properties of the tomatoes, analysis of variance (ANOVA) and Tukey's multiple comparison test were performed with a significance level of 5% using Statistica 7.0 software (StatSoft Inc., Tulsa, Oklahoma, USA).

3. Results and discussion

3.1 *In vitro* cytotoxicity of CNF

Cellulose nanofibers (CNFs) derived from cassava peel through enzymatic hydrolysis have promising potential as stabilizers of food matrices and reinforcement for biodegradable packaging, among other applications. Given the intended use of new materials in human consumption, it is imperative to carry out toxicity studies to ensure biosafety and biocompatibility before commercialization (Mejía-Jaramillo et al., 2023). In this study, the *in vitro* cytotoxicity of CNFs was evaluated. Caco-2 cells were exposed to various concentrations of CNF for 24 hours to evaluate potential cytotoxic effects. The impact of CNF on Caco-2 cell viability is depicted in Figure 1. The observed effect on cell viability appeared to correlate with the post-exposure CNF concentration. The increase in CNF concentration decreased the viability of Caco-2 cells only above 3.75% (w/w) ($p \leq 0.05$). Cell viability was from 98.50% to 88.77% compared to the positive control. Thus, within the concentration range investigated (0.01% to 1% w/w CNF), the results suggest that CNFs did not exert a toxic effect on cells.

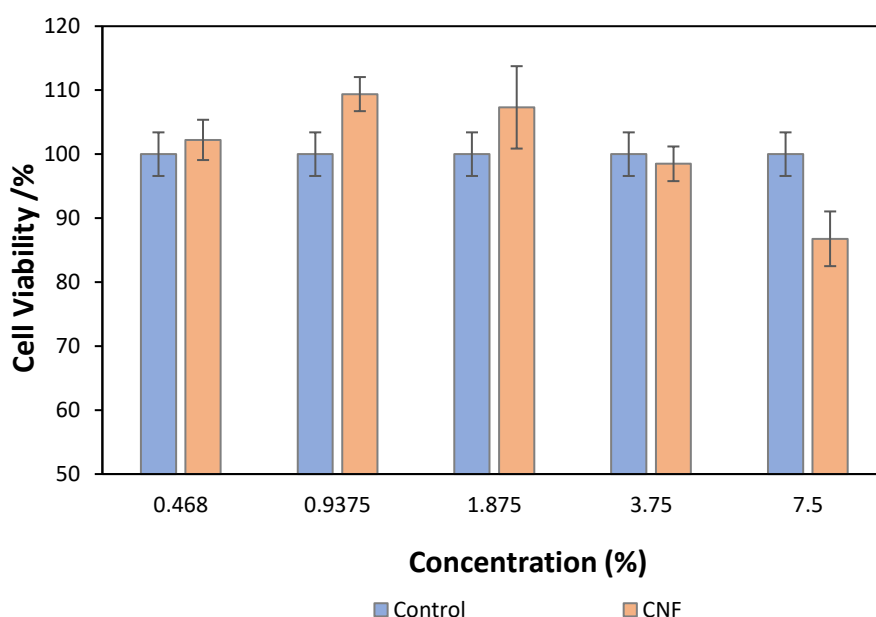


Figure 1. CNF effect on Caco-2 cell viability after 24 h of incubation (bars represent standard deviation).

3.2 Films properties

3.2.1 Rheological properties

The rheological properties of FFS directly affect the properties of the films. A frequency sweep was performed to evaluate the storage (G') and loss (G'') moduli as a function of frequency (Figure 2). FFS showed predominant elastic behavior ($G' > G''$) regardless composition, showing physical characteristics of weak gel (Silva-Weiss et al., 2014) because G' was frequency dependent. Flow curves were well-fitted to power law equation (Table 1), showing a shear thinning behavior (n between 0.31 and 0.42) with viscosity decreasing with increasing shear rate. Addition of different components to FFS can influence the viscosity of the FFS and, consequently, the drying time of the films (Ren et al., 2021). Furthermore, the stability of emulsions is directly proportional to viscosity, as high viscosity can delay PE phase separation during film drying. CNF are capable of increasing viscosity, through fiber entanglement, forming networks within FFS matrix (Fein et al., 2020). However, the addition of CNF and PE reduced the viscosity at low shear rate (important considering that drying occurs in quiescent conditions), favoring a shorter drying time of the FFS. Due to shear thinning behavior, as the shear rate increases, the particles gradually move in the same direction and the intermolecular force of the formed networks decreases, breaking the interactions and reducing the viscosity of the FFS. Thus, the combination of pseudoplasticity with more complex composition provided a lower viscosity (Liu and Tang, 2011; Ren et al., 2021) under process conditions used in films production such as extrusion and spreading.

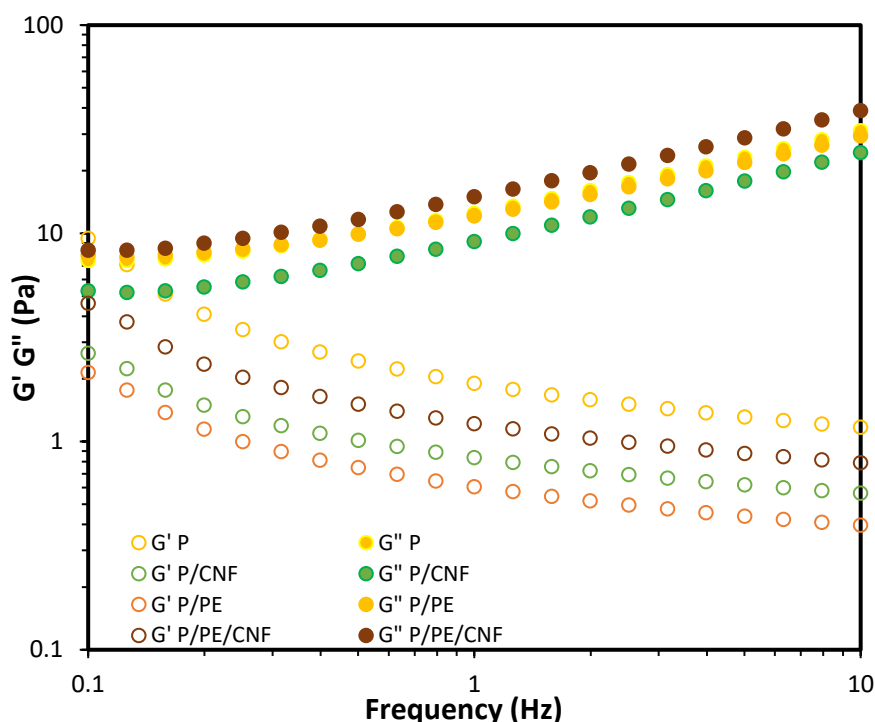


Figure 2. Oscillatory rheology of FFS. Storage (G') and loss (G'') moduli as a function of frequency. P: pectin film; P/CNF: pectin film reinforced with CNF; P/PE: pectin film added with PE and P/PE/CNF: pectin film added with PE and CNF.

Table 1. Rheological properties obtained from power law equation fitted to flow curves of FFS. Viscosity values (η) were evaluated at a shear rate of 10 s^{-1} .

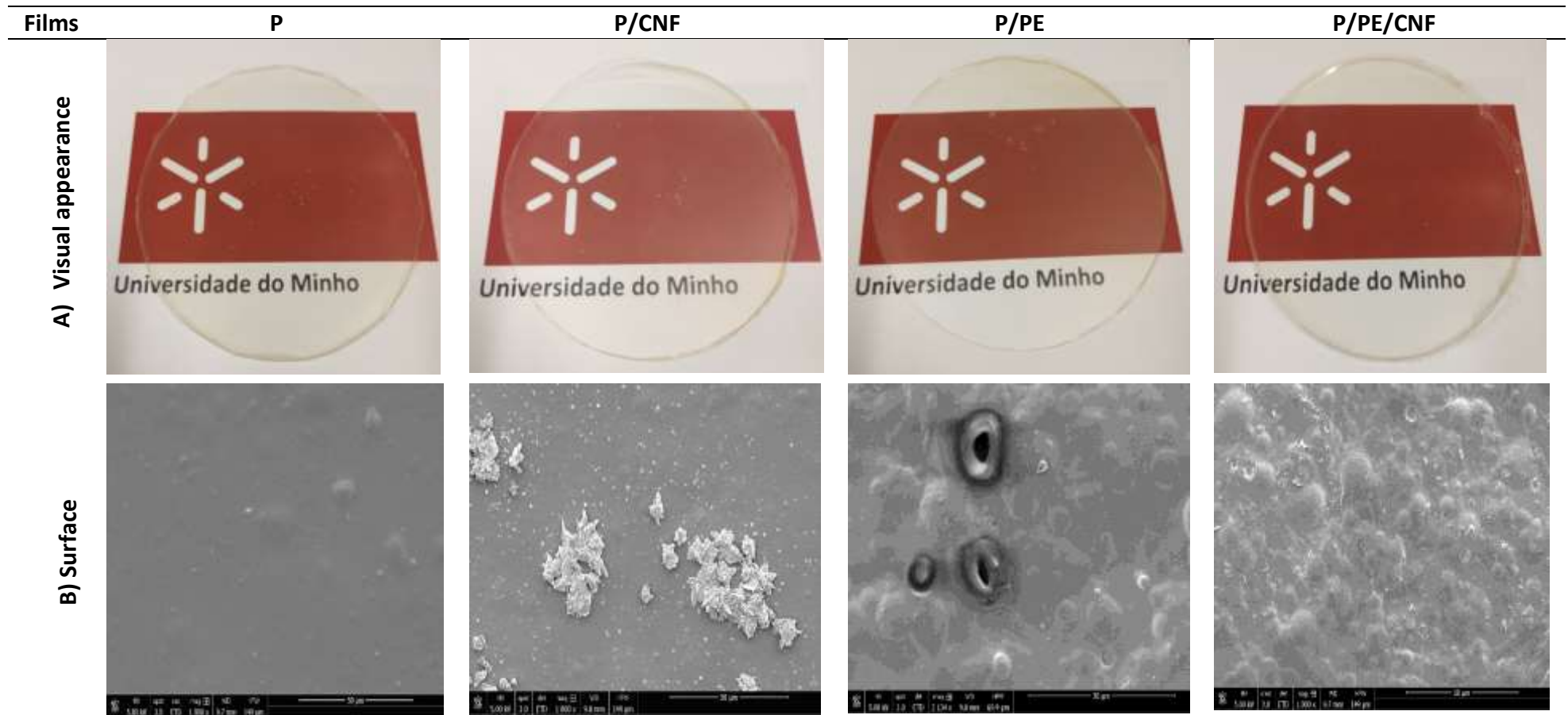
FFS	$k (\text{Pa.s}^n)$	n	$\eta (\text{Pa.s})$
P	18.37 ± 1.63^A	0.31 ± 0.02^B	7.02 ± 0.11^A
P/CNF	8.90 ± 0.45^B	0.40 ± 0.01^A	2.77 ± 0.75^B
P/PE	8.51 ± 1.10^{BC}	0.34 ± 0.02^B	1.92 ± 0.21^B
P/PE/CNF	6.09 ± 0.40^C	0.42 ± 0.09^{AB}	2.72 ± 1.47^B

Different letters indicate significant differences ($p < 0.05$).

3.2.2 Structure and appearance

Macroscopic appearance, as well as surface and cross-section morphology of films can be seen in Figure 3. Differences in the structure of the films were observed with addition of CNF and/or PE. P/CNF films showed a compact structure, but presented agglomeration of some CNF particles both on the surface and in the cross-section of the film. Possibly, the FFS homogenization time was not enough to allow the complete incorporation of CNF into the pectin matrix. The presence of cavities and oil droplets

that tend to aggregate on the surface of the films were observed with PE addition to the films. The holes observed on the film surface became even more evident in the cross-section of the films. Regarding P/PE/CNF film, it was possible to observe the presence of oil droplets on the surface and some cavities in the cross section of the film, predominantly due to PE addition (Zhao et al., 2022). However, in general, the appearance of the films was quite similar, regardless of composition.



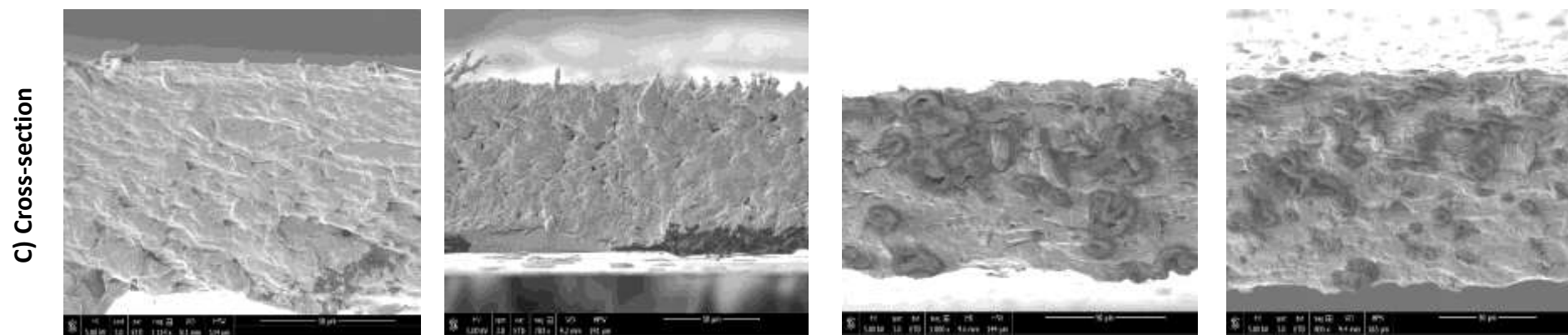


Figure 3. Visual appearance (A), surface (B) and cross-section (C) morphology of the films: P: pectin film; P/CNF: pectin film reinforced with CNF; P/PE: pectin film added with PE and P/PE/CNF: pectin film added with PE and CNF.

3.2.3 Fourier-transform infrared (FTIR) spectroscopy

The FTIR spectra of CNF and films (P; P/CNF; P/PE and P/PE/CNF) are shown in Figure 4. The broad peak observed around $3,300\text{ cm}^{-1}$ corresponds to the stretching vibrations of the -OH groups of P, CNF and water molecules (Zambuzi et al., 2021). Peaks around $2,900\text{ cm}^{-1}$ are attributed to asymmetric and symmetric stretching vibrations of methylene from aliphatic C - H bonds (Zhang et al., 2019). The peaks at $1,650$ and 1450 cm^{-1} are characteristic of the asymmetric and symmetric modes of stretching vibration of CO groups, respectively (Dai et al., 2023).

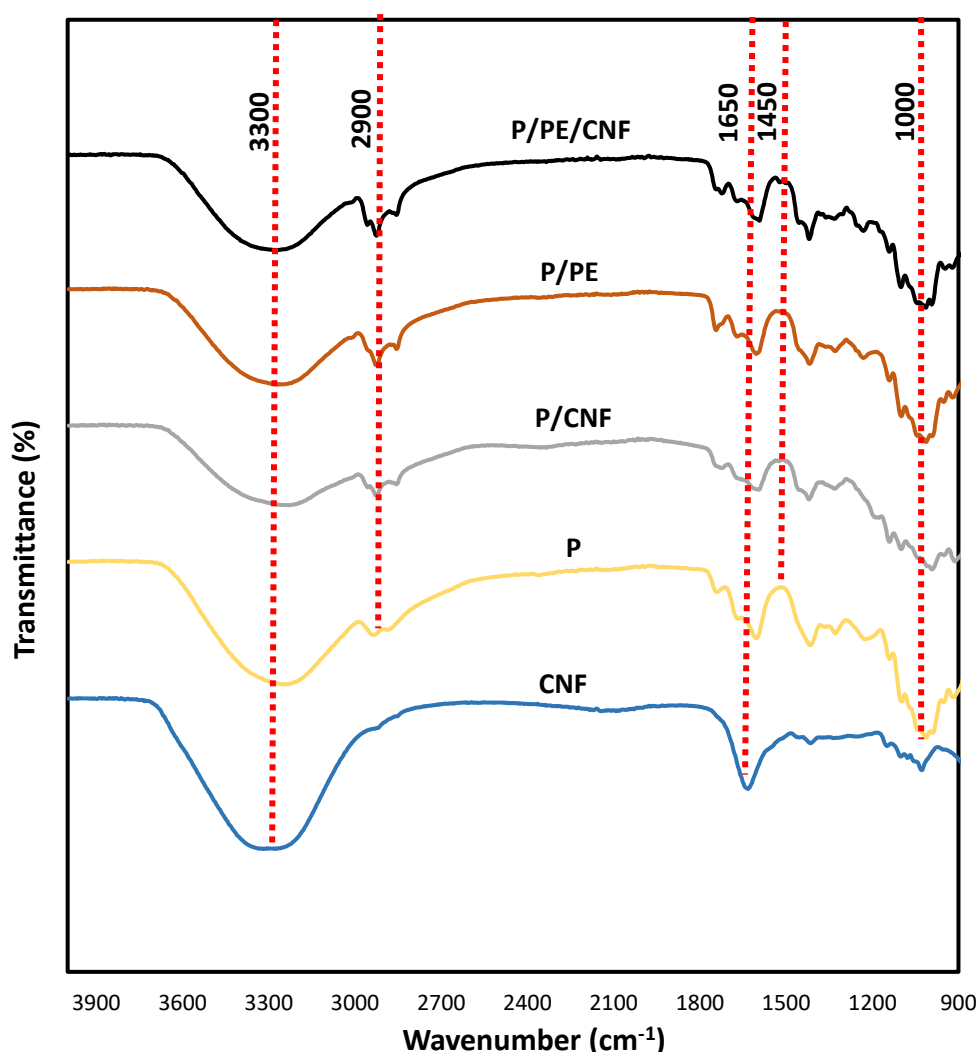


Figure 4. FTIR spectra of CNF and films. P: pectin film; P/CNF: pectin film reinforced with CNF; P/PE: pectin film added with PE and P/PE/CNF: pectin film added with PE and CNF.

The absorption band around $1,160\text{--}1,010\text{ cm}^{-1}$ may be associated with C–O stretching vibrations in glycerol, lignin and P (as glycosidic bonds) (Zhang et al., 2023). The transition

from cellulose I to II in CNF was confirmed by the expressive absorption region around 1,160-1,102 cm^{-1} (Costa et al., 2018). In general, the spectra were very similar and dominated by the presence of pectin and with small contributions from the other components.

3.2.4 Thickness, MC, SW, WCA and WVP

Table 2 presents the thickness, MC, WCA, WVP and SW results of the films. In general, film thicknesses were very similar because the amount of film-forming solution added to the Petri dishes was controlled. Regarding MC, it can be observed that P film presented a higher MC value than the other film samples ($p < 0.05$). Both the addition of CNF and PE led to a reduction in MC. Considering that the drying time was the same, these results may be associated with the higher viscosity of the control films (without addition of PE and/or CNF) and, consequently, lower drying rate and higher MC. CNF is able to bind to pectin, forming a dense and highly entangled structure, which increases the tortuosity of the film network, hindering the water vapor diffusion mechanism (Zhang et al., 2022, although this effect seems to not prevail over the viscosity of the FFS.

WCA was determined to investigate the surface hydrophobicity (resistance to water) or wettability of films (Xue et al., 2019; Zhao et al., 2023). The commonly used threshold to distinguish between hydrophilicity and hydrophobicity is 65° (Miao et al., 2022). P films showed a WCA of around 60° . This hydrophilicity is due to the large amount of hydroxyl groups, which is the main disadvantage for the application of P films in food products. As can be seen in Table 2, the addition of PE significantly increased the WCA of the films. Addition of PE to P film introduces the presence of sunflower oil + OEO droplets, creating a more hydrophobic surface or reducing the hydrophilicity of the films (Pelissari et al., 2017a; Tessaro et al., 2021). Although reports have associated the addition of CNF with the prevention of the formation of hydrogen bonds between P and water with a consequent increase in surface hydrophobicity (Zhang et al., 2023), the concentration of CNF added was not sufficient to significantly modify the WCA results (Table 2). SW is another important parameter to be investigated and is associated with hydrophilicity, being crucial to verify the feasibility of applying the film to food. Addition of PE significantly decreased ($p < 0.05$) the SW value, possibly due to the addition of hydrophobic substances (oil droplets), decreasing the availability of hydrophilic groups. In addition, some changes in the microstructural arrangement of the polymer chain may occur with possible interactions between the

biopolymer (pectin) and emulsion components (Liu et al., 2020). Despite the reduction in hydrophilicity with the addition of PE demonstrated by WCA and SW values, this was not enough to significantly alter WPV. However, according to the microstructure of the P/PE and P/PE/CNF films (Figure 2), some cavities were observed in the structure of the films, which possibly promoted the passage of water vapor that reduced MC.

Table 2. Thickness, moisture content (MC), water contact angle (WCA), water vapor permeability (WVP) and water solubility (SW) of the films. P: pectin film; P/CNF: pectin film reinforced with CNF; P/PE: pectin film added with PE and P/PE/CNF: pectin film added with PE and CNF.

Sample	Thickness (mm)	MC (%)	WCA (°)	WPV× 10 ¹⁰ (g m ⁻¹ s ⁻¹ Pa ⁻¹)	SW (%)
P	0.09±0.01 ^{AB}	27.12±0.48 ^A	60.43±2.67 ^B	8.46±2.11 ^A	62.13±0.42 ^A
P/CNF	0.10±0.02 ^{AB}	19.11±0.80 ^C	64.40±2.44 ^B	8.25±3.87 ^A	60.63±2.08 ^A
P/PE	0.12±0.01 ^A	20.88±0.70 ^B	73.40±1.70 ^A	10.50±2.18 ^A	55.49±0.74 ^B
P/PE/CNF	0.08±0.01 ^B	21.15±0.58 ^B	71.87±1.33 ^A	8.99±2.11 ^A	57.89±2.55 ^{AB}

^{A-C} Different letters in the same column indicate a statistically significant difference ($p < 0.05$) between samples.

3.2.5 Color and Opacity

Consumer acceptance of food products is directly influenced by vision. Therefore, the packaging needs to be attractive, as it is the first impression that the consumer has of the product. In this sense, the color and opacity of films is a very relevant parameter (Zhao et al., 2023). Table 3 presents the values of the color parameters L^* , a^* , b^* and opacity of the films. Regarding L^* parameter, all films showed similar high luminosity ($L^* > 93$). The a^* values also did not differ significantly from each other ($p > 0.05$), in addition to showing that the green-red coloration was not relevant to the films (value close to zero). On the other hand, the b^* values of P/PE/CNF films increased significantly compared to P films ($p < 0.05$), indicating that films became more yellow. Although some authors have observed that CNF (obtained from banana peel) incorporated into bio-based films has increased their opacity due to the formation of a network between CNF and the biopolymeric matrix (Pelissari et al., 2017b; Tibolla et al., 2019), our results showed no significant difference with the addition of CNF ($p > 0.05$). However, the addition of PE to P films significantly affected film opacity ($p < 0.05$), as the addition of essential oil affects the optical properties of the material due to the droplets dispersed in the P matrix (Bonilla et al., 2018; Zhao et al., 2023).

Table 3. Color parameters and opacity of the films. P: pectin film; P/CNF: pectin film reinforced with CNF; P/PE: pectin film added with PE and P/PE/CNF: pectin film added with PE and CNF.

Sample	L*	a*	b*	Opacity (%)
P	94.63±0.34 ^A	-0.05±0.08 ^A	7.10±0.23 ^B	10.14±0.13 ^B
P/CNF	93.91±0.70 ^A	0.02±0.11 ^A	7.78±0.60 ^{AB}	11.45±1.06 ^{AB}
P/PE	94.60±0.57 ^A	0.04±0.12 ^A	7.85±1.99 ^{AB}	13.61±0.47 ^A
P/PE/CNF	93.16±0.76 ^A	0.17±0.10 ^A	10.42±0.59 ^A	12.60±1.94 ^{AB}

^{A-B} Different letters in the same column indicate a statistically significant difference between samples ($p < 0.05$).

3.2.6 UV/Vis light barrier properties

Exposure to UV/VIS light during transport or storage of food products can cause deterioration and loss of nutrients or intrinsic properties of the food. Typically, the most desired optical characteristics of packaging are high transparency and low UV transmission. A high transparency can be observed in Figure 2 and Table 3 indicates that the transparency of the films (or opacity) was not significantly affected by the addition of PE and/or CNF to the P film matrix. On the other hand, the evaluation of light transmission is important as a way to verify the reliability of the packaging materials (Zhao et al., 2022). The UV and visible light transmission curves of the films are shown in Figure 5. P/PE and P/PE/CNF films completely block UV light (from 100 to 380 nm), while P and P/CNF films showed a transmittance of 50% and 10%, respectively, at 240 nm. This result indicates that the addition of CNF contributes to the reduction of UV transmittance, although to a lesser extent when compared to the addition of PE. P/PE/CNF and P/PE films showed low transmittance values (around 5 and 10%, respectively) at the visible light region (380 to 800 nm). The films without PE presented higher transmittance values in the visible region, although P/CNF film showed a lower value (around 22%) than the P film (around 75%). Results indicate that the addition of PE and CNF was beneficial to the UV blocking properties of the films, as well as reducing the transmittance in the visible spectrum. Possibly, the phenolic hydroxyl groups present on OEO and the chromophore present on CNF structure are strongly absorbed at UV light wavelengths (Wang et al., 2019). This is extremely advantageous, as packaging with low UV/Vis transmittance is usually preferred as a way to prevent food oxidation (Kowalczyk et al., 2021).

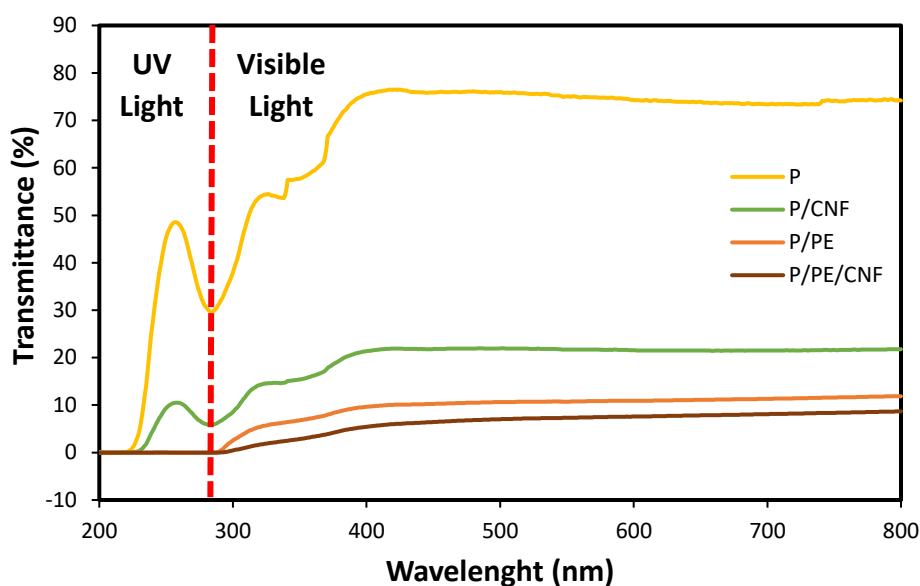


Fig. 5. Light transmittance as a function of wavelength in films. P: pectin film; P/CNF: pectin film reinforced with CNF; P/PE: pectin film added with PE and P/PE/CNF: pectin film added with PE and CNF.

3.2.7 Mechanical properties

The mechanical properties of the films (rigidity and elasticity) were evaluated as they are decisive factors in validating the integrity of the packaging. The mechanical properties of the films are defined by the intermolecular interactions and the distribution of components in the FFS matrix (Jridi et al., 2020; Zhang et al., 2023). Therefore, the morphology observed in the films (Figure 3) must be directly related to the mechanical properties of the films. According to Table 4, YM of P/PE and P/PE/CNF films decreased when compared to P film ($p < 0.05$). The reduction of YM with the incorporation of PE is due to the small oil droplets that cause an increase in the specific surface area of the oil, hindering polymer-polymer interactions and resulting in a loose polymeric structure (Fattahi and Seyedain-ardabili, 2021).

Without the presence of PE, the addition of CNF to P films increased EB values (Table 4), demonstrating the ability of CNF to induce molecular rearrangement along the tensile direction and favor the formation of more ductile films ($p < 0.05$) (Huang et al., 2021). The addition of PE did not change the ductility of the film. In summary, the results showed that the mechanical properties of the films can be modulated by modifying the formulation, as more rigid packages are formed by continuous polymeric networks (without PE and CNF), while greater ductility is achieved with the addition of cellulose nanofibers. However, considering that the addition of PE was beneficial for several properties, such as reducing

transmittance and hydrophilicity, it is suggested that an increase in the concentration of the polymer (pectin) could reduce the effect of reducing packaging strength promoted by PE.

Table 4. Mechanical properties of the films. P: pectin film; P/CNF: pectin film reinforced with CNF; P/PE: pectin film added with PE and P/PE/CNF: pectin film added with PE and CNF.

Film	Young modulus (MPa)	Elongation at break (%)
P	0.12±0.02 ^A	31.49±20.07 ^B
P/CNF	0.05±0.06 ^{AB}	89.93±33.25 ^A
P/PE	0.03±0.01 ^B	42.92±14.74 ^{AB}
P/PE/CNF	0.03±0.01 ^B	35.25±5.93 ^{AB}

^{A-B} Different letters in the same column indicate statistically significant differences ($p < 0.05$).

3.3. Shelf-life of coated tomatoes

3.3.1 Physicochemical analyses

The pH, weight loss and TSS values of control and coated tomatoes during storage are shown in Figure 6. The pH did not vary over the 12 days of storage for either uncoated and coated tomatoes (Figure 6A). In addition, pH values are within the normal pH range for tomatoes, which typically ranges between 4.30 and 4.9 (Perera et al., 2022). Weight loss was influenced by the addition of coatings to tomatoes. Figure 6B shows higher weight loss of coated tomatoes (especially with P/PE) than uncoated tomatoes. This result was not expected, as it is usually reported in several studies that the weight loss of coated tomatoes is lower than that of uncoated tomatoes, i.e., the coatings preserve the weight of the fruits (Ahmed et al., 2023; Ali et al., 2024). However, other research also report greater weight loss in coated fruits (Perera et al., 2022). Possibly, the increase in weight loss in coated tomatoes was due to the reduction of endogenous oxygen in the fruit, which can damage the internal tissue, leading to the production of fermentative substances such as alcohols that can excessively hydrate the epidermis and favor weight loss (Gallardo et al., 2012). Furthermore, the coating itself, being rich in water, can also lose weight to the environment due to the moisture concentration gradient.

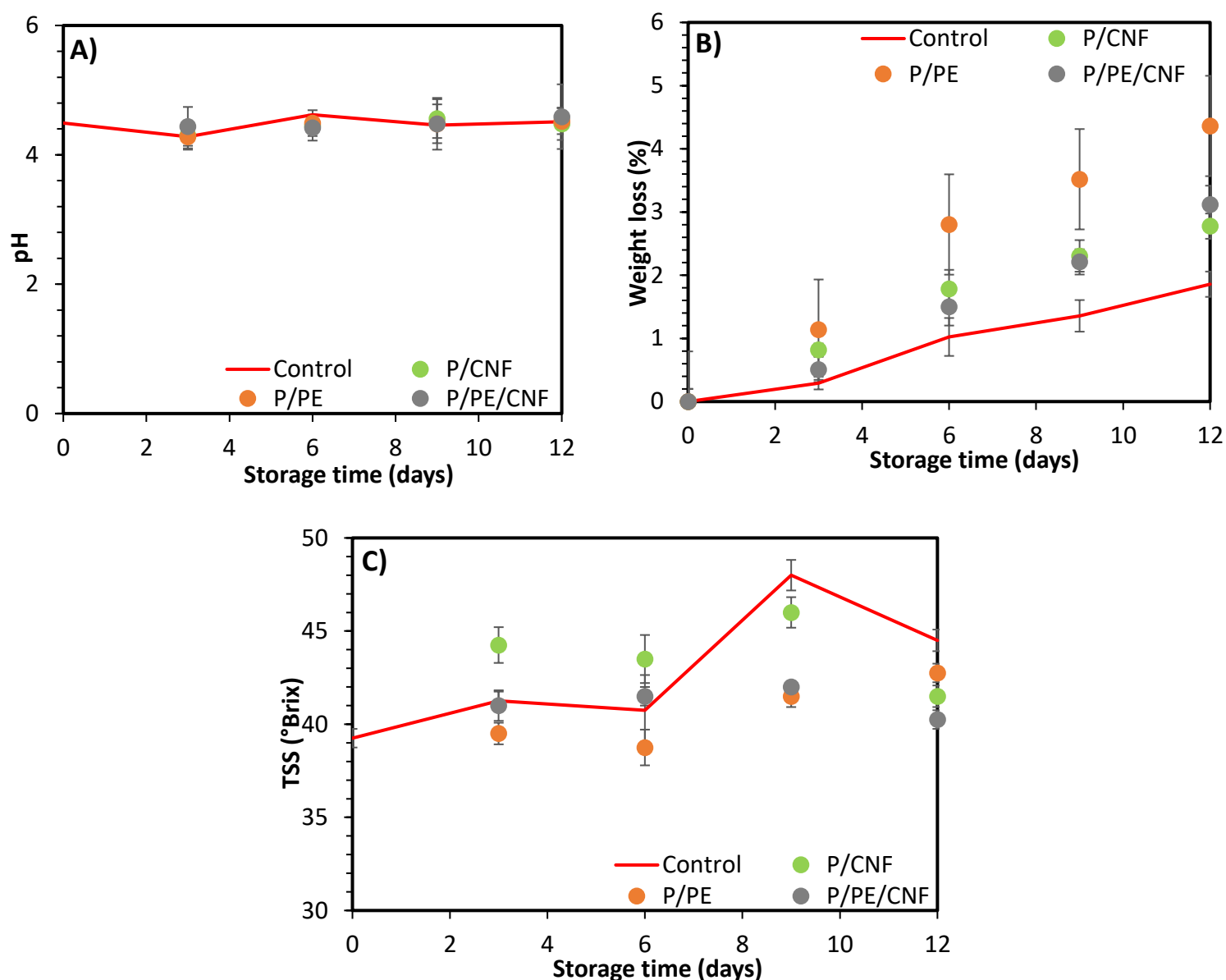


Figure 6. Variation of A) pH, B) weight loss and C) total soluble solids (TSS) of uncoated (Control) and coated tomatoes (P/PE, P/CNF and P/PE/CNF) over 12 days of storage.

For consumer acceptance, it is extremely important to investigate TSS and titratable acidity of tomatoes. Sugars and other nutrients constitute the TSS content present in fruits (Gao et al., 2019; Melo et al., 2021). The TSS in tomatoes gradually increased during storage, reaching a significant TSS peak after 9 days of storage (Figure 6C), especially evident for uncoated tomatoes. This significant increase in TSS is related to fruit ripening, which occurred because climacteric fruits, such as tomatoes, convert sucrose into glucose over time, resulting in the accumulation of free sugars (Silva et al., 2024). It is important to mention that all coated tomatoes showed lower TSS values after 12 days of storage compared to the uncoated control (Figure 6C). In general, TA values of uncoated tomatoes decreased over time (Figure 7), which

can be explained by the consumption of organic acids (such as citric acid) in the natural respiratory process of tomatoes (Vieira et al., 2016). However, this trend is not so clear for tomatoes coated with P/CNF and P/PE/CNF. During storage, tomatoes coated with films added with CNF showed TA values varying around the initial value, demonstrating the ability of these coatings to maintain the TA of tomatoes (Figure 7).

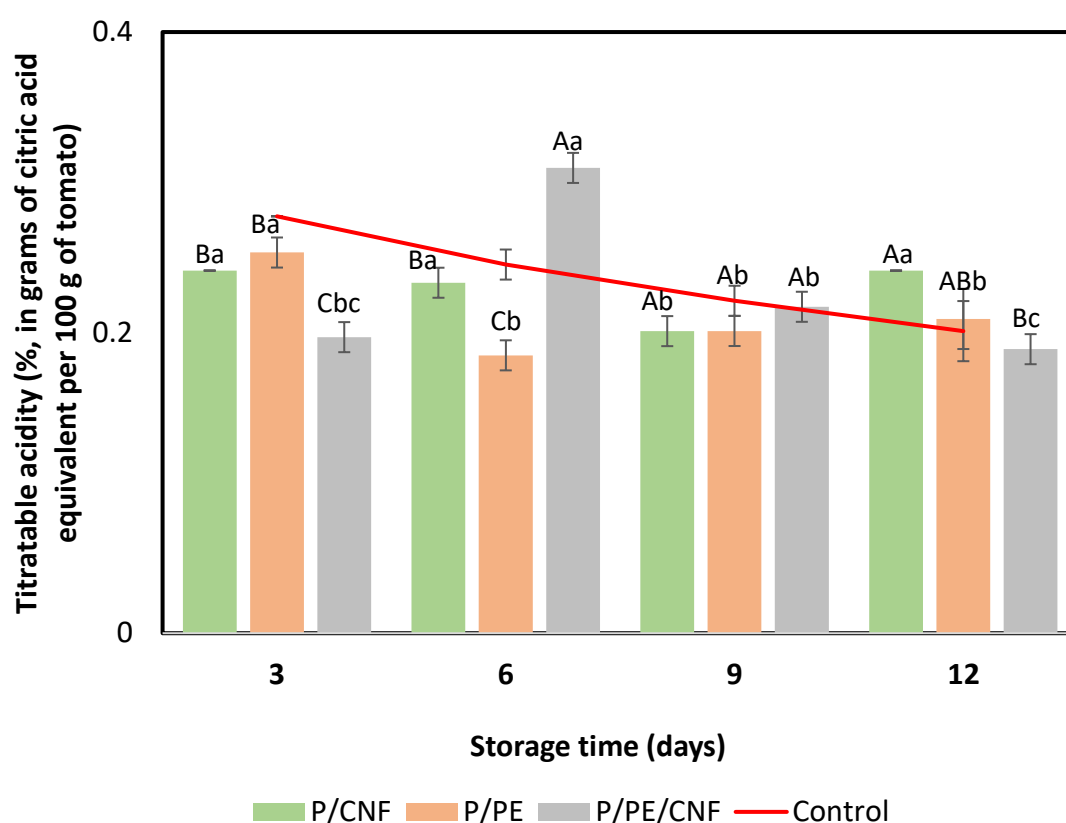


Fig. 7. Titrateable acidity (TA) (%) of tomatoes over storage time for uncoated samples (Control) and for samples coated with P/PE; P/CNF and CF. Different letters indicate significant differences ($p < 0.05$) between TA values. Capital letters: differences between different coating treatments and the same storage time. Lowercase letters: differences between different storage times and the same coating treatment.

During storage, loss of firmness in fruits and vegetables is the most common textural change and one of the main determining factors for consumption of tomatoes. Composition of the cell wall, biochemical components, organelles and moisture content determine the texture of the fruit. Texture degradation and, ultimately, unwanted changes in product quality are the result of changes in external or internal factors over storage (Das et al., 2022). Figure 8 shows the effect of coatings on tomato firmness during 12 days of storage. In general, a decrease in the firmness of coated tomatoes was observed over the days of storage, not

statistically different from uncoated tomatoes. This result demonstrates that the coatings had no effect on maintaining the texture of the tomatoes. The weight loss results (Figure 6B) already indicated possible structural/textural modification, since weight loss may indicate less firmness (Sun et al., 2017).

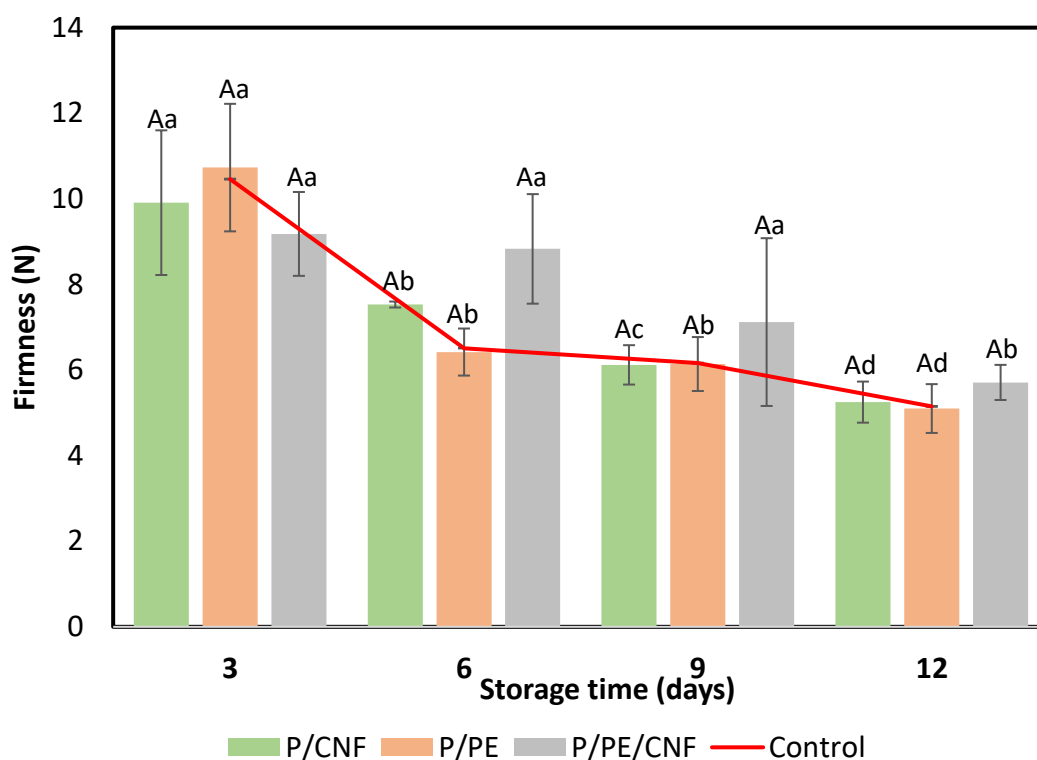


Figure 8. Firmness of tomatoes over 12 days of storage. Different letters indicate significant differences ($p < 0.05$) between firmness values. Capital letters: differences between different coating treatments and the same storage time. Lowercase letters: differences between different storage times and the same coating treatment.

Color is linked to visual appearance and is considered an essential indicator of tomato quality. Figure 9 shows L^* , a^* and b^* parameters of uncoated (control) and coated tomatoes over the 12 days of storage. As the days of storage passed, luminosity (L^*) tended to decrease for all treatments, although they did not differ statistically from each other (for the same day of storage). This was expected because tomatoes darken as they ripen, as chlorophyll in chloroplasts decreases while carotenoid and anthocyanins increase (Das et al., 2022). Small fluctuations in the a^* and b^* parameters were observed over the days of storage, but without significant differences between coated and uncoated tomatoes. These results indicate that

the intensity of the red (a^*) and yellow (b^*) color was maintained for all samples, showing no significant effect of the coatings on the color of the tomatoes.

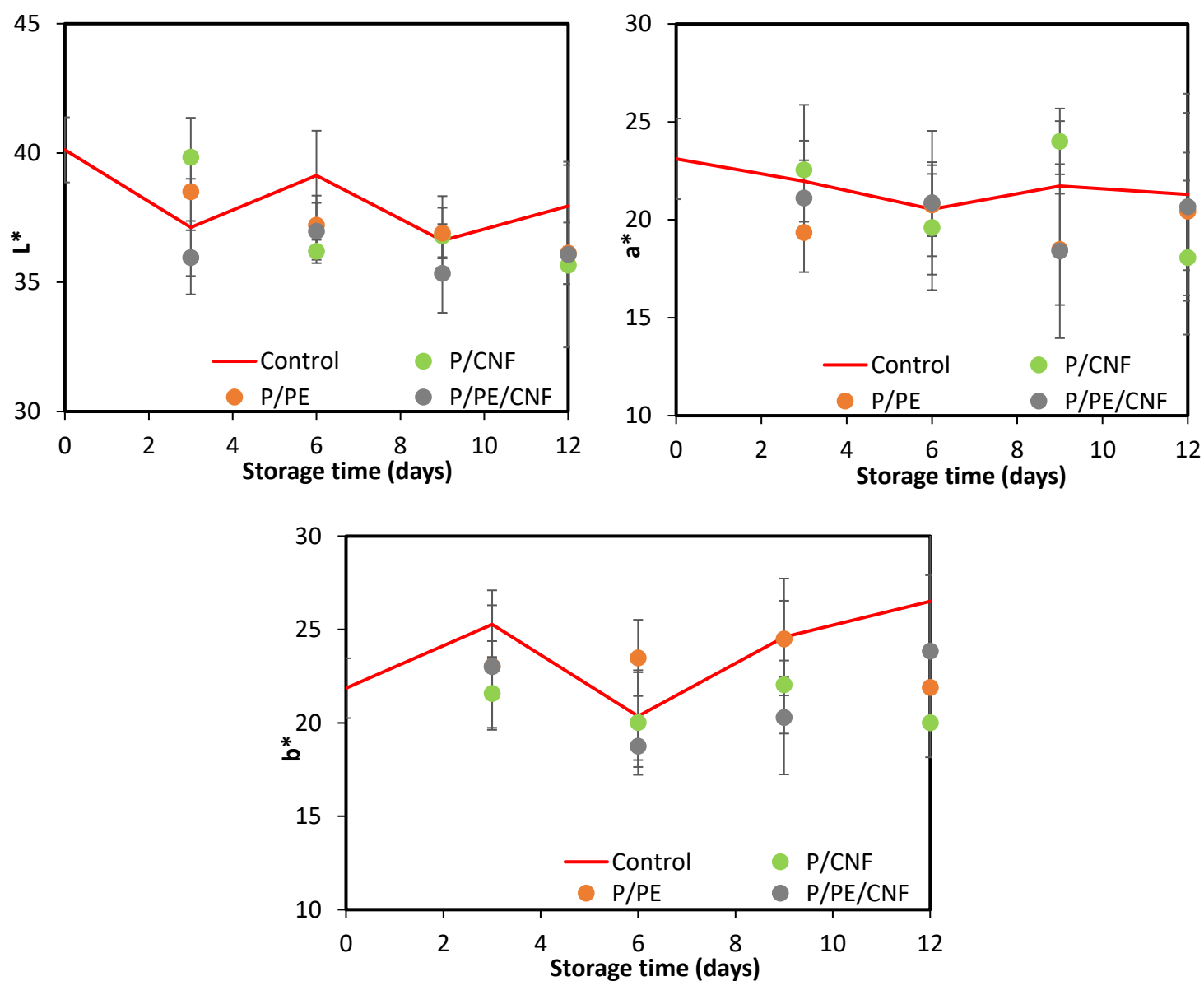


Figure 9. Color parameters (L^* ; a^* and b^*) of tomatoes over storage time for uncoated (Control) and coated tomatoes with P/PE; P/CNF and P/PE/CNF films.

3.3.2 Microbiological analyses

During post-harvest storage and improper handling, some oxidative damage may occur, as well as potential contamination of the fruits by microorganisms, which leads to substantial deterioration of the fruits. Tables 5 and 6 show the total viable count (TVC) and molds and yeasts count, respectively. Results showed an increase on microbial growth over storage time. At 12 days of storage, TVC for uncoated tomatoes (control) was higher than that

of coated tomatoes, with tomatoes coated with P/PE/CNF films having the lowest TVC value (Table 5). Regarding molds and yeasts count, uncoated tomatoes had higher count than tomatoes coated with P/PE and P/PE/CNF after 12 days of storage. Thus, OEO-containing coatings were effective in retarding microbial growth during storage, which may be due to the ability of the coatings to act as a barrier to gases and other nutrients necessary for microbial growth and activity (Quadros et al., 2020). Furthermore, the hydrophilic and antimicrobial properties of thymol and carvacrol allow their penetration through the polysaccharide membrane of the coating, acting as active components. Such diffusion causes a barrier to microbial growth (Souza, 2021).

Table 5. Total viable counts (TVC) during storage of tomatoes for 12 days.

Samples	TVC (CFU/g)				
	0 day	3 days	6 days	9 days	12 days
Control	<10	<10	<10	2.7×10^2	6.9×10^3
P/CNF	-	<10	1.6×10^2	2.8×10^2	5.3×10^2
P/PE	-	<10	1.0×10^2	1.1×10^2	5.5×10^2
P/PE/CNF	-	<10	<10	1.2×10^2	2.2×10^2

Table 6. Molds and yeast count during storage of tomatoes for 12 days.

Samples	Molds and yeasts (CFU/g)				
	0 day	3 days	6 days	9 days	12 days
Control	<10	2.0×10^2	5.0×10^2	1.2×10^3	1.4×10^4
P/CNF	-	<10	<10	1.0×10^2	9.1×10^2
P/PE	-	<10	<10	<10	<10
P/PE/CNF	-	<10	<10	<10	1.0×10^2

4. Conclusion

Pectin films and coatings were produced and, regardless of the addition of emulsions (PE) and cellulose nanoparticles (CNF), they were compact and transparent. However, some agglomerates were observed when CNF was added and cavities formation was detected when PE was incorporated. The addition of PE reduced solubility in water and increased water contact angle of the pectin films, showing a reduction in the hydrophilicity of the film surface properties that is beneficial for food application. However, this reduction in hydrophilicity with the addition of PE was not enough to significantly change water vapor permeability. Despite the transparency of the films, they proved to be an effective barrier to UV light with the addition of PE, which is extremely desirable to prevent food oxidation. Although the addition of PE and CNF reduced the network strength, cellulose nanofibers significantly increased the

elongation at break of the films. Thus, the results show that the combination of PE+CNF was beneficial for the properties of pectin films. Regarding the analysis of the shelf-life of tomatoes, it was observed that the pH value and titratable acidity of the coated tomatoes were maintained during 12 days of storage. However, coated tomatoes showed higher weight loss and consequently, lower firmness after 12 days of storage. In contrast, coated tomatoes were effective in retarding microbial growth compared to uncoated tomatoes. Therefore, in general the incorporation of CNF and PE was positive, especially with the antimicrobial activity of OEO against molds and yeasts in tomato. However, better homogenization in the addition of components during the matrix formation process would need to be better investigated and studied, so that a more homogeneous structure could be obtained, without the formation of cavities that can favor moisture diffusion and weight loss. In general, the gains with the incorporation of CNF are clearly observed, mainly in relation to mechanical properties, while PE favors a reduction in hydrophilicity and the use of oregano oil provided greater microbiological quality to the tomato.

ACKNOWLEDGMENTS

This study was financed by Coordenação de Aperfeiçoamento de Pessoal de Nível Superior – Brazil (CAPES) - Finance Code 001 and Fundação de Amparo à Pesquisa do Estado de São Paulo - FAPESP (2019/27354-3). Chevalier thanks CAPES-Brazil for the scholarship (88887.479720/2020-00) and CNPq for Sandwich Doctorate Abroad - SWE scholarship (200248/2022-7). Cunha thanks CNPq (307094/2021-9) for the productivity grant. Cunha and Chevalier thanks CNPq (404753/2023-0). The authors thank the Laboratório Ibérico Internacional de Nanotecnologia (INL) (Braga- Portugal) for SEM analyses and TGA. This study was also supported by the Portuguese Foundation for Science and Technology (FCT) under the scope of the strategic funding of UIDB/04469/2020 unit, with DOI 10.54499/UIDB/04469/2020 and by LABBELS – Associate Laboratory in Biotechnology, Bioengineering and Microelectromechanical Systems, LA/P/0029/2020. Martins acknowledges FCT for her Assistant Research contract obtained under the scope of Scientific Stimulus Employment with reference 2022.00788.CEECIND/CP1718/CT0024, with DOI 10.54499/2022.00788.CEECIND/CP1718/CT0024.

References

- Ahmed, M., Saini, P., Iqbal, U., 2023. Bio cellulose-based edible composite coating for shelf-life extension of tomatoes. *Food Humanit.* 1, 973–984.
<https://doi.org/10.1016/j.foohum.2023.08.016>
- Ali, Q., Seckin, M., Mujtaba, M., Wahed, A., Dogan, A., Kaya, M., Toksoy, E., Akyuz, B., Erkan, M., 2024. Scientia Horticulturae Shelf life of cocktail tomato extended with chitosan , chia mucilage and levan. *Sci. Hortic. (Amsterdam)*. 323, 112500.
<https://doi.org/10.1016/j.scienta.2023.112500>
- Arkoumanis, P.G., Norton, I.T., Spyropoulos, F., 2019. Pickering particle and emulsifier co-stabilised emulsions produced via rotating membrane emulsification. *Colloids Surfaces A* 568, 481–492. <https://doi.org/10.1016/j.colsurfa.2019.02.036>
- Arnon-rips, H., Poverenov, E., 2018. Improving food products quality and storability by using Layer by Layer edible coatings. *Trends Food Sci. Technol.* 75, 81–92.
<https://doi.org/10.1016/j.tifs.2018.03.003>
- Bonilla, J., Poloni, T., Lourenço, R. V, Sobral, P.J.A., 2018. Antioxidant potential of eugenol and ginger essential oils with gelatin / chitosan films. *Food Biosci.* 23, 107–114.
<https://doi.org/10.1016/j.fbio.2018.03.007>
- Bonilla, J., Sobral, P.J.A., 2016. Investigation of the physicochemical , antimicrobial and antioxidant properties of gelatin-chitosan edible fi lm mixed with plant ethanolic extracts. *Food Biosci.* 16, 17–25. <https://doi.org/10.1016/j.fbio.2016.07.003>
- Chen, Q., Zhou, M., Yuan, J., Cai, J., Xie, H., Zhu, M., Cai, L., Wei, P., Chang, C., 2023. High-strength and recyclable hydroplastic films from hydrophobic cellulose nanofibers produced via deep eutectic solvents. *Chem. Eng. J.* 476, 146771.
<https://doi.org/10.1016/j.cej.2023.146771>
- Chevalier, R.C., JÚNIR, F.D.O., Cunha, R.L., 2024. Modulating digestibility and stability of Pickering emulsions based on cellulose nanofibers. *Food Res. Int.* 178, 113963.
<https://doi.org/10.1016/j.foodres.2024.113963>
- Coelho, C.C.S., Cerqueira, M.A., Pereira, R.N., Pastrana, L.M., Freitas-silva, O., Vicente, A.A., Cabral, L.M.C., Teixeira, J.A., 2017. Effect of moderate electric fields in the properties of starch and chitosan films reinforced with microcrystalline cellulose. *Carbohydr. Polym.* 174, 1181–1191. <https://doi.org/10.1016/j.carbpol.2017.07.007>
- Costa, A.L.R., Gomes, A., Tibolla, H., Menegalli, F.C., Cunha, R.L., 2018. Cellulose nanofibers from banana peels as a Pickering emulsifier: High-energy emulsification processes.

- Carbohydr. Polym. 194, 122–131. <https://doi.org/10.1016/j.carbpol.2018.04.001>
- Cuq, B., Gontard, N., Cuq, J.-L., Guilbert, S., 1996. Functional Properties of Myofibrillar Protein-based Biopackaging as Affected by Film Thickness. *J. Food Sci.* 61, 580–584.
- Dai, H., Chen, Y., Chen, H., Fu, Y., Ma, L., Wang, H., Yu, Y., Zhu, H., Zhang, Y., 2023. Gelatin films functionalized by lignocellulose nanocrystals-tannic acid stabilized Pickering emulsions : Influence of cinnamon essential oil. *Food Chem.* 401, 134154. <https://doi.org/10.1016/j.foodchem.2022.134154>
- Das, S.K., Vishakha, K., Das, S., Chakraborty, D., Ganguli, A., 2022. Carboxymethyl cellulose and cardamom oil in a nanoemulsion edible coating inhibit the growth of foodborne pathogens and extend the shelf life of tomatoes. *Biocatal. Agric. Biotechnol.* 42, 102369. <https://doi.org/10.1016/j.bcab.2022.102369>
- Fattahi, R., Seyedain-ardabili, M., 2021. A comparative study on the effect of homogenization conditions on the properties of the film-forming emulsions and the resultant films. *Food Chem.* 352, 129319. <https://doi.org/10.1016/j.foodchem.2021.129319>
- Fein, K., Bous, D.W., Gramlich, W.M., 2020. The influence of versatile thiol-norbornene modifications to cellulose nanofibers on rheology and film properties. *Carbohydr. Polym.* 230. <https://doi.org/10.1016/j.carbpol.2019.115672>
- Gallardo, A.P.-, Mattinson, S.D., Lazcano-peralta, A., Fellman, J.K., Regalado, C., Garcí, B., Barbosa-ca, G., 2012. Effect of native and acetylated-crosslinked waxy corn starch-beeswax coatings on quality attributes of raspberries during storage. *Starch J.* 64, 665–673. <https://doi.org/10.1002/star.201200005>
- Gao, Y., Tian, P., Li, Juan, Cao, Y., Xu, W., Li, Jianshe, 2019. Transcriptional changes during tomato ripening and influence of brackish water irrigation on fruit transcriptome and sugar content. *Plant Physiol. Biochem.* 145, 21–33. <https://doi.org/10.1016/j.plaphy.2019.10.025>
- Guillard, V., Broyart, B., Bonazzi, C., Guilbert, S., Gontard, N., 2003. Preventing Moisture Transfer in a Composite Food Using Edible Films : Experimental and Mathematical Study. *J. Food Sci.* 68.
- Huang, J., Lu, Z., Li, J., Ning, D., Jin, Z., Ma, Q., Hua, L., Songfeng, E., Zhang, M., 2021. Improved mechanical and ultraviolet shielding performances of hydroxyethyl cellulose film by using aramid nanofibers as additives. *Carbohydr. Polym.* 255, 117330.

- <https://doi.org/10.1016/j.carbpol.2020.117330>
- Jafari, H., Pirouzifard, M., Khaledabad, M.A., Almasi, H., 2016. Effect of chitin nanofiber on the morphological and physical properties of chitosan / silver nanoparticle bionanocomposite films. *Int. J. Biol. Macromol.* 92, 461–466.
<https://doi.org/10.1016/j.ijbiomac.2016.07.051>
- Jridi, M., Abdelhedi, O., Salem, A., Kechaou, H., Nasri, M., Menchari, Y., 2020. Physicochemical , antioxidant and antibacterial properties of fish gelatin-based edible films enriched with orange peel pectin : Wrapping application. *Food Hydrocoll.* 103, 105688. <https://doi.org/10.1016/j.foodhyd.2020.105688>
- Kowalczyk, D., Szymanowska, U., Skrzypek, T., Basiura-cembala, M., Katarzyna, Ł., 2021. Corn starch and methylcellulose edible films incorporated with fireweed (*Chamaenerion angustifolium* L .) extract : Comparison of physicochemical and antioxidant properties. *Int. J. Biol. Macromol.* 190, 969–977. <https://doi.org/10.1016/j.ijbiomac.2021.09.079>
- Kumar, M., Tomar, M., Saurabh, V., Mahajan, T., Punia, S., Contreras, M., Rudra, S.G., Kaur, C., Kennedy, J.F., 2020. Emerging trends in pectin extraction and its anti-microbial functionalization using natural bioactives for application in food packaging. *Trends Food Sci. Technol.* 105, 223–237. <https://doi.org/10.1016/j.tifs.2020.09.009>
- Liu, F., Tang, C., 2011. Cold , gel-like whey protein emulsions by microfluidisation emulsification : Rheological properties and microstructures. *Food Chem.* 127, 1641–1647. <https://doi.org/10.1016/j.foodchem.2011.02.031>
- Liu, Z., Lin, D., Shen, R., Yang, X., 2020. Characterizations of novel konjac glucomannan emulsion films incorporated with high internal phase Pickering emulsions. *Food Hydrocoll.* 106088. <https://doi.org/10.1016/j.foodhyd.2020.106088>
- Mejía-Jaramillo, A.M., Gómez-Hoyos, C., Guitierrez, A.I.C., Correa-Hincapié, N., Gallego, R.Z., Triana-Chávez, O., 2023. Tackling the cytotoxicity and genotoxicity of cellulose nanofibers from the banana rachis : A new food packaging alternative. *Heliyon* 9. <https://doi.org/10.1016/j.heliyon.2023.e21560>
- Melo, F. De, Henrique, G., Nunes, D.S., 2021. Phenotypic variability , diversity and genetic-population structure in melon (*Cucumis melo* L .) Associated with total soluble solids. *Sci. Hortic.* 278. <https://doi.org/10.1016/j.scienta.2020.109844>
- Mendes, C.G., Martins, J.T., Lüdtke, F.L., Geraldo, A., Pereira, A., Vicente, A., Vieira, J.M., 2023. Chitosan Coating Functionalized with Flaxseed Oil and Green Tea Extract as a Bio-

Based Solution for Beef Preservation 1–19.

Miao, W., Tian, Y., Jiang, L., 2022. Bioinspired Superspreading Surface: From Essential Mechanism to Application. *Acc. Chem. Res.* 55, 1467–1479.

<https://doi.org/10.1021/acs.accounts.2c00042>

Olveira-Bouzas, V., Pita-Calvo, C., Vázquez-Odériz, M.L., Romero-Rodríguez, M.Á., 2021.

Evaluation of a modified atmosphere packaging system in pallets to extend the shelf-life of the stored tomato at cooling temperature. *Food Chem.* 364.

<https://doi.org/10.1016/j.foodchem.2021.130309>

Pelissari, F.M., Andrade-Mahecha, M.M., Sobral, P.J. do A., Menegalli, F.C., 2017a.

Nanocomposites based on banana starch reinforced with cellulose nanofibers isolated from banana peels. *J. Colloid Interface Sci.* 505, 154–167.

<https://doi.org/10.1016/j.jcis.2017.05.106>

Pelissari, F.M., Andrade-Mahecha, M.M., Sobral, P.J. do A., Menegalli, F.C., 2017b.

Nanocomposites based on banana starch reinforced with cellulose nanofibers isolated from banana peels. *J. Colloid Interface Sci.* 505, 154–167.

<https://doi.org/10.1016/j.jcis.2017.05.106>

Perera, K.Y., Sharma, S., Duffy, B., Pathania, S., Jaiswal, K., Jaiswal, S., 2022. An active

biodegradable layer-by-layer film based on chitosan-alginate-TiO₂ for the enhanced shelf life of tomatoes. *Food Packag. Shelf Life* 34, 100971.

<https://doi.org/10.1016/j.fpsl.2022.100971>

Quadros, C. da C. de, Lima, K.O., Bueno, C.H.L., Fogaça, F.H. dos S., Rocha, M. da, Prentice,

C., 2020. Effect of the edible coating with protein hydrolysate on cherry tomatoes shelf life. *J. Food Process. Preserv.* 1–9. <https://doi.org/10.1111/jfpp.14760>

Ren, Z., Li, Z., Chen, Z., Zhang, Y., Lin, X., Weng, W., Yang, H., Li, B., 2021. Characteristics and application of fish oil-in-water pickering emulsions structured with tea water-insoluble proteins / κ -carrageenan complexes. *Food Hydrocoll.* 114, 106562.

<https://doi.org/10.1016/j.foodhyd.2020.106562>

Sahraee, S., Milani, J.M., Ghanbarzadeh, B., Hamishehkar, H., 2017. Physicochemical and

antifungal properties of bio-nanocomposite film based on gelatin-chitin nanoparticles. *Int. J. Biol. Macromol.* 97, 373–381. <https://doi.org/10.1016/j.ijbiomac.2016.12.066>

Silva-weiss, A., Bifani, V., Ihl, M., Sobral, P.J.A., Gómez-guillén, M.C., 2014. Polyphenol-rich extract from murta leaves on rheological properties of film-forming solutions based on

- different hydrocolloid blends. *J. Food Eng.* 140, 28–38.
<https://doi.org/10.1016/j.jfoodeng.2014.04.010>
- Silva, A.C.P. da, Barbosa, J.R., Araújo, C. da S., Batista, J.T.S., Neves, E.M.P.X., Cardoso, D.N.P., Joele, M.R.S.P., Lourenço, L. de F.H., 2024. A new edible coating of fish gelatin incorporated into açaí oil to increase the post-harvest shelf life of tomatoes. *Food Chem.* 438. <https://doi.org/10.1016/j.foodchem.2023.138047>
- Souza, E.L. De, 2021. Insights into the current evidence on the effects of essential oils toward beneficial microorganisms in foods with a special emphasis to lactic acid bacteria – A review. *Trends Food Sci. Technol.* 114, 333–341.
<https://doi.org/10.1016/j.tifs.2021.06.011>
- Sun, X., Zhou, B., Luo, Y., Ference, C., Baldwin, E., Harrison, K., Bai, J., 2017. Effect of controlled-release chlorine dioxide on the quality and safety of cherry / grape tomatoes. *Food Control* 82, 26–30. <https://doi.org/10.1016/j.foodcont.2017.06.021>
- Tessaro, L., Vinícius, R., Martelli-tosi, M., Jos, P., 2021. Gelatin / chitosan based films loaded with nanocellulose from soybean straw and activated with “ Pitanga ” (*Eugenia uniflora* L.) leaf hydroethanolic extract in W / O / W emulsion. *Int. J. Biol. Macromol.* 186, 328–340. <https://doi.org/10.1016/j.ijbiomac.2021.07.039>
- Tibolla, H., Pelissari, F.M., Martins, J.T., Lanzoni, E.M., Vicente, A.A., Menegalli, F.C., Cunha, R.L., 2019. Banana starch nanocomposite with cellulose nano fi bers isolated from banana peel by enzymatic treatment : In vitro cytotoxicity assessment. *Carbohydr. Polym.* 207, 169–179. <https://doi.org/10.1016/j.carbpol.2018.11.079>
- Vieira, J.M., Flores-lópez, M.L., Jasso, D., Rodríguez, D., Sousa, M.C., Vicente, A.A., Martins, J.T., 2016. Effect of chitosan – Aloe vera coating on postharvest quality of blueberry (*Vaccinium corymbosum*) fruit. *Postharvest Biol. Technol.* 116, 88–97.
<https://doi.org/10.1016/j.postharvbio.2016.01.011>
- Wang, K., Wang, Yifan, Cheng, M., Wang, Yirong, Zhao, P., Xi, X., Lu, J., Wang, X., Han, X., Wang, J., 2024. Preparation and characterization of active films based on oregano essential oil microcapsules / soybean protein isolate / sodium carboxymethyl cellulose. *Int. J. Biol. Macromol.* 258, 128985. <https://doi.org/10.1016/j.ijbiomac.2023.128985>
- Wang, X., Wang, Shanyong, Liu, W., Wang, Si, Zhang, L., Sang, R., 2019. Facile fabrication of cellulose composite fi lms with excellent UV resistance and antibacterial activity 225, 1–8. <https://doi.org/10.1016/j.carbpol.2019.115213>

- Xu, J., He, M., Wei, C., Duan, M., Yu, S., Li, D., Zhong, W., Tong, C., Pang, J., Wu, C., 2023. Konjac glucomannan films with Pickering emulsion stabilized by TEMPO-oxidized chitin nanocrystal for active food packaging. *Food Hydrocoll.* 139, 108539. <https://doi.org/10.1016/j.foodhyd.2023.108539>
- Xue, F., Gu, Y., Wang, Y., Li, C., Adhikari, B., 2019. Encapsulation of essential oil in emulsion based edible films prepared by soy protein isolate-gum acacia conjugates. *Food Hydrocoll.* 96, 178–189. <https://doi.org/10.1016/j.foodhyd.2019.05.014>
- Zambuzi, G.C., Camargos, C.H.M., Ferreira, M.P., Rezende, C.A., Freitas, O. De, Francisco, K.R., 2021. Modulating the controlled release of hydroxychloroquine mobilized on pectin films through film-forming pH and incorporation of nanocellulose. *Carbohydr. Polym. Technol. Appl.* 2, 100140. <https://doi.org/10.1016/j.carpta.2021.100140>
- Zhang, S., Cheng, X., Fu, Q., Li, Y., Wu, P., Qiao, Y., Yan, J., Si, L., Waterhouse, G.I.N., Li, H., Ai, S., 2023. Pectin-nanolignin composite films with water resistance , UV resistance , and antibacterial activity. *Food Hydrocoll.* 143, 108783. <https://doi.org/10.1016/j.foodhyd.2023.108783>
- Zhang, W., Shu, C., Chen, Q., Cao, J., Jiang, W., 2019. The multi-layer film system improved the release and retention properties of cinnamon essential oil and its application as coating in inhibition to penicillium expansion of apple fruit. *Food Chem.* 299, 125109. <https://doi.org/10.1016/j.foodchem.2019.125109>
- Zhao, R., Guan, W., Zhou, X., Lao, M., Cai, L., 2022. The physiochemical and preservation properties of anthocyanidin / chitosan nanocomposite-based edible films containing cinnamon-perilla essential oil pickering nanoemulsions. *LWT* 153, 112506. <https://doi.org/10.1016/j.lwt.2021.112506>
- Zhao, Y., Ren, Z., Shi, L., Zhang, Y., Weng, W., 2023. Effects of pre-emulsion prepared using sucrose esters with different hydrophile-lipophile balances on characteristics of soy protein isolate emulsion films. *Food Res. Int.* 165, 112542. <https://doi.org/10.1016/j.foodres.2023.112542>
- Zheng, K., Li, B., Liu, Y., Wu, D., Bai, Y., Xiang, Q., 2023. Effect of chitosan coating incorporated with oregano essential oil on microbial inactivation and quality properties of refrigerated chicken breasts 176, 1–10.

CAPÍTULO VI

DISCUSSÃO GERAL

6.1 DISCUSSÃO GERAL

A premissa deste trabalho foi baseada na ausência de trabalhos na literatura que tivessem utilizado nanofibras de celulose simultaneamente como estabilizante de emulsões Pickering e como material de reforço em matrizes filmogênicas. Foi estudado desde a produção da nanofibra até a aplicação da embalagem em um produto, visando avaliar toda a cadeia produtiva. Diante desse desafio e o da pandemia da COVID-19 (dois primeiros anos da tese), primeiramente foi feito um estudo teórico voltado a entender o efeito dos diferentes métodos de produção das nanofibras sobre suas propriedades visando posteriores aplicações, enquanto a parte experimental foi efetivamente realizada nos últimos dois anos.

O levantamento teórico das diferentes fontes de celulose e dos variados processos isolados ou combinados foi feito de forma que pudessem ser identificadas e escolhidas as melhores estratégias para a produção das CNFs. Como a celulose é o polímero natural mais abundante e de baixo custo, existe um apelo sustentável para sua utilização em substituição a polímeros convencionais na potencial aplicação em diferentes setores industriais como biomedicina, embalagens de alimentos e materiais optoeletrônicos (Hu et al., 2024). Entretanto, apesar de apresentar muitas propriedades desejáveis para diversas aplicações, como elevada resistência mecânica, biocompatibilidade e biodegradabilidade, a celulose apresenta a desvantagem em relação à sua baixa solubilidade em água. Entre os métodos de obtenção das nanofibras de celulose, os mais utilizados são os químicos e físicos por serem mais simples. No entanto, os métodos químicos geram muito efluentes químicos, originando gastos na neutralização e descarte. Já os métodos físicos estão associados a grande desgaste de equipamentos e energia. Com isso, apesar dos métodos biotecnológicos, como a hidrólise enzimática, apresentarem um elevado custo pela utilização de enzimas, estes mostram a vantagem de serem tecnologias verdes e ambientalmente amigáveis. Além disso, a concentração utilizada de enzima pode ser otimizada visando a redução do custo de processo. Um ponto a se destacar é a dificuldade em se estabelecer uma relação entre as propriedades das nanofibras frente aos diferentes métodos de obtenção, uma vez que, em geral, é necessária uma combinação de técnicas para transformar as fibras de celulose em nanofibras. Os numerosos métodos associados à produção de CNF e a complexidade das fontes de celulose são fatores que dificultam a escolha para obter desejáveis características dos CNF.

A primeira etapa experimental consistiu na produção de nanofibras a partir de um resíduo agroindustrial, a casca de mandioca, utilizando pré-tratamento alcalino, seguido por hidrólise ácida ou hidrólise enzimática e, por fim, ultrassom. Nanofibras de etilcelulose foram adicionalmente produzidas com o objetivo de comparar um material mais hidrofóbico com as nanofibras de celulose. As nanofibras de celulose e etil celulose foram caracterizadas quanto a diferentes propriedades como tamanho (comprimento e raio), potencial zeta e ângulo de contato com água e óleo. Estas nanofibras foram avaliadas quanto à capacidade de estabilização de emulsões e digestibilidade *in vitro*. A maior estabilidade foi observada nas emulsões estabilizadas com CNF-C (nanofibra obtida por hidrólise ácida) e CNF-EC (nanofibra de etil celulose). A boa estabilidade das emulsões CNF-EC foi atribuída à capacidade de redução da tensão interfacial, enquanto a da emulsão CNF-C foi associada ao menor diâmetro das nanofibras facilitando o recobrimento das gotas. Como as CNF-C e CNF-ENZ (nanofibra obtida por hidrólise enzimática com xilanase) não apresentaram redução na tensão interfacial, considerou-se que um mecanismo predominantemente tipo-Pickering promoveu a estabilização das emulsões. Em relação à digestibilidade, todas as emulsões apresentaram baixa liberação de ácido graxos livres, sendo uma possibilidade sua incorporação em dietas de baixo valor calórico. E por fim, apesar da CNF-ENZ apresentar um resultado inferior como estabilizante de emulsões, nossa hipótese foi que o aprimoramento do processo de hidrólise enzimática poderia promover uma quebra mais pronunciada das nanofibras e a formação de uma rede similar à CNF-C, aumentando assim sua capacidade estabilizante de emulsões.

Diante do exposto, nosso segundo estudo teve como objetivo a produção de CNF utilizando uma associação de enzimas usando primeiramente xilanase seguida de celulase. Foram mantidas as mesmas condições do primeiro estudo para a xilanase, enquanto a celulase atuou por um período de 3, 6, 12 ou 24 horas. Observou-se que as nanofibras obtidas nos limites inferior e superior do tempo de hidrólise da celulase (3 e 24 horas) tinham aspecto bem distinto à CNF-C, pois eram fechadas e aglomeradas no menor tempo, e bastante isoladas no maior tempo de hidrólise. Assim, as nanofibras obtidas com 6 e 12 horas, que apresentaram fibras mais semelhantes à CNF-C, foram selecionadas para produzir as emulsões Pickering. Devido ao objetivo de sua incorporação em matrizes filmogênicas e produzir um filme ativo, a fase dispersa dessas emulsões teve a adição do óleo essencial de orégano (OEO). Os óleos essenciais possuem múltiplas atividades, como antioxidantes, antimicrobianos, anti-

inflamatórias e anticancerígenas, dependendo de sua composição. Entretanto, a elevada volatilidade e instabilidade (Ebrahimi et al., 2023) é uma desvantagem em processos que impliquem em aumento de temperatura, como é o caso da secagem de filmes e a emulsificação. Diante disso, óleo de girassol (SO- óleo de girassol) foi misturado com OEO para minimizar perdas do OEO durante o processo de produção de filmes, além de aumentar a viscosidade da fase oleosa e, conseqüentemente, a estabilidade das emulsões. A fase oleosa foi mantida fixa (10% m/m), enquanto a razão de OEO:SO foi 0:10; 5:5; 8:2; 10:0. A composição da fase oleosa exerceu influência no tamanho das gotas, e conseqüentemente na estabilidade das emulsões. Os menores tamanhos de gotas foram observados nas emulsões com fase oleosa mista (5:5 e 8:2 OEO:SO), independente do tipo de CNF. O mecanismo de estabilidade das emulsões não foi puramente Pickering, pois uma redução da tensão interfacial foi observada. O OEO foi um eficiente antimicrobiano contra diferentes bactérias e o fungo *Alternaria alternata*, responsável pela deterioração de diversos frutos. Estes resultados mostraram que foi possível produzir emulsões com propriedades adequadas para a aplicação em filmes biodegradáveis.

Na terceira etapa, filmes de pectina incorporados de emulsões Pickering estabilizadas por CNF e reforçados com CNFs foram produzidos para entender o papel das CNFs nas matrizes filmogênicas. A razão 8:2 de OEO: SO e as CNFs produzidas com 12 horas de hidrólise com celulase foram escolhidas por produzirem emulsões com menor tamanho de gota e maior estabilidade. Além disso, a emulsão contendo 8:2(OEO:SO), seguida da emulsão com apenas OEO, foi a que apresentou os melhores resultados em relação a atividade antimicrobiana frente as bactérias *S. aureus*, *Listeria sp.*, *E.coli* e do fungo *A.alternata*. De forma geral, os filmes eram transparentes, o que é muito desejado para embalagens de alimentos. Porém, apesar da transparência, os filmes com adição de emulsões apresentaram barreira à luz UV, característica também muito desejada, uma vez que a incidência de luz pode causar a degradação do óleo (oxidação) ou de outros componentes fotossensíveis (Santos-López et al., 2023). Por outro lado, a permeabilidade ao vapor de água (WPV) não melhorou com a incorporação da emulsão Pickering, o que pode ser devido a cavidades na estrutura do filme promovendo a passagem de vapor de água. Já a maior solubilidade foi observada para o filme de pectina, uma vez que a incorporação da emulsão Pickering promove a adição de substâncias hidrofóbicas (óleo) que diminui a disponibilidade de grupos hidrofílicos. A adição

de CNFs aos filmes aumentou os valores de EB (elongação na ruptura), devido à capacidade dos CNFs de induzir o rearranjo molecular ao longo da direção da tração (Huang et al., 2021). A incorporação da emulsão Pickering reduziu o módulo de elasticidade dos filmes, o que pode ser atribuído a uma ação plastificante do óleo quando adicionado a filmes à base de hidrocolóides (Galus, 2018). Estas matrizes filmogênicas foram usadas para recobrir tomates que foram armazenados e avaliados quanto a diversas propriedades por 12 dias em ambiente refrigerado. O pH, cor e os sólidos solúveis não mostraram diferenças ao longo do armazenamento. No entanto, os tomates com recobrimento mostraram maior perda de peso que os tomates não recobertos. Isso pode ser devido à redução do oxigênio endógeno que pode danificar o tecido interno do fruto, levando à produção de substâncias fermentativas como álcoois e à hidratação excessiva da epiderme, favorecendo a perda de peso (Gallardo et al., 2012). A análise microbiológica mostrou a contagem total superior nos tomates não revestidos, sendo a menor observada em tomates revestidos com película contendo a emulsão e o reforço de CNFs. O comportamento foi similar para bolores e leveduras, porém a adição de emulsões foi muito eficiente para a inativação destes microrganismos. Os resultados mostraram o potencial de uso dessas emulsões em matrizes filmogênicas visando a preservação de frutos perecíveis, embora aprimoramento das formulações seja ainda necessário para o prolongamento da vida útil.

Referências

- Ebrahimi, R., Fathi, M., & Ghoddusi, H. B. (2023). Nanoencapsulation of oregano essential oil using cellulose nanocrystals extracted from hazelnut shell to enhance shelf life of fruits : Case study : Pears. *International Journal of Biological Macromolecules*, 242(P1), 124704. <https://doi.org/10.1016/j.ijbiomac.2023.124704>
- Gallardo, A. P.-, Mattinson, S. D., Lazcano-peralta, A., Fellman, J. K., Regalado, C., Garci, B., & Barbosa-ca, G. (2012). Effect of native and acetylated-crosslinked waxy corn starch-beeswax coatings on quality attributes of raspberries during storage. *Starch Journal*, 64, 665–673. <https://doi.org/10.1002/star.201200005>
- Galus, S. (2018). Functional properties of soy protein isolate edible films as affected by

rapeseed oil concentration. *Food Hydrocolloids*, 85, 233–241.

<https://doi.org/10.1016/j.foodhyd.2018.07.026>

Hu, P., Wang, S., Yi, H., Wang, Z., Kang, J., & Wang, Y. (2024). Hybridized Cellulose Nanocrystals Enhanced the Temperature Resistance and Viscoelasticity of the Fracturing Fluid Network. *Journal of Molecular Liquids*, 124269.

<https://doi.org/10.1016/j.molliq.2024.124269>

Huang, J., Lu, Z., Li, J., Ning, D., Jin, Z., Ma, Q., Hua, L., Songfeng, E., & Zhang, M. (2021). Improved mechanical and ultraviolet shielding performances of hydroxyethyl cellulose film by using aramid nanofibers as additives. *Carbohydrate Polymers*, 255(October 2020), 117330. <https://doi.org/10.1016/j.carbpol.2020.117330>

Santos-López, G., Soto-castro, D., León-Matínéz, F. M., Hernández-Martínez, Á. R., & Gutiérrez, M. C. (2023). Characterization of gelatin films functionalized with silver nanoparticles or polysorbate 20 as UV – vis light controllers. *Food Packaging and Shelf Life*, 40(October). <https://doi.org/10.1016/j.fpsl.2023.101208>

CAPÍTULO VII

CONCLUSÃO GERAL

7.1 CONCLUSÃO GERAL

Nanofibras de celulose foram produzidas, caracterizadas e usadas tanto como estabilizante de emulsões Pickering como material de reforço em filmes. A emulsão foi incorporada pela capacidade de reduzir as limitações dos filmes biopoliméricos quanto à alta permeabilidade ao vapor de água, enquanto as nanofibras poderiam contornar as pobres propriedades mecânicas dos filmes. As nanofibras de celulose foram produzidas a partir da casca da mandioca, um resíduo agroindustrial, e métodos químico (hidrólise ácida), físico (ultrassom) e enzimático foram usados na produção dessas nanofibras. Em todos os casos, uma concentração muito baixa de nanofibras de celulose foi necessária para a estabilização das emulsões. Apesar das nanofibras de celulose obtidas pelo método de hidrólise química apresentarem melhor capacidade de estabilização das emulsões, hidrólise enzimática foi avaliada em maior profundidade por ser um processo verde. A melhora das propriedades das nanofibras de celulose produzidas por hidrólise enzimática foi alcançada por uma associação de enzimas, xilanase seguida de celulase.

Emulsões foram formadas com a incorporação do óleo essencial de orégano para produzir filmes nanocompósitos com atividade antimicrobiana. No entanto, a volatilidade deste óleo essencial era um grande problema tecnológico e, como solução, óleo de girassol foi misturado com o óleo essencial de orégano utilizando diferentes proporções. Essa mistura, além de reduzir a volatilidade da fase oleosa, aprimorou a atividade antimicrobiana das emulsões. Estas emulsões foram incorporadas em filmes e coberturas de pectina, juntamente com nanofibras que tinham o papel de reforçar as propriedades mecânicas. As coberturas foram aplicadas em tomates que foram avaliados durante o armazenamento, mostrando potencial para serem usadas para ampliação da vida útil após otimização da composição das matrizes filmogênicas. Algumas lacunas foram observadas, principalmente no estudo dos filmes, uma vez que um estudo deveria ter sido feito usando diferentes métodos para que a incorporação de todos os materiais na estrutura fosse mais efetiva. No entanto, de forma geral, este trabalho que trouxe um estudo amplo indo desde a extração dos nanomateriais até chegar à aplicação em um produto, abriu caminhos para novas ideias e aplicações do uso de nanofibras de celulose.

SUGESTÃO DE TRABALHOS FUTUROS

- Melhoramento da estrutura dos filmes e maior diversidade de composição dos filmes;

- Avaliação da digestibilidade dos filmes e tomates revestidos;
- Estudo mais detalhado do *shelf-life* principalmente em relação a produção do etileno, e em tempos maiores.
- Estudo do filme com embalagem em diversos produtos alimentícios.

CAPÍTULO VIII

REFERÊNCIAS GERAIS

- Cengiz-Çallıoğlu, F. (2011). *Silindirli elektro lif çekim yöntemi ile poliüretan nano lif üretimi. 2011. Tese de Doutorado. Üniversitesi Fen Bilimleri Enstitüsü, Doktora Tezi, Süleyman Demirel , Isparta.*
- Chevalier, Y., & Bolzinger, M. (2013). Emulsions stabilized with solid nanoparticles: Pickering emulsions. *Colloids and Surfaces A: Physicochemical and Engineering Aspects*, 439, 23–34.
- Ebrahimi, R., Fathi, M., & Ghoddusi, H. B. (2023). Nanoencapsulation of oregano essential oil using cellulose nanocrystals extracted from hazelnut shell to enhance shelf life of fruits : Case study : Pears. *International Journal of Biological Macromolecules*, 242(P1), 124704. <https://doi.org/10.1016/j.ijbiomac.2023.124704>
- Fujisawa, S.;Togawa, E.; Kuroda, K. (2017). Nanocellulose-stabilized Pickering emulsions and their applications. *Science and Technology of Advanced MaTerialS*, 18(1), 959–971.
- Khan, S., Hashim, S. B. H., Arslan, M., Zhang, K., Bilal, M., Zhiyang, C., Zhihua, L., Elrasheid, H., Zhai, X., Rezaul, M., Shishir, I., & Zou, X. (2024). Berry wax improves the physico-mechanical , thermal , water barrier properties and biodegradable potential of chitosan food packaging film. *International Journal of Biological Macromolecules*, 261(P2), 129821. <https://doi.org/10.1016/j.ijbiomac.2024.129821>
- Li, J., Alamdari, N. E., Aksoy, B., Parit, M., & Jiang, Z. (2023). Chemosphere Integrated enzyme hydrolysis assisted cellulose nanofibril (CNF) fabrication : A sustainable approach to paper mill sludge (PMS) management. *Chemosphere*, 334(April), 138966. <https://doi.org/10.1016/j.chemosphere.2023.138966>
- Liu, Z., Lin, D., Shen, R., & Yang, X. (2020). Characterizations of novel konjac glucomannan emulsion films incorporated with high internal phase Pickering emulsions. *Food Hydrocolloids*, 106088. <https://doi.org/10.1016/j.foodhyd.2020.106088>
- Nikfarjam, N.; Qazvini, N. T.; Deng, Y. (2015). Surfactant free Pickering emulsion polymerization of styrene in w/o/w system using cellulose nanofibrils. *European Polymer Journal*, 64, 179–188.
- Patel, A. R. (2020). Functional and Engineered Colloids from Edible Materials for Emerging Applications in Designing the Food of the Future. *Advanced Functional Materials*, 30(18), 1–34. <https://doi.org/10.1002/adfm.201806809>
- Pelissari, F. M., Andrade-Mahecha, M. M., Sobral, P. J. do A., & Menegalli, F. C. (2017). Nanocomposites based on banana starch reinforced with cellulose nanofibers isolated from banana peels. *Journal of Colloid and Interface Science*, 505, 154–167. <https://doi.org/10.1016/j.jcis.2017.05.106>
- Pérez-Córdoba, L. J., Norton, I. T., Batchelor, H. K., Gkatzionis, K., Spyropoulos, F., & Sobral, P. J. A. (2018). Physico-chemical, antimicrobial and antioxidant properties of gelatin-chitosan based films loaded with nanoemulsions encapsulating active compounds. *Food Hydrocolloids*, 79, 544–559. <https://doi.org/10.1016/j.foodhyd.2017.12.012>
- Riaz, S., Aslam, A. M., Butt, M. S., & Khan, M. K. I. (2024). Valorization of agricultural residues in the development of biodegradable active packaging films. *Industrial Crops & Products*, 215(April), 118587. <https://doi.org/10.1016/j.indcrop.2024.118587>
- Silva, A. C. P. da, Barbosa, J. R., Araújo, C. da S., Batista, J. T. S., Neves, E. M. P. X., Cardoso, D. N. P., Joele, M. R. S. P., & Lourenço, L. de F. H. (2024). A new edible coating of fish gelatin incorporated into açaí oil to increase the post-harvest shelf life of tomatoes. *Food Chemistry*, 438(May 2023). <https://doi.org/10.1016/j.foodchem.2023.138047>
- Tavernier, I. et al., Wijaya, W., Meeren, P. Van der, & Dewettinck, K. (2016). Food-grade particles for emulsion stabilization. *Trends in Food Science & Technology*, 50, 159–174.

- Travalini, A. P., Lamsal, B., Magalhães, W. L. E., & Demiate, I. M. (2019). Cassava starch films reinforced with lignocellulose nanofibers from cassava bagasse. *International Journal of Biological Macromolecules*, 139, 1151–1161. <https://doi.org/10.1016/j.ijbiomac.2019.08.115>
- Yang, W., Zhang, S., Hu, Y., Fu, Q., Cheng, X., Li, Y., Wu, P., Li, H., & Ai, S. (2024). Pectin-based film activated with carboxylated cellulose nanocrystals-stabilized oregano essential oil Pickering emulsion. *Food Hydrocolloids*, 151(January), 109781. <https://doi.org/10.1016/j.foodhyd.2024.109781>
- Yang, Y. et al., Fang, Z., Chen, X., Zhang, W., & Xie, Y. (2017). An overview of Pickering emulsions: solid-particle materials, classification, morphology, and applications. *Frontiers in Pharmacology*, 8, 287.
- Zhang, X. et al., Ren, S., Han, T., Hua, M., & He, S. (2018). New organic–inorganic hybrid polymers as Pickering emulsion stabilizers. *Colloids and Surfaces A: Physicochemical and Engineering Aspects*, 542, 42–51.
- Zhang, Y., Xie, J., Ellis, W. O., Li, J., Appaw, W. O., & Simpson, B. k. (2024). Bioplastic films from cassava peels : Enzymatic transformation and film properties. *Industrial Crops & Products*, 213(August 2023), 118427. <https://doi.org/10.1016/j.indcrop.2024.118427>
- Ebrahimi, R., Fathi, M., & Ghoddusi, H. B. (2023). Nanoencapsulation of oregano essential oil using cellulose nanocrystals extracted from hazelnut shell to enhance shelf life of fruits : Case study : Pears. *International Journal of Biological Macromolecules*, 242(P1), 124704. <https://doi.org/10.1016/j.ijbiomac.2023.124704>
- Gallardo, A. P.-, Mattinson, S. D., Lazcano-peralta, A., Fellman, J. K., Regalado, C., Garcı, B., & Barbosa-ca, G. (2012). Effect of native and acetylated-crosslinked waxy corn starch-beeswax coatings on quality attributes of raspberries during storage. *Starch Journal*, 64, 665–673. <https://doi.org/10.1002/star.201200005>
- Galus, S. (2018). Functional properties of soy protein isolate edible films as affected by rapeseed oil concentration. *Food Hydrocolloids*, 85, 233–241. <https://doi.org/10.1016/j.foodhyd.2018.07.026>
- Hu, P., Wang, S., Yi, H., Wang, Z., Kang, J., & Wang, Y. (2024). Hybridized Cellulose Nanocrystals Enhanced the Temperature Resistance and Viscoelasticity of the Fracturing Fluid Network. *Journal of Molecular Liquids*, 124269. <https://doi.org/10.1016/j.molliq.2024.124269>
- Huang, J., Lu, Z., Li, J., Ning, D., Jin, Z., Ma, Q., Hua, L., Songfeng, E., & Zhang, M. (2021). Improved mechanical and ultraviolet shielding performances of hydroxyethyl cellulose film by using aramid nanofibers as additives. *Carbohydrate Polymers*, 255(October 2020), 117330. <https://doi.org/10.1016/j.carbpol.2020.117330>
- Santos-López, G., Soto-castro, D., León-Matínéz, F. M., Hernández-Martínez, Á. R., & Gutiérrez, M. C. (2023). Characterization of gelatin films functionalized with silver nanoparticles or polysorbate 20 as UV – vis light controllers. *Food Packaging and Shelf Life*, 40(October). <https://doi.org/10.1016/j.fpsl.2023.101208>

CAPÍTULO IX

APÊNDICE

Apêndice I: Atividades Gerais e Divulgação dos Resultados

Artigos completos publicados em periódicos

1. **CHEVALIER, RAQUEL COSTA**; OLIVEIRA JÚNIOR, FERNANDO DIVINO; CUNHA, ROSIANE LOPES. Modulating digestibility and stability of Pickering emulsions based on cellulose nanofibers. FOOD RESEARCH INTERNATIONAL, v. 178, p. 113963, 2024.

Resumos simples publicados em Anais de Congressos

1. **CHEVALIER, R. C.**; ALMEIDA, N. A.; ROCHA, L. O.; CUNHA, R. L. TECHNOFUNCTIONAL PROPERTIES OF OREGANO OIL PICKERING EMULSIONS STABILIZED BY CELLULOSE NANOFIBERS. In: 15º Simpósio Latino Americano de Ciência de Alimentos e Nutrição - SLACAN, 2023, CAMPINAS. A Revolução da Ciência de Alimentos e Nutrição: Alimentando o Mundo de Forma Sustentável, 2023.
2. **CHEVALIER, R. C.**; VIEIRA, J. M. M.; MARTINS, J. T. R.; VICENTE, A.; CUNHA, R. L. CELLULOSE NANOFIBERS: REINFORCING AND STABILIZING MATERIAL FOR PICKERING EMULSIONS IN FILM-FORMING MATRICES. In: 15º Simpósio Latino Americano de Ciência de Alimentos e Nutrição - SLACAN, 2023, CAMPINAS. A Revolução da Ciência de Alimentos e Nutrição: Alimentando o Mundo de Forma Sustentável, 2023.
3. **CHEVALIER, R. C.**; DIVINO, F.J.O; CUNHA, R. L. DESIGNING CELLULOSE NANOFIBERS TO MODULATE RHEOLOGY AND STABILITY OF PICKERING EMULSIONS. In: Workshop on Mesostructures and Microfluidics, 2023.

Participação em eventos científicos

1. 15º SLACAN - Simpósio Latino Americano de Ciência de Alimentos e Nutrição. TECHNOFUNCTIONAL PROPERTIES OF OREGANO OIL PICKERING EMULSIONS STABILIZED BY CELLULOSE NANOFIBERS. 2023. (Simpósio).
2. Workshop on Mesostructures and Microfluidics. Designing cellulose nanofibers to modulate rheology and stability of pickering emulsions. 2023. (Simpósio).

Estágio de Capacitação de Docente

1. Participação como bolsista do Programa de Estágio Docente (PED), categoria C, na Disciplina “TA932 – Projeto Industrial”, sob orientação da Professora Ana Carla K. Sato. Participação como bolsista voluntária.

2. Participação como bolsista do Programa de Estágio Docente (PED), categoria C, na Disciplina “TA631 – Operações Unitárias I”, sob orientação da Professora Rosiane Lopes da Cunha. Participação como bolsista PED.

Estágio de Pesquisa no exterior

A Doutoranda realizou estágio de pesquisa no exterior no período de Março de 2023 a Agosto de 2023 na Universidade do Minho – Braga, Portugal. Financiado pelo CNPq (200248/2022-7).

RC ⓘ 🔍



Modulação da digestibilidade e estabilidade de emulsões Pickering à base de nanofibras de celulose
Autor: Raquel Costa Chevalier, Fernando Divino Oliveira Júnior, Rosiane Lopes Cunha
Publicação: Pesquisa Alimentar Internacional
Editor: Elsevier
Data: Fevereiro de 2024
© 2024 Elsevier Ltd. Todos os direitos reservados.

Direitos do autor do periódico

Observe que, como autor deste artigo da Elsevier, você mantém o direito de incluí-lo em uma tese ou dissertação, desde que não seja publicado comercialmente. A permissão não é necessária, mas certifique-se de mencionar o periódico como fonte original. Para obter mais informações sobre este e outros direitos retidos, visite: <https://www.elsevier.com/about/our-business/policies/copyright#Author-rights>

VOLTARJANELA FECHADA